GEOPHYSICAL FLUID DYNAMICS LABORATORY

ACTIVITIES – FY96
PLANS – FY97

U.S. DEPARTMENT OF COMMERCE
National Oceanic and Atmospheric Administration
Environmental Research Laboratories

GEOPHYSICAL FLUID DYNAMICS LABORATORY

ACTIVITIES - FY96

PLANS - FY97

OCTOBER 1996

GEOPHYSICAL FLUID DYNAMICS LABORATORY
PRINCETON, NEW JERSEY

UNITED STATES
DEPARTMENT OF COMMERCE

MICHAEL KANTOR
SECRETARY OF COMMERCE

NATIONAL OCEANIC AND
ATMOSPHERIC ADMINISTRATION

D. JAMES BAKER
UNDERSECRETARY FOR OCEANS
AND ATMOSPHERE

ENVIRONMENTAL
RESEARCH
LABORATORIES

ALAN R. THOMAS
DIRECTOR

NOTICE

Mention of a commercial company or product does not constitute an endorsement by NOAA Environmental Research Laboratories. Use for publicity or advertising purposes of information from this publication concerning proprietary products or the tests of such products is not authorized.

PREFACE

This document is intended to serve as a summary of the work accomplished at the Geophysical Fluid Dynamics Laboratory (GFDL) and to present a glimpse of the near future direction of its research plans.

It has been prepared within GFDL and its distribution is primarily limited to GFDL members, to Princeton University affiliates, to interested offices of the National Oceanic and Atmospheric Administration (NOAA), to other relevant government agencies and national organizations, and to interested individuals.

The organization of the document encompasses an overview, project activities and plans for the current and next fiscal year, and appendices. The overview covers highlights of the three major research areas that correspond to Strategic Plan Elements in NOAA's Environmental Assessment and Prediction Portfolio: Advance Short-Term Forecasts and Warnings; Seasonal to Interannual Climate Forecasts; and Predict and Assess Decadal to Centennial Changes. The body of the text describes goals, specific recent achievements and future plans for the following major research categories: Climate Dynamics; Middle Atmosphere Dynamics and Chemistry; Experimental Prediction; Oceanic Circulation; Planetary Circulations; Observational Studies; Hurricane Dynamics; and Mesoscale Dynamics. These categories, which correspond to the GFDL organization of research groups, are different from the NOAA categories and are far from being mutually exclusive. Interaction occurs among the various groups and is strongly encouraged.

The appendices contain the following: a list of GFDL staff members and affiliates during Fiscal Year 1996; a bibliography of relatively recent research papers published by staff members and affiliates during their tenure with GFDL (these are referred to in the main body according to the appropriate reference number or letter); a description of the Laboratory's computational support and its plans for Fiscal Year 1997; a listing of seminars presented at GFDL during Fiscal Year 1996; a list of seminars and talks presented during Fiscal Year 1996 by GFDL staff members and affiliates at other locations.

Although the specific names of individuals are not generally given in the overview, an entire listing of project participants can be found in Appendix A. Research staff personnel can normally be identified by consulting the cited Appendix B references or the names listed in the body of the text.

The Scientific Editor for this year's report was John Sheldon, with Wendy Marshall serving as Technical Editor. This report is the culmination of a team effort involving a large majority of the GFDL staff and their Princeton University collaborators. Special thanks are extended to all who contributed to this substantial effort.

September 1996

Geophysical Fluid Dynamics Laboratory/NOAA
P.O. Box 308, Princeton, New Jersey 08542

(609) 452-6500
http://www.gfdl.gov

TABLE OF CONTENTS

AN OVERVIEW

SCOPE OF THE LABORATORY'S WORK

The Geophysical Fluid Dynamics Laboratory is engaged in comprehensive long lead-time research fundamental to NOAA's mission.

The goal of this research is to expand the scientific understanding of the physical processes that govern the behavior of the atmosphere and the oceans as complex fluid systems. These systems can then be modeled mathematically and their phenomenology can be studied by computer simulation methods. In particular, GFDL research concerns the following:

- the predictability of weather on large and small scales;
- the structure, variability, predictability, stability and sensitivity of global and regional climate;
- the structure, variability and dynamics of the ocean over its many space and time scales;
- the interaction of the atmosphere and oceans, and how the atmosphere and oceans influence and are influenced by various trace constituents;
- the Earth's atmospheric general circulation within the context of the family of planetary atmospheric circulations.

The scientific work of the Laboratory encompasses a variety of disciplines including meteorology, oceanography, hydrology, classical physics, fluid dynamics, chemistry, applied mathematics, and numerical analysis. Research is also facilitated by the Atmospheric and Oceanic Sciences Program (AOSP), which is a collaborative program at GFDL with Princeton University. Under this program, regular Princeton faculty, research scientists, and graduate students participate in theoretical studies, both analytical and numerical, and in observational experiments in the laboratory and in the field. The program is supported in part by NOAA funds. AOSP scientists may also be involved in GFDL research through institutional or international agreements.

The following sections describe the GFDL contributions to three major research areas that correspond to Strategic Plan Elements in NOAA's Environmental Assessment and Prediction Portfolio.

HIGHLIGHTS OF FY96

and

IMMEDIATE OBJECTIVES

In this section, some research highlights are listed that may be of interest to those persons less concerned with the details of GFDL research. Selected are items that may be of special significance or interest to a wider audience.

Items in this section are placed in the NOAA Strategic Plan Elements:

Advance Short-Term Forecasts and Warnings

Seasonal to Interannual Climate Forecasts

Predict and Assess Decadal to Centennial Changes

These categories are organized rather differently than the GFDL research project areas presented in the main body of the report. The parentheses refer to references in GFDL Activities, FY96; Plans, FY97.

ADVANCE SHORT-TERM FORECASTS AND WARNINGS

The need for short-term warning and forecast products covers a broad spectrum of environmental events which have lifetimes ranging from several minutes up to a month or so. Some examples of these events are tornadoes, hurricanes, tsunamis, and coastal storms, as well as "spells" of unusual weather (warm, cold, wet, or dry). Benefits of these products can be measured in terms of lives saved, injuries averted, and expenses spared. NOAA's vision for improvement in this area involves operational modernization and restructuring, strengthening of observing and prediction systems, and improved applications and dissemination of products and services.

Efforts at GFDL are centered around the development of numerical models which may be used in the prediction of "short-term" atmospheric and oceanic phenomena. Simulations from these models are studied and compared with observed data to aid in the understanding of the processes which govern the behavior of the various phenomena.

With regard to tropical weather systems, efforts are aimed at the genesis, growth, and decay of tropical storms and hurricanes. In extratropical regions, interest includes the development of severe weather systems, the interaction of medium-scale atmospheric flow with that on larger scales, and the influence of the underlying topographic features. Experimental prediction of regional-scale weather parameters weeks to months in advance is being pursued; included in this context is the study of "ensemble forecasting." With regard to the marine environment, forecasts of coastal conditions on a day-to-day basis can be made by coupling of ocean and atmosphere models. Ocean models are also used to simulate coastal bays and estuaries, the response of coastal zones to transient atmospheric storms, and Gulf Stream meanders and rings.

ACCOMPLISHMENTS FY96

A method has been developed for assimilating satellite-derived winds into the GFDL hurricane model. Preliminary results suggest that including the satellite winds does have a beneficial impact on hurricane track forecasts (2.4.3).

A careful study of methods for selecting the initial conditions of ensemble forecasts was performed using simple numerical models. The conclusions are that a simple random sample of the observational error is probably the most effective method for generating ensemble forecasts. The use of random samples could have significant impacts on the usefulness of ensemble forecasts produced by operational prediction centers (4.1).

An operational Coastal Ocean Forecast System (COFS) is providing daily predictions for the U.S. east coast, and has been upgraded for use with a higher resolution atmospheric prediction model and an improved ocean model configuration (5.4.3).

Performance of the GFDL Hurricane Prediction System, which became an official operational model for the National Weather Service in the 1995 hurricane season, was carefully monitored. The system made 257 forecasts in the Atlantic and 105 forecasts in the Eastern pacific. It produced substantial improvement in track forecasts, *e.g.*, 35% error reduction at forecast times beyond one day relative to the Cliper model in the Atlantic. An accurate track guidance for two to three days ahead will provide increased lead time to prepare for the approach of tropical cyclones (7.1.1).

Collaboration with the U.S. Navy has resulted in the successful combination of the GFDL Hurricane Prediction System with their global forecast/analysis system. Officially adopted by the Navy in 1996, the new combined system provides forecasters with operational guidance for typhoon prediction in the Western Pacific. An arrangement was instituted to carry out parallel runs of the GFDL model using the NCEP analysis (7.1.3).

A sensitivity study was initiated to evaluate the utility of the satellite water vapor wind data for tropical cyclone track forecasts. In the preliminary investigation, improvement due to the additional data was found in some cases examined (7.2.1).

A coupled model consisting of the GFDL hurricane model and the Princeton ocean model was constructed. A coupled simulation experiment was performed for one case of Hurricane Gilbert (1988) interacting with the water of the Gulf of Mexico. The over-intensification of the hurricane in simulation run without ocean coupling was considerably reduced, resulting in an improved intensity forecast (7.3.2).

Regression analysis has revealed a distinct difference in the characteristics of cyclone-scale evolution during periods of high and low forecast skill. One important feature affecting the quality of forecasts is the intensity of a ridge in the eastern Pacific, with high and low forecast skill corresponding to a weak and strong ridge, respectively. Consequently, the trajectories of cyclones into North America are substantially different during periods of high and low skill (8.1.1).

New versions of the hydrostatic and nonhydrostatic terrain-following Zeta models are expressed in spherical coordinates to more accurately simulate planetary scale and synoptic scale dynamics and to facilitate intermodel comparisons (8.4).

PLANS FY97

- Implementation of an operational data assimilation system will be made part of the eastern Coastal Ocean Forecasting System. This should improve operational forecasts of coastal sea level and sea surface temperature.

- Hurricane forecast experiments with increased resolution will be initiated.

- A new version of hurricane model initialization method, including a generalized scheme of vortex generation, will be extensively tested. It is anticipated that consideration of effects of the environmental flow in the vortex generation will lead to an improvement in storm intensity prediction.

- A GFDL coupled tropical cyclone-ocean forecast system will be designed in a cooperative effort with the University of Rhode Island.

- The investigation of topographic influences on cyclones and mesoscale systems will continue. Topographic wave drag will be assessed by means of three-dimensional model simulations. The effects of compressibility, the Boussinesq approximation, and nonhydrostatic motions on mesoscale circulations will continue to be evaluated. These high resolution studies will facilitate improvements to the parameterizations of wave drag in larger scale models and GCMs.

- The development of limited area models will emphasize the incorporation of moist physics and boundary layer processes into the new, high resolution hydrostatic and non-hydrostatic models expressed in spherical coordinates

SEASONAL TO INTERANNUAL CLIMATE FORECASTS

Seasonal to interannual climate fluctuations have far-reaching consequences for agriculture, fishing, water resources, transportation, energy consumption, and commerce, among others. Short-term climate anomalies which persist from a season to several years affect rainfall distributions, surface temperatures, and atmospheric and oceanic circulation patterns. Reliable climate forecasts may be used to reduce the disruption, economic losses, and human suffering that occur in connection with these anomalies. NOAA's vision for improvement in this area is based on better predictive capability, enhanced observations, greater understanding of climate fluctuations, and assessment of impacts.

The study of seasonal to interannual climate fluctuations at GFDL is based on both theoretical and observational studies. Available observations are analyzed to determine the physical processes governing the behavior of the oceans and atmosphere. Mathematical models are constructed to study, simulate, and predict the coupled ocean-atmosphere, land-surface, sea-ice system.

Simulations based on the numerical models maintained at GFDL, in conjunction with observations, are used to study climate variations on seasonal and longer time scales. Processes under study include large-scale wave disturbances and their role in the general circulation, the effects of boundary conditions such as sea surface temperature and soil moisture, influence of clouds, radiation, and atmospheric convection, and the "teleconnection" of atmospheric anomalies across the global atmosphere. Furthermore, experimental model forecasts are used to evaluate atmospheric predictability and to assess skill in forecasting atmospheric and oceanic climate anomalies, both in general and in

connection with the El Niño-Southern Oscillation phenomenon. Also, a more accurate representation of the state of the global ocean is being studied through data assimilation for better initialization of seasonal-interannual forecasts.

ACCOMPLISHMENTS FY96

Numerical experiments with a simple model of soil-water balance have elucidated the dependence of the soil-water decay time scale on climatic and land-surface parameters. In systems where damping of soil-water fluctuations is dominated by the runoff process, the temporal dynamics of soil water are closely tied to the storm arrival process (1.2.3).

The mid-winter suppression of eddy amplitudes in the Pacific storm track has been found to be clearly evident in R30 climate model simulations. A series of perpetual insolation integrations, using insolation appropriate for November, December, January, February, and March, show an even clearer minimum in the strength of the Pacific storm track in January, as compared with November or March. These model simulations should help in isolating the mechanism underlying this peculiar seasonal cycle of the Pacific storm track (1.4.1.2).

Observations indicate a distinct increase in tropical-mean greenhouse trapping of ~2 W/m^2 associated with a ~0.4 K warming of the tropical oceans during their evolution from colder La Niña conditions in early 1985 to warmer El Niño conditions in late 1987. The observed increase compares favorably with climate model simulations of both the dynamically and thermodynamically driven changes in greenhouse trapping during ENSO (2.4.1).

A new modular modeling system is being built to facilitate the development of improved atmospheric and coupled ocean-atmosphere models. Flexible dynamical cores for both B-grid and spectral atmospheric models have been completed using Fortran-90. A large number of modular physics parameterizations have been completed and tested in the B-grid model. Modular support tools such as a diagnostic output module have also been completed and integrated into the B-grid model (4.2.1).

A new version of the Modular Ocean Model with greatly enhanced vertical resolution has been completed and tested in coupled model integrations. The new model gives improved simulations of the upper ocean thermal structure, particularly the position of the equatorial thermocline which is vital to successful seasonal predictions (4.2.2).

The impact of convection and cloud parameterizations on seasonal and interannual forecasts has been studied through a number of 18-month forecasts. The use of the Relaxed Arakawa-Schubert convection scheme and prescribed low-level cloudiness appear to have significantly improved coupled model performance in the tropical Pacific (4.3.1).

An ensemble of coupled model forecasts has been produced in order to study the potential predictability of the ocean-atmosphere system. Forecasts of sea surface

temperatures and extratropical atmospheric fields for some years are found to be considerably more potentially predictable than for other years. The potential predictability of the extratropical atmosphere is extremely limited in many years, but occasionally it might be possible to make useful forecasts with lead times of two seasons or more (4.3.2).

Ensemble simulations with an atmospheric model forced by observed sea surface temperatures do a good job in reproducing the number of tropical storms occurring over the North Atlantic Ocean each year. This suggests that coupled model predictions of the expected number of tropical storms could be produced with lead times of several seasons (4.3.6).

The sigma-coordinate Princeton Ocean Model (POM) has been shown to successfully reproduce observed interannual and interdecadal sea level changes in the Atlantic Ocean during the period 1950-1989 when forced with observed sea surface temperature and surface winds (5.4.4).

A comparison has been made between model experiments with SST changes prescribed in the tropical Indian and Pacific Oceans, respectively. It is demonstrated that the polarity of the global atmospheric response to Indian Ocean SST changes is opposite to that of the response to tropical Pacific anomalies. This result may be primarily attributed to the spatial displacement of the near-equatorial rainbelt when a SST anomaly in the tropical Pacific is replaced by a SST anomaly of the same sign in the Indian Ocean (6.3.1).

The mechanisms connecting the warming in the Pacific to the warming in the other tropical oceans during El Niño events have been investigated with observational and model-generated data. In each ocean, the change in net heat flux across the air-sea interface is due to a different combination of changes in cloud cover and evaporation. The latter changes are, in turn, linked to perturbations in the atmospheric circulation resulting from El Niño-related forcing in the tropical Pacific (6.3.2).

A high degree of consistency was found among satellite-based and surface-based observations of cloud patterns accompanying extratropical cyclone waves and low-latitude convective disturbances. This comparison study demonstrates the usefulness of both types of datasets for studying various facets of recurrent circulation systems (6.4.1).

A series of studies of planetary and cyclone scale waves has identified significant differences in their interaction with the mean circulation. Planetary scale waves tend to equilibrate anticyclonically, whereas smaller cyclone scale waves always equilibrate cyclonically. These results could have an important impact on the interannual variability of the position and strength of storm tracks, depending on whether the environment favors cyclonic scale or planetary scale development (8.2.2).

PLANS FY97

- Analyses of trends and natural variability of runoff and river discharge will be extended and refined by inclusion of precipitation observations and by extension of the river discharge dataset. Information on natural variability of runoff and discharge will be used as a context within which to evaluate both observed discharge changes and modeled sensitivities of runoff to anthropogenic changes of radiative forcing.

- An analysis of temporal characteristics of soil water will be extended to include seasonality and atmospheric feedbacks. A companion GCM study of soil-water predictability will also be conducted, with relevance also to seasonal climate predictability.

- Work on the modular modeling system will continue with completion of additional physics modules, the creation of a general circulation model built around the spectral dynamical core, and the addition of more modular support tools. The B-grid model and the new spectral model will be evaluated by coupling these models to the high resolution ocean model and examining both forecasts and long "climate" integrations.

- Analysis of seasonal coupled model ensemble predictions will be expanded to examine both potential predictability and forecast quality. Additional ensemble members will be produced as needed to increase the significance of interesting results and to examine additional seasons. In particular, coupled model ensemble forecasts of tropical storm frequency will be evaluated to see if this model is capable of making useful forecasts with lead times of one or more seasons.

- A careful analysis of the interactions between clouds, convection and radiation in coupled model forecasts and in observations will be undertaken. The interaction between these atmospheric parameterizations and the upper layers of the tropical ocean is known to be a weakness in the current coupled model system. Possible improvements to parameterizations will be incorporated and tested in coupled model predictions.

- A new isopycnal diffusion scheme will be incorporated into the ocean model of the coupled prediction system. The impact of this more theoretically grounded diffusion scheme on the ocean circulation will be evaluated in ocean-only simulations and coupled model integrations.

- Inverse modeling techniques will be applied to atmospheric CO_2 observations to produce a preliminary estimate of the year-by-year changes in the atmospheric carbon budget during the 1980s.

- The relationships between the atmospheric circulation and the cloud properties associated with stratus decks and subtropical frontal zones will be further explored. The

mesoscale cloud organization in frequently occurring circulation systems will be studied using satellite cloud products with higher spatial resolution.

- Multiple runs of a high-resolution version of the GFDL Climate GCM with SST forcing corresponding to selected El Niño-Southern Oscillation events will be analyzed. The findings from these integrations will be compared to previous runs based on the same model with lower resolution.

- An investigation into the seasonal evolution of the storm track and the synoptic scale disturbances within it will employ both data analyses and idealized model simulations. One particular goal will be the accurate modelling of the poleward deflection of the storm track during the transition from autumn to winter. This will also help clarify how the development of blocking by the Eastern Pacific ridge affects the trajectory of winter storms over North America.

PREDICT AND ASSESS DECADAL TO CENTENNIAL CHANGES

Events such as the Sahel drought, the dust bowls in the Midwest, the Little Ice Age, stratospheric ozone depletion, and global warming may define eras in history. Events such as these have lifetimes of decades to centuries and their causes may be either natural or anthropogenic. An ability to predict such changes and to assess the causes is essential in long-range policy making. Adaptation to the changes and reduction of the effects of human induced changes require enhanced predictive capability. NOAA's vision for improvement in this area is based on a commitment to research in climate and air quality, as well as to insure long-term climate and chemical records.

The related research efforts at GFDL require judicious combinations of theoretical models and specialized observations. The modeling efforts draw on principles from the atmospheric, oceanic, chemical, and biological sciences. One area of focus is long-term climate variability and secular change associated with the atmosphere and oceans. This area encompasses a number of topics, including the effects of changes in the concentration of atmospheric gases such as carbon dioxide, the simulation of past climates, and the variability of the oceanic thermohaline circulation. Another area of focus is the formation, transport, and chemistry of atmospheric trace constituents. This area addresses problems such as: the transport of quasi-conservative trace gases; the biogeochemistry of climatically significant long-lived trace gases; the transport, sources, and sinks of aerosols; the chemistry of ozone and its regulative trace species; the effects of clouds and aerosols on chemically important trace gases; and the impact of anthropogenic chlorofluorocarbons on stratospheric ozone amounts. Yet another area of focus relates to the modeling of the marine environment. It includes the dispersion of geochemical tracers in the world oceans, the oceanic carbon cycle and trace metal geochemistry, and ecosystem structures.

ACCOMPLISHMENTS FY96

A 120-year simulation with the higher resolution (R30) version of the GFDL coupled climate model contains a decadal-scale variability pattern similar to recent observed decadal changes in the tropical and subtropical Pacific. Thus the model shows promise as a tool for helping discriminate between natural decadal-scale variability and externally forced changes in this region (1.1.2).

In the coupled ocean-atmosphere model, a pattern was identified in which anomalously warm Northern Hemisphere temperatures are associated with land areas poleward of 40°N being anomalously warm and the ocean being anomalously cold. This cold ocean-warm land pattern is almost identical to that found in an analysis of observed surface air temperature data (1.1.3).

Substantial 50 to 60 year oscillations of ocean temperature and salinity occur in the Nordic Seas region of a coupled ocean-atmosphere model. These fluctuations, which are reminiscent of the observed Great Salinity Anomaly, are associated with large-scale anomalies of salinity which propagate out of the Arctic, down the East Greenland current, and around the North Atlantic subpolar gyre. Atmospheric temperature and wind anomalies are also associated with this variability (1.1.4).

A coupled ocean-atmosphere GCM with higher computational resolution has been developed. The improvements in the performance of the model include more realistic simulations of El Niño/Southern Oscillations and decadal oscillations in the North Pacific Ocean. The computational requirements of the model are small enough to allow the many long-term integrations needed to study climate variability (1.1.6).

Power spectra of monthly runoff aggregated over large river basins in a climate model were found typically to display white-noise behavior. In contrast, the time series of observed river discharges have red-noise spectra. It is inferred that groundwater and surface water storage, not considered in the climate model, are important controls on monthly to annual river discharge (1.2.1.1).

Preliminary analyses of observed annual river discharges from major basins of the world revealed large (typically 10-50%/century) trends. For the most part, however, the trends were not significant in a formal statistical sense, due to the large natural interannual variability of flows (1.2.1.2).

Intercomparisons of stand-alone responses of numerous land-surface parameterizations revealed the importance of non-water stressed stomatal resistance. Preliminary analysis of a GCM sensitivity experiment showed that the stand-alone sensitivity to such resistance is significantly modified by atmospheric feedbacks, which may be either negative (boundary-layer and radiation) or positive (precipitation). The net effect of the feedbacks is a reduced sensitivity (1.2.2).

Forced by both greenhouse gases and sulphate aerosols, a coupled ocean-atmosphere model successfully reproduced the increase of global mean surface air temperature during the last 100 years, as well as the magnitude of its fluctuation at interannual to interdecadal time scales (1.1.1). Because of the increase of sulphate aerosols which reflect solar radiation, the so-called mid-continental summer dryness did not materialize in this numerical experiment until the beginning of the 21st century (1.2.4).

In response to a massive discharge of fresh water into the ocean, a coupled ocean-atmosphere model reproduces the so-called abrupt climate change which frequently occurred in the North Atlantic Ocean and surrounding regions during the last glacial and deglacial periods (1.3.2).

Models of Jupiter's atmospheric circulation have been adapted to take into account the vertical wind data provided by the recent "Galileo" probe. A study of vortex genesis in Galilean structures leads to simulations of the Great Red Spot with realistic scales, speeds, and oscillations and suggests that Jupiter's winds extend to a depth of about 500 km (1.5.2).

An underestimate occurring in the specifications of the gas optical depths near line centers in the solar line-by-line calculations has been corrected. This results in an increase in the computed solar heating rates due to O_2, CO_2, and H_2O in the upper stratosphere (2.1.2).

The outgoing clear-sky longwave irradiances computed by the new GFDL longwave radiation algorithm using analyzed fields of temperature and moisture have been compared with those observed by the Earth Radiation Budget Experiment satellites. The agreement between the computed and measured fluxes is encouraging (2.2.2).

A three-dimensional cloud-system model, with a domain of hundreds of kilometers, has been integrated for the complete life cycle of a convective system.This is among the first such integrations of its type. The development, dissipation, and convective- and stratiform-dominated stages of the system are modeled in good agreement with observations. Strong interactions between radiation and microphysics play an important role in the behavior of the convective system (2.3.2).

A study of GCM climate responses to combined greenhouse (*e.g.*, trace gas increases) and midlatitude Northern Hemisphere albedo forcings (*e.g.*, anthropogenic sulfate aerosol increases) reveals that, in the absence of cloud feedbacks, the resulting temperature and precipitation changes are approximately similar to that expected from a simple arithmetic sum of the responses to the individual forcings, thus suggesting a linearly additive behavior of the climate system (2.3.6).

A study of the direct sulfate aerosol radiative effect in the limited-area-nonhydrostatic model indicates that sub-grid scale variations of relative humidity markedly affect the computation of the forcing performed over large domains typical of coarser grid models (*e.g.*, GCMs) (2.3.7).

Incorporation of the new water vapor continuum formulation ("CKD 2.1") in the SKYHI GCM results in a substantial cooling of the upper troposphere, with warming occurring below. This is in contrast to the effects of the non-CO_2 trace gases which act to warm the upper troposphere (2.5.1).

The complex effects of chlorine, bromine and heterogeneous chemistry have now been added to the ozone chemistry module for the SKYHI troposphere-stratosphere model. The new chemistry is currently being tested. This advance creates the potential for key three-dimensional calculations of anthropogenic influences on ozone in the lower stratosphere and upper troposphere (3.1.1).

A detailed study of the sources and transport of atmospheric reactive nitrogen (NO_y), the key precursor to ozone chemical processes, has shown that human sources of NO_y dominate the continental lower troposphere, while lightning sources dominate in the tropical troposphere. NO_y transported from the stratosphere dominates in the northern hemisphere upper troposphere, and much of the entire southern hemisphere troposphere. This is found to be the case even though the global total anthropogenic sources of NO_y dominate the stratospheric source by nearly two orders of magnitude (3.1.4).

Using the above calculations of global NO_y, a new evaluation of the likely impact of human activities in tropospheric ozone amounts has been completed. The results indicate that today's ozone is more than twice pre-industrial values in the summer northern hemisphere lower troposphere. Ozone amounts increase by 20-50% in the middle troposphere, but increase by less than 20% in the upper troposphere (3.1.5).

An integration for the May-June period using a version of the SKYHI model at $0.6° \times 0.72°$ resolution was found to produce a simulation of the SH polar night jet that is markedly improved over that obtained at lower model resolution (3.2.4).

A long integration using the SKYHI model with an imposed quasi-biennial oscillation in the tropical stratosphere was performed. The results show that the model is able to reproduce the observed extratropical effects of the equatorial wind variations, notably the observed tendency for the NH polar vortex to be weaker when the tropical winds near 40 mb are easterly. A version of the SKYHI model with sophisticated photochemistry has been run with the same imposed quasi-biennial oscillation in the wind field. This model produces a quasi-biennial modulation of the ozone concentrations that is in very good agreement with observations (3.2.7).

A new analysis of the energy balance in the GFDL Modular Ocean Model (MOM) has been carried out which quantifies, for the first time, the work done by buoyancy forces (mainly heating and cooling) and wind forces. The analysis shows that the work done by buoyancy forces is surprisingly small relative to the work done by the winds in a model configuration which includes an Antarctic Circumpolar Current (5.1.1).

A global ocean circulation model has been constructed which employs discrete isopycnal layers of varying thickness in its vertical dimension. Isopycnal layers provide a more natural coordinate system for determining the effects of advection and mixing in the ocean's interior (5.1.4).

A simulation of the transient uptake of CFC-11 shows that the GFDL coupled ocean-atmosphere climate model is capable of predicting past CFC penetration into the Southern Ocean. The tracer study lends credence to the climate change forecasts of the coupled model (5.1.6).

A new isopycnal mixing scheme has been developed for use within the discrete-depth framework of the GFDL Modular Ocean Model (MOM). The new scheme allows lateral mixing in the model to be oriented along surfaces of constant potential density, and is a significant improvement over the previous isopycnal mixing scheme. This improvement will soon be released to MOM users worldwide (5.3.2).

A carbon cycle model has been embedded in the GFDL coupled ocean-atmosphere climate model to predict changes in oceanic CO_2 uptake associated with an enhanced greenhouse effect. Predicted future CO_2 uptake is found to be reduced due to a weakened thermohaline circulation in the ocean (5.5.1).

PLANS FY97

- The natural, internally generated variability of climate will be studied using numerical simulations of millennium scale, which will be generated by an improved version of the coupled ocean-atmosphere GCM with higher computational resolution.

- The combined and separate effects of increasing greenhouse gases and sulphate aerosols upon climate will be investigated by use of an improved version of the coupled ocean-atmosphere GCM with higher computational resolution.

- An attempt will be made to simulate the very cold climate of the last glacial maximum using a coupled ocean-atmosphere GCM.

- The sensitivity of a climate model to inclusion of non-water-stressed stomatal resistance will be explored in detail, with a comprehensive evaluation of atmospheric feedbacks. In connection with this study, an estimate of sensitivity to stomatal resistance doubling will also be made, providing a partial basis for assessing the direct impact of atmospheric carbon-dioxide increase on the global water cycle.

- A variety of idealized eddy-resolving models will be used to test proposed schemes for eddy-flux closure in ocean models based on homogeneous turbulence theory.

- Comparisons between "benchmark" radiative transfer computations and available observations will be used to evaluate the accuracy of the computed fluxes and heating rates. Effects of new radiative parameterizations on biases in the GCM simulations will be analyzed.

- The sensitivity of climate to changes in the concentrations of tropospheric and stratospheric greenhouse gases, ozone and aerosols, and to changes in the physical properties of clouds, will continue to be investigated using GCMs. The explicit simulation of the liquid and the solid phases of H_2O in GCMs and the associated cloud-radiative interactions will also be studied.

- Quantitative differences between computed and observed radiative fluxes, as obtained from satellite and field experiments, will continue to be analyzed, including investigations of the atmospheric hydrologic cycle (*e.g.*, water vapor and clouds) and its effect on the global radiation budget.

- Satellite data will be used to understand the variations in the hydrologic and radiative parameters on different spatial and temporal scales. Comparisons between model simulations and satellite data will continue to be used to evaluate and improve the quality of simulation.

- Radiative-convective equilibria will be obtained with a three-dimensional model of moist convection, in a doubly periodic domain over a horizontally homogeneous lower boundary with fixed temperature. Water vapor and clouds will be fully interactive with radiative transfer. This model will be used to study moist convective organization, the maintenance of CAPE (convective available potential energy) in the tropics, and cloud feedback mechanisms.

- The statistical characteristics of vertical-velocity and microphysical variations at small scales in a three-dimensional cloud-system model will be used to evaluate a cumulus parameterization which includes these processes. These processes are important in governing interactions between convection, clouds, and radiation.

- The semi-empirical tropospheric ozone chemistry will continue to be refined and will be applied to a range of key problems. Particular emphasis will be placed on quantification of anthropogenic influences on tropospheric ozone and on the relative roles of transport and chemistry on regional scales.

- Intensive effort will be made to evaluate and test the performance of the new SKYHI ozone chemistry module that includes effects of chlorine, bromine, and aerosols on ozone destruction processes. Particular emphasis will be placed upon improving understanding of their importance in the higher-latitude lower stratosphere.

- A number of SKYHI integrations that test the capability of various tracer advection schemes will be analyzed in detail to assess their relative strengths and weaknesses.

- The broad-based effort to improve the applicability of SKYHI to a wide range of tropospheric and stratospheric subject areas will continue. Emphasis will be placed on careful analysis of the impacts of the various SKYHI upgrades on the model's performance.

- Experimental integrations of the SKYHI model at higher horizontal and vertical resolutions will be analyzed in depth. These pioneering studies are providing key insights into the effects of unresolved processes and inaccurate physical parameterizations on the capability of the model.

- Detailed analysis will be made of various SKYHI, mechanistic, and theoretical approaches to gain a more quantitative understanding of the role of gravity waves in influencing atmospheric circulation and transport characteristics. Attention will be devoted to developing more physically correct parameterizations of gravity wave effects.

- A new energy analysis for the GFDL Modular Ocean Model (MOM) will be applied to decadal and century-scale fluctuations observed in ocean-only and coupled models. This should provide new insights into the mechanisms governing long-term oceanic variability.

- A new isopycnal-coordinate ocean model will be examined for its utility in climate studies. Comparisons will also be made between the new isopycnal model and MOM set up with its new isopycnal mixing scheme. MOM's isopycnal mixing scheme should mimic some of the isopycnal effect in an isopycnal-coordinate model within a traditional vertical grid.

- A new release of MOM 2 is planned which will include new third-order and fourth-order advection schemes, NCAR's K-profile boundary layer parameterization (KPP), and the new GFDL isopycnal mixing scheme.

PROJECT ACTIVITIES FY96

PROJECT PLANS FY97

1. CLIMATE DYNAMICS

GOALS

To construct mathematical models of the atmosphere and of the coupled ocean-atmosphere system which simulate the global large-scale features of climate.

To study the dynamical interaction between large-scale wave disturbances and the general circulation of the atmosphere.

To identify and elucidate the physical and dynamical mechanisms which maintain climate and cause its variation, and to examine their generality in the context of paleoclimate and the atmospheres of other planets.

To evaluate the impact of human activities on climate.

1.1 OCEAN-ATMOSPHERE INTERACTION

1.1.1 Response to CO_2 and Sulphates

J. Haywood *R.J. Stouffer*
S. Manabe *R.T. Wetherald*
V. Ramaswamy

ACTIVITIES FY96

In order to investigate the past and future changes of climate in response to the combined effect of increasing greenhouse gases and sulphate aerosols, a numerical experiment was conducted using the GFDL coupled climate model. The temporal variations of both sulphate aerosols and the CO_2-equivalent of all greenhouse gases used for this experiment are similar to those used by Mitchell et al. (1995)[1]. (The temporal variation of CO_2-equivalent from 1765 to 1990 AD was based upon the 1990 IPCC report. After 1990, it was assumed to increase by 1%/year. The horizontal distribution of aerosol loading up to 1990 AD was based on the calculated annual mean distribution for the 1980s, scaled by the estimated sulphate emissions. In addition, the IPCC estimated global mean thermal forcing of sulphate aerosols (-0.6 W/m^2) in 1990 was imposed. Starting from an initial condition which was in a quasi-equilibrium state, numerical time integration of the coupled model was performed with the thermal forcing of combined greenhouse gases and aerosols described above.

Figure 1.1 illustrates the temporal variation of the globally averaged, annual mean surface air temperature anomaly of the coupled model over the 300-year period from 1765 to

1. Mitchell, J.F.B., T.C.Johns, J.M.Gregory, and S.F.B.Tett, Climate response to increasing levels of greenhouse gases and sulfate aerosols, *Nature, 376*, 501-504, 1995.

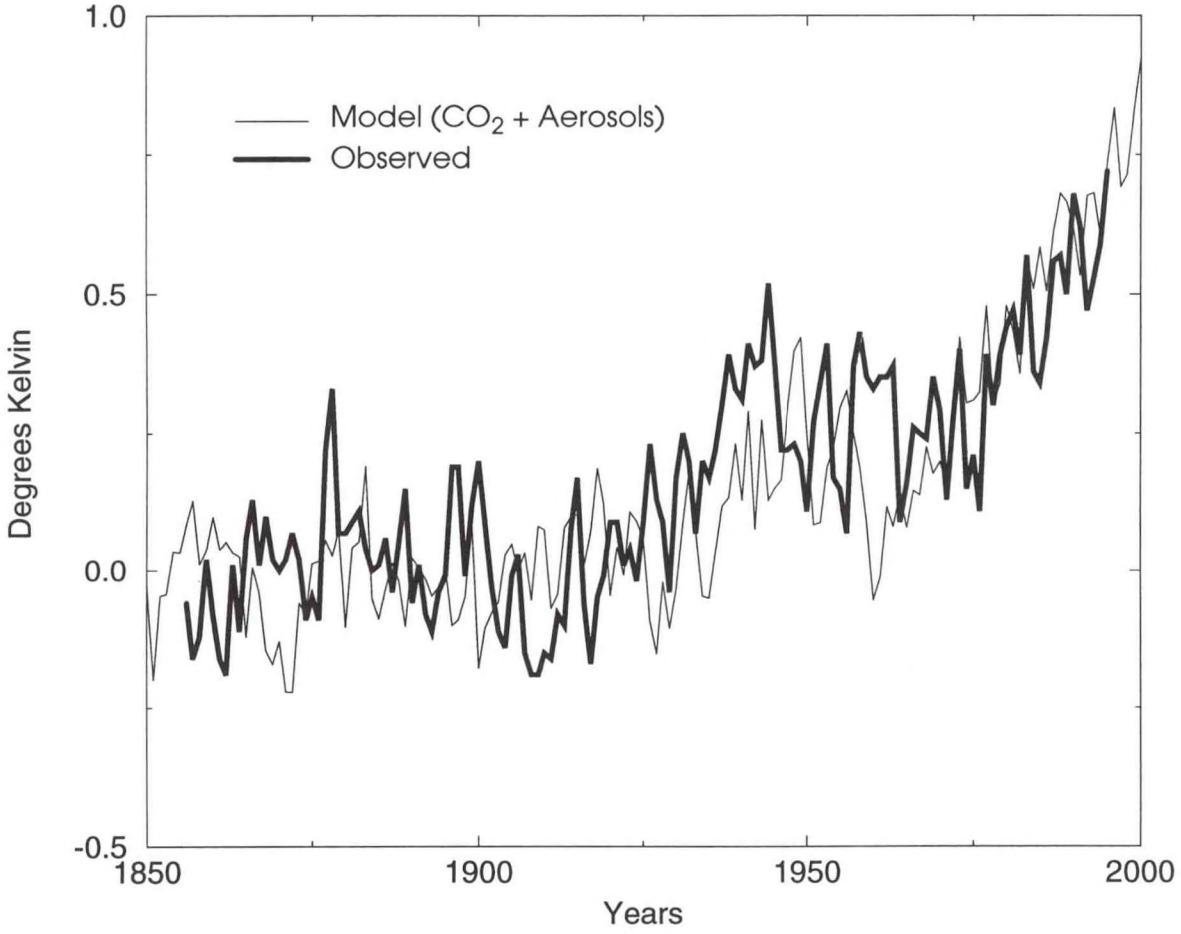

Fig. 1.1 Time series of globally averaged, annual mean surface air temperature anomalies (*i.e.*, deviations from 1880-1920 mean). Thick solid line: observed (Jones et al., 1996[2]). Thin solid line: simulated. The coupled model successfully simulates the observed warming trend.

2065 AD. For comparison, the time series of global mean surface air temperature anomaly compiled by Jones et al. (1996)[2] is added to the same figure. This figure indicates that the coupled model successfully simulates the observed warming trend of global mean surface air temperature during the last 100 years. The model also reproduces the observed variability of interannual to decadal time scales reasonably well (1201 and 1359).

The equilibrium response of the simplified coupled model (in which the oceanic GCM is replaced by a mixed layer ocean model) to the doubling of atmospheric CO_2 is 3.7°C, which lies in the upper half of the range of 1.5°C~4.5°C estimated by IPCC. Nevertheless, the successful simulation of the warming trend during the last century encourages one to speculate that the sensitivity of the coupled model may be realistic. Obviously, a more

2. Jones, P., et al., Personal communication. Data obtained from UEA Web Site (http://www.cru.uea.ac.uk/cru/press/pj9601/data.htm) in August 1996.

reliable determination of the thermal forcing of aerosols is required for a critical assessment of model sensitivity.

PLANS FY97

In order to investigate the oceanic uptake of atmospheric CO_2, the numerical experiment described above will be repeated, incorporating carbon chemistry and transport into the oceanic component of the model.

1.1.2 Tropical Storm Response to Increased CO_2

T. Knutson *S. Manabe*

ACTIVITIES FY96

The impact of increased CO_2 on tropical storm activity has been explored using the GFDL R30 resolution global climate model. The simulated tropical storms are much weaker and broader in horizontal extent than those observed, and do not display an "eye" region. However, they do depict several realistic features, including: pronounced cyclonic flow that decreases with height through the troposphere, weak anticyclonic outflow aloft; a pronounced mid-to-upper tropospheric warm core; and strong precipitation and rising motion near the storm center. The seasonal cycle of tropical storm days is fairly well simulated over the Northwest and Southwest Pacific basins and the North Indian Ocean, but the number of storm days is substantially under-simulated in other basins. The internally generated interannual variability of tropical storm days over the Northwest Pacific basin is smaller than the observed interannual variability in that region by about a factor of two.

A composite model tropical storm was constructed for both the control and high-CO_2 climates in order to explore features of the storm response to CO_2-induced warming. There is no evidence in the model of a substantial change in storm intensities with elevated CO_2 concentrations. For example, although precipitation in the composite storm region increased by 14%, the composite surface windspeed changed relatively little (+2-3%). A heat balance analysis indicates that changes in the model's vertical temperature structure allow the additional precipitation and atmospheric heating to occur without a substantial strengthening of the vertical velocities. Finally, an analysis of seasonal maps of maximum surface windspeeds in the model indicate relatively little CO_2-induced change in the domain of tropical storms, despite a large (factor of ~2) increase in the area of relatively warm (>28°C) SSTs.

PLANS FY97

Investigations of the response of the tropical storms in the global climate models will continue.

In collaboration with the Hurricane Dynamics group at GFDL, exploratory studies are planned using the GFDL Hurricane Prediction Model to address important questions regarding

CO_2-induced warming and tropical storms (7.3.3). The GFDL climate model simulations will be used as a source of boundary conditions for such experiments.

1.1.3 Cold Ocean-Warm Land Pattern

A.J. Broccoli M.J. Nath
N.-C. Lau

ACTIVITIES FY96

A method developed for analyzing observed variations in surface air temperature (Wallace et al., 1995)[3] was applied to a 1000-year integration of the GFDL coupled atmosphere-ocean model with constant forcing. The method identifies the spatial pattern in monthly mean surface air temperature anomaly whose amplitude has the largest correlation with the spatially-averaged temperature anomaly. When applied to surface air temperature anomalies from Northern Hemisphere land areas taken from the coupled model, the pattern that emerges has large positive coefficients over the high latitude interiors of North America and Eurasia and smaller negative coefficients in maritime regions and some low latitudes (Fig. 1.2, left). This implies that when the Northern Hemisphere is anomalously warm, the land areas poleward of 40°N are anomalously warm and the ocean is anomalously cold. An almost identical pattern was found in observed surface air temperature data by Wallace et al.[3] and dubbed the cold ocean-warm land (COWL) pattern (Fig 1.2, right).

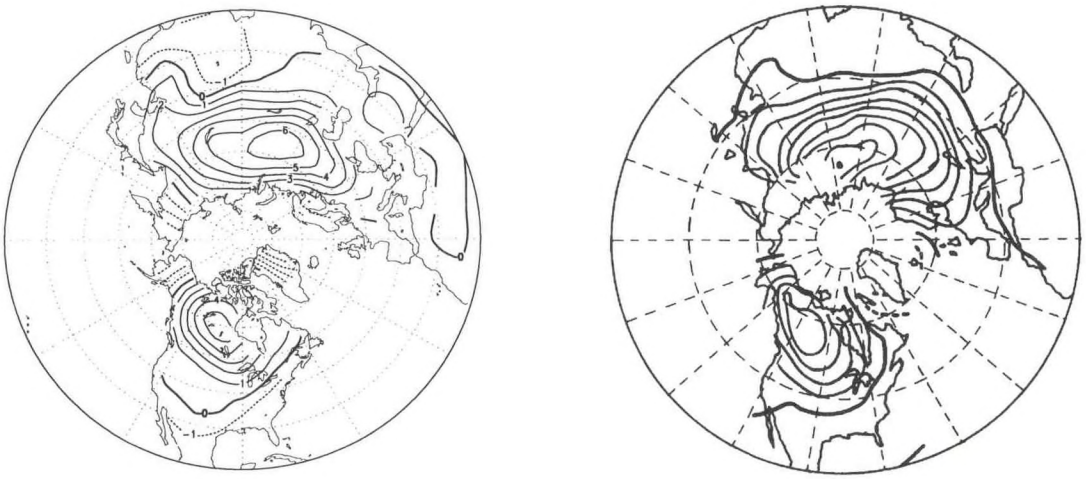

Fig. 1.2 Spatial pattern of surface air temperature anomaly deviation from spatial mean whose amplitude has the largest correlation with the spatially-averaged surface air temperature anomaly. Contour interval is 1 K per degree K, the zero contour is thickened, and negative contours are dashed. Left: 1000-year integration of coupled atmosphere-ocean model. Right: Observed data (from Wallace et al. 1995[3]). The pattern that appears in the coupled model integration is very similar to that which appears in the observed data.

3. Wallace, J.M., Y. Zhang, and J.A. Renwick, Dynamic Contributions to Hemispheric Mean Temperature Trends, *Science, 270(5237),* 780-783, 1995.

The time series of hemispheric mean temperature from the coupled model was decomposed into two components: the COWL pattern and a residual. Analysis of the power spectra of these components indicates that the fraction of variability associated with the COWL pattern is largest at high frequencies and decreases steadily as the time scale increases. At the one-year time scale, the COWL pattern accounts for ~33% of the variability, decreasing to ~21% at five years and ~16% at 10 years. Thus the residual contains most of the variability at time scales of several years and beyond.

To determine if this decomposition is useful for separating short-term variability from long-term climate trends, the same analysis was applied to a coupled model integration forced by the historical variations in greenhouse gas and tropospheric aerosol forcing. The COWL pattern that emerges from this analysis is almost indistinguishable from that of the constant forcing integration, and its amplitude shows no evidence of trend. Instead, virtually all of the trend in simulated Northern Hemisphere temperature was found in the residual. This supports the interpretation of the COWL pattern as a manifestation of high frequency climate variability induced by atmospheric dynamics.

Additional insight into the physical mechanism producing the COWL pattern was obtained by extending the analysis to two additional long climate model integrations that differ from the coupled model integration in their treatment of the ocean. In one of these, the atmospheric model is coupled to a simple mixed-layer ocean, while in the other the climatological spatial and seasonal distribution of sea surface temperature is prescribed. When subjected to the same analysis technique, both of these integrations yield COWL patterns that are virtually identical to that of the coupled model. This suggests that the primary function of the ocean in the existence of the COWL pattern is to provide thermal inertia. It strongly supports the interpretation of the COWL pattern as resulting from the difference in thermal inertia between land and sea, which allows larger variability of surface air temperature over land in response to intermonthly changes in atmospheric circulation.[3]

PLANS FY97

Investigation of this topic will continue by examining how the distributions of other climatic variables are related to the COWL pattern in the coupled model. The availability of a dynamically-consistent three-dimensional distribution of atmospheric quantities from the coupled model should allow an examination of variables that would be problematic using observed data. The impact of using other spatial domains for the analysis will also be explored.

1.1.4 Sea Surface Temperature Variability in the Greenland Sea

T. Delworth *R.J. Stouffer*
S. Manabe

ACTIVITIES FY96

Analysis of a multi-century integration of the coupled ocean-atmosphere model has revealed pronounced oscillations of ocean temperature and salinity in the Greenland Sea.

The oscillations, involving both the surface and subsurface layers, have a time scale of approximately 50-60 years, and are associated with fluctuations in the intensity of the East Greenland Current. The Greenland Sea temperature and salinity variations are preceded by large-scale changes in near-surface salinity in the Arctic, which appear to propagate out of the Arctic through the East Greenland Current. These anomalies then propagate around the subpolar gyre into the Labrador Sea and the central North Atlantic. This propagation pathway from the Arctic to the central North Atlantic can be seen in the darkly shaded regions of Fig. 1.3, which shows the spatial pattern of sea surface salinity (SSS) anomalies associated with the oscillations. The oscillations are coherent with previously identified (1182) multi-decadal fluctuations in the intensity of the North Atlantic thermohaline circulation.

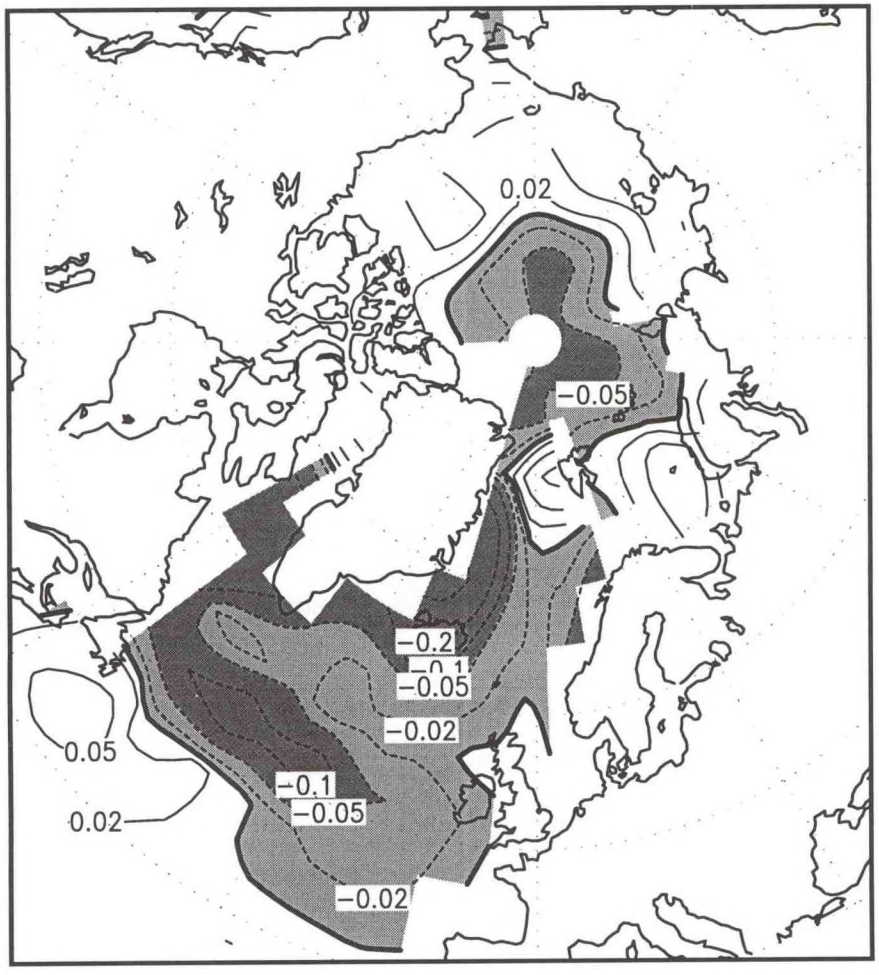

Fig. 1.3 The darker shading in this figure indicates the path of fresh water anomalies associated with the Greenland Sea SST oscillation. Anomalies move from the Arctic, through the Greenland and Labrador Seas, into the central North Atlantic. The values contoured are regressions of annual mean sea surface salinity (SSS) at each grid point versus the time series of annual mean SST in the model Denmark Strait (off the southeast coast of Greenland). The contoured values are the slopes of the regression lines multiplied by -2, and indicate the anomalous SSS conditions associated with an SST anomaly of -2°C. Values between 0 and -0.05 are lightly shaded, and values less than -0.05 are darkly shaded. Units are parts per thousand per -2°C SST anomaly.

These oscillations in SSS and SST are associated with atmospheric variations as well. Negative anomalies of surface air temperature are associated with cold SST anomalies in the Greenland Sea, with amplitudes up to 2°C near Greenland declining to several tenths of a degree C over northwestern Europe. The cold SST anomalies and intensified East Greenland Current are also associated with enhanced northerly winds over the Greenland Sea (db).

PLANS FY97

Further analyses will be conducted to investigate the mechanisms responsible for this large signature in the interdecadal variability in the coupled ocean-atmosphere model.

1.1.5 Decadal to Multi-decadal Variability of the Tropical Pacific

T. Knutson *S. Manabe*

ACTIVITIES FY96

Decadal averages of SST in the tropical and subtropical Pacific have been shown to exhibit substantial variability during the past century. A crucial question regarding these changes is what portion of this variability, if any, was due to external forcing such as increased greenhouse gases, and what portion was due to natural internal variability of the climate system. A 120-year simulation with a medium resolution (R30) version of the GFDL coupled ocean-atmosphere climate model shows promise as a tool for addressing these questions. The internally generated decadal to multi-decadal SST variability pattern from this model (Fig. 1.4b) bears a strong resemblance to the observed variability on this time scale (Fig. 1.4a). For both model and observation, the warm phase is comprised of a triangular-shaped warm region which extends in the eastern Pacific from about 35°S to the Gulf of Alaska, and in the east-west direction across the Pacific basin at low latitudes. This triangular warm anomaly pattern is flanked by cool regions in the subtropics and midlatitudes of both hemispheres. The amplitudes of the composite anomalies are comparable between the model and observations, although regional discrepancies can be seen.

The occurrence of a similar pattern of decadal to multi-decadal variability in the model and observations suggests that the model may be helpful in discriminating between natural variability and externally forced variations over the Pacific region. It may also be useful for examining possible mechanisms for the decadal to multi-decadal variability.

PLANS FY97

The investigation of decadal to multi-decadal variability in the model Pacific will continue and will include a comparison between the observed structure and that of the modeled climate response to increased greenhouse gases.

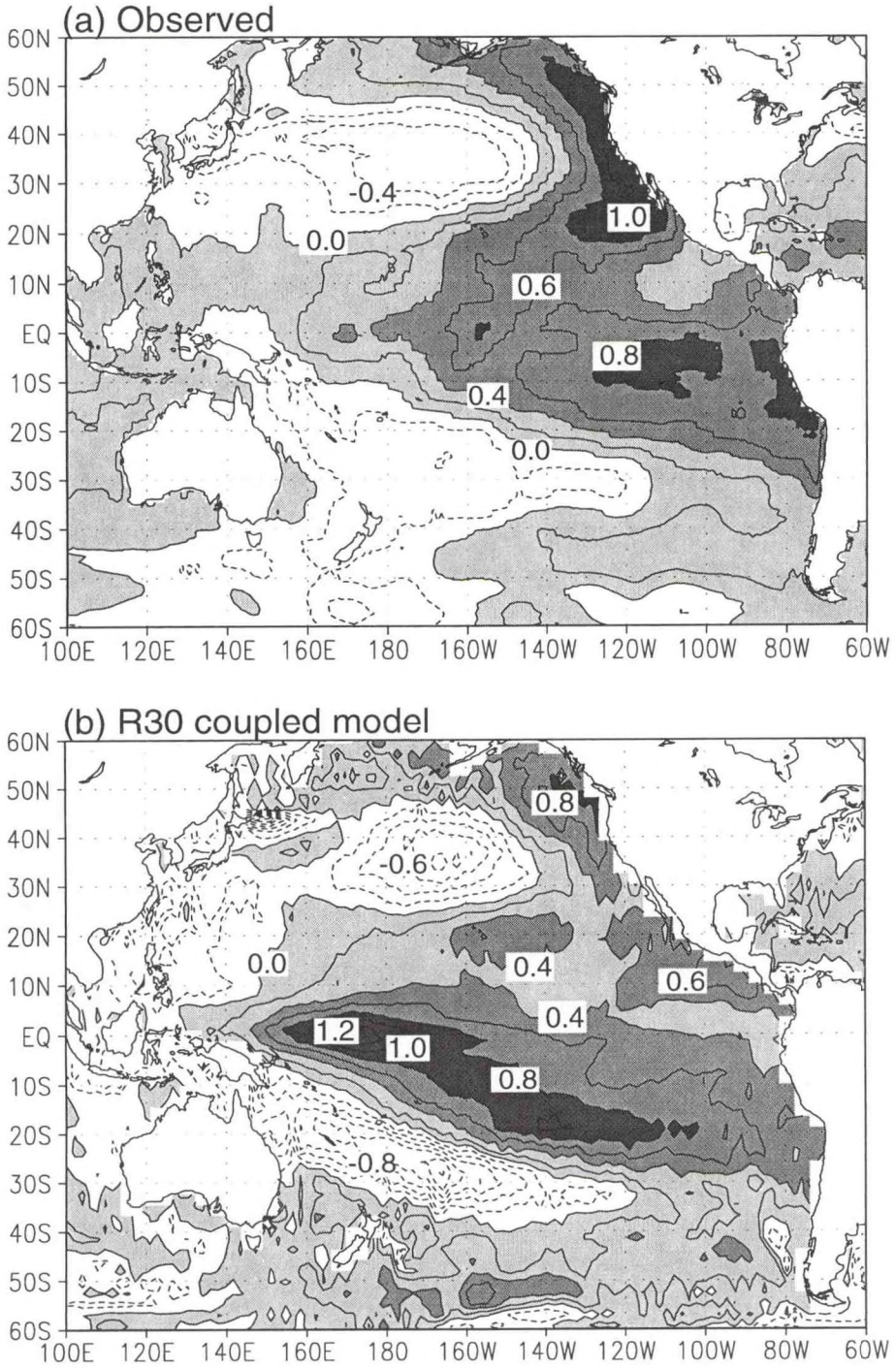

Fig. 1.4 Comparison of modeled and observed decadal to multi-decadal SST variability patterns for the Pacific region. Shown is the warm minus cold composite based on the first principal component of the time-filtered (>7 year) data. The observed composite (4 warm and 3 cold events) is from the Hadley Centre's GISST2 dataset (1903-1994). The model composite (5 warm and 6 cold events) is from a 120-year simulation using a GFDL R30 resolution coupled model. The contour interval is 0.2°C, with positive values shaded. The results show that the model-generated decadal to multi-decadal variability bears a strong resemblance to the observed variability on this time scale.

1.1.6 Coupled Model Development

T. Delworth *M.J. Spelman*
K. Dixon *R.J. Stouffer*
T. Knutson

ACTIVITIES FY96

A coupled ocean-atmosphere model with low resolution (the "LR" model; with grid size ~ 500 km, 9 atmospheric and 12 oceanic levels) has been used to study the natural and anthropogenic variations of climate (1201, 1192, 1359). However, the simulated climate of the LR model has some unrealistic features. During the last few years, a coupled ocean-atmosphere model with medium computational resolution (the "MR" model: grid size ~ 250 km, 14 atmospheric and 18 oceanic levels) has produced many encouraging results.

Our evaluation indicates that the MR model is superior in a number of ways to the LR model in simulating the coupled ocean-atmosphere system. Among the climate features that are better simulated by the MR model are the central Asian and North American arid regions in middle latitudes, the sharpness and intensity of the tropical rainbelt, the strong westerlies and thick cloudiness in the Circumpolar Ocean of the Southern Hemisphere, and precipitation and runoff at high latitudes.

Although the physical mechanism of the El Niño/Southern Oscillation (ENSO) as simulated by the LR model is quite realistic (aw), its amplitude is only ~40% of the observed. This shortcoming of the LR model has been improved substantially in the MR model. Fig. 1.5 indicates that the amplitude of ENSO produced by the MR model is much more realistic than that of the LR model. The performance of the MR model is quite surprising given that the resolution of the model in the tropics is much lower than that of most other models which are currently used for the ENSO prediction. One remaining deficiency in the MR model simulation, however, is the SST variability in the eastern part of the basin, which is smaller than observed. This deficiency is believed to be caused by remaining problems in the simulation of the mean climatology. Efforts are underway to overcome this difficulty through an improved flux adjustment technique.

In addition to the simulation of ENSO in the tropical Pacific, the MR model is substantially better at simulating the dominant mode of interdecadal variability in the North Pacific Ocean. Shown in Fig. 1.6 is the dominant mode of non-ENSO SST variability obtained from the LR and MR models, compared to the corresponding results from observations. The MR model bears a stronger resemblance to the observations than the LR model. In addition, this variability "stands out" from the background red noise spectrum to a much greater degree in the MR model than in the LR model, suggesting a more distinct physical phenomenon in the MR model. The improved simulation of climate variability by the MR model should provide a unique opportunity to explore not only the physical mechanisms of these phenomena, but also their sensitivity to long term climate changes such as global warming.

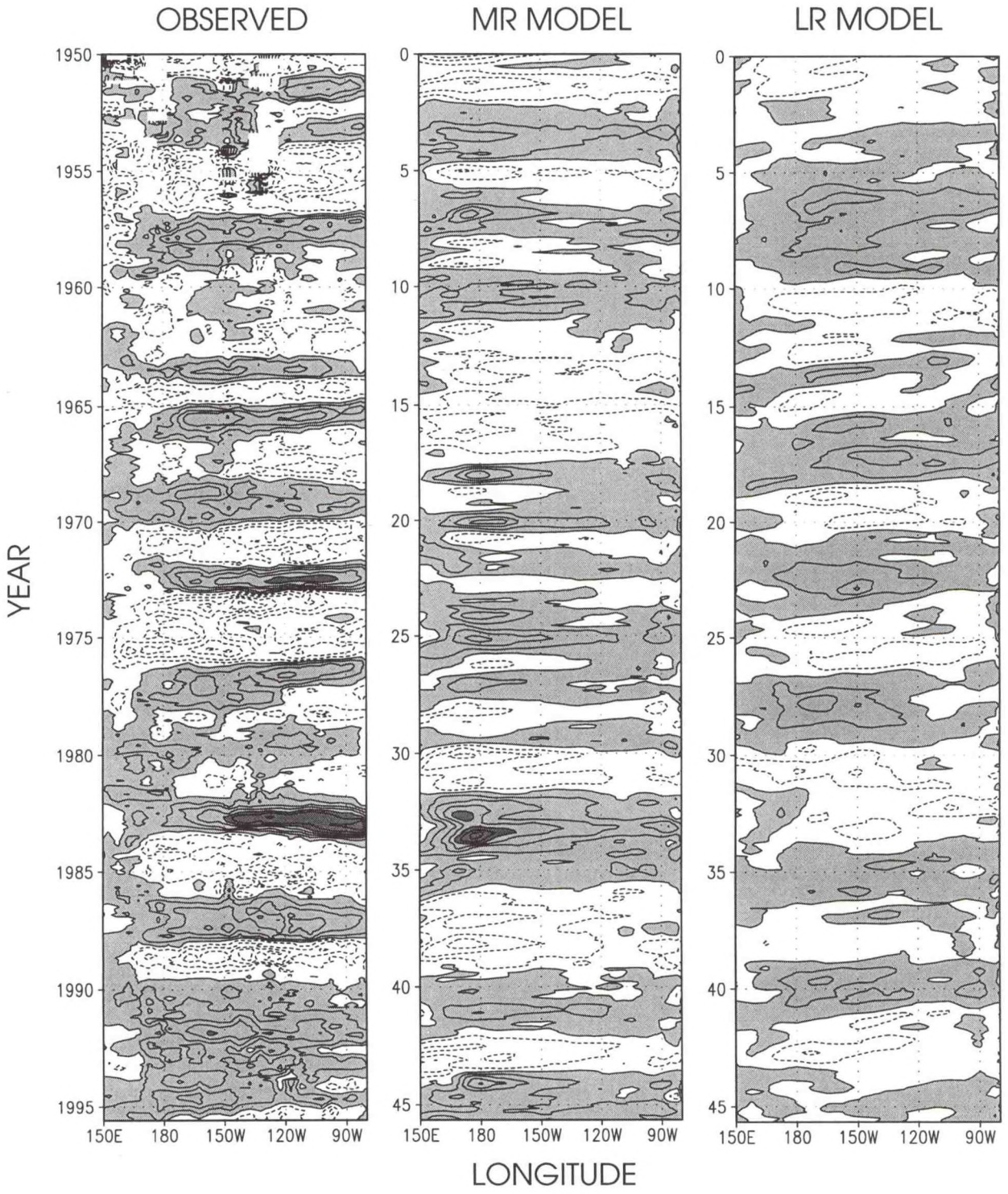

Fig. 1.5 SST anomalies along the equator from observations and from medium and low-resolution (MR=R30, LR=R15) versions of a GFDL coupled ocean-atmosphere GCM. The observations are from the Hadley Centre MOHS, ST6 dataset. The anomalies are 7-month running means, with the seasonal cycle removed, shown in a longitude vs. time format. The contour interval is 0.5°C with positive anomalies shaded. Note that the amplitude of the simulated El Niño events is more realistic in the higher resolution model.

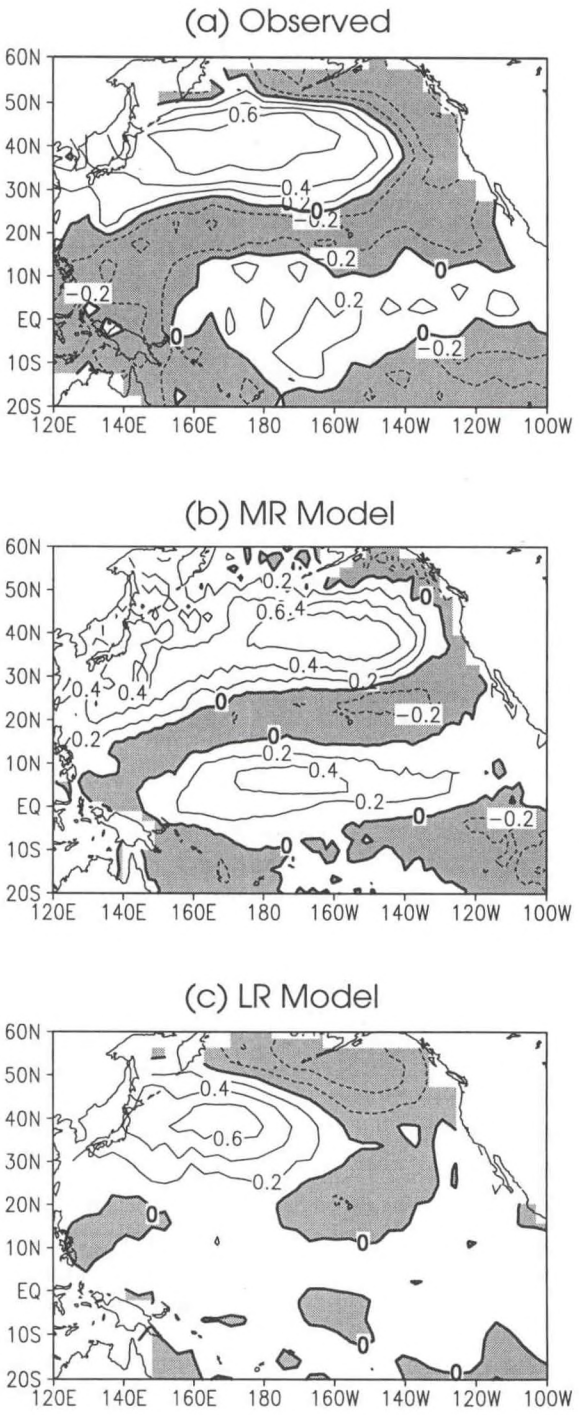

Fig. 1.6 The dominant spatial patterns of variability, extracted using an Empirical Orthogonal Function (EOF) analysis and winter mean values of SST over the Pacific. The patterns shown correspond to the second EOF over the domain, indicating a preferred pattern of variability (the first EOF is associated with ENSO). (a) Observational results using the period 1950-1991. (b) Results from the medium-resolution (MR) model. (c) Results from the low-resolution (LR) model.

A remaining shortcoming of the MR model is its tendency to drift away from a realistic initial condition over the period of several decades, despite the use of the so-called flux adjustment technique. This drift makes it very difficult to reliably interpret the results from a numerical experiment. By conducting a large number of trial integrations, it has been determined that one of the factors which affects the climate drift is the magnitude of the oceanic subgrid scale diffusion coefficients.

PLANS FY97

As soon as the drift of the MR model climate is reduced sufficiently, many sets of numerical experiments will be conducted in order to explore the physical mechanisms responsible for the natural and anthropogenic variations of climate.

1.2 CONTINENTAL HYDROLOGY AND CLIMATE

1.2.1 Modeled and Observed Runoff and River Discharge

1.2.1.1 Spectral Analysis of Modeled and Observed Runoff and Discharge

*K.A. Dunne** *R.T. Wetherald*
*P.C.D. Milly**

**U.S. Geological Survey*

ACTIVITIES FY96

Temporal variability of runoff and river discharge is being assessed using climate-model computed runoff and observed river discharges. Analyses are all based on areal averages over a set of geographic areas corresponding to several major gauged river basins of the world. The model runoff is from a 1000-year integration of the GFDL coupled atmosphere-ocean climate model (1201). Observations have been provided by national hydrological services and are typically of 50-100 years duration.

For most of the basins considered, the power spectra of modeled monthly runoff and precipitation are both nearly white, indicating little dependence of power on frequency. In some midlatitude basins, there is a slight reddening of runoff and precipitation spectra, with reduced variability appearing at annual and shorter time scales. In some high-latitude basins, the model transforms the white-noise precipitation to a blue-noise runoff; preliminary analysis suggests that this transformation is explained by snow storage and the snowmelt process.

Power spectra of observed river discharge, in contrast to those of model runoff, resemble spectra generated by a red-noise process, with characteristic time scales ranging from weeks to months. Spectra of corresponding precipitation are yet to be computed, but are believed to be much closer to white than are the discharges. It appears that the main difference between the spectral characteristics of the (white) model runoff and (red) observed discharge can be explained by the presence of significant storage in the river basins. Inferred basin residence times appear to be smallest in those high-latitude basins that

are known to be underlain by permafrost. This suggests that groundwater storage may be the dominant component of basin storage elsewhere.

PLANS FY97

A gridded monthly precipitation set will be obtained and aggregated over river basin areas to complement the existing model outputs and observational data. Relations between precipitation and runoff/discharge variability will be explored in more detail.

1.2.1.2 Trend Analysis of Observed River Discharge

*K.A. Dunne** *R.T. Wetherald*
*P.C.D. Milly**

** U.S. Geological Survey*

ACTIVITIES FY96

The time series of observed annual discharge from nine large (0.6-3.2x10^6 km^2) river basins of the middle and high latitudes were analyzed. Best-fit linear trends of annual discharge for the most recent 50 years of available record ranged from -30%/century (Amur River) to +49%/century (Mississippi RIver, Fig. 1.7). Various statistical evaluations of the significance of these trends were undertaken, including a method that uses climate-model

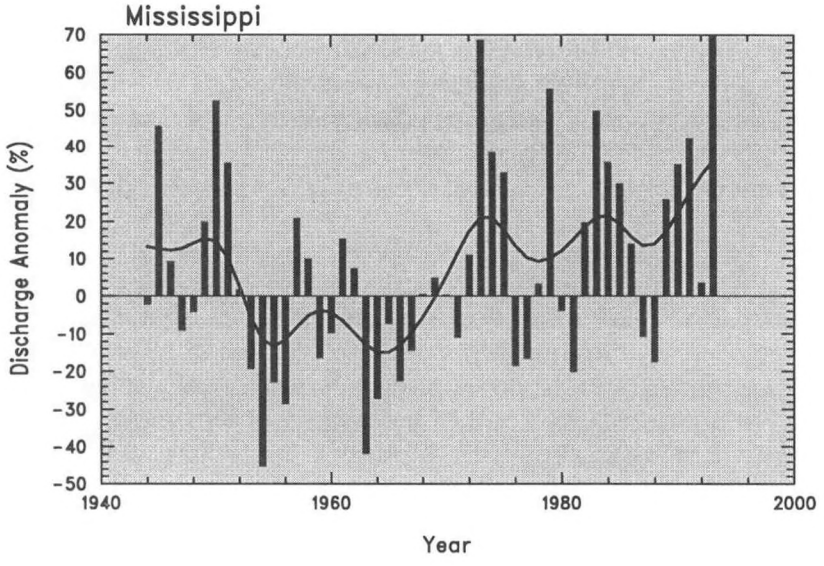

Fig. 1.7 Annual discharge anomaly of the Mississippi River, 1944-1993, as percent of mean discharge. Smooth curve obtained using a 21-point binomial filter. Fitted trend of unfiltered values (48%/century) is not significant at 95% level, according to linear-regression and Mann-Kendall statistics. This example illustrates the general result that even a large trend in river discharge is difficult to detect, given the high natural variability of discharge.

output to estimate the character of natural low-frequency variability. Generally, these analyses suggested that none of the noted trends was strongly significant in a statistical sense. This was a direct consequence of the high natural variability of annual river discharge and suggested that substantial changes may occur before such changes are formally judged to be statistically significant.

PLANS FY97

The river database will be extended in space and time, and the analyses of long-term trends will be repeated and refined.

1.2.2 Project for Intercomparison of Land-Surface Parameterization Schemes

K.A. Dunne P.C.D. Milly**

**U.S. Geological Survey*

ACTIVITIES FY96

The Project for Intercomparison of Land-Surface Parameterization Schemes (PILPS) is an international project with the objective of identifying the essential differences among the many parameterizations used to characterize water and energy exchange at land surface in GCMs. GFDL and USGS are participating mainly by assisting in experimental design and analysis.

PILPS Phase 1 used synthetic forcing to drive 16 land-surface schemes. Recent analysis identified two quantities that were strongly predictive of the water- and energy-flux partitioning by land-surface schemes, regardless of their internal dynamics and level of detail. The first is the efficiency of the soil evapotranspiration sink, integrated over the active soil water range. The second is the fraction of the active soil water range over which runoff is generated.

PILPS Phase 2(a) used one year of atmospheric, radiative, and turbulent-flux measurements from Cabauw in the Netherlands. Responses of 23 land-surface schemes to the observed forcing were computed and compared with observed flux data and with each other (bq). The most significant predictor of model output was found to be the inclusion or neglect of a term representing stomatal resistance to transpiration under conditions of negligible soil-water shortage. However, it was also shown that relations between soil-water storage and runoff differed widely across schemes. In an environment less humid than the study site, such differences would presumably have much greater impact on computed water and energy balances.

Non-water stressed stomatal resistance has been shown to be an important control of water and energy balances in PILPS Phases 1 and 2, both of which have used prescribed atmospheric and radiative forcing of stand-alone land-surface schemes. In stand-alone experiments, inclusion of such resistance reduces evaporation and increases runoff. A GCM

experiment has been run at GFDL to provide a basis for evaluating the importance of atmospheric feedbacks in modifying the sensitivities of land-surface balances to stomatal resistances. Preliminary analysis identifies several feedbacks of importance, including drying and warming of the atmospheric boundary layer (negative feedback), increase of surface net radiation (negative feedback), and reduction of precipitation (positive feedback).

PLANS FY97

Analyses of both stand-alone and GCM experiments will continue.

1.2.3 Temporal Variability of Soil Water Content

*P.C.D. Milly** *C.A. Schlosser*

**U.S. Geological Survey*

ACTIVITIES FY96

A stochastic model of land-surface water balance (1242) has been used to examine the temporal characteristics of depth-integrated soil water content. The model tracks the water-storage changes that result from alternating random precipitation episodes and intervening periods of constant evaporative potential. Precipitation is characterized as a series of independent, instantaneous pulses, with a Poisson arrival process and with storm precipitation depth exponentially distributed. Evaporation efficiency (ratio of actual to potential) is set equal to relative soil saturation, and runoff occurs only upon saturation. For a given set of parameters, the model can be run many times to obtain statistics describing the temporal variability of water storage. Initially, analyses have been carried out for the case where seasonality is absent and atmospheric feedbacks are negligible.

Several related measures of soil-water persistence have been computed for this model. These include i) the soil-water decay time scale identified in earlier studies at GFDL, ii) the expected length of time between sign changes of a soil-water anomaly, and iii) the expected length of time until an existing soil-water anomaly changes sign. Each of these time scales can be expressed in the form $N^{-1}f(R, W)$, in which N is the mean storm arrival rate, R is the evaporative index of dryness (ratio of annual evaporative demand to expected annual precipitation), and W is the ratio of soil-water storage capacity to the expected value of storm depth. This dependence is illustrated in Fig. 1.8 for the soil-water decay time scale; the other time scales exhibit similar behaviors. For sufficiently large W, with R greater than one, soil saturation and runoff almost never occur. In this case the decay time scale is that expected from the established evaporative-damping red-noise theory, and is independent of storm arrival rate. For sufficiently large W, with R less than one, the decay time scale is independent of storage capacity and, for a given R, directly proportional to the mean storm interarrival time, N^{-1}. In this case, soil is always near saturation. For very small R in this regime, almost every storm event saturates the soil, so the memory reflected in the decay time scale is only on the order of the mean storm interarrival time. However, as R is increased, the probability of a given storm saturating the soil decreases, and the memory of the system, as measured by the decay time scale, increases. Over many combinations of R and W of practical interest, the decay

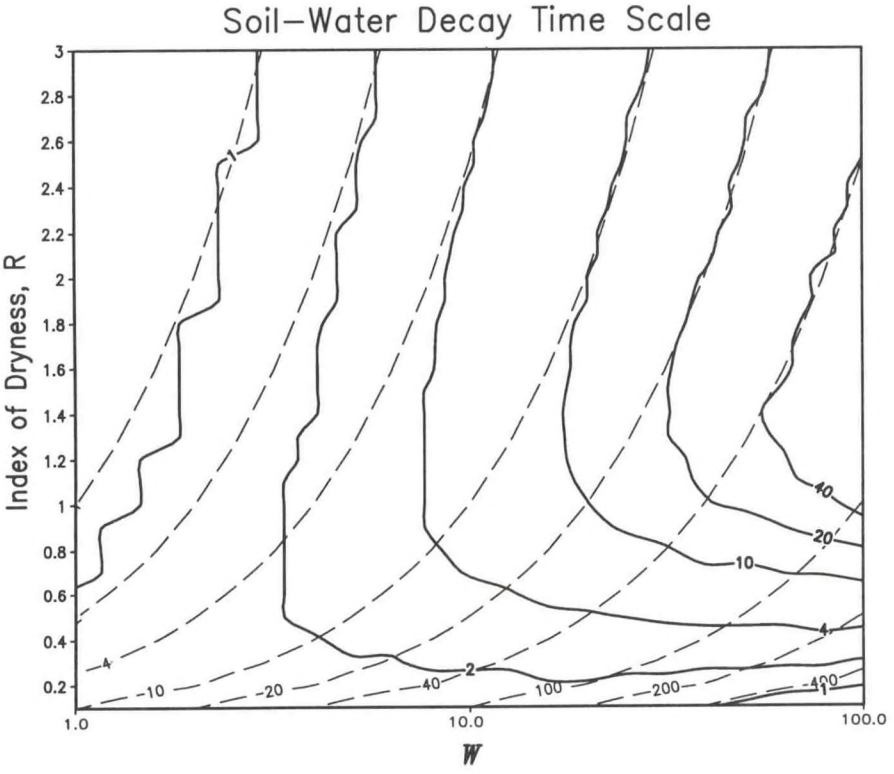

Fig. 1.8 Soil-water decay time scale (expressed as dimensionless multiple of mean storm interarrival time) as a function of dimensionless storage capacity *W* (ratio of soil-water storage capacity to mean storm depth) and index of dryness *R* (ratio of potential evaporation to mean precipitation.) Solid lines: Estimates from Monte-Carlo runs. Dashed lines: theoretical values for evaporative damping only. The figure indicates that soil-water anomalies tend to last longest in climates where precipitation and evaporative demand are nearly equal.

time scale is affected by both evaporative damping and runoff and is therefore smaller than would be predicted by consideration of either process alone.

PLANS FY97

The analysis of soil water persistence will be extended to include seasonality and atmospheric feedbacks, and the implications for soil-water predictability will be explored. A companion GCM study of soil-water predictability will be conducted, with potential application to evaluating seasonal climate predictability on the basis of soil-water initialization.

1.2.4 Mid-Continental Summer Dryness

S. Manabe *R.T. Wetherald*
R.J. Stouffer

ACTIVITIES FY96

A project exploring the hydrologic response of the R15 coupled ocean-atmosphere model to an increase of greenhouse gases and sulphate aerosols was initiated (1.1.1). The goal of this project is to determine how the inclusion of sulphate aerosols modifies the greenhouse-gas warming of the model atmosphere, with emphasis upon the midlatitude continental summer dryness obtained in previous studies (795, 1067). Two regions were selected for detailed analysis: (a) Central North America (CNA) and (b) Southern Europe (SEU). Both regions are defined according to the 1995 IPCC report.

An example of the above response is given in Fig. 1.9 which shows the decadal time series of the percentage differences of soil moisture averaged over the CNA and SEU regions during the summer season (June-July-August) for greenhouse gases and sulphate aerosols.

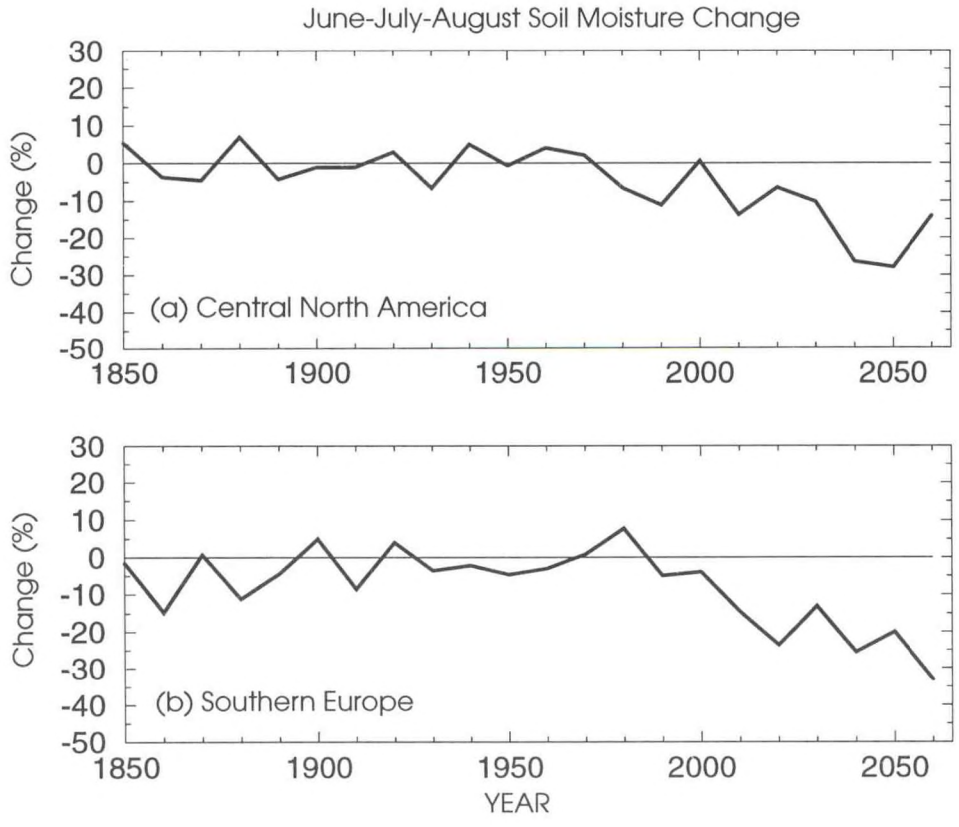

Fig. 1.9 Time series of percentage differences of area averaged soil moisture for June-July-August in the regions (a) Central North America (35°-50°N, 85°-105°W) and (b) Southern Europe (35°-50°N, 10°W-45°E). The time series consists of the percentage differences between the decadal means of soil moisture for the integration with greenhouse gases and sulfate aerosols, and the corresponding control run simulation averaged over the period of 1000 years. Units are in %. The inclusion of sulfate aerosols in the coupled model delays the effects of greenhouse warming on surface hydrology.

According to Fig. 1.9, a significant degree of summer dryness does not occur until approximately the year 2000 of the integration. These results indicate that the inclusion of sulphate aerosols in the coupled ocean-atmosphere model delays the effects of greenhouse warming on surface hydrology.

PLANS FY97

The above analysis will be expanded to include changes in other quantities, such as precipitation and river runoff.

1.3 PALEOCLIMATE

1.3.1 Tropical Cooling at Last Glacial Maximum

A.J. Broccoli

ACTIVITIES FY96

As part of the Paleoclimate Model Intercomparison Project (PMIP), a simulation of the climate of the last glacial maximum was conducted using an R30L20 version of the atmosphere-mixed layer ocean model. The forcing was provided by changing the orbital parameters to their values at 21,000 years before present, reducing sea level by 105 m, imposing continental ice sheets as reconstructed by a geophysical inverse calculation, and reducing atmospheric carbon dioxide by approximately 25%. The experimental design is thus very similar to previous experiments (707,769,1354), but with a number of significant improvements in the model, including an increase in both the horizontal and vertical resolution, the use of a heat flux adjustment to mimic the effects of ocean heat transport, and the incorporation of sea ice dynamics.

As in the previous experiments, the imposition of glacial forcing produces a substantial global cooling, with the greatest cooling in the Northern Hemisphere regions near the North American and Eurasian ice sheets. The low latitude (30°N-30°S) reduction of surface air temperature averages 2°C but varies in magnitude considerably, ranging from 1-6°C. Several mechanisms influence the distribution of tropical cooling. On the largest scale, the northern tropics cool more than the southern tropics due to the interhemispheric asymmetry in radiative forcing that results from the existence of expanded continental ice sheets in the Northern Hemisphere. There is more cooling over land than ocean, due to the combination of an elevation effect associated with the sea level lowering, negative radiative forcing that results from the replacement of ocean by land with higher albedo, and the requirement that sensible heating must compensate for a greater fraction of the radiatively-induced perturbation in the energy balance over land due to its lower moisture availability. The smallest cooling occurs over the subtropical oceans of the Southern Hemisphere, where an equatorward shift in the dry regions associated with the descending branch of the Hadley circulation produces an increase in upper tropospheric relative humidity and thus a smaller positive water vapor feedback.

Comparison of the model results with paleoclimatic reconstructions suggests that the magnitude of the simulated oceanic cooling in low latitudes is within the wide range of estimates from current techniques. Over the continents, the reconstructed cooling appears larger than that simulated by the model.

PLANS FY97

More detailed comparisons will be conducted between the simulated and reconstructed changes in climate using a wider array of paleoclimatic estimates. The analysis of the simulation of the last glacial maximum will also be extended beyond the tropics. Comparison of the GFDL model results with those of other research groups contributing to PMIP will be undertaken.

1.3.2 Abrupt Climate Change

S. Manabe *R.J. Stouffer*

ACTIVITIES FY96

The isotopic analysis of Greenland ice cores suggests that large and rapid changes of climate occurred frequently during the last glacial and post-glacial periods. For example, the isotopic ($\delta^{18}O$) temperature dropped very rapidly approximately 13,000 years ago, followed by the so-called Younger Dryas (Y-D) when the isotopic temperature was almost as low as the last glacial maximum. Faunal and palynological analysis indicate that, during the period of the Y-D cooling, surface temperature was very low not only over the northern North Atlantic but also over Western Europe. The cold Y-D period, which lasted several hundred years, ended abruptly as indicated by the records from Greenland ice cores.

This study explores the responses of the GFDL coupled ocean-atmosphere model to the discharge of freshwater into the North Atlantic Ocean. In the first numerical experiment in which freshwater is discharged into high North Atlantic latitudes over the period of 500 years, the thermohaline circulation (THC) in the Atlantic Ocean weakens, reducing surface air temperature over the northern North Atlantic and Greenland and, to a lesser degree, over the Arctic Ocean, the Scandinavian Peninsula, and the Circumpolar Ocean and the Antarctic Continent of the Southern Hemisphere (Fig. 1.10a). Upon the termination of the water discharge at the 500th year, the THC begins to intensify, regaining its original intensity in a few hundred years. With the exception of the Pacific sector of the Circumpolar Ocean of the Southern Hemisphere, where surface air temperature continues to decrease beyond the 500th year (see Fig. 1.10b), the climate of the northern North Atlantic and surrounding regions also resumes its original distribution. The evolution of the ocean-atmosphere system described above resembles the Younger Dryas (Y-D) event as inferred from the comprehensive analysis of ice cores and deep sea and lake sediments.

In the second experiment, in which the same amount of freshwater is discharged into the subtropical North Atlantic again over the period of 500 years, the THC and climate evolve in a manner qualitatively similar to the first experiment. The magnitude of the THC response,

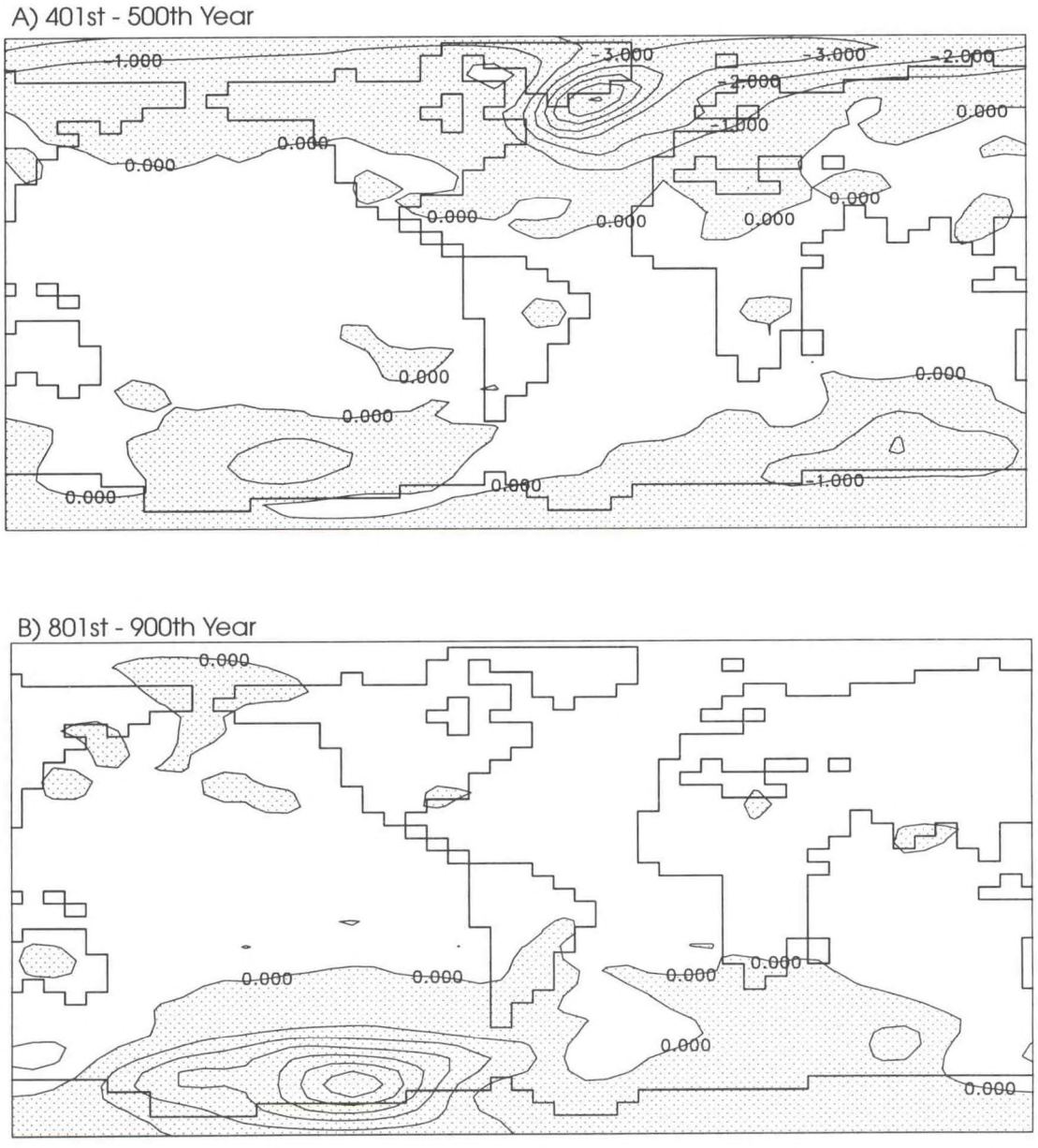

Fig. 1.10 The geographical distributions of surface air temperature anomalies (°C) from the first experiment in which freshwater is discharged into high North Atlantic latitudes (50°N-70°N). (a) 401st-500th year. (b) 801st-900th year. The evolution of the computed ocean-atmosphere system resembles the abrupt climate change of the Younger-Dryas event.

however, is 4-5 times smaller. In both experiments, the capping of oceanic surface by relatively fresh, low density water is responsible for reducing convective activity, and accordingly, weakening the THC. However, the freshwater discharge is particularly effective in doing so when it is applied to the sinking regions of the THC in the high North Atlantic latitudes.

PLANS FY97

The role of ocean circulation in cold glacial and warm Cretaceous climates will be the subject of continued investigation.

1.4 PLANETARY WAVE DYNAMICS

1.4.1 Baroclinic Instability, Geostrophic Turbulence, and Extratropical Dynamics

S. Chen
I. Held
P. Kushner
V. Larichev
P. Phillipps
K. Swanson
A.-M. Treguier

ACTIVITIES FY96

1.4.1.1 Baroclinic Eddy Flux Parameterization

Theoretical developments on the fundamentals of quasi-geostrophic turbulence generated by baroclinic instability (1337,1362,1369) have been described in earlier reports. Besides contributing to our fundamental understanding of atmospheric dynamics, these developments have implications for the problem of parameterizing the effects of mesoscale baroclinic eddies in ocean climate models, and some of these implications have been described earlier (bm). A key component of such a parameterization is the "eddy induced thickness flux", the net mass flux between isopycnal surfaces resulting from the presence of the eddies. In this paper, kinematic and dynamic constraints on possible diffusive theories for this flux are discussed, and the appropriate boundary conditions near the surface described.

An eddy-resolving two-layer quasi-geostrophic model of a mid-ocean subtropical gyre has also been constructed in order to provide a test-bed for eddy flux closures. The model produces strongly inhomogeneous eddy fields, and work is underway in comparing these eddy statistics with the predictions of theories based on homogeneous turbulence.

Multi-layer homogeneous turbulence simulations are also underway to study how the vertical stratification typical of the ocean affects turbulent fluxes in a homogeneous environment.

1.4.1.2 Barotropic Models of Midlatitude Storm Tracks

The understanding of the longitudinal structure of the midlatitude storm tracks is incomplete, one of the central issues being the relative importance of variations in low-level baroclinicity and the structure of the upper level flow. In particular, simple models of the effects of upper-tropospheric flow on storm track eddies are needed in order to improve the intuitive understanding of this part of the storm track problem. Several simple barotropic models have recently been analyzed (ce) that provide new insights into the modulation of the eddy field by zonal variations in the strength of the upper-tropospheric jet. The key to this work is the

approximate representation of the upper tropospheric potential vorticity field as consisting of a small number of regions of uniform potential vorticity. "Wave action" and "pseudo-energy" conservation laws then take on a simple form which can be used to predict how the eddy amplitudes will be modulated as they propagate through a zonally varying jet. Eddy energies are found to be smallest in the regions of the weakest jet, but the amplitude of the meridional particle trajectories, a good measure of the potential for nonlinearity, is maximized in these regions. Based on this linear theory, a semi-quantitative theory for the loss of wave action due to wave breaking in the jet-exit region was also developed and tested against nonlinear simulations using contour dynamics. This work should help provide the requisite background for a more satisfying understanding of storm track structure.

The surprising result that the frequency of the eddy field is lowered when breaking occurs in the jet-exit region was also discovered in these simulations, but remains to be explained. This result may provide a new perspective on the observed tendency for extratropical low frequency variability to be found in the jet exit regions.

1.4.1.3 Idealized Models of Baroclinic Wave Packets

Previous work at GFDL has highlighted the fact that large-scale eddies in midlatitudes are often organized into coherent wave packets. These packets move with a group velocity that is larger than the phase velocity of the individual cyclone waves, so that new disturbances are continually forming on the leading (easternmost) edge of the packet. These disturbances mature as they migrate westward with respect to the packet itself, eventually breaking or forming vortices and dissipating at the trailing edge. In work nearing completion, a quasi-geostrophic model of a baroclinically unstable jet has been used to generate very coherent packets. The life cycles of the eddies within the packet are analyzed by averaging eddy statistics after moving into the frame of reference moving with the packet itself. The pseudomomentum conservation equation then provides a particularly clean way of describing the eddy dynamics. The picture that emerges is one of nearly equivalent barotropic eddies that are energized by relatively small baroclinic production at the leading edge of the packet. The amount of pseudomomentum in the packet is determined by a balance between this small source and the barotropic decay at the trailing edge. By changing the meridional shape of the jet, one can manipulate the characteristics of the waveguide within which these waves propagate, increasing or decreasing the rate of wave breaking at the trailing edge, thereby changing the eddy amplitudes, even though the baroclinic source is hardly affected.

PLANS FY97

Work will continue on problems related to baroclinic equilibration, storm track dynamics, geostrophic turbulence, and eddy flux parameterization using a variety of idealized models.

1.4.2 Generation of Tropical Transient Waves

D.G. Golder *A. Numaguti*
Y. Hayashi

ACTIVITIES FY96

During FY95, control experiments were conducted (az) using an idealized general circulation model with moist convective adjustment to examine the effects of evaporation-wind feedback (EWF) and saturation-triggering (ST) mechanisms on the generation of tropical low- and high-frequency transient waves. The EWF mechanism hypothesizes that some transient waves coupled with moist convection are destabilized through interaction between low-level wind and the surface fluxes of latent and sensible heat. The ST mechanism hypothesizes that some transient waves are triggered by the intermittent onset of moist convection, upon saturation, to neutralize any pre-existing unstable stratification. It was concluded that simulated 40-50- and 25-30-day tropical intraseasonal oscillations (TIOs) were primarily generated through the EWF mechanism, while simulated superclusters as well as Kelvin, mixed Rossby-gravity, and gravity waves were primarily generated through the ST mechanism. These results were qualitatively consistent with quasi-linear EWF theory (ba) based on a simplified scheme of moist convective adjustment, except that the growth rate of the 25-30-day TIO mode was too weak to explain this mode by linear EWF instability.

During FY96, several nonlinear effects of evaporation and condensation on the EWF mechanism have been examined with the use of an idealized general circulation model. The model prescribes globally uniform distributions of sea-surface temperatures and insolation conditions. It also prescribes the zonal-mean component U of the zonal velocity in the parameterized surface fluxes of latent heat and sensible heat, while allowing the deviation from the zonal mean to fluctuate. It was concluded that the effect of positive-only condensational heating enhances the EWF instability of the 25-30-day TIO more effectively than the 40-50-day TIO. On the other hand, this effect suppresses the EWF instability of superclusters. Without this effect, the TIO periods become too long, consistent with linear EWF theory. It was also found that the dominant period of the TIOs shifts from 40-50 to 25-30 days through nonlinear effects of the EWF mechanism when prescribed easterly values of U are increased from -2 to -5 m/s. This shift may partly account for the interannual variation of observed TIO periods that depend on the ENSO-related variation of low-level winds.

To explain why eastward-moving superclusters consist of westward-moving cloud clusters, a high-resolution (one degree) two-dimensional (longitude-height) model of superclusters has been constructed (bk). This model incorporates moist convective adjustment and the beta effect (*i.e.*, the effect of the latitudinal gradient of the Coriolis force) that results in east-west asymmetry. It does not, however, include the basic zonal wind or the EWF mechanism. The model simulates the life cycle of cloud activity and demonstrates the importance of interactions between gravity waves and cloud activity. Moist convection, triggered upon saturation, first produces a low-level shallow cloud which develops into deep convection, becomes a top-heavy cloud, and finally decays. Deep- and shallow-mode gravity-wave packets are excited by the growth and decay of the cloud, propagating both eastward and westward with zonally asymmetric amplitudes and phases. The upper-level

cloud activity is coupled with the westward-moving shallow-mode gravity-wave packet and forms westward-moving cloud clusters. To the east of the original convection, on the other hand, a new convective cloud is triggered, upon saturation, only after the middle level is sufficiently moistened by the cooperative effects of the deep- and shallow-mode gravity-wave packets. The quasi-periodic emergence of the new convective cloud to the east of the original convection results in an eastward movement of the envelope of cloud clusters, forming an eastward-moving supercluster. Fig. 1.11 demonstrates that eastward-moving

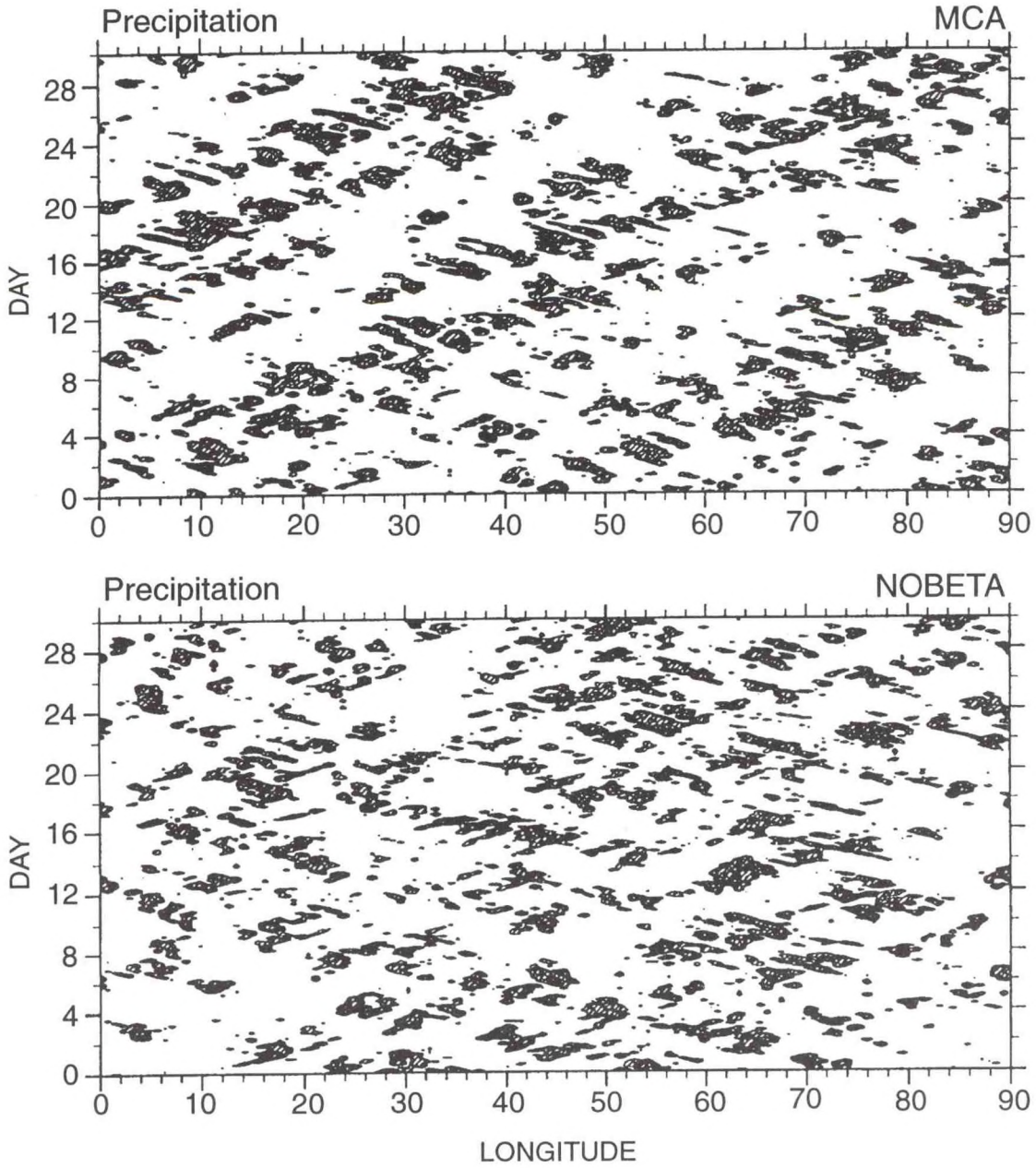

Fig. 1.11 Longitude-time distributions of precipitation for the two-dimensional supercluster models with (upper) and without (lower) the beta effect. Eastward-moving superclusters are well simulated in the model with the beta effect, but suppressed in the absence of this effect.

superclusters consisting of westward-moving cloud clusters are well simulated in the two-dimensional model with the beta effect (upper panel), while the superclusters are suppressed in the absence of this effect (lower panel).

PLANS FY97

With the use of the idealized model, further experiments will be conducted to examine the sensitivity of tropical transient waves to convective-adjustment time scale and parameterized re-evaporation. The relationship between the two- and three-dimensional superclusters will also be examined.

1.4.3 NOAA/University Joint Study of the Maintenance of Regional Climates and Low Frequency Variability in GCMs

I. Held *P. Phillipps*
N.-C. Lau *J. Zhang*
M.J. Nath *Q. Zhang*

ACTIVITIES FY96

A collaboration between GFDL, NOAA/Climate Diagnostic Center, MIT, the Universities of Washington, Chicago, and Illinois, and the Lamont Doherty Earth Observatory has continued its study of the interrelated problems of stationary waves, storm tracks, low-frequency variability, and the response of the atmosphere to perturbations in boundary forcing. The group has collaborated in designing experiments to be performed at GFDL. Further information about this project has been provided in the annual reports from previous years.

1.4.3.1 Effective Linear Operators

A recent development in atmospheric dynamics has been the construction of approximations to atmospheric models consisting of a linear operator forced by white noise. Both the operator and the covariance structure of the noise are obtained by attempting to fit the space-time covariance statistics of the full model with this linear, stochastic system. This is a new approach to using linear dynamics to analyze atmospheric variability. Here the linear operator being studied is not obtained by linearizing the equations of motion about some more or less arbitrarily chosen basic state, but rather from a statistical fitting procedure. The resulting operator is referred to as an "effective linear operator", or ELO.

The ELO corresponding to an idealized GCM with zonally symmetric climate has been constructed, using the one-day lag covariance statistics of the GCM. This operator can then be used as a Green's function for the computation of the response to various kinds of perturbations, such as tropical heating and the introduction of surface topography. This algorithm promises to provide a way of improving linear stationary wave theory. For example, there is no need to remove the singularity at critical latitudes that plagues standard linear stationary wave theory, and the effects of transient eddies on the response are automatically

taken into account. The structure of the ELO, its relationship to the operator obtained by linearizing about the time mean flow, and the accuracy of its predictions of the response to stationary forcing are all under investigation.

1.4.3.2 Midwinter Suppression of the Pacific Storm Track

The seasonal cycle of the North Pacific storm track has become the focus of considerable interest because of its counter-intuitive behavior: while the maximum strength of the north-south temperature gradient occurs in January, maximum energy levels occur in November and March. Therefore, one cannot understand this seasonal cycle in terms of a theory in which the strength of the storm track is simply a function of the local baroclinicity. This and related problems are being addressed from several perspectives.

A study of interannual variability, using the R30 model results, has demonstrated that those individual Januarys with stronger jet streams in the Pacific sector also tend to have weaker storm tracks. Therefore, this anomalous relationship between jet strength and storm track intensity holds not only for the seasonal cycle, but for interannual variability as well. This result seems to rule out one possible explanation for this relationship -- that the colder sea-surface temperatures in mid-winter result in less latent heat release which, in turn, results in weaker eddies. In the GCM, the sea-surface temperatures are prescribed, with no interannual variability.

A series of R30 GCM integrations have been performed with insolation and surface boundary conditions taken in turn from the individual months October, November, December, January, February, and March. The results show a very clearly defined mid-winter minimum in the Pacific storm track once again, which is even more prominent than in the seasonal model. These perpetual-insolation integrations will therefore provide an excellent laboratory for studying the dynamics of this phenomenon.

A linear stochastic model has been constructed to attempt to simulate this phenomenon. The underlying linear operator is obtained by linearizing about the model's time mean flow in an individual month. This model can be tuned to provide an accurate simulation of the January storm tracks, including the relative strength of the Atlantic and Pacific variance maxima, but is not capable of simulating the details of the seasonal cycle of the storm tracks, including the mid-winter suppression in the Pacific.

1.4.3.3 Statistical Analysis of Low-Frequency Variability

A new modification to EOF analysis has been developed which is optimized for the description of oscillatory phenomena. This technique takes as its starting point the procedure of statistically fitting the time evolution of the data with a linear model, but in contrast to POP (Principal Oscillation Pattern) analysis, the time derivative in the statistical model uses centered, rather than forward, differencing.

1.4.3.4 Idealized GCM Integrations

The generation of a series of GCM integrations with idealized boundary conditions has continued, using the 14-level R30 model and a dry model with various resolutions. These integrations include a series of runs with zonally symmetric boundary conditions designed to study the response of the midlatitude storm track to changes in the mean temperature and the north-south temperature gradient, and a series of integrations focusing on the extratropical response to sea surface temperature anomalies.

PLANS FY97

Work will continue on both idealized and realistic GCMs, in collaboration with several university scientists. In collaboration with the Experimental Prediction Group, new higher resolution (R30 or T42) integrations will be performed to replace the R15 "GOGA" ensemble of integrations in which the atmospheric model is run for 40 years with observed sea surface temperatures. Integrations with similar or higher resolution idealized models will continue to focus on storm track, stationary wave, and midlatitude SST interactions.

The application of this method to the study of tropical intraseasonal variability in a GCM, and an analysis of its relationship to other methods -- POPs, canonical correlation analysis, and rotated EOFs, will be described in a paper in preparation.

1.5 PLANETARY ATMOSPHERES

G.P. Williams

ACTIVITIES FY96

The Jovian atmospheres may have close dynamical ties with Earth's atmosphere and oceans, exhibiting conventional meteorological and oceanographic processes such as jets, eddies, and vortices. Although Jupiter seems to behave like a larger, faster-spinning Earth, significant differences occur because of its unbounded vertical structure. To improve the definition and understanding of the circulation, 3-D primitive equation models are used to examine the role of structure in forming the various turbulent and coherent phenomena.

The main problem in defining Jupiter's meteorology is that the nature and extent of the atmosphere and its motions are not generally known for the region below the clouds. The main hypothesis involved - that the atmospheric circulation is relatively thin and driven by baroclinicity - has been examined with a wide range of meteorological models over the years. The present study extends these models by considering the influence of vertical structure more specifically and experimentally.

To understand and define Jupiter's circulation requires that fundamental questions concerning the stability and genesis of vortices and jets be addressed. In particular, it must be determined: 1) why vortices exist and why they last so much longer on Jupiter than in Earth's

oceans; 2) what processes generate the various single and multiple vortex states seen in the various anticyclonic zones; 3) how the various jets are generated in low and midlatitudes for unbounded atmospheres in a way that is consistent with vortex stability and genesis; 4) what causes the onset of the equatorial super-rotation in such a multi jet-vortex system. Answers to these questions have been found that are mutually consistent, and define the vertical structure of the motions, while showing how the multiple jets and vortex sets are generated.

The nature of the Jovian problem was radically altered on December 7, 1995 when the "Galileo" space probe entered the Jovian atmosphere and provided, for the first time in history, data on the vertical structure of the circulation down to 100 km below the tropopause at a latitude of 6.5°N. The general qualitative nature of the winds ("fairly constant", "increasing with depth") was described in EOS on January 30, 1996 and was immediately incorporated into vortex calculations (1400). The actual qualitative details of the winds (Fig. 1.12) were released in Science on May 10, 1996 and immediately incorporated into

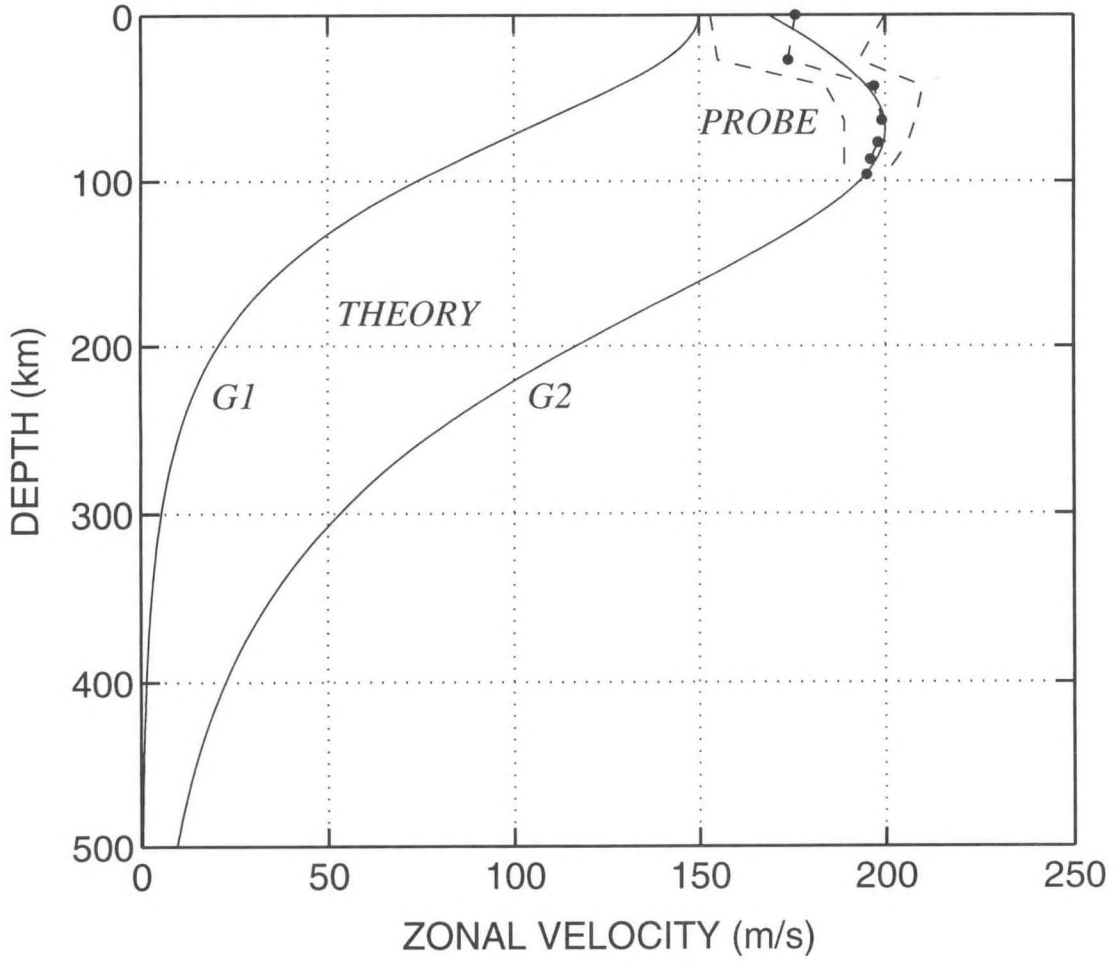

Fig. 1.12 The vertical profiles of the zonal wind compare the flow observed by the "Galileo" spacecraft probe (solid dots) with the theoretical generic (G1) and Galilean (G2) structures used in the vortex solutions. Long-lived vortices resembling the Great Red Spot can be generated by jets matching the probe data provided they have the G2 form. This implies that Jupiter's circulation extends to a depth of 500 km, but only if the probe data is globally representative.

additional vortex calculations (bi). This rapid assimilation of revolutionary data into existing models was possible because the appropriate generic structures had been derived beforehand in an extensive fundamental study. Their inclusion into existing manuscripts and rapid publication were made possible by timing this submission carefully.

1.5.1 Vortex Stability, Structure, and Genesis

Planetary vortices occur in Earth's oceans near the Gulf Stream and in Jupiter's atmosphere in the anticyclonic jet zones where they last for decades or centuries depending on their size. This longevity is reproduced by calculations with a primitive equation model that isolates the parameters and structures for which vortices last indefinitely (1400). Calculations over a wide range of conditions reveal that generic vortex stability depends primarily on the thickness of the active layer relative to the abyss ($\delta = h/H$), and on the size of the storm relative to the Rossby deformation scale. In particular, large anticyclones with a large thickness ratio of $\delta \sim 1/5$ are quasi-stable in that they remain coherent but tend to migrate toward the equator where they disperse rapidly. Thinner vortices with $\delta \sim 1/10$ migrate more slowly and can be made conditionally stable by the blocking action of weak easterly jets. Even thinner vortices with $\delta \sim 1/20$ are absolutely stable, remaining coherent indefinitely and not migrating at all, just propagating steadily westward.

When zonal currents are confined to thin atmospheres with $\delta \leq 1/20$, the easterly jets develop baroclinic instabilities that take on the form of solitary waves rather than the usual periodic waves seen in thick atmospheres with $\delta \geq 1/5$. The solitary waves grow into vortices that exhibit a variety of configurations and evolutionary paths. Most cases result, after a series of mergers, in a single vortex state or a state that can also arise at the start and persist thereafter. SIngle vortex states resembling all phases of the Great Red Spot, with sizes ranging from 15° to 50° in longitude and with velocities in the observed range, can be generated either directly or by mergers.

1.5.2 The "Galileo" Probe and Jupiter's Vertical Structure

Observations of the vertical structure of Jupiter's circulation are limited to those made near the equator by the "Galileo" probe. Theoretically, however, planetary vortices exist so selectively for special generic structures that they can be used to probe the Jovian atmospheres in other regions. The Galileo data is seriously limited in that it samples only the outer 1/700th of the envelope and is taken from a complex transitional zone between the equatorial and tropical regimes that may differ completely from the regimes where the major vortices lie. Nevertheless, a study of vortex genesis with the primitive equation model that compares the generic and Galilean structures shown in Fig. 1.12 leads to realistic simulations of the Great Red Spot in both cases while indicating that Jupiter's winds extend to a depth of about 500 km at most. The three-dimensional form of planetary vortices like the Great Red Spot, as given by the isothermal surface in Fig. 1.13, shows that it consists of an asymmetric keel-shaped basin connected near the tropopause to the warm easterly jet from which it arose.

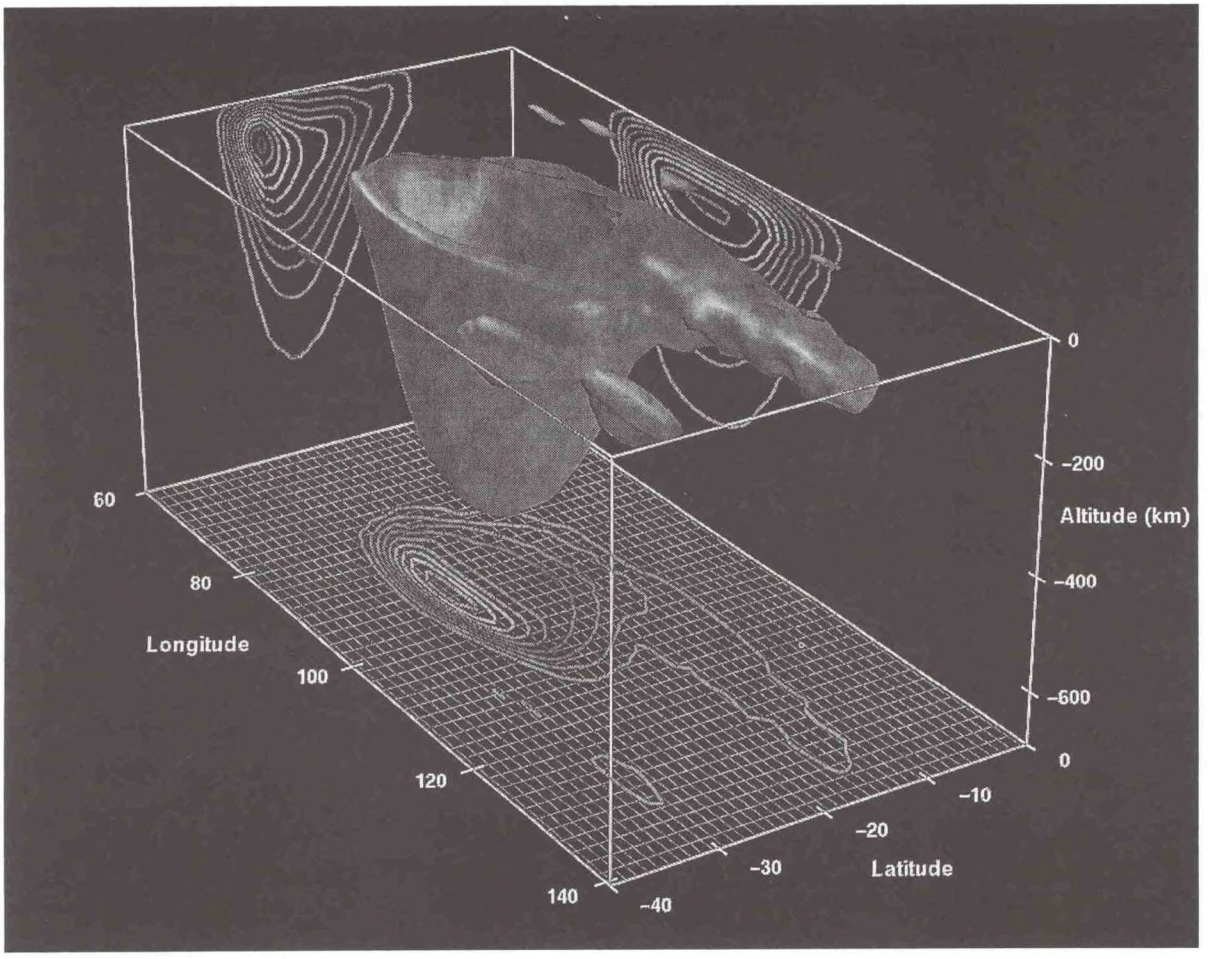

Fig. 1.13 The three-dimensional temperature structure of a generic vortex resembling the Great Red Spot is defined by an isothermal surface and by sections taken through the vortex center and top and projected onto the boundaries. The keel-shaped vortex extends to a depth of 500 km and remains self-contained except for a residual connection near the tropopause to the warm easterly jet from which it arose.

1.5.3 Stability and Genesis of Multiple Jets and Vortex Sets

Calculations with the primitive equation model subject to heating functions appropriate to Jupiter's atmosphere produce different types of jet streams in midlatitudes, low latitudes, and at the equator. All currents, however, are driven by baroclinicity acting over a thin layer. Some of these jets generate sets of vortices in different anticyclonic zones with the same scales as the Great Red Spot, the Large Ovals, the Small Ovals, etc., becoming smaller with increasing latitude. Evolutionary paths are more complex in heated systems when vortex regeneration becomes a factor. New vortex forms resembling terrestrial blocking phenomena are generated at 30° latitude.

1.5.4 Model Development

Isolating the Jovian parameters and structures and simulating the global circulation is difficult because observations are limited and the dynamical processes are highly nonlinear. Consequently, many calculations are needed to solve any problem definitively but are expedited by GFDL's highly interactive computing system and by the form of the model and analyses programs. These programs are constantly being modified to improve accuracy, efficiency and content.

PLANS FY97

Further calculations will be made to produce global circulations that achieve a fuller synthesis of the various jets and vortex sets. Additional study of the processes underlying the genesis of the different jets and vortices will also be carried out. The full implications of the Galileo data will be assessed. The primitive equation models and analysis programs will be further developed, as needed, to extend and refine the understanding and simulation of circulations in vertically confined atmospheres, as well as explore their terrestrial connection.

2. RADIATION AND CLOUDS

GOALS

To investigate the characteristics of convection-cloud-radiative interactions on a variety of space and time scales, leading to the understanding of their role in weather, climate and climate change.

To use satellite and other meteorological observations for diagnostic analyses of climate processes, and for evaluating and improving physical parameterizations employed in general circulation models.

To study fundamental aspects of atmospheric radiative transfer, and to investigate the climatic effects of natural and anthropogenic radiatively-active trace gases and aerosols.

ACTIVITIES FY96

2.1 SOLAR SPECTRUM

S.M. Freidenreich J. Li
J.M. Haywood V. Ramaswamy

2.1.1 Multiple-scattering Approximation

The formulation of, and analysis of results from the new four-stream spherical harmonic expansion approximation have been completed (1364). Additionally, as reported in A95/ P96, the new formulation has been combined with the GFDL line-by-line (LBL) algorithm to study the absorption and reflection in inhomogeneous clouds (ao). A comparison of the ratio of the computed visible-to-near-infrared reflectances with observations does not indicate any "anomalous" absorption of solar radiation by vertically inhomogeneous clouds. Using the LBL algorithm, a prescription for estimating the solar spectral irradiance at low cloudtops in a general manner has been obtained (ay).

2.1.2 Benchmark Computations

A computational error was uncovered in the assignment of the gas optical depths for the solar LBL calculations, with values corresponding to frequencies within 0.1 cm^{-1} of a line center being mostly underestimated. This led to an underestimate in absorption when the spectral lines become extremely narrow, especially in the upper stratosphere. The problem has now been rectified. The correction results in an increase in the estimates of the solar heating rates, with the difference increasing with height in the stratosphere ($P < 100$ mb). The correction has a negligible impact on the tropospheric heating rates, and on the atmospheric absorbed flux in clear atmospheres. The gas most affected by this error is CO_2. Previously derived benchmark results for both cloud absorbed flux and boundary fluxes in overcast atmospheres were found to be negligible.

Additional line-by-line + doubling-and-adding (LBL + DA) calculations across the entire solar spectrum have been performed for clear-sky with aerosol scattering and more computationally intensive cases, *e.g.*, overcast sky with molecular scattering. Clear-sky computations performed for three different atmospheric profiles reveal that the upward flux at the top of the atmosphere varies by only a small amount (3%) between the moist tropical and the dry sub-arctic winter profiles. These benchmark results will permit an accurate assessment of the biases in solar parameterizations which purport to treat both the absorption and scattering processes.

Fourteen groups have participated in a comprehensive intercomparison project involving column calculations of the direct radiative forcing due to sulfate aerosols. Comparisons have been completed for different aerosol size distributions, surface reflectances, and solar zenith angles. While many of the groups have used approximate methods for calculating the radiative forcing, the 16-stream LBL + DA calculations performed at GFDL provide an appropriate "benchmark" against which results from other groups may be compared. The calculations include radiative forcing at 0.55 microns, as well as over the entire solar spectrum. An example of the results provided for the intercomparison is shown in Fig. 2.1 which plots normalized radiative forcing in this benchmark with analogous results from the radiation code within the Hadley Centre GCM. From this, it is concluded that GCM radiation codes have to pay attention to capturing the sensitivity of the forcing with respect to solar zenith angle.

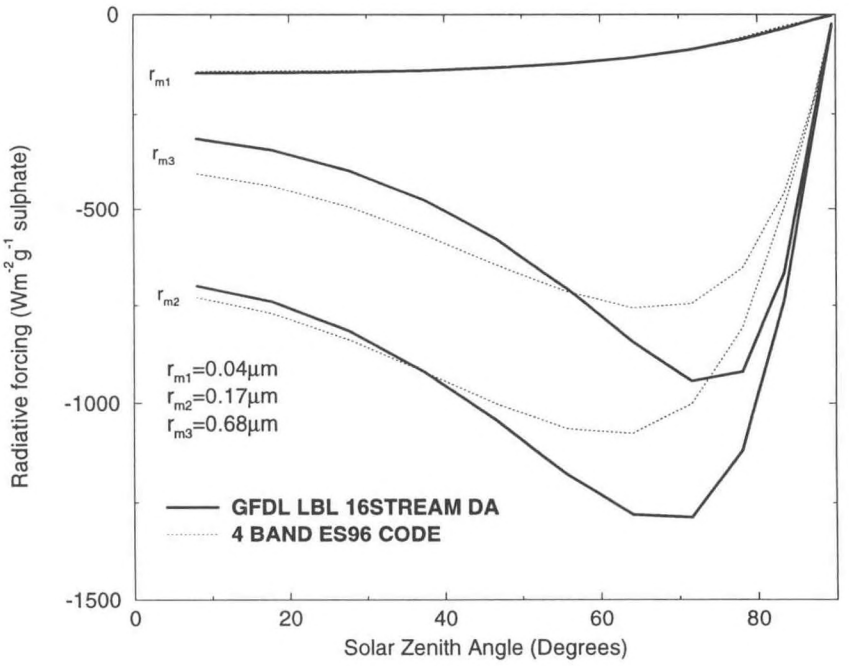

Fig 2.1 The normalized radiative forcing for sulfate aerosol as a function of solar zenith angle for a surface reflectance of 0.15 using the 16-stream GFDL LBL + DA code. The radiative forcing determined using the 4 spectral bands within the Hadley Centre GCM (ES96) is also shown for comparison purposes. Three different mode radii (r_m) of the aerosol distributions are considered. Note the differences of approximately 20% in the forcing by the Hadley Centre radiative GCM radiation code.

2.1.3 Parameterizations

The previously described multi-band parameterization (A95/P96) was modified to correct for the underestimate in the stratospheric heating uncovered in the reference results (2.1.2). To capture the increased stratospheric H_2O heating, additional terms were added to the previously derived exponential-sum fit, thus increasing slightly the total number of terms in the parameterization. In order to accurately simulate the increased CO_2 and O_2 (visible and near-infrared) stratospheric heating, a different functional dependence of gas transmission on absorber amount was devised. This yields an acceptable accuracy when compared with the reference heating profiles for these gases. With these modifications, the error in the total stratospheric heating due to the parameterization when all gases are present is found to be $< 5\%$, which is a considerable improvement over the previous formulation employed.

The broadband parameterizations for CO_2 and H_2O (A95/P96) were reformulated to account for the additional stratospheric heating (2.1.2). For H_2O, 4 additional terms were added to the modified Lacis-Hansen parameterization. For CO_2, a new parameterization was developed (combination of Sasamori-type expressions for the stratosphere and troposphere separately). Also, a broadband (visible+near infrared) parameterization was developed for O_2. The error in the individual heating rate for each gas from these parameterizations is generally $< 20\%$.

2.1.4 Solar H_2O and CO_2 Effects in the Stratosphere

Experiments examining the effect of improved broadband parameterizations on stratospheric temperatures computed with the fixed-dynamical heating (FDH) model (A95/P96) were repeated using the reformulated CO_2 and H_2O parameterizations. The heating due to CO_2 in the middle and upper stratosphere is substantially greater than previously determined, with the values increasing with height. The corresponding FDH results yield an increase in the middle and upper stratospheric temperatures. In the tropics, at 45 km, the difference with respect to the earlier formulation is ~2 K. In the tropical lower stratosphere, the increase due to the new $CO_2 + H_2O$ parameterization is also ~2 K.

2.1.5 Improvements to SKYHI GCM

The new multi-band shortwave parameterization has been incorporated in SKYHI, and experiments have been run to determine the changes in radiative quantities compared to results using the old shortwave parameterization. Fig. 2.2 shows the change in the heating due to the new parameterization for July 1 clear-sky conditions. Heating increases are due mostly to CO_2 and range from a few tenths to greater than 1 K in the polar summer upper stratosphere.

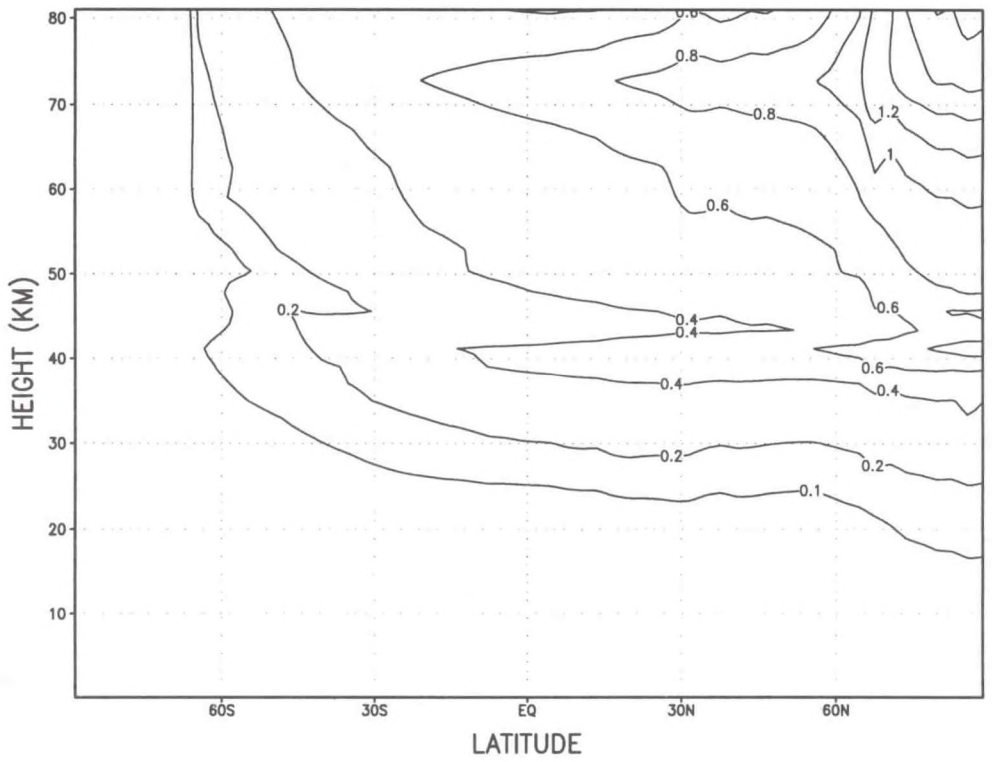

Fig. 2.2 Difference in the zonal-mean vertical profile of the solar heating rate (K d^{-1}) between the new and the old parameterizations in SKYHI GCM for July 1 conditions. Note the substantial increase in the middle and upper stratosphere.

The surface albedo specifications in the SKYHI GCM have been updated. Over oceanic regions, a zenith angle-dependent formulation developed by P. Hignett and colleagues (personal communication) based on aircraft measurements has been incorporated. Over land regions, the values have been adopted from the GFDL Climate GCM. Fig. 2.3 shows the resulting change in the outgoing reflected solar flux at the top of the atmosphere for July 1 conditions. Most notable is the increase over the Sahara region with values > 50 W/m^2 noted. This helps correct a substantial underestimate in the outgoing flux noted there in a comparison of the earlier model results (using the older albedo specification) with ERBE observations.

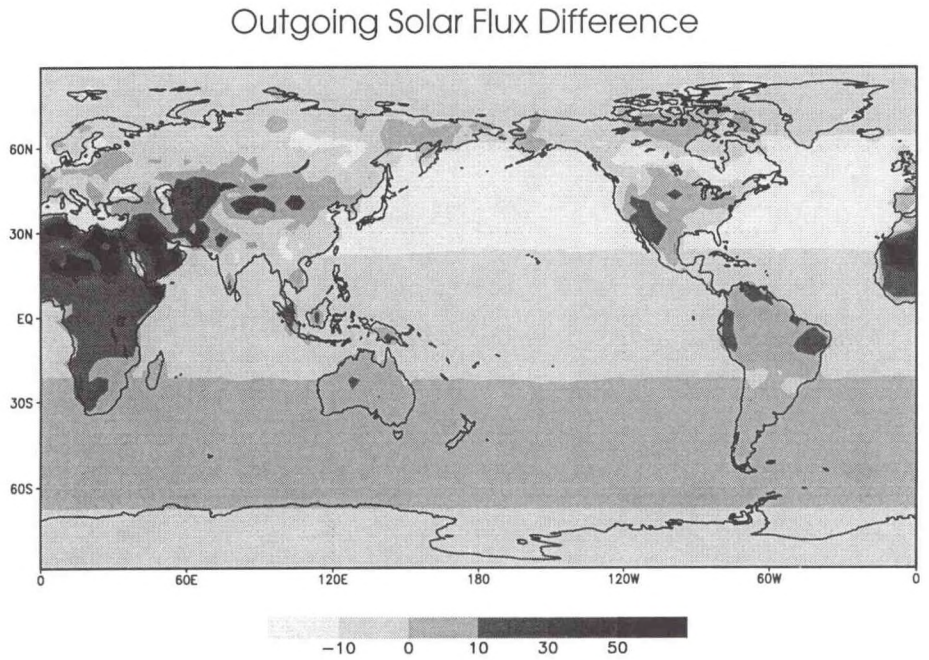

Fig. 2.3 Difference in the outgoing July solar reflected flux (W m^{-2}) at the top-of-the-atmosphere due to the new specification of surface albedos in the SKYHI GCM. The new results generally agree better with ERBE observations, especially over land regions.

PLANS FY97

The "benchmark" calculations with aerosols and clouds will be analyzed further. Comparison of the fluxes and heating rates obtained from the new shortwave parameterization with those from the previous model version will continue. The new shortwave parameterization will also be implemented in the Climate Group's GCM and simulations with that model will begin.

Comparisons of computed irradiances with satellite top-of-the-atmosphere and surface measurements will be analyzed to help determine computational versus instrumental biases.

The SKYHI GCM simulation, run with the new shortwave parameterization, will be evaluated further. In particular, both tropospheric and stratospheric temperature changes will be examined.

2.2 LONGWAVE SPECTRUM

M.D. Schwarzkopf V. Ramaswamy

ACTIVITIES FY96

2.2.1 Parameterization

The GFDL longwave radiative transfer algorithm (1034) has now been modified to represent the effects of the H_2O continuum using the "CKD 2.1" method (A95/P96). LBL cooling rate calculations for a standard ICRCCM (Intercomparison of Radiation Codes in Climate Models) atmospheric profile using the new approach reveal substantial increases in upper tropospheric cooling rates compared to the previous (Roberts) method. There is also a significant change in the net outgoing infrared flux at the tropopause and the top of the atmosphere. The new parameterization has been shown to reproduce these fluxes, with an accuracy of ~10 percent. The code has been incorporated into the GFDL SKYHI GCM.

2.2.2 Comparison of Line-by-Line Calculations with Observations

For the first time, top-of-the-atmosphere (TOA) irradiances computed using the GFDL longwave radiative transfer algorithm have been compared with measured irradiances. The observed irradiances are clear-sky values for each day of July 1987, measured by the ERBE instrument. The corresponding co-located atmospheric profiles are obtained from ECMWF analyses. Clear-sky irradiance calculations using the longwave algorithm have been computed under three assumptions: 1) inclusion of the radiative effects of H_2O, CO_2 and O_3, with the Roberts H_2O continuum formulation (Roberts 3gas); 2) adding the effects of CH_4, N_2O, and the halocarbons F11, F12, F113, and F22 (Roberts 9gas); 3) including the effects of the same nine gases, but employing the CKD 2.1 H_2O continuum formulation (CKD2.1). The difference between these calculations (zonally and monthly averaged) and the observations are shown in Fig. 2.4. The results indicate that the effect of the new continuum formulation and the additional species is a ~8 W/m^2 decrease in the computed outgoing irradiance. The results also demonstrate encouraging agreement between observations and the new parameterization.

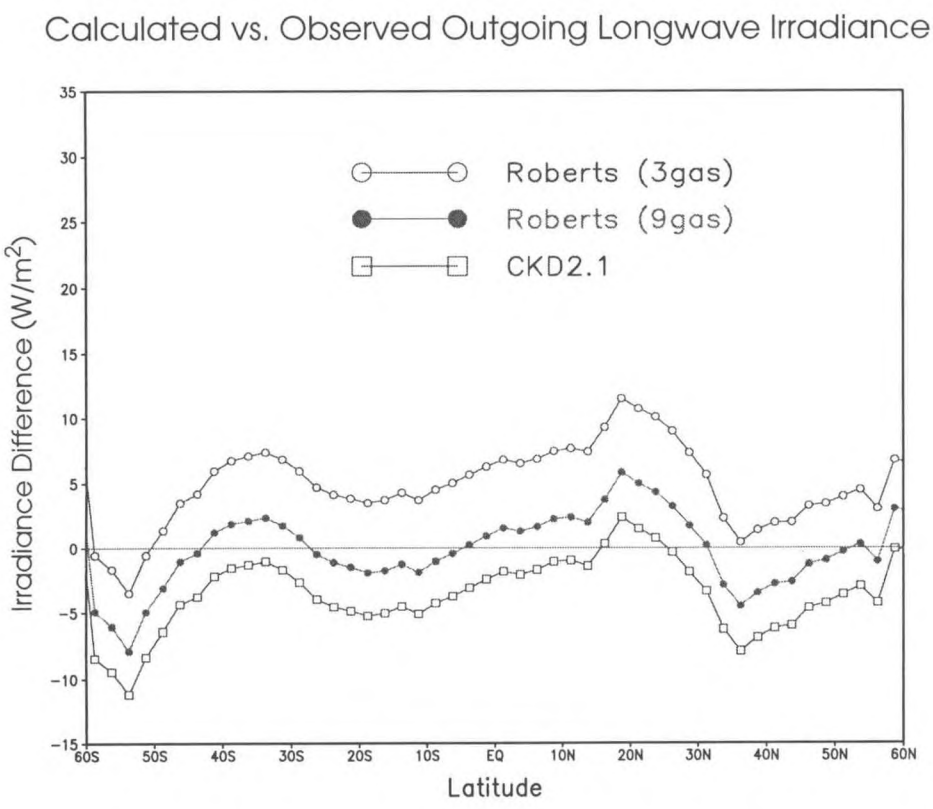

Fig. 2.4 Difference between calculated and observed zonally and monthly-averaged clear-sky outgoing longwave irradiances at the top of the atmosphere, for July 1987, for three versions of the radiation algorithm. The combined effects of the additional trace gases and the new H_2O continuum yield a top-of-the-atmosphere (TOA) irradiance that is within the measurement uncertainties.

PLANS FY97

Analysis of the differences between LBL and observed radiances will continue. The calculations will be extended to additional cases involving different atmospheric soundings.

The longwave radiation algorithm will be changed to include on-line computation of CO_2, CH_4 and N_2O transmissivities. The resulting codes will be implemented into GFDL GCMs, including the Climate Group GCM. Analysis of changes in SKYHI GCM temperature, moisture and wind profiles due to the algorithm modifications will continue.

Comparison of observed and computed irradiances will be extended to additional months. Analysis will continue of an intercomparison exercise involving LBL, wide-band, and narrow-band radiative transfer model calculations of the effects of CH_4, N_2O, F11 and F12, conducted as part of the ICRCCM project.

2.3 CONVECTION-CLOUDS-RADIATION-CLIMATE INTERACTIONS

2.3.1 Cumulus Parameterization

L. Donner

ACTIVITIES FY96

Interactions between cumulus convection and atmospheric radiation represent a difficult and important problem in the study of climate and climate change. Cumulus convection interacts with atmospheric radiation through several processes; among the most significant are the controls on the vertical distribution of water vapor exerted by cumulus convection and feedbacks involving clouds in convective systems with both short-wave and long-wave radiation. To address these problems in the context of general circulation models (GCMs), a parameterization for cumulus convection, which provides a physical basis for treating radiative interactions, has been developed (1133).

The parameterization places unique emphasis on the statistical aspects of convective-scale vertical velocities and microphysics (1349). Two strategies for evaluating these critical aspects of the parameterization have been adopted. The first involves using a high-resolution limited-area nonhydrostatic model as a test bed for the GCM parameterization. This approach is described briefly in 2.3.2. The second involves the design of a field experiment which would observe both the water budget of a convective system and its large-scale environment. An experiment which has analyzed both has never been carried out. Plans for such an experiment have been drafted.

As a preliminary step toward incorporating the parameterization in GCMs, a simple closure has been developed. The key closure assumption is that the vertically integrated forcing provided by the convective system balances large-scale destabilization. This provides an equilibrium between large-scale forcing and convective response, but neglects the details of the interactions between convective subensembles.

PLANS FY97

The closure will be combined with the aspects of the parameterization described in (1133) to provide a one-dimensional column version. This version will be incorporated in the SKYHI GCM for a series of studies of convection, microphysics, and radiation in the general circulation.

2.3.2 Limited-Area Nonhydrostatic Model Development

L. Donner *T. Reisin*
R. Hemler *C. Seman*
V. Ramaswamy

ACTIVITIES FY96

The Lipps-Hemler (885) limited-area nonhydrostatic model was used to study interactions between large-scale flows and cloud microphysics and radiation. The purpose of this study was twofold, including both an evaluation of cumulus parameterizations, such as that described in 2.3.1, and an analysis of the basic character of these interactions. A three-dimensional simulation of convective systems during a typical easterly wave in the east Atlantic was completed. The behavior of the modeled system agrees well with observations. Strong interactions between cloud microphysics and radiation were found in this and other two-dimensional integrations. An example is illustrated in Fig. 2.5, which shows the change in horizontally averaged total condensate in a convective system in parallel integrations with and without radiative interactions. Radiative interactions increased the condensate concentrations in the stratiform anvil. These interactions also tended to destabilize the stratiform anvil while stabilizing the middle troposphere. A new approach to microphysics in the model has also been implemented. This approach consists of prognostic equations for several moments of the particle-size distributions. A model integration in which particle-size statistics were calculated for deep convection is undergoing analysis.

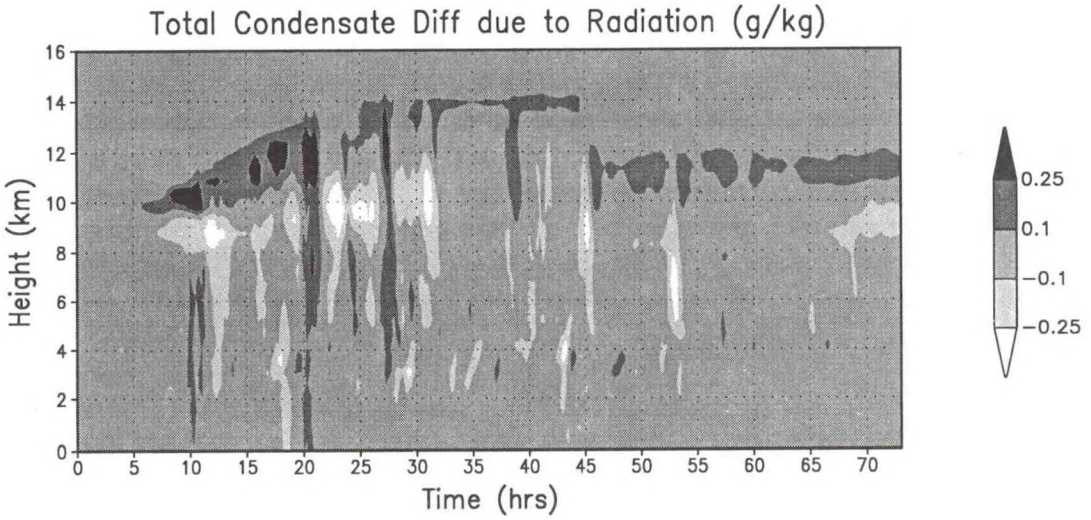

Fig. 2.5 Horizontally averaged differences in total condensate (sum of cloud water, rain, and snow) between two integrations of the GFDL LAN model, with and without radiation. Radiation generally increases condensate, especially in the stratiform anvil above 10 km.

PLANS FY97

Emphasis will be placed on analyzing the roles of the convective and stratiform parts of the convective system and using this decomposition to evaluate the parameterization described in 2.3.1. The water budgets and statistical distributions of convective-scale vertical velocities, which are important for interactions between convection and radiation, will be studied in the model and compared with data from field experiments where available. Further analysis of the particle size distribution and its impact on radiation interactions is planned.

2.3.3 Radiative-convective Equilibria with Explicit Moist Convection

I. Held *S. Klein*

ACTIVITIES FY96

In the recent literature, two theories for the CAPE (convective available potential energy) of atmospheres in radiative-convective equilibrium have been published. These theories are quite similar, but differ in their closure for the cumulus mass flux. These theories have been compared and a new formula for CAPE has been developed (ca). With cloud resolving models, it is possible to test this new formula and those already published.

Several parameter studies with a two-dimensional version of the radiative-convective model have been completed. These will serve as background for evaluation of the full three-dimensional integrations to be conducted in the coming year.

PLANS FY97

Radiative-convective equilibria will be obtained with a three-dimensional model of moist convection, in a doubly periodic domain over a horizontally homogeneous lower boundary with fixed temperature. Water vapor and clouds will be fully interactive with radiative transfer. This model will be used to study moist convective organization, the maintenance of the CAPE in the tropics, and cloud feedback mechanisms.

2.3.4 Atmospheric Ice Clouds

L. Donner *B. Soden*
R. Hemler *J. Warren*
C. Seman

ACTIVITIES FY96

Ice clouds influence both the shortwave and longwave radiation balance of the earth-atmosphere system and thereby play a delicately balanced role in climate. A parameterization for ice clouds (Heymsfield and Donner, 1990)[1] has been incorporated in the SKYHI GCM and linked to its hydrological cycle. Unlike many cloud parameterizations, very little of the ice reaches the surface as precipitation; most of the ice in a given cloud eventually sublimates, and the ice clouds can persist across model time steps. Another novel feature of the parameterization is its prediction of cloud vertical extents on a scale finer than the GCM vertical resolution. The parameterization has also been linked to both solar and longwave radiative transfer in SKYHI. Variations in ice-particle sizes are parameterized based on field observations. Large-scale variations in both ice content and particle sizes are important for regional variations in cloud albedo and emissivity.

Several SKYHI integrations with the parameterization have been analyzed. The principal regions of observed large-scale ice clouds are captured by the integrations, as can be seen in Fig. 2.6. (Mean SKYHI biases in temperature, humidity, and vertical velocity have been accounted for in the parameterization used in this integration.) The net effect of the large-scale ice clouds is warming of the earth-atmosphere system. Both shortwave and longwave forcing depend on ice-water path and mean crystal size, but differently. As a result, the geographical patterns of shortwave and longwave forcing also differ. The statistical distributions of large-scale ice clouds generally agree with those inferred from satellite observations, but with some differences due to secondary cloud-formation processes neglected by the parameterization. Ice clouds act to increase the temperatures in the upper tropical troposphere in the SKYHI integrations.

PLANS FY97

Ice-clouds formed by convective, rather than large-scale, processes will be studied, based on the cumulus parameterization described in 2.3.1.

---

1. Heymsfield, A.J., and L.J. Donner, A scheme for parameterizing ice-cloud water content in general circulation models, *J. Atmos. Sci.,47*, 1865-1877, 1990.

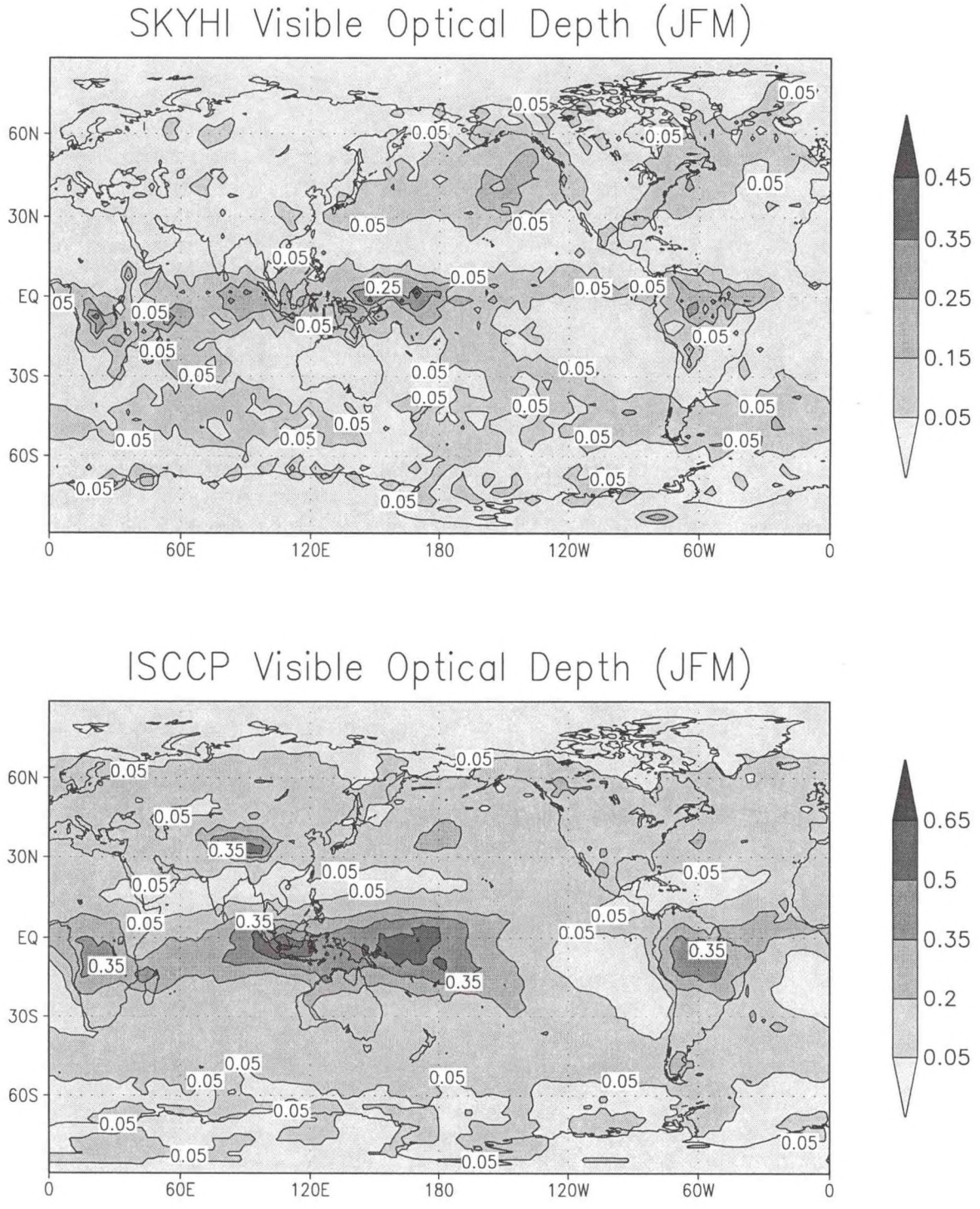

Fig. 2.6 Visible optical depths for non-convective cirrus clouds inferred from (a) SKYHI integrations and (b) ISCCP (International Satellite Cloud Climatology Program). Averages for January, February, and March. SKYHI integrations included a correction in the ice parameterization to account for the time-mean biases in temperature, humidity, and vertical velocity. The results show that key regions of satellite-observed cirrus clouds are captured in SKYHI.

2.3.5 Interactions Between Water Vapor, Radiation, and Circulation

B. Soden

ACTIVITIES FY96

The tropics exhibit large regional variations in water vapor which reflect complex interactions between water vapor, radiation, and the atmospheric circulation. In the tropics, the distribution of upper tropospheric moisture is strongly regulated by the large-scale circulation, yet variations in tropospheric moisture also play an important role in determining the strength of the tropical circulation. Thus water vapor and the tropical circulation are closely coupled, yet there has been little investigation of the nature and importance of this coupling. To address this issue, a series of GCM experiments were performed to elucidate the role of water vapor radiative heating in regulating the strength and distribution of the large-scale tropical circulation.

Three experiments were performed to examine the impact of regional variations in radiative heating by total column moisture, upper tropospheric moisture (above 500 hPa) and lower tropospheric moisture (below 500 hPa). At each grid box within the 30°N-30°S tropical belt, the water vapor concentration used to determine the infrared radiative heating was replaced with the tropical-mean water vapor for that vertical level determined from a 5-year control run. The area-mean water vapor was utilized only by the radiative calculations, in all other computations (*e.g.*, evaporation, condensation, convective adjustment) the moisture was unaltered. In all three cases the strength of the Hadley circulation was dramatically weakened by ~30-50%, with the largest reduction occurring for changes in upper tropospheric moisture. Inspection of the radiative cooling profiles indicated that the circulation changes primarily result from increased downwelling radiation in the dry subtropical regions. These results confirm the importance of water vapor, particularly water vapor in dry subtropical regions, in regulating the tropical circulation.

PLANS FY97

Further analysis during FY97 will focus on the differences between the moisture variations at various levels and the manner in which the vertical distribution of cooling rates impacts the circulation.

2.3.6 Radiative Forcing and Climate Response

C.-T. Chen *V. Ramaswamy*

ACTIVITIES FY96

Analysis continued with respect to the GCM equilibrium experiments reported in A95/P96, which were designed to investigate whether climate response to combined greenhouse and albedo forcings were linearly additive. In particular, the characteristics of the zonal-mean precipitation response were investigated (cv). There is a differential precipitation response in the northern (a decrease) and southern (an increase) tropical regions when a

midlatitude northern hemispheric forcing is present (*e.g.*, anthropogenic sulfate aerosol). The greenhouse forcing obtained by increasing carbon dioxide concentrations in the model exhibits no such differential quality. The simultaneous albedo and greenhouse forcings yield a differential response that resembles approximately that obtained when only the albedo forcing is considered. This is a further confirmation that the model's response patterns for the forcing types considered (see A95/P96) is approximately linearly additive.

Another GCM experiment was performed in which the albedo forcing was even more localized, confined to the Eurasian region. One motivation for this experiment is the anticipated large radiative forcing in this area due to increases in future sulfate emissions in Asia. The global-mean climate sensitivity of this experiment is reasonably similar to that of the other localized forcings investigated previously (1381, av).

PLANS FY96

Further analyses will involve a comparative look at the total and the individual feedbacks, and will include a summary of the forcing-response characteristics for the variety of GCM experiments performed.

2.3.7 Aerosol Radiative Forcing

L. Donner *V. Ramaswamy*
J.M. Haywood

ACTIVITIES FY96

The GFDL limited-area non-hydrostatic model (2.3.2), with a horizontal spatial resolution of 2 km by 2 km, was used to assess the importance of sub-grid scale variations in relative humidity and clouds in estimates of the direct radiative forcing by tropospheric sulfate aerosols. The radiative forcing from the limited-area model for both clear and cloudy regions was analyzed and the results compared against those that are obtained using GCM parameterizations that perform the computations over very coarse horizontal grids. It was found that, in both clear and cloudy cases, the GCM calculations underestimate the radiative forcing due to sulfate aerosols when sub-grid scale variations are not taken into account.

PLANS FY97

The results from the LAN model study of the effects of sub-gridscale effects of relative humidity upon the radiative forcing of sulfate aerosol will be incorporated into future studies with the R30 GFDL Climate Model.

2.4 DIAGNOSTIC ANALYSES USING SATELLITE OBSERVATIONS

ACTIVITIES FY96

2.4.1 Variations in Tropical Greenhouse Forcing During ENSO

B. Soden

Observations of the clear-sky outgoing longwave radiation and sea surface temperature were combined to examine the evolution of the tropical greenhouse effect from colder La Niña conditions in early 1985 to warmer El Niño conditions in late 1987 (ch). The greenhouse trapping (G) was defined as the difference between the clear-sky outgoing longwave radiation (F_{clr}) and the Planck surface emission (σT_s^4), $G = \sigma T_s^4 - F_{clr}$, where T_s is the sea surface temperature. Although comparison of individual months can suggest a decrease in greenhouse trapping from cold to warm conditions, when the entire 4-year record was considered, a distinct increase in tropical-mean greenhouse trapping of ~2 W/m^2 is observed in conjunction with a ~0.4 K increase in tropical-mean sea surface temperature. This observed increase compares favorably with AMIP GCM simulations of the change in the clear-sky greenhouse effect during ENSO (Fig. 2.7). Superimposed on top of the SST-driven change in greenhouse trapping are dynamically-induced changes in tropical moisture apparently associated with a redistribution of SST during ENSO. The GCM simulations also successfully reproduce this feature, thus offering encouraging support for the ability of GCMs to simulate both dynamically and thermodynamically driven changes in greenhouse trapping.

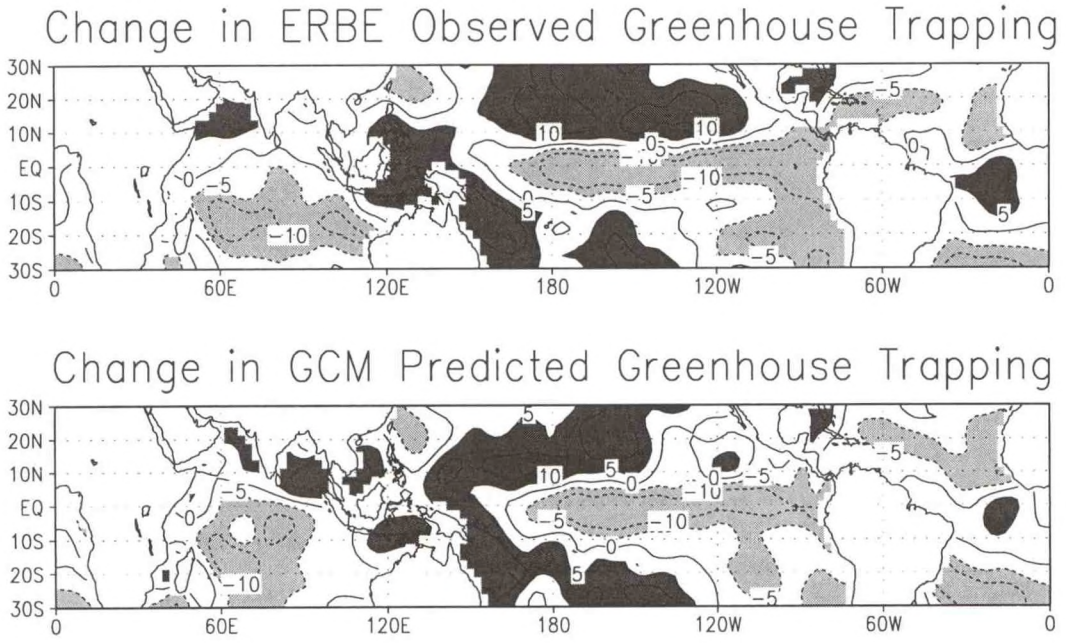

Fig. 2.7 Map of the difference in greenhouse trapping DG in W/m^2 between April 1985-April 1987 for ERBE observations (top) and GCM simulations (bottom).

2.4.2 Tracking Upper Tropospheric Water Vapor

B. Soden

A pattern tracking algorithm was applied to GOES 6.7 μm radiance measurements to identify moisture trajectories from sequential, time-lagged water vapor imagery. The trajectories were used to determine upper tropospheric winds and, combined with contemporaneous information on upper tropospheric humidity (UTH), to describe Lagrangian characteristics of upper tropospheric moisture. This provided what is perhaps the first climatological study of the Lagrangian tendencies of UTH, its relation to the formation and dissipation of clouds, and to upper level dynamics.

Maximum UTH coincides with areas of upper-level divergence, and minimum UTH occurs over regions of upper-level convergence, confirming the strong role which the tropical circulation plays in regulating upper tropospheric moisture. Observational estimates of the Lagrangian tendency in UTH were also computed. The humidity tendencies are directly proportional to the vertical velocity and thus provide valuable insight into the dynamics of the tropical upper troposphere. In clear regions, the humidity tendencies were predominantly negative, indicating that in the absence of convection, the upper troposphere is dominated by large-scale subsidence. The upper level air parcels dry out faster over the subtropics relative to the tropics, implying a greater rate of subsidence for the subtropics, which is consistent with the observed divergence patterns. Backwards time-lagged trajectories were also computed to examine the origin and Lagrangian behavior of air parcels arriving in the subtropics. It was found that the dry subtropical air originated from both the tropical convective systems as well as from midlatitude storms, suggesting that extratropical transport may play an important role in determining the moisture for the subtropics.

2.4.3 Impact of Satellite Winds on Hurricane Forecasts

B. Soden *C. Velden**
R. Tuleya

**University of Wisconsin*

Reliable predictions of hurricane tracks are dependent upon having accurate wind observations with which to initialize the forecast models. Unfortunately, conventional measurements are currently not available over much of the tropics where hurricanes originate. One supplement to conventional wind measurements are "cloud" and "water vapor" winds derived by objectively tracking water vapor or cloud features from sequential geostationary images. A scheme for assimilating the satellite winds into the GFDL hurricane model was developed and a series of model forecasts were performed to assess the impact of the GOES winds upon hurricane track predictions for portions of the 1994 and 1995 Atlantic hurricane season.

On average, the satellite winds had little net impact on the 12-24 hour forecasts, however, for the later forecasts there appears to be systematic improvement (Fig. 2.8). This is particularly apparent for the 36-48 hour forecast period where the mean track errors are reduced by ~10-15%. An analysis based upon a student's t-test suggests that the 36-48 hour improvement is statistically significant at the 95% level. The number of improved forecasts was

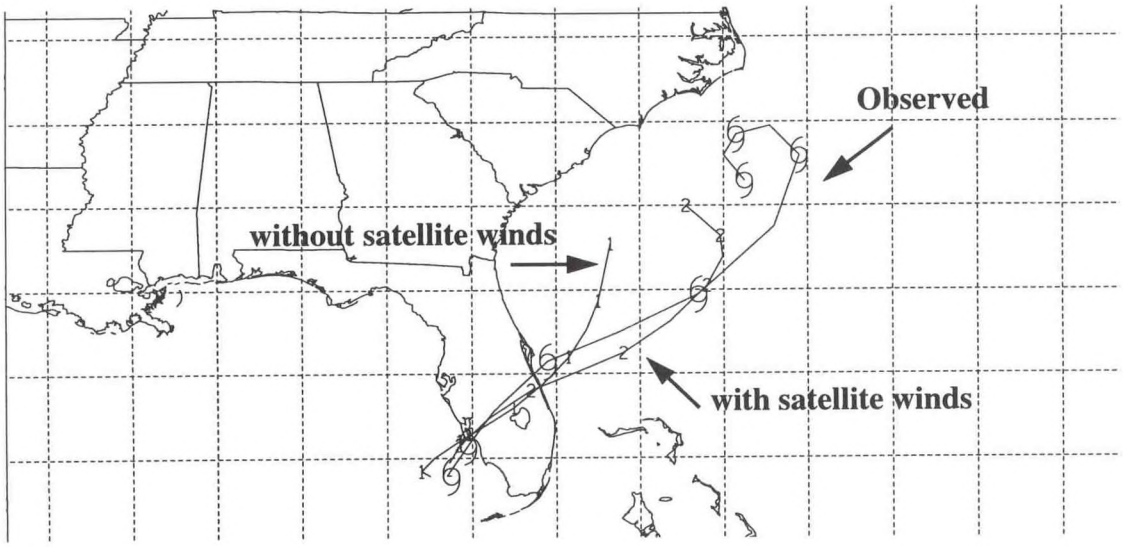

Fig. 2.8 Observed and model predicted track for hurricane Gordon on Nov 16, 1994, 00 GMT. Track of Hurricane Gordon, compared to model forecasts with and without satellite wind information. Use of satellite wind data can significantly improve hurricane forecasts at 36-48 hour range.

also systematically larger for the 36-48 hour period, where more than 55% of the forecasts were improved. These results suggest that the satellite-derived winds contain information that could improve hurricane forecasts.

PLANS FY97

The variations of greenhouse trapping will be extended to cover the ENSO events of 1983 and early 1990s using a newly developed clear-sky OLR dataset. The variations in greenhouse trapping at various spectral wavelengths will also be examined.

The analysis will continue on the GOES pattern tracking results. An algorithm for tracking temporal patterns in UTH will be developed and applied to a 15 year archive of TOVS pentad data. The TOVS data will enable a global analysis of the seasonal and interannual variations in the moisture transport.

The impact of satellite winds for the 1996 hurricane season will be analyzed further. The impact of upgrades in the NCEP analysis system upon the results will be investigated, as will their sensitivity to various assimilation strategies.

2.5 EFFECT OF CHANGES IN ATMOSPHERIC COMPOSITION

J.D. Mahlman *V. Ramaswamy*
R. Orris *M.D. Schwarzkopf*

ACTIVITIES FY96

2.5.1 "CKD 2.1" H_2O Continuum

The GFDL SKYHI GCM (latitude-longitude resolution: 3x3 degrees) has been used to study the changes in upper tropospheric and lower stratospheric climate due to inclusion of the radiative effects of the foreign-broadened H_2O continuum included in the CKD 2.1 formulation (2.2.1). Ten years of model integration have been completed. Fig 2.9 shows that the annually and zonally-averaged temperature response (compared to the Roberts 9-gas formulation) is a cooling of ~ 0.5-1 K throughout the upper troposphere, with warming occurring below. A larger cooling (up to ~1.6 K) occurs near the tropical tropopause.The temperature changes in the lower stratosphere are generally under 0.5 K. These results are broadly consistent with expectations from instantaneous cooling rate changes. The new simulation also leads to a decrease in upper tropospheric moisture concentrations, with a shift

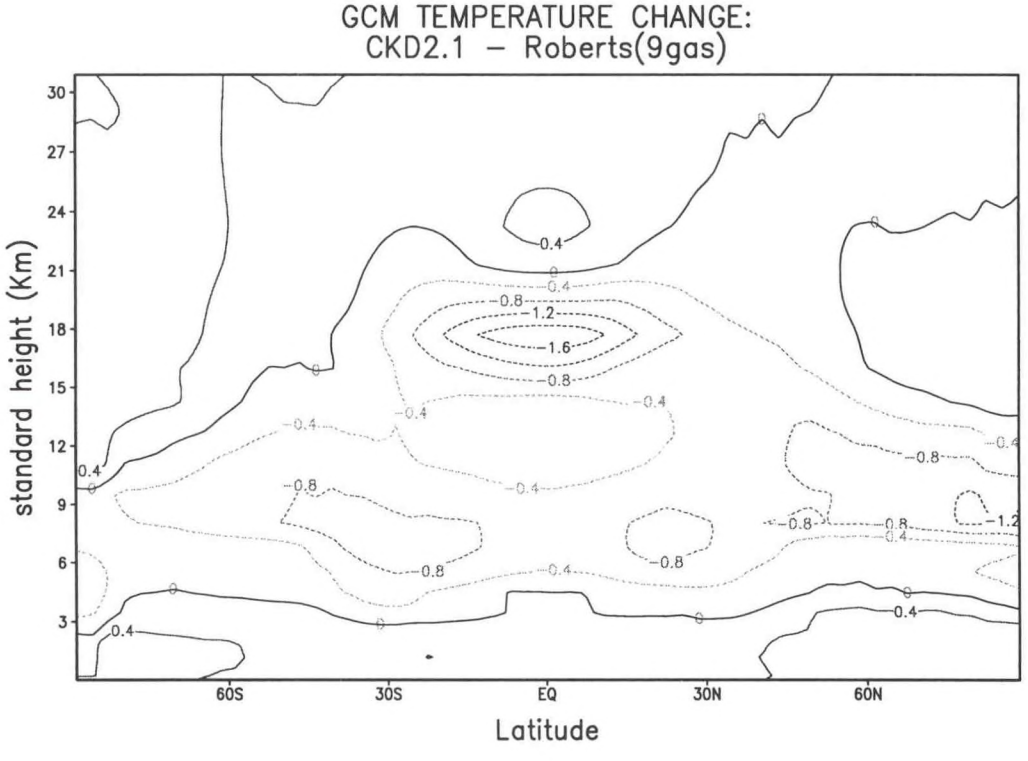

Fig. 2.9 Difference in annually and zonally-averaged temperature between GCM simulations using the Roberts H_2O continuum formulation and the CKD 2.1 approach. Each simulation is a ten-year run. The tropical upper troposphere undergoes a substantial cooling using the CKD2.1 formulation.

in the latitudes of the annually-averaged upper tropospheric zonal wind maxima towards the equator. The temperature changes are in contrast to those resulting from the introduction of additional (non-CO_2) trace gases (A95/P96). The combined effect of the additional trace gases and the new H_2O continuum algorithm is a small (~0.3 K) increase in tropical tropospheric temperatures and small decreases in lower stratospheric and mid-tropospheric temperatures.

2.5.2 Temperature Changes Due to the Observed 1979-1990 Ozone Loss

Analysis of the GCM simulation of the effects of decadal lower stratospheric ozone losses have been completed (1393, 1384). It was determined that a statistically significant lower stratospheric cooling computed by the GCM simulations has a close seasonal, latitudinal and altitude correspondence with the observed pattern of decadal temperature change in the lower stratosphere. This leads to the conclusion that, since the ozone loss is likely due to human influences, the observed temperature change is a fingerprint indicating a human-induced climate change in the lower stratosphere. The simulation of upper tropospheric temperature decreases due to reductions in lower stratospheric ozone concentrations leads to an improved correspondence between observed and simulated patterns of the altitude profile of temperature change during the 1980s (1384).

A GCM simulation of the observed decadal (1979-1990) lower stratospheric ozone losses, with the altitude profile of ozone depletion extending to higher altitudes than in previous calculations (1393), has been completed. The new range is intended to reproduce more closely the observed altitude range of ozone loss in the southern polar latitudes. Results show increased cooling, compared to previous results (1393) of the lower stratospheric temperatures in southern polar latitudes, and, as expected, an upward extension of the lower stratospheric cooling at all latitudes.

2.5.3 Ozone-Temperature Relation in the Stratosphere

Work continued regarding the radiative consistency of ozone and temperature observations in the middle and upper stratosphere. Temperatures derived from the fixed dynamical heating (FDH) model calculations, employing heating rates from the 1-degree resolution SKYHI GCM and the Upper Atmospheric Research Satellite (UARS) Microwave Limb Sounder (MLS) ozone, show closer agreement with MLS and LIMS temperatures than with Barnett and Corney (BC) temperatures. However, significant differences still persist between the modeled and observed temperatures.

Estimates have been obtained of the sensitivity of the FDH modeled temperatures to uncertainties of 5% in the longwave and shortwave radiative heating rates. Such uncertainties could arise due to inaccuracies in the line parameters as well as approximations associated with the parameterizations. Uncertainties in the ozone mixing ratio of 10% below 1 mb and 20% above 1 mb have also been examined to determine their effect on the FDH modeled temperatures. One important contribution to the uncertainty in the FDH calculation is the interannual variability of the 1-degree latitude resolution SKYHI GCMs temperatures and dynamical heating rates. The FDH modeled temperatures in the tropics using two different years of dynamical heating rates differ by as much as 5 K. The variability of the temperature

in 25 years of data from the 3-degree latitude resolution SKYHI GCM has been examined, and found to exhibit a tendency for successive years to exhibit similar temperature deviations from the mean. There is also evidence of a low frequency (~10 years) variation in the 3-degree model's temperatures. This variability is a significant source of uncertainty because the dynamical heating rates used for the FDH calculations were derived from a single year of the 1-degree SKYHI GCM simulation. Examination of the three years of the 1-degree GCM simulation, newly available, suggest that even simulations of this length are not enough to eliminate the existence of interannual variability suggested by the 3-degree model's statistics. An important conclusion emerging from the SKYHI GCM simulations is that very long-term records are essential to evaluate "true" averages. Assuming such low frequency variation in the real atmosphere, even several years of measurements may not be enough to determine the "climatological" averages of temperatures and dynamical heating rates. The uncertainty introduced into the comparison of FDH modeled temperatures and measurements due to interannual variability is estimated to be about 8 K near 1 mb in the tropics.

Comparison of the global-mean values of the FDH modeled and comparisons with measured temperatures have been performed on pressure surfaces. The global-mean calculations show that the year to year values of UARS MLS temperatures are within 2 K. MLS and LIMS temperatures agree to within 2 K in the global-mean at pressures of 1 mb and greater. The global-mean BC temperatures between 2-10 mb are found to be significantly warmer (3.5-5.0 K) than either the MLS or LIMS temperatures for most months. Given these results, it is concluded that BC temperatures do not accurately represent the temperature of the stratosphere between 2-10 mb.

Comparisons of global-mean SKYHI temperatures with measured temperatures show the SKYHI temperatures to be about 5 K colder at all pressure levels for all months. When account is taken of the uncertainties in the FDH calculation and the uncertainty in the measured temperatures, only "marginal" agreement is found between the SKYHI temperatures and both the MLS and LIMS temperatures.

PLANS FY97

Further analysis of the GCM simulation using the CKD 2.1 formulation will continue. Comparison with FDH calculations will be undertaken to determine the relative significance of radiative and dynamical effects.

GCM simulations using the Climate Dynamics Group model will be undertaken to determine the effects of the inclusion of trace gases, and of varying ozone, in a model with predicted cloud fields and sea surface temperature. This will allow evaluation of the tropospheric effects due to the radiative perturbations. Additionally, the Climate Group's GCM will be used to study the climatic changes in the concentrations of different types of aerosols.

Analysis of the GCM simulation in which the ozone loss extends to higher altitudes in the stratosphere will continue. Temperature changes obtained from the current experiment will be

compared to those obtained from GCM simulations of realistic changes in CO_2 and other trace gases, as well as changes in aerosols.

Uncertainties in the FDH investigation of the ozone-temperature radiative consistency problem will be further explored, especially regarding radiative heating rates and the interannual variability of relevant quantities.

3. MIDDLE ATMOSPHERE DYNAMICS AND CHEMISTRY

GOALS

To understand the interactive three-dimensional radiative-chemical-dynamical structure of the middle atmosphere (10-100 km), and how it influences and is influenced by the regions above and below.

To understand the dispersion and chemistry of atmospheric trace gases.

To evaluate the sensitivity of the atmospheric system to human activities.

3.1 ATMOSPHERIC CHEMISTRY AND TRANSPORT

*W.L. Chameides** *J.D. Mahlman*
A.I. Hirsch *W.J. Moxim*
*S. Fan*** *S. Oltmans*****
*P.S. Kasibhatla**** *L.M. Perliski*
*A. Klonecki*** *S. Taubman*
H. Levy II

**Georgia Institute of Technology*
***Princeton University*
****MCNC/Environmental Program*
*****Climate Monitoring and Diagnostics Laboratory/NOAA*

ACTIVITIES FY96

3.1.1 In situ Photochemical Module Development

A version of SKYHI with a detailed treatment of stratospheric photochemistry has now been run for a total of six model years. The photochemical scheme is described in detail in A95/P96. These simulations show that SKYHI is capable of generating generally realistic distributions of important stratospheric trace constituents. The version of SKYHI employed to perform the photochemical calculations does not have a parameterization of gravity wave drag, therefore the cold pole bias still exists in the calculations and has an effect on the trace species distributions through temperature-dependent photochemical processes.

A scheme has been developed to calculate photolysis rates on-line in SKYHI. This scheme will result in more realistic sensitivities of photolysis rates to surface albedo, overhead ozone column and temperature. In addition, the scheme will permit aerosol scattering processes to influence calculated photolysis frequencies. The previous photolysis rate computation used in SKYHI allowed sensitivity to solar zenith angle changes only. The new photolysis calculation is currently being optimized for efficient use in SKYHI.

The photochemical scheme currently being tested in SKYHI does not include a treatment of halogen chemistry (chlorine and bromine compounds). This was done for computational economy during model development, and it was also the strategy adopted for modelling the "pre-industrial" stratosphere when chlorine and bromine abundances were a small fraction of present day levels. A photochemical scheme that includes a full treatment of chlorine and bromine chemistry including heterogeneous processes has been developed and tested in box and column models. The new chemical scheme includes a diagnostic calculation of type I and II polar stratospheric clouds (PSCs). Background stratospheric aerosol abundances are currently prescribed from SAGEII observations and latitude-dependent percent weights of sulfuric acid are assumed.

The polar stratospheric cloud parameterizations mentioned above assume that type I polar stratospheric clouds are composed of nitric acid trihydrate. Recent observational evidence and laboratory measurements suggest that it is likely that most type I PSC's are actually liquid ternary solutions of water, nitric acid and sulfuric acid. An algorithm to calculate the abundances, volumes and composition of these aerosols has been obtained from Carslaw and co-workers at the Max-Planck Institut für Chemie in Mainz, Germany and is being added to the one-dimensional version of SKYHI's halogenated photochemical scheme for testing purposes and eventual incorporation into the GCM.

3.1.2 Off-line Photochemical Module Development

In recognition of the computational cost, chemical complexity, and inherent empirical nature of explicit photochemical schemes for the polluted boundary layer, such as the one under development in A94/P95, a simple empirical parameterization has been developed which depends on the atmospheric level of NO_x, the season, and the latitude. This parameterization, which can be applied to both pre-industrial, present, and future conditions, was developed and implemented in the 11-level Global Chemical Transport Model (GCTM). One of the primary goals of this study is to quantify the global and regional impact of ozone produced in the polluted boundary layer. Based on observed empirical relationships between NO_y compounds and O_3 and theoretical calculations of O_3 produced per NO_x consumed, the net rate of O_3 photochemical production was assumed to be proportional to the rate at which NO_x molecules were oxidized to HNO_3 by reaction with hydroxyl radicals (OH). The proportionality constant (k) was chosen to be:

$k(NO_x) = 8.5$ for $NO_x > 1$ ppbv, and

$k(NO_x) = \{8.5 - 60*\log10(NO_x)\}$, for $NO_x < 1$ ppbv.

The values of the individual parameters were constrained by current understanding of regional smog chemistry and were chosen to reproduce the observed levels of O_3 in the polluted boundary layer. To simulate the seasonal and latitudinal variation of the net O_3 production efficiency (OPE) in the extratropics, $k(NO_x)$ was multiplied by **S**(month). For the 30°N-90°N and 30°S-90°S belts, **S** was specified using the seasonal variation of the net OPE calculated by for Harvard Forest, MA. For the tropics (30°N-30°S) **S** was held constant at 1.0.

This approach was deemed the most reasonable way to extrapolate the values of k and A based on analyses at a few specific geographic locations, to the globe as a whole.

A chemical gas-phase box model with CO-CH_4-NO_x chemistry was used to produce tables of the rate of ozone production or destruction (the ozone chemical tendency) for the clean troposphere over the entire globe for all months of the year. The box model calculations were performed for four seasons (January, April, July, October), nine latitudes (80°S, 60°S, 40°S, 20°S, equator, 20°N, 40°N, 60°N, 80°N), and 7 pressure surfaces (990 mb, 940 mb, 835 mb, 685 mb, 500 mb, 315 mb, 190 mb). To account for different concentrations of CO and different values of albedo over land and sea, separate tables were constructed for each. Zonally averaged values of input parameters were used; with water and temperature fields taken from observations and CO concentration taken from a GCTM model run. The calculations were carried out with a 60 second time step until the diurnally averaged ozone chemical tendency did not change by more than 1% from day to day, but for not fewer than 5 days. The net O_3 chemical tendency for each GCTM time-step can then be interpolated from the off-line chemical tendency table, using either specified or model determined values of O_3 and NO_x.

3.1.3 Advection Schemes

A model experiment was designed to test the ability of several different advection schemes to produce realistic distributions of water vapor and atmospheric tracers such as N_2O. The schemes tested were 1) SKYHI's default advection scheme, 2) a centered difference scheme that is 4th order accurate in the vertical and 2nd order accurate in the horizontal, 3) a new pseudo-4th-order vertical and horizontal centered difference scheme, and 4) a higher-order upstream difference scheme developed by Lin and Rood. The NCAR semi-Lagrangian scheme is currently being added to SKYHI for further study of the differences between various treatments of constituent advection.

The first set of advection scheme experiments involve running a simulation of water vapor in SKYHI for each advection scheme for three model years. The stratospheric water vapor in the tropics generally shows a great deal of vertical structure compared to the Lin and Rood scheme which appears to be significantly drier than the centered difference schemes. The vertical structure apparent in the stratospheric water vapor calculated with the centered difference schemes may be due either to dispersion errors associated with the schemes, or perhaps horizontal transport processes which may be smeared out by the more diffusive Lin and Rood scheme. More analysis is required to settle this issue.

The second set of advection scheme experiments involves a three-year SKYHI simulation of N_2O for each advection scheme. The results of these experiments suggest that the best simulation of the N_2O horizontal gradient near the polar vortex edge is obtained using the pseudo-4th-order centered difference scheme. The Lin and Rood and mixed 4th-2nd order centered difference schemes produce a much weaker N_2O gradient across the vortex, implying that more N_2O is diffused into the vortex than for the pseudo-4th-order scheme. The pseudo-4th-order effect is roughly equivalent to running a higher spatial resolution calculation and thus has implications for more economical modeling of polar vortex ozone depletion chemistry.

3.1.4 Tropospheric Reactive Nitrogen

Analysis of the global and regional budgets of tropospheric reactive nitrogen and the relative contributions of natural and pollution sources was completed. Both the pre-industrial and present distributions were simulated with a GCTM employing off-line calculations of the gas-phase interconversion rates among NO_x, HNO_3 and peroxyacetyl nitrate and the nighttime heterogeneous conversion of NO_2 to HNO_3 on sulfate aerosol, via NO_3 and N_2O_5. The pre-industrial sources of NO_x, which existed before there was a significant human presence on earth, are comprised of soil-biogenic emissions (3.6 tgN/yr), natural wildfires (~1tgN/yr), lightning emissions (3 tgN/yr) and stratospheric injection (0.6 tgN/yr). The present level of emissions also includes anthropogenic contributions from fossil fuel combustion (21.2 tgN/yr), greatly increased biomass burning (~8.3 tgN/yr) and enhanced soil-biogenic emissions due to fertilization (~1.5 tgN/yr), all in the atmospheric boundary layer, plus aircraft emissions (.45tgN/yr), primarily in the upper troposphere (1051, 1167, 1243, 11307, zr).

Given that most of the anthropogenic increase in NO_x emissions from a pre-industrial level of ~8 tgN/yr to a present level of more than 40 tgN/yr has occurred in the atmospheric boundary layer, it is not surprising that current NO_x levels in the lower troposphere are dominated by surface pollution. With the exception of the remote tropics, NO_x levels are elevated by at least a factor of two over the globe and by more than a factor of 10 in the heavily polluted Northern Hemisphere midlatitudes. In the mid-troposphere, natural emissions from lightning dominate in the tropics, while both natural emissions and pollution that has been transported from the surface contribute to the NO_x levels in the extratropics. Currently, the impact of NO_x emissions from rapidly increasing aircraft traffic in the upper-troposphere is of great concern. The simulated NO_x levels at 190 mb, as well as relative contributions from aircraft and surface pollution, are shown in Fig. 3.1. Surface pollution has little impact at 190 mb in the NH, while aircraft contribute more than 30% over a broad midlatitude belt. Note that all pollution sources contribute less than 40% of the NO_x in most of the SH, which is dominated by lightning emissions and stratospheric injection.

3.1.5 Tropospheric Ozone

Tropospheric ozone, which both controls the chemical reactivity of the lower atmosphere and is a significant greenhouse gas, is thought to have increased significantly in a number of regions, possibly throughout much of the globe, over the last 100 years. The key issues to be addressed are the magnitude of the impact of human activity on tropospheric ozone levels and the mechanism, or mechanisms, responsible. A variety of observational, analytical and numerical techniques are being applied to this general problem.

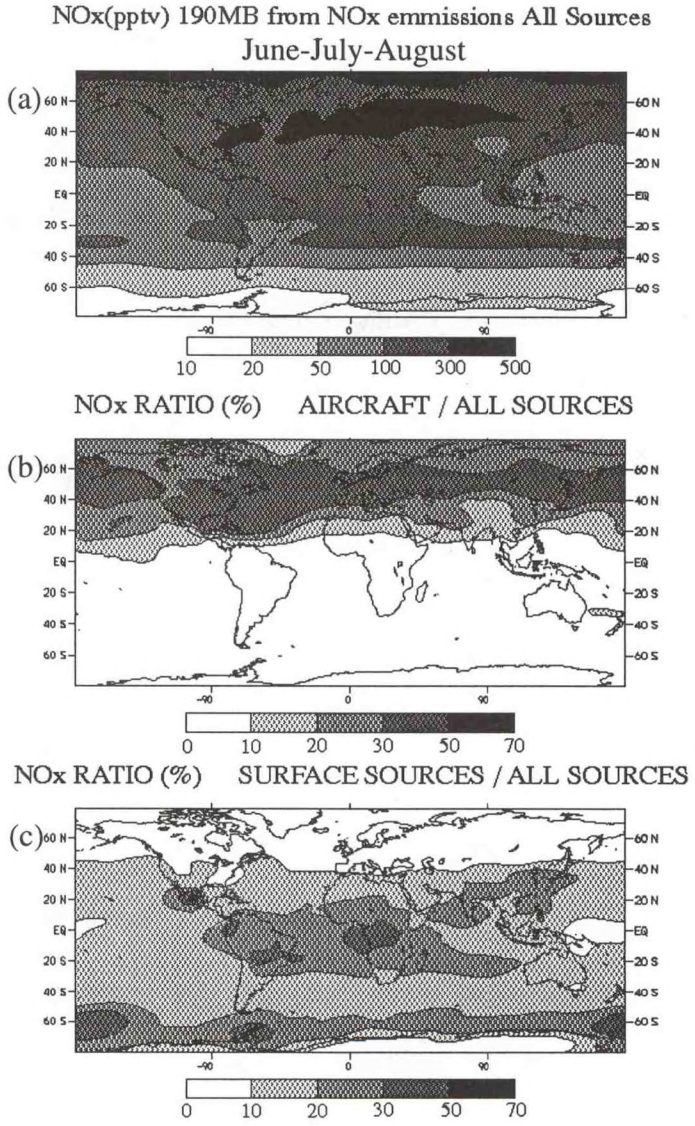

Fig. 3.1 Summer NO_x mixing ratios at 190 mb: (a) all sources; (b) the fractional contribution from aircraft; and (c) the fractional contribution from surface emissions (fossil fuel combustion, biomass burning, and biogenic processes). Aircraft contribute significantly to NO_x concentrations in the Northern Hemisphere, but all pollution sources combined contribute less than 40% of the NO_x in the tropics and Southern Hemisphere.

Collaborations continue with colleagues from the Air Ocean Chemistry Experiment (AEROCE) over the North Atlantic, focusing on measurements of tropospheric ozone and both their chemical precursors and tracers of atmospheric transport. A program of ozonesonde measurement and analysis continues with Sam Oltmans of CMDL. The AEROCE Theme 1 field campaign, which included aircraft measurements of H_2O, CO, O_3, NO, and hydrocarbons, surface measurements of a similar suite of species at Bermuda, and coordinated ozonesonde measurements from Indiana, Virginia, Maryland and Bermuda, was successfully completed in the spring of 1996 and the analysis is now in progress.

The 11 level GFDL GCTM was used to extend a preliminary regional study of summertime ozone over the North Atlantic (zj) to the full globe for all seasons. The ozone chemical tendencies discussed in 3.1.2, along with ozone transported from the stratosphere and the formation of ozone in the polluted boundary layer (see 3.1.2), were used to calculate the distribution of ozone throughout the troposphere. The present and pre-industrial ozone distributions were simulated with the previously calculated present and pre-industrial distributions of NO_x (see 3.1.4). Measurements from 12 surface and 21 ozonesonde sites were used to evaluate the global simulation of present ozone levels. With the exception of the wintertime high-latitude Northern Hemisphere (NH), the Southern Hemisphere (SH) tropics during its biomass burning season, and certain remote SH island sites, the model was in good agreement (± 25% or better) with an extensive set of observations, producing realistic global distributions of tropospheric ozone. The simulated July ratios of present to pre-industrial ozone for the surface, mid-troposphere, and upper troposphere are shown in Fig. 3.2. Preliminary

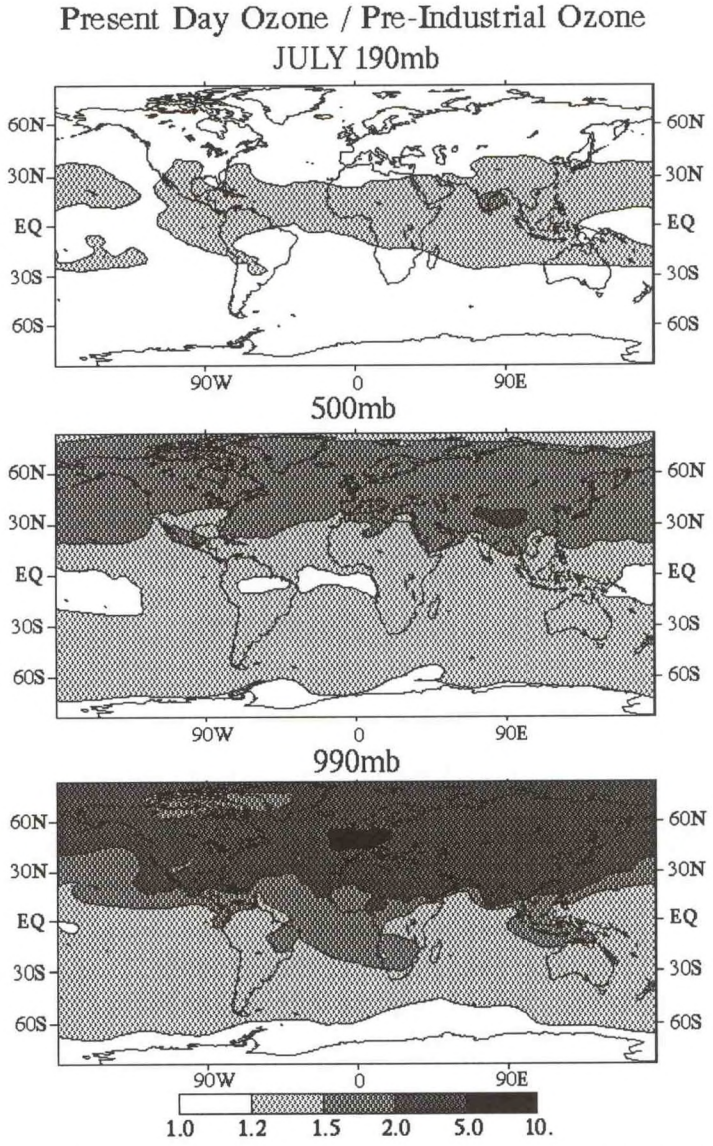

Fig. 3.2 Ratio of present day to pre-industrial July ozone for the upper, middle, and lower troposphere.

analysis indicates that, during the summertime, pollution more than doubled ozone levels not only in the polluted continental boundary layer, but throughout most of the NH boundary layer as well, with an increase of more than 50% in the NH mid-troposphere. Conversely, there is a significantly smaller increase (20-50%) in the wintertime NH and throughout the year in the SH. Anthropogenic emissions have little impact (<20%) in most of the upper troposphere.

3.1.6 Atmospheric Sulfur Chemistry and Transport

A detailed analysis of the anthropogenic sulfur simulations with the 11-level GCTM has been completed. Monthly-mean simulated column burdens of SO_4 have been compiled and are being used to calculate the clear-sky direct radiative forcing of sulfate aerosols, which in turn will be incorporated into the GFDL climate model.

3.1.7 Atmospheric Transport

The photochemistry and transport of CFC-11 in the 40-level GCM has been simulated. A time-dependent source for the gas is based on annual emission rates estimated by the Chemical Manufacturer's Association for the years 1978-1981, and is released into the lowest model layer. CFC-11 is lost in the atmosphere via photolysis and reaction with $O(^1D)$. The rates of loss were calculated monthly using an off-line photochemical and radiative transfer model and a prescribed ozone climatology. The model results for 1980-1981 are in good agreement with observations with respect to inter-site and intra-site variabilities (*e.g.*, meridional gradient and annual trend). The vertical gradients are negative in the NH where CFC-11 is emitted at the surface and transported upward, and positive in the troposphere of the SH where it is transported from the upper to the lower troposphere. This indicates that the north-to-south transport is mainly via the upper troposphere.

Simulations using the SKYHI GCM have also been conducted of the transport of radioactive tracers 85Kr, 222Rn, and 210Pb. Both observations and model results of 85Kr show a subtropical barrier against meridional exchange. However, the model and the observational data differ on the location of this barrier. It is not clear whether this is a model error or whether it reflects inter-annual and/or longitudinal variabilities. Lead-210 is rapidly removed by precipitation in the intertropical convergence zone (ITCZ), within which the model predicts a lifetime for soluble aerosols that ranges from less than two days in the lower troposphere to a few days in the free troposphere. However, observational data for these tracers are sparse and concentrations of the tracers are highly variable in space and in time owing to their short lifetime.

The 11-level GCTM was used to develop techniques for inverse modeling of CO_2 sources and sinks. A series of transport simulations have been conducted in the GCTM for fossil fuel, biospheric, and oceanic CO_2 sources, and seventeen regional CO_2 sources. When realistic atmosphere-biosphere and air-sea CO_2 fluxes, together with fossil fuel CO_2 source, are used in the simulation, good agreement is obtained with observed seasonal cycles at surface sites scattered around the globe. These results will be compared with the increasing number of aircraft measurements. The regional CO_2 tracers may provide a means of diagnosing air mass origins in various parts of the atmosphere. For example, it may be possible to assess the

relative influences of African, South American, and Northern Hemispheric sources on air pollution in the South Atlantic basin.

PLANS 97

Sources and sinks of NH_3 and NH_4^+ will be added to the NO_x/NO_y GCTM.

The Asia-RAINS NO_x emission inventory will be incorporated in the NO_y GCTM and the impact of future Asian emissions on the troposphere will be studied.

A detailed analysis of the global impact of human activity on tropospheric ozone will be completed.

Available water vapor data will be mapped on a 5x5 global grid and used in the ozone tendency calculations to account for the impact of its longitudinal variability. A GCTM simulation of tropospheric ozone will employ the new chemical tendencies.

A set of NO_y off-line interconversion tables will be constructed. A self-consistent CO-NO_y-O_3 simulation for the 11-level GCTM will be developed using the new tables and the feedback interactions of ozone and NO_x will be examined.

A more thorough analysis is underway to understand the differences between the advection schemes tested in 3.1.3. In addition, the NCAR semi-Lagrangian scheme will be tested in a similar manner. Simulations at higher vertical and horizontal resolution will also be tested since the comparative accuracy of various schemes can change with increasing resolution.

A new version of SKYHI with halogen photochemistry and heterogeneous chemistry will be run.

The new tropospheric NO_x sources will be added to SKYHI's troposphere in order to more realistically simulate the chemistry of the upper troposphere.

Detailed mechanistic analysis of tropospheric transport in the SKYHI will continue and regional transport characteristics as well as zonal mean meridional circulations will be examined. Simulated 222Rn and 210Pb distributions will be compared with observations.

3.2 ATMOSPHERIC DYNAMICS AND CIRCULATION

D.G. Golder *C. Kerr***
K. Hamilton *J.D. Mahlman*
Y. Hayashi *L. Perliski*
R. Hemler *R.J. Wilson*
*P.W. Jones**

**Los Alamos National Laboratories/DOE*
***International Business Machines*

ACTIVITIES FY96

3.2.1 SKYHI Model Development

A number of components of the planned SKYHI physics upgrade have been independently developed and evaluated. A new short-wave radiation code which better resolves the solar spectrum is now available. An improved surface albedo scheme sensitive to land-sea differences has been produced. The longwave radiation package incorporated into SKYHI in FY95 has been further refined to include a parameterization of the water vapor continuum. An examination of existing ozone measurements, with their biases and strengths, has led to the creation of a new ozone climatology for SKYHI, which should be more accurate and self-consistent than that previously used. These individual components are now being brought together in a new version of the standard SKYHI model.

SKYHI now includes the option to use the standard prescribed clouds, a prognostic cloud scheme, or a scheme which uses the prescribed water clouds but predicts ice clouds. The prognostic option is now being tested and refined.

The ability to use a centered pseudo-fourth order transport scheme for all model prognostic variables is now available and is undergoing evaluation. An option to transport water vapor and/or selected tracers with the NCAR semi-Lagrangian algorithm has been added, and is being tested.

Additional flexibility is being added to the SKYHI model structure. The ability to run SKYHI with arbitrary vertical and horizontal resolution is being developed, requiring that initial data for an arbitrary model structure be easily produced, and that the data generated by an arbitrarily configured model be readily analyzable. Procedures to provide these capabilities are under development. The ability to calculate and archive zonal integrals as the model is being integrated is also now available.

3.2.2 SKYHI Control Integrations and Basic Model Climatology

The control integration with the 40-level 1° x 1.2° latitude-longitude version of the SKYHI model was continued. The portion completed on the CRAY YMP and C90 with no changes in model formulation now extends for over 24 months. Another integration starting from early

March (using initial conditions slightly perturbed from the main control run) of the second year was undertaken and continued into July. These integrations have resulted in three independent realizations of the June-early July period which were used in comparison with the even higher resolution experiment discussed in 3.2.4. An extended integration of a version of the model with 48 levels up to about 95 km has begun. Preliminary results suggest that the mesospheric zonal jet structures and the eddy driving in the mesosphere are not greatly affected by raising the model top.

3.2.3 Studies of Diurnal Variability

A diurnal integration of a version of the SKYHI model with enhanced vertical resolution and extending up to ~95 km has been commenced. This will be analyzed to examine tidal behavior in the mesosphere and lower thermosphere.

The role of latent heat release in forcing the upward-propagating diurnal tide is a subject of a collaboration with J. Forbes (University of Colorado) and M. Hagan (NCAR). A linear tidal calculation forced with a diurnal heating source modelled roughly on the observed diurnal rainfall oscillation has been performed. Results suggest that the latent heat forcing may produce non-migrating tidal components that can account for a significant fraction of the diurnal wind variance in the tropical mesosphere.

3.2.4 High Resolution Integration with SKYHI

The integration of a version of the 40-level SKYHI model with 0.6° x 0.72° latitude-longitude resolution was extended from early May into early July. Analysis of the results has proceeded, concentrating on a comparison of the SH winter circulation with that found in lower resolution versions of the model. The most striking aspect of the middle atmospheric circulation in the high resolution experiment is the considerable improvement in the simulation of the polar night jet and associated high-latitude temperature structure. The peak jet strength in the 0.6° x 0.72° simulation is about 110 $m\text{-}s^{-1}$. While this is still stronger than observed, it is a substantial improvement (by ~20 $m\text{-}s^{-1}$) over the 1° x 1.2° results. The jet structure is also much more realistic in the high resolution model, notably in displaying an equatorward tilt with height in the mesosphere. It appears that the 0.6° x 0.72° SKYHI model is the first GCM without an imposed drag that has captured this feature of the SH winter circulation.

While the middle atmospheric circulation in SH winter clearly improves when the model resolution is increased to 0.6° x 0.72°, there are aspects of the tropospheric circulation that become less realistic. In particular, both the meridional eddy transport of zonal momentum and the strength of the midlatitude surface westerly winds are increased to unrealistically strong values in the high resolution model. Many moderate resolution GCMs include a topographic gravity wave drag parameterization to reduce the surface westerlies in the NH. Since topographic drag is presumably much less important in the SH, the present results suggest that when GCMs are run at very high resolution the problem of excessive surface westerlies may emerge in the SH.

3.2.5 Resolved Gravity Waves in the SKYHI Model

Analysis of the resolved gravity wave field in the SKYHI control simulations has continued. Earlier results of spectral analysis of the waves have been summarized and updated (1376). In collaboration with M. Charron (McGill University), a modified principal component analysis of the wind and temperature field over continental-sized regions has been undertaken. The procedure adopted successfully isolates nearly monochromatic gravity wavetrains in the model fields.

A project in collaboration with R. Sica (University of Western Ontario) to compare the high-frequency variability in the SKYHI simulation with lidar data has commenced.

3.2.6 Parameterized Gravity Wave Drag in the SKYHI Model

An experiment was undertaken to diagnose the zonal drag needed to bring the 3° x 3.6° SKYHI model simulation of the zonal-mean middle atmospheric circulation into close agreement with observations. Near the solstices the results indicate that the model needs strong westerly (easterly) drag in the summer (winter) extratropical mesosphere. This is in accord with the basic notions of the effects of the filtering of a broad gravity wave spectrum during propagation through the polar night (summertime easterly) jet and subsequent wave breaking at high levels. The inferred drag was compared with that predicted by the gravity wave parameterization scheme of Lindzen. With reasonable values of the wave input parameters, the parameterization can capture many of the features of the diagnosed solstitial drag distribution, but only if some modification of the Lindzen procedure is adopted to allow the region of parameterized wave breaking to extend to lower heights (cr). Some preliminary integrations of the SKYHI model including a version of the Lindzen scheme have also been completed and are being analyzed.

3.2.7 GCM Simulation with an Imposed Tropical Quasi-biennial Oscillation

The simulation using the 3° x 3.6° SKYHI model with an imposed zonal momentum source designed to force a realistic quasi-biennial oscillation (QBO) in the tropical stratosphere was continued for 48 years. The imposed forcing was restricted to within about 20° of the equator and above 100 mb, and it succeeds in forcing rather realistic wind and temperature QBOs within the tropics. Interestingly, the model simulation of the tropical mean winds shows the observed asymmetry between the strength of westerly and easterly QBO shear zones, as well as the observed tendency for the initial westerly QBO accelerations to appear in a narrow region near the equator. Neither of these features is explicitly included in the imposed momentum source.

The model results have been extensively analyzed to look for the global effects of the tropical QBO. Fig. 3.3 shows the correlation coefficient for the boreal winter, zonal-mean wind at all latitudes and heights with the equatorial value at 40 mb. This is based on the last 45 years of the experiment and, assuming 45 independent samples, any values of the correlation coefficient greater in magnitude than 0.288 are significant at the 95% level. Only contours for these statistically-significant regions are plotted. The stacked positive, negative and positive regions right on the equator simply reflect the downward propagation of the imposed QBO

winds in the model. The region of positive correlation at high latitudes reveals a tendency for the NH winter polar vortex to be weaker when the equatorial middle stratospheric winds are easterly. This effect has been found in many earlier observational studies, and the distribution shown in Fig. 3.3 has a strong resemblance to the comparable observational result presented by Baldwin and Dunkerton[1]. The model results also show that the mean NH winter planetary wave structure in the stratosphere is affected by the phase of the QBO, with more intense waves seen at high latitudes during the easterly QBO phase. Again this aspect of the model simulation has a very strong resemblance to earlier observations of the QBO effects on NH stationary waves.

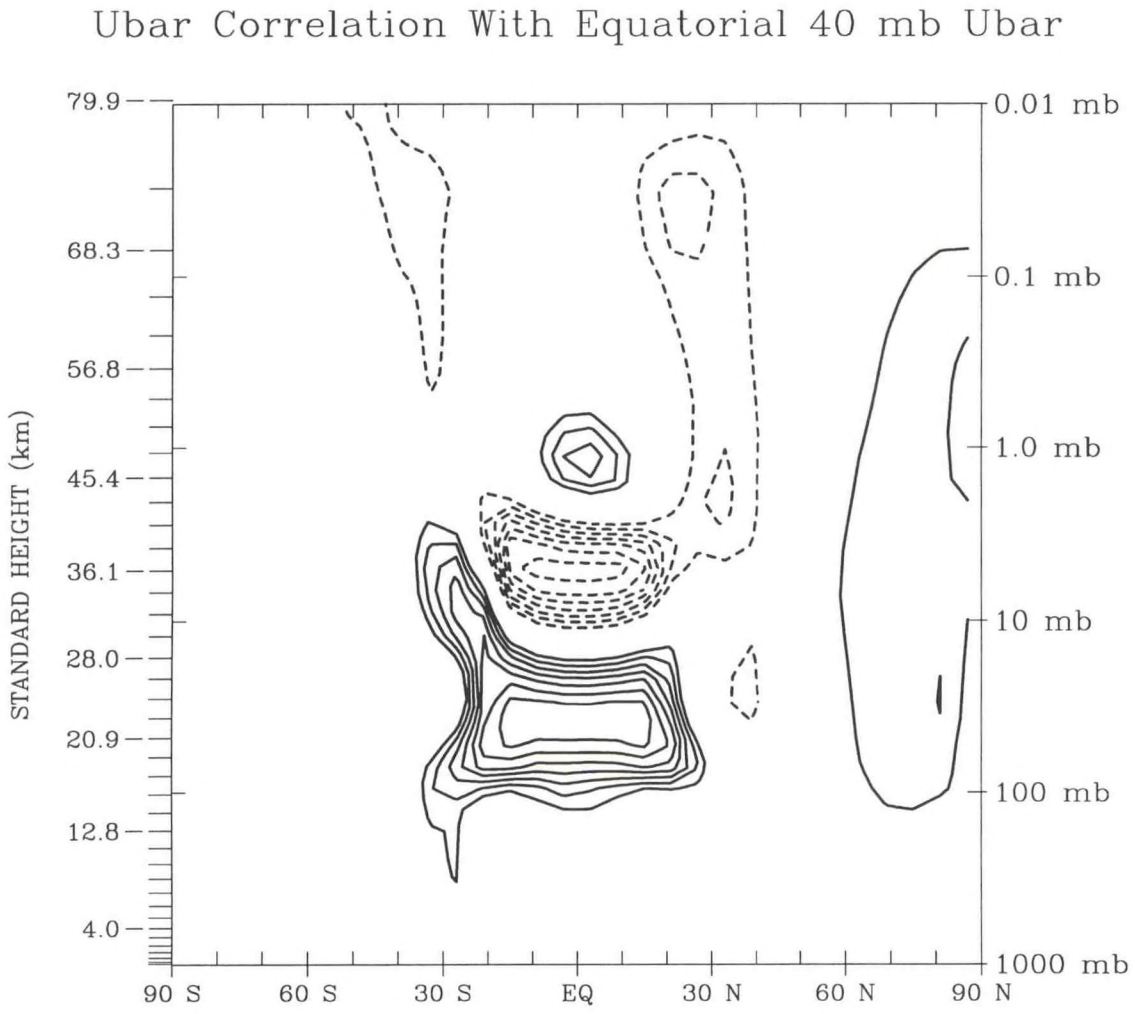

Fig. 3.3 The correlation coefficient between the December-February zonal mean zonal wind with the equatorial zonal wind at 40 mb. Results from 45 years of the QBO SKYHI experiment. The contour interval is 0.1 and negative correlations are denoted by dashed contours. Only contours for values with magnitude greater than or equal to 0.3 are plotted.

1. Baldwin, Mark P., and Timothy J. Dunkerton, Quasi-Biennial Oscillation Above 10 mb, *Geophysical Research Letters, 18*, 1205-1208, 1991.

A very interesting aspect of Fig. 3.3 is the region of positive correlation that extends into the SH subtropical troposphere. This indicates a statistically-significant tropospheric effect of the stratospheric QBO. While this effect in the model is fairly modest (about 1 $m\text{-}s^{-1}$ difference in mean wind strength in the upper troposphere between easterly and westerly QBO phases), the result does have implications for extended range weather forecasting. The stratospheric QBO is the one aspect of atmospheric circulation that clearly can be predicted with skill for periods up to 1 year. If the SKYHI model QBO-troposphere connection holds in the real atmosphere as well, then QBO forecasts could provide useful input to extended range weather predictions for the SH.

3.2.8 GCM Simulation of the Ozone Quasi-biennial Oscillation

An integration of the SKYHI model with stratospheric chemistry and incorporating the QBO forcing described in 3.2.7 has now proceeded for one complete QBO cycle (27 months). Fig. 3.4 shows that the simulation is able to produce a reasonable peak-to-peak ozone QBO amplitude of about 25 DU. The total ozone QBO is also in phase with the maximum westerlies and warmest temperatures at 40 hPa, in agreement with observations and theory. These results

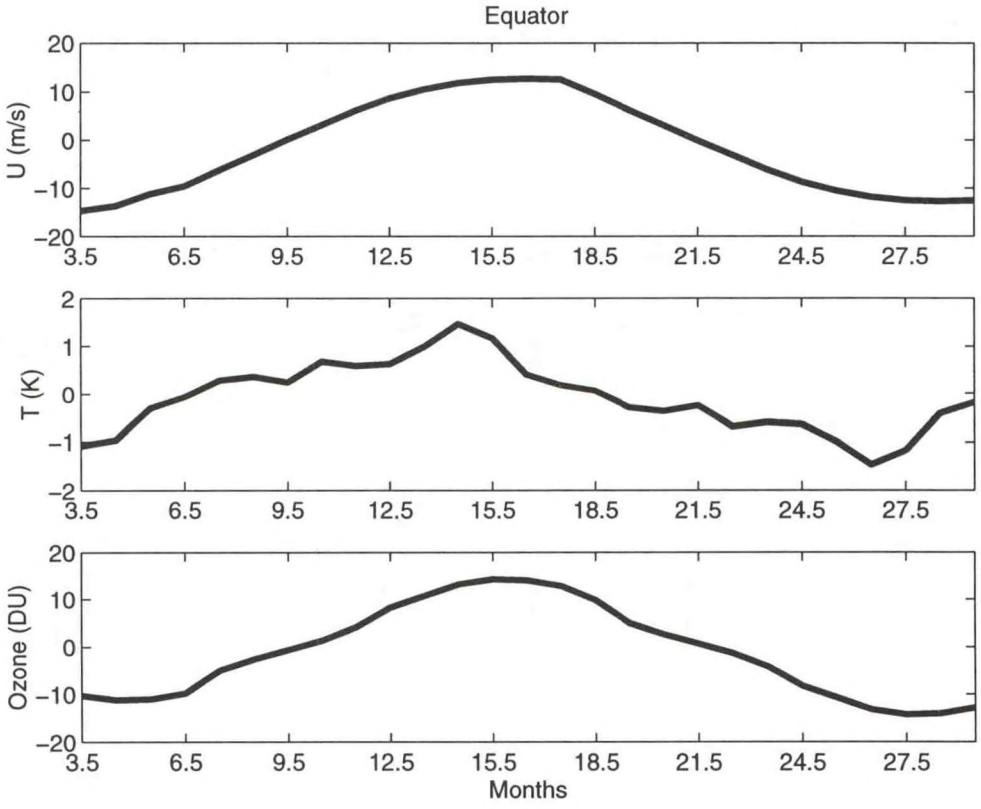

Fig. 3.4 Monthly averaged 40 mb equatorial zonal wind (top), temperature (middle), and total column ozone (bottom). All harmonics of the annual cycle have been removed from the time series. The amplitude of the ozone variation, and its correlation with the winds and temperatures at 40 mb, are in good agreement with observations and theory, indicating reasonable performance on the part of the photochemical model.

suggest that the photochemical model is producing reasonable ozone profiles in the tropics, although the calculated total ozone columns tend to be 10-15% higher than observed. This difference is likely due to the lack of halogen chemistry in the model. Although one QBO cycle may be used to examine transport differences between the westerly and easterly phases, a model run covering at least four QBO cycles with halogen chemistry included is currently in preparation.

3.2.9 Tropical Waves Observed in High-Resolution Radiosonde Data

Very high resolution radiosonde data taken at six stations in the tropical Western Pacific during 120 days of the TOGA-COARE have been analyzed. At very long periods some rather coherent temperature fluctuations are seen near the tropopause and in the lowest part of the stratosphere. Fig. 3.5 shows the height-time temperature fluctuations at Majuro (7°N, 171°E) filtered to include periods between 30 and 40 days. Between about 16 and 20 km a wave with downward phase propagation and vertical wavelength ~3 km can be clearly seen. This oscillation has counterparts in the temperature data at the other low latitude stations. The temperature fluctuations in the 30-40 day band appear quite coherent even over the 35° longitude spread of the stations considered. The temperature perturbations travel eastward with a phase speed of about 3 $m\text{-}s^{-1}$. This phenomenon is reasonably attributed to a large-scale equatorial Kelvin wave that is the stratospheric expression of the familiar intraseasonal oscillations of the tropical troposphere.

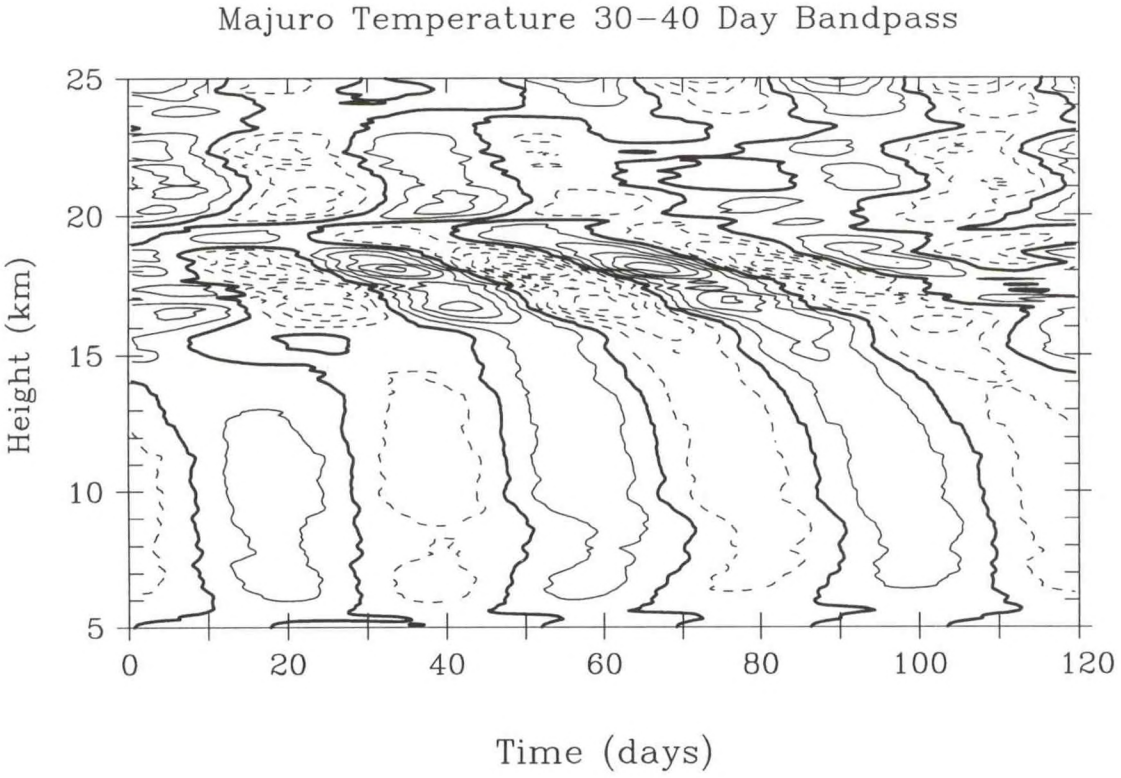

Fig. 3.5 Height-time section of radiosonde observations of temperature at Majuro for the period November 1, 1992 through February 28 1993. The data have been band-passed to retain only periods between 30 and 40 days. The contour interval is 0.4°C and dashed contours are used for negative values.

The very short vertical wavelength seen near the tropopause in Fig. 3.5 make this phenomenon extremely difficult to observe with either satellite data or radiosonde data as conventionally archived. Thus the present results illustrate the importance of routinely archiving radiosonde data at very high resolution. Earlier studies (*e.g.*, 1341) have shown how such data can be used in examining small scale variability at individual stations. The present study has shown the value of the high resolution data in the investigation of planetary-scale phenomena.

3.2.10 SKYHI Simulations with an Imposed Kelvin Wave Forcing

Integrations of the SKYHI model in which a single upward-propagating monochromatic Kelvin wave was excited by an imposed arbitrary heating were described in A95/P96. These have been repeated with the 2° x 2.4° version of the model. Analysis of earlier integrations with the 3° x 3.6° model indicated that the subgrid-scale vertical mixing parameterizations were crucial for the dissipation of the Kelvin wave in the tropical mesosphere. This should be even more evident in a higher-resolution model with a more complete spectrum of explicitly resolved gravity waves.

3.2.11 Tropical Gravity Waves Simulated by the High-Resolution SKYHI Model

It has previously been hypothesized (1272), on the basis of wave analysis of SKYHI and observed tropical transient waves, that the vertical momentum flux due to small-scale gravity waves could play a more important role than large-scale Kelvin and mixed Rossby-gravity waves in the forcing of the quasi-biennial oscillation (QBO) in the tropical stratosphere. It has also been hypothesized that these waves could be triggered by the intermittent onset of moist convection. The latter hypothesis is consistent with control experiments with an idealized general circulation model having moist convective adjustment (az). In order to examine the effect of horizontal resolution on convective heating and gravity-wave momentum flux, tropical gravity waves simulated by a high-resolution (0.6° x 0.72° latitude-longitude grid size) SKYHI model (ck), integrated at the Los Alamos National Laboratory, have been compared with those simulated by lower-resolution (3.0° x 3.6° and 1.0° x 1.2°) SKYHI models integrated at GFDL.

As illustrated in Fig. 3.6, grid-scale precipitation becomes more confined in space and time as the resolution is increased. The grid-scale precipitation mimics observed cloud clusters and is organized into planetary-scale superclusters. The westward propagation of cloud clusters and eastward propagation of superclusters are better simulated in the high-resolution model. The model results also indicate that the stratospheric gravity-wave momentum flux is dominated by high-frequency components having periods shorter than one day, although the high- and low-frequency components are associated with comparable values of kinetic energy. The momentum flux is doubled as the resolution is increased from 3.0° x 3.6° to 0.6° x 0.72°. The 3.0° x 3.6° SKYHI model simulates only a very weak QBO (1274). A further increase in the horizontal and vertical resolutions could substantially enhance the gravity-wave momentum flux convergence and thus the model-simulated QBO.

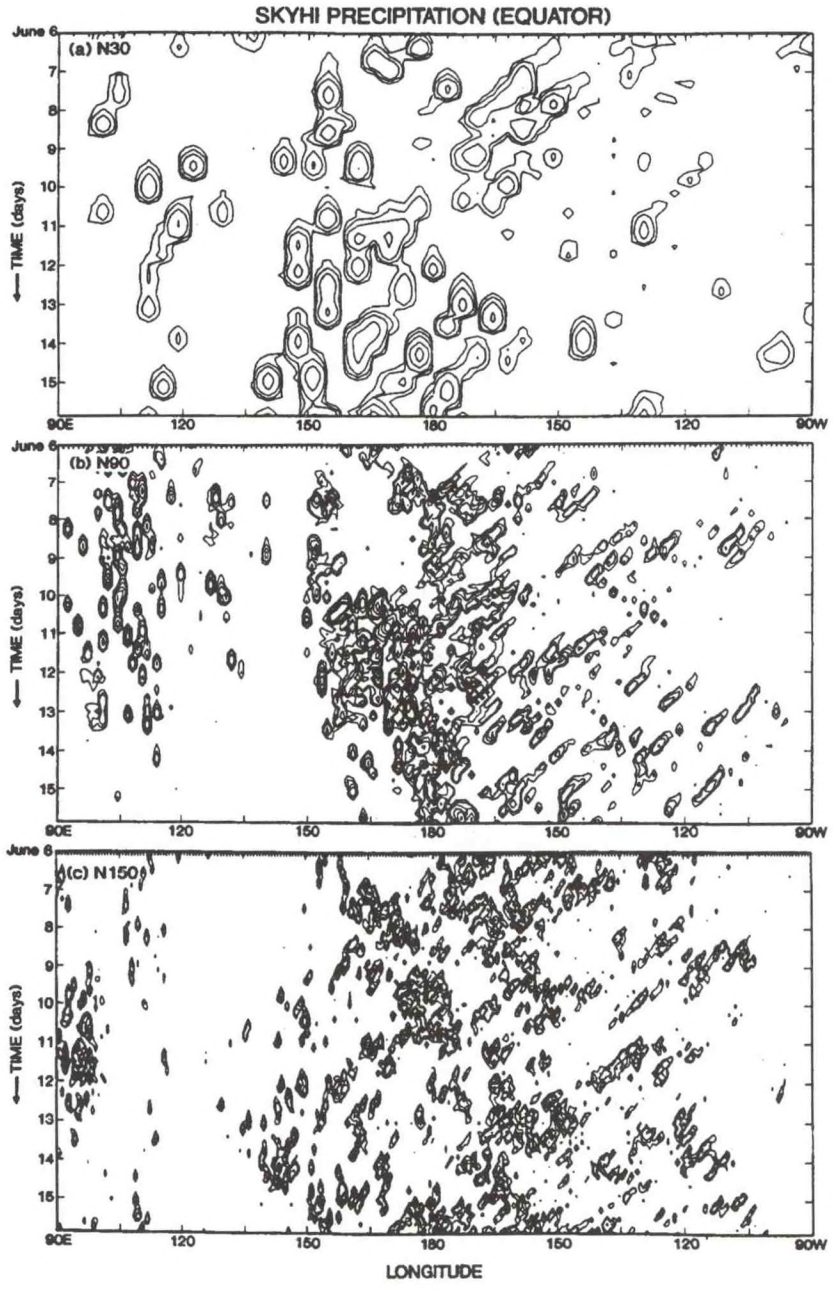

Fig. 3.6 Longitude-time distributions of three-hourly equatorial precipitation over 90°E-90°W during June 6-16 simulated by SKYHI models having latitude-longitude resolutions of (a) 3.0° x 3.6°, (b) 1.0° x 1.2°, and (c) 0.6° x 0.72°.

3.2.12 Dynamics of the Martian Atmosphere

Dust in the Martian atmosphere has a profound influence on the dynamics of the general circulation as a consequence of radiative effects. In particular, winds associated with the Hadley circulation and the thermal tides respond strongly to the evolving spatial distribution of aerosol-induced heating. In turn, the circulation plays a major role in determining the sources, sinks and transport of the dust. In an effort to explore this interaction, annual cycle simulations for a variety of dust scenarios have been carried out with the recently developed Mars GCM. This model has been derived from the SKYHI model and incorporates aerosol transport, radiation parameterizations for a variably dusty atmosphere, and surface physics for the CO_2 condensation cycle. A more detailed description of the model, as well as some features of the simulations and an extensive discussion of the thermal tides, are given in (1370).

A critical element of this work is the comparison of the model circulation with available observations. A notable success has been the realistic simulation of a winter hemisphere polar warming observed by the Viking orbiters following the onset of a global dust storm. The simulated warming is largely a result of the expansion of the Hadley circulation due to the increased heating from a deep and broad distribution of aerosol. The simulations indicate a marked decrease in transient and stationary wave activity as the polar warming develops. This is consistent with the distribution of potential vorticity such that the region of strong meridional gradient is tightly confined to the polar cap and elsewhere is almost uniformly near-zero. The evolution towards a relatively symmetric state is in contrast to the case of the terrestrial stratospheric sudden warming where the transience of forced, near-stationary planetary waves plays a dominant role.

Analysis is continuing on characterizing the influence of topography on the near-surface winds. For example, the near-surface winds associated with the thermal tides are strongly modified by the local topographic slope, and the lower branch of the Hadley circulation is modulated by the planetary scale topography. These effects are likely to be significant for transport of dust and water vapor. Work has begun on relating dust-raising to the local surface stress.

PLANS FY97

The assembly of the various independently produced pieces for the SKYHI upgrade will be completed and a new standard version of the model will be produced.

Development of the procedures needed to both generate initial data and analyze model output for models with arbitrary resolution will continue.

Further analyses of the tropical gravity-wave activity simulated by high- and low-resolution SKYHI models, as related to the QBO, will be performed.

Integrations of SKYHI with both high vertical and horizontal resolution will be run on the GFDL CRAY T90 to evaluate model errors and the viability of the SKYHI subscale closure parameterizations.

Integrations of SKYHI with parameterizations of stratospheric and mesospheric gravity wave drag will continue.

Investigation of the diurnal cycle in the SKYHI model will continue.

Analysis of the SKYHI experiments with imposed QBO forcing will continue.

An extended QBO experiment with stratospheric photochemistry will be run.

The comparison of small-scale wind and temperature variations in the SKYHI GCM with lidar, rocket, and radar observations will continue.

Development of a simple, dry, planar-geometry model for studies of vertical wave propagation will continue.

Investigation will continue into the behavior and effects of breaking gravity waves under a variety of physical conditions to evaluate their quantitative effects on the large-scale circulation.

Parameterization of dust lifting based on surface stress will be developed for the Mars GCM to examine the role of feedback between dust lifting by the tidal and Hadley circulations and subsequent increased solar heating in obtaining a global dust storm initiation. This will involve a careful examination and treatment of the boundary layer.

4. EXPERIMENTAL PREDICTION

GOALS

To develop methods of stochastic-dynamic prediction capable of extracting as much useful forecast information as possible from numerical prediction models given imperfectly observed initial conditions.

To develop and improve numerical models of the atmosphere-ocean-land system in order to produce useful forecasts with lead times of several weeks, months, seasons or years.

To understand the limits of predictability of the ocean-atmosphere system with emphasis on quantifying the amount of useful forecast information that could be available at lead times of several weeks, months, seasons or years.

To develop methods for the assimilation of ocean observations into dynamical models in order to improve predictions of the ocean and atmosphere.

4.1 STOCHASTIC-DYNAMIC PREDICTION

J. Anderson *A. Wittenberg*
J. Ploshay

ACTIVITIES FY96

4.1.1 Selection of Initial Conditions for Ensembles

A fundamental problem in ensemble prediction is the selection of initial conditions for different ensemble forecast members (1355). Operational atmospheric prediction centers have developed techniques for selecting ensemble initial conditions. Most of these techniques are predicated on the notion that constraints derived from the dynamics of the forecast model should be used to constrain the initial conditions (ca). A set of simple dynamical systems has been used to demonstrate that the use of randomly selected initial conditions (bd) (*i.e.*, initial conditions that are consistent with the observational error distribution) is superior to the use of dynamically constrained initial conditions for most standard measures of forecast skill. The most important strength of randomly selected ensemble initial conditions is that there exists a simple analytic theory that describes the characteristics of the resulting ensemble forecasts.

Traditionally, the use of randomly selected initial conditions has been associated with ensembles with insufficient variance. A non-linear normal mode initialization scheme was implemented in a low order dynamical system in order to demonstrate that insufficient

variance is associated with the inappropriate use of dynamic initialization algorithms on ensemble initial conditions. The results from low order systems suggest that the use of randomly selected ensemble initial conditions could improve the usefulness of operational ensemble predictions.

4.1.2 Predictability from Forced Atmospheric Model Ensembles

Long integrations of atmospheric models, forced by observed sea surface temperatures (SSTs) are widely used to bound the potential predictability of the atmosphere (1300). Ensembles of forced integrations of an atmospheric GCM are used to investigate how strongly the atmospheric circulation is constrained by an observed SST pattern. Since the atmosphere is unable to feed back on the ocean in forced integrations, the dynamics of atmosphere-only runs are conceivably different from the dynamics of the coupled ocean-atmosphere system.

Experiments with simple dynamical systems were used to evaluate the validity of using forced atmospheric ensembles to evaluate potential predictability. First, a long integration of a fully-coupled model was performed. An ensemble of runs of the simple atmosphere model was then performed in a forced mode with the ocean prescribed from the fully-coupled integration. Statistical tools were used to show that the forced atmosphere ensemble was inconsistent with the atmospheric portion of the fully-coupled integration. This implies that the use of forced atmosphere GCM integrations to evaluate potential predictability may be unwarranted.

PLANS FY97

An investigation of methods for producing random ensemble initial conditions will be initiated. A study of the characteristics of different types of ensembles in models with systematic errors will provide insight into optimal methods for producing ensemble forecasts. The consistency of SST forced integrations will be investigated using higher order dynamical models of the coupled ocean-atmosphere system.

4.2 DEVELOPMENT OF MONTHLY TO SEASONAL FORECAST MODELS

ACTIVITIES FY96

4.2.1 Atmospheric Model Development

4.2.1.1 Global Atmospheric Grid Point Model

B. Wyman

Development continued on the B-grid atmospheric general circulation model (AGCM) in two phases: an initial conversion from the E-grid (1351) to the B-grid and the reorganization to a modular model. The initial B-grid model was integrated with complete physical parameterizations for up to 10 years at resolutions up to N45L18. The climatology

appears to be superior to that of its E-grid predecessor. In particular, the simulation of the polar night stratosphere has improved.

In the second phase, the B-grid model's dynamics and physical parameterizations (4.2.1.3) were rewritten in a modular format in Fortran-90. All physical parameterizations from the preceding model were converted and testing of the modular version has commenced.

A ten year integration of the E60L25 E-grid Global Eta Model (1351) was completed for both the sigma and eta vertical coordinates. This long integration at higher resolution provides a more robust comparison of the eta and sigma vertical coordinates. Increased vertical resolution added in the boundary layer and stratosphere did not improve the unusually strong polar night jet in the eta coordinate simulation.

4.2.1.2 Spectral Dynamical Core

J. Anderson *P. Phillips*
I. Held *A. Weill-Zrahia*

A flexible spectral dynamical core was written in Fortran-90. This core is designed so that a variety of different spectral models, from barotropic models through complete GCMs, can be constructed using the same core routines. The spectral core provides straightforward support for arbitrary resolution, physical space grid windowing, reduced physical space grids, and generalized semi-implicit timestepping.

A parallel version of the spectral dynamical core's transform routines has been completed and evaluated on several parallel architectures. The transforms were parallelized using the transpose method in which a reorganization of the data takes place before each step of the transform; the data dimension that is required for a particular transform step is always available on a single processor. Reasonable speedups were obtained by the parallel transforms on both a CRAY T3D and IBM SP2.

4.2.1.3 Modular Physics Parameterizations

J. Anderson *W. Stern*
C.T. Gordon *B. Wyman*
J. Sirutis

A complete set of Fortran-90 modular physical parameterizations was written and incorporated into the B-grid AGCM (4.2.1.1). Details involving the allocation of data and interaction between physics modules were examined. Parameterizations currently in the B-grid model include moist convective adjustment, large scale condensation, Mellor-Yamada turbulent closure, Monin-Obukhov similarity theory, surface temperature prediction, Fels-Schwarzkopf radiation, bucket hydrology, and vertical diffusion. A modular version of the Relaxed Arakawa-Schubert (RAS) cumulus convection parameterization scheme was also written and tested in the B-grid atmospheric model. A modular mountain gravity wave drag scheme was completed and work has begun on a modular version of a predicted cloud scheme (1097).

4.2.1.4 Support Tools for Modular Models

J. Anderson *J. Ploshay*

Several support tools for modular GCMs were written using Fortran-90 and object-oriented coding techniques. Standard error-handler and diagnostic output tools were completed and are in use in the B-grid AGCM (4.2.1.1). The diagnostic output tool provides data buffering and averaging and produces output in NetCDF (network Common Data Form). Work is underway on a tool that will manage time and date calculations for both single model and coupled model integrations.

4.2.1.5 Development of Subgrid-scale Parameterizations

C.T. Gordon *J. Sirutis*
S. Klein *W. Stern*

The RAS cumulus convection parameterization scheme was incorporated in the spectral AGCM. A parameterization for the evaporation of convective scale precipitation was also developed and included in the spectral model as part of the RAS package. Without the evaporation of convective scale precipitation, the lower part of the atmosphere was too dry compared to the full Arakawa-Schubert scheme and observations.

A prognostic cloud water parameterization, based upon the Del Genio formulation, is being developed. The scheme incorporates bulk parameterizations of various cloud microphysical processes.

4.2.2 Ocean Model Development

4.2.2.1 Ocean Model Simulations

R. Gudgel *A. Rosati*
M. Harrison

To calibrate the ocean component of the coupled model, the MOM ocean model was driven with operational wind analyses. These simulations were compared to observations and systematic model errors and the impact of surface forcing were evaluated. The model was upgraded to MOM 2 and the vertical resolution increased to 50 levels, with 30 levels in the upper 225 m. Preliminary results show an improvement in the simulation of the upper ocean thermal structure, particularly the equatorial thermocline, compared to the previous 15 level model.

A comparison of observed wind stress products is underway. This study contrasts the climatologies and the interannual variability of the COADS, Hellerman-Rosenstein, FSU, and NCEP reanalysis products. The ECMWF reanalysis will soon be included in this comparison. One finding is that the NCEP reanalysis appears to have unrealistically weak equatorial trade winds.

4.2.2.2 Sensitivity to Subgrid Scale Parameterizations

The implementation of the TAO moorings in the equatorial Pacific offers a unique opportunity to compare model simulations to observations. Based on findings from such comparisons, the horizontal and vertical mixing schemes are being modified to better represent the thermal and current structure observed at the mooring sites.

4.2.2.3 Isopycnal Diffusion Schemes

S. Griffies

An analysis of the parameterization of ocean tracer diffusion, which occurs predominantly along isopycnal surfaces, has led to the implementation and testing of a new isopycnal diffusion scheme in the GFDL MOM2 ocean model. In collaboration with the Ocean Group, extensive tests are underway for this scheme in order to fine-tune its details.

PLANS FY97

B-grid model development will focus on testing additional physics modules, optimizing performance, and reducing model bias. Additional parameterizations to be incorporated into the model include predicted cloud schemes (for convective and stratiform clouds), prognostic cloud water, the RAS convective scheme, and mountain gravity wave drag. The object-oriented date-time tool will be completed and incorporated in the B-grid model. The B-grid model will be extensively tested in coupled model integrations with the 50-level ocean model.

A soil/vegetation/atmosphere transfer model will be developed and incorporated in the B-grid atmospheric model. This model will, hopefully, yield the benefits of including the effects of vegetation on the surface fluxes without the complexity and cost of the full SiB (Simple Biosphere) model.

Implementation of the flexible spectral core will be completed. An AGCM will be constructed around the spectral core and evaluated for use as a seasonal prediction model. The complete array of modular parameterizations originally developed in the B-grid model will be tested in the spectral model.

The isopycnal diffusion scheme will be incorporated into the ocean model in order to assess the impact of a more adiabatic ocean model on processes affecting equatorial and midlatitude ocean and coupled ocean-atmosphere dynamics.

Blocking frequency will be examined in the 10 year integrations of the E60L25 E-grid models and compared to the NMC reanalysis data.

The comparison of various wind stress products and their impact on ocean simulations will continue. Ocean model integrations with various configurations of subgrid-scale parameterizations will be compared to observations.

4.3 ATMOSPHERIC AND OCEANIC PREDICTION AND PREDICTABILITY

ACTIVITIES FY96

4.3.1 ENSO Forecasts

T. Gordon *A. Rosati*
R. Gudgel *J. Sirutis*

Ten 18-month coupled model forecasts were produced for the period 1985-1994 utilizing a T42L18 atmospheric model with Arakawa-Schubert convection (cl) and prescribed ISCCP low level clouds. Comparison with previous forecasts (xt) shows a westward shift of the region of highest skill and increased skill in the North Pacific. Ten year integrations of the coupled model show that the model's tropical Pacific SST oscillates with variance 0.8°C and maximum amplitude in March compared to the observed variance of 1.5°C with a maximum in January.

4.3.2 Coupled Model Predictability

J. Anderson *R. Gudgel*

A five-member ensemble of fully-coupled, one year model predictions was produced starting from 1 January of each year from 1985 through 1994. The potential predictability (1365) of both the SSTs and the atmospheric variables was evaluated as a function of forecast lead time for each year. A forecast for a given scalar quantity (*i.e.*, SST at a single ocean point) in a given year is said to be potentially predictable if the ensemble distribution for that year is significantly different from the model climatological distribution for the same forecast lead time. Although much of the potentially predictable SSTs were in the tropical Pacific Ocean, large areas of potential predictability were also found in the extratropical oceans for lead times exceeding six months (Fig. 4.1). Atmospheric quantities are also found to retain limited amounts of potential predictability for several seasons (Fig. 4.2). Results to date indicate that potential predictability results obtained from AGCMs forced by observed SSTs are significantly overoptimistic (4.1.2). Despite this, there do appear to be areas in the extratropics for which important atmospheric fields are potentially predictable for lead times of at least several seasons.

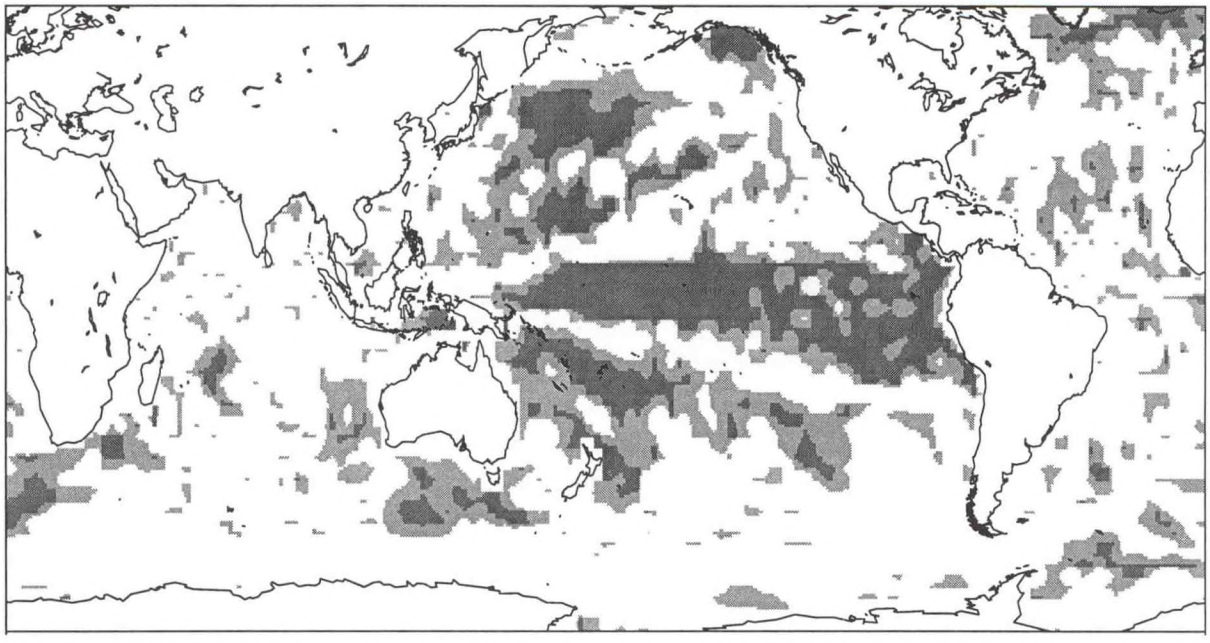

Fig. 4.1 Potential predictability of SST for 6-month lead ensemble forecast valid June 1989. Light shading indicates 90% confidence and dark shading 99% confidence. With this model, one could hope to make a useful 6-month prediction of SSTs only in the shaded regions.

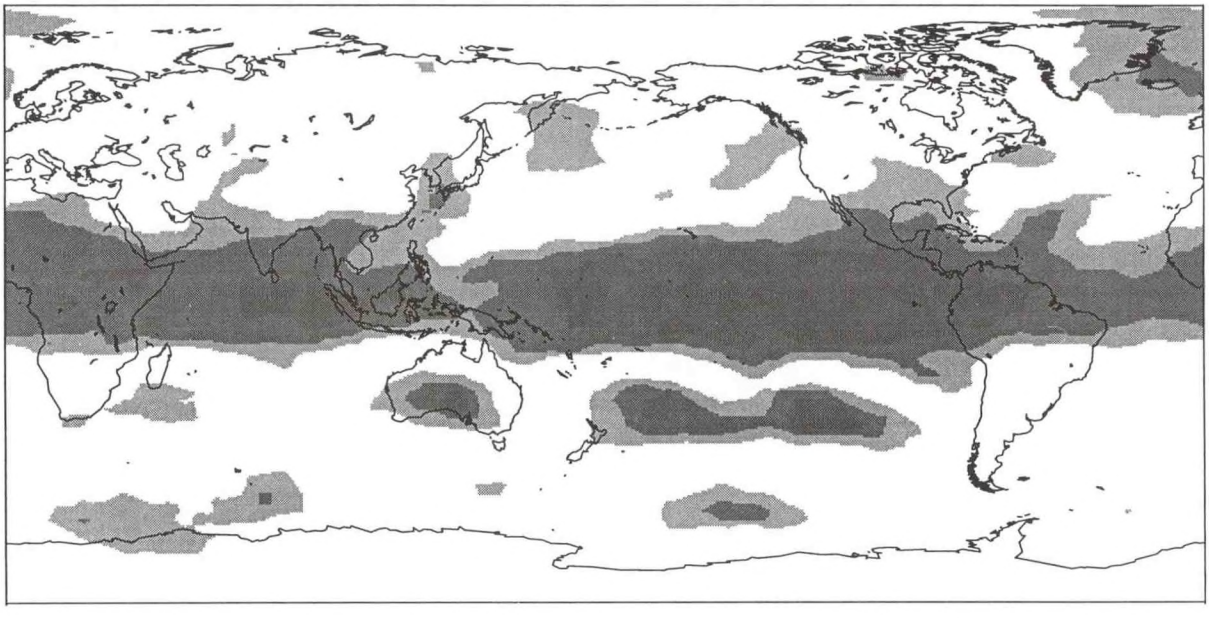

Fig 4.2 Potential predictability of 300 hPa heights for 6-month lead ensemble forecast valid June, 1989. Light shading indicates 90% confidence and dark shading 99% confidence. The shaded regions are those where one might hope to make a useful 6-month prediction of the upper tropospheric circulation with this model.

4.3.3 Impact of Improved Seasonal Cycle on Seasonal Forecasts

C.T. Gordon *A. Rosati*
R. Gudgel *J. Sirutis*

In coupled model forecasts with predicted low clouds over the ocean, the marine stratus cloud regime in the tropical eastern Pacific is not adequately simulated. This was rectified in a set of forecasts by specifying low clouds from the monthly mean climatology of ISCCP (International Satellite Cloud Climatology Project). The annual cycle of SST in the equatorial eastern Pacific is significantly amplified in the latter forecasts, consistent with previous results from multi-year integrations (cn). The correlation between predicted and observed monthly mean SST anomalies improves substantially at lead times of 12 to 18 months. The improvement in forecast skill is apparently due to dynamical feedbacks, since the dominant local radiative forcing is located further east.

In the western tropical Pacific the coupled model exhibits a cold bias in SST. This bias was increased when the ISCCP low level clouds were used. The coupled model was found to be very sensitive to the convective parameterization scheme. Replacing the moist convective adjustment scheme with RAS led to a significant reduction in the cold bias. Daily values of the components of the surface heat balance were compared to observations revealing that excessive long wave and evaporative fluxes were the source of the SST cooling.

4.3.4 Sensitivity of Seasonal Forecasts to Subgrid-Scale Parameterizations

C.T. Gordon *W. Stern*

The sensitivity of the Asian Summer Monsoon simulated by an AGCM with specified SSTs to changes in initial snow depth, specified field capacity of soil moisture, and snow albedo parameterization over the Tibetan Plateau. Analyses indicate that the hydrologic spin-up time for snow cover in the Tibetan region is greatly increased if the initial snow depth is artificially enhanced. Also, the spin-up time is shorter and the seasonal snow melt occurs slightly earlier using an updated snow albedo parameterization; this improved climatology for snow-cover may improve the simulation of the monsoon circulation.

4.3.5 Simulation of Intraseasonal Variability in the Tropics

J. Anderson *W. Stern*
R. Smith

An ensemble approach was used to investigate the behavior of tropical intraseasonal oscillations (TIO) in the spectral AGCM forced by observed SSTs. Ensemble mean power spectra from the collection of nine T42L18 integrations are plotted for each year from 1980 to 1988 in Fig. 4.3. The time mean GCM spectra has a peak at 30 days (zs) while observations peak at 45 to 60 days. Statistical tools applied to the ensemble suggest that the simulated interannual variability of these modes is significant; in particular 1982 and 1984 show high levels of significance (cj). This hint of a relationship between TIO and ENSO suggests that it is possible that TIO must be properly simulated in the coupled model in order to reliably predict ENSO onset.

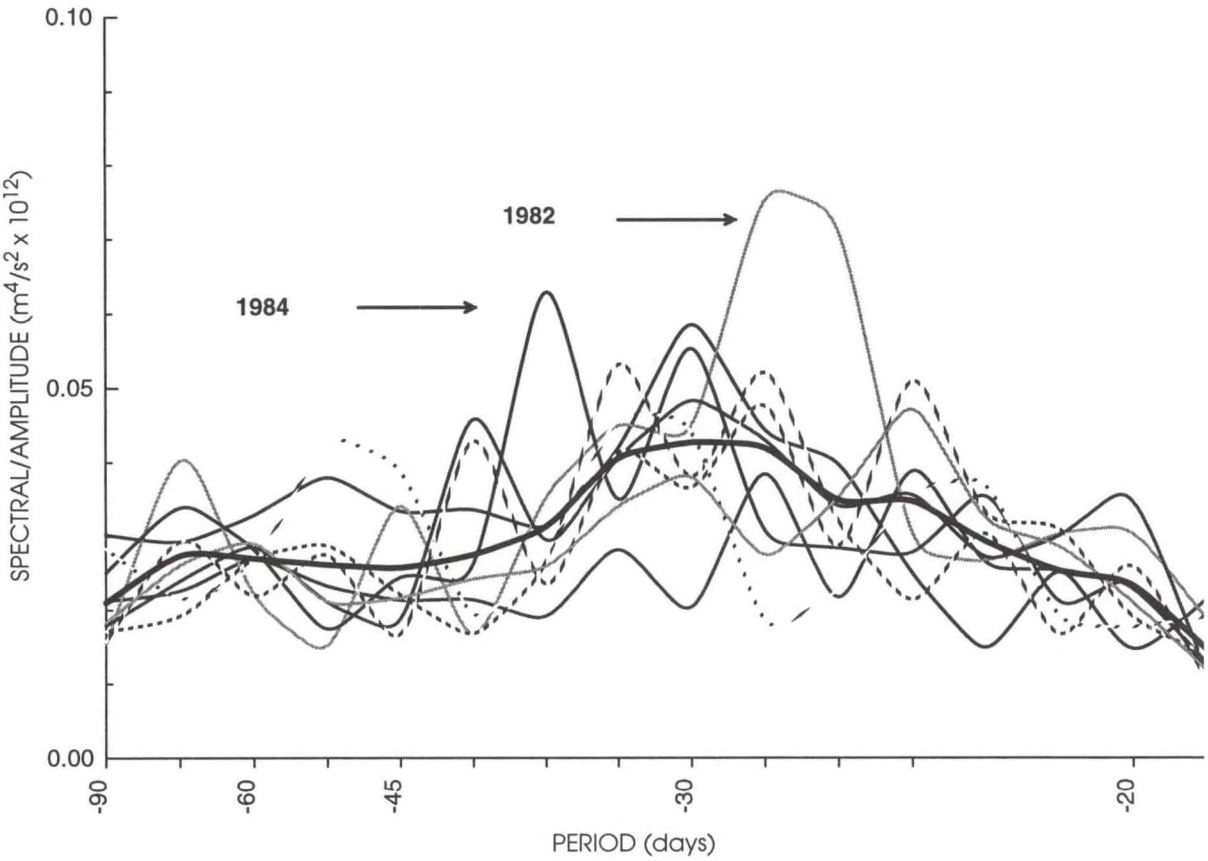

Fig. 4.3 GCM ensemble mean wavenumber 1 power spectra for χ_{850}. 80-88 climatology is indicated in bold. The details of tropical intrasesaonal oscillations may be predictable in years like 1982 and 1984. Successful prediction of these tropical oscillations may lead to improved forecasts of ENSO.

4.3.6 Simulation of Tropical Storm Frequency

J. Anderson F. Vitart

A nine-member ensemble of 10-year integrations of a spectral AGCM forced by observed SSTs has been studied to investigate the potential for producing forecasts of the expected number of tropical storms during a given season with lead times of a season or more. Both the potential predictability and the verisimilitude of the ensemble simulation have been carefully evaluated with a number of statistical tools. The simulations are found to be of high quality over some ocean basins including the North Atlantic (bt). In addition, there is good agreement between measures of potential predictability and simulation quality; this means that when the ensemble spread is small (*i.e.*, the model is quite sure about how many tropical storms will occur) the number of storms simulated is close to that observed. Despite the caveats raised in section 4.1.2, this study suggests that coupled GCMs may be able to produce skillful forecasts of the number of tropical storms in the North Atlantic with lead times of several seasons.

The interaction between the large scale circulation and tropical storm frequency simulated by the ensemble is under investigation. Vertical wind shear and low level vorticity seem to play an important role in the model tropical storm frequency, as has been found previously in observations.

4.3.7 Atmospheric Initial Conditions for Coupled Model Predictions

J. Anderson *A. Rosati*
R. Gudgel

Integrations of coupled forecast models to lead times of one year have shown unexpected dependence on the details of the atmospheric initial conditions. Integrations in which ocean initial conditions for a given year are combined with atmospheric initial conditions for a different year are found to be significantly different from integrations in which atmospheric initial conditions are for the same year as the ocean. Although this result appears intuitively obvious, it is contrary to the generally accepted notion that the atmosphere rapidly adjusts to the ocean initial condition so that details of the atmospheric initial condition can be viewed as noise. This result may indicate that coupled assimilation algorithms will eventually be an essential part of an optimal coupled model seasonal prediction system.

4.3.8 Thermohaline Circulation Predictability and Impacts of Coupling Frequency

K. Bryan *E. Tziperman*
S. Griffies

A major goal of current research programs, such as NOAA's Atlantic Climate Change Program and the World Ocean Circulation Experiment, is to quantify our ability to forecast low-frequency climate fluctuations. An effort is underway to characterize the predictability of the GFDL climate model's thermohaline variability in hopes of gaining insight for use in the forecasting of such natural phenomena. Work has produced a characterization of the dominant spatial patterns of this variability in the model's North Atlantic as well as their ensemble predictability (cm). Most notably, the results indicate that the dominant modes of dynamic topography are quite predictable for 10-15 years. Additionally, the amount of predictability appears to be directly related to the amplitude of the decadal variability, larger decadal variability implying enhanced predictability.

PLANS FY97

Additional ENSO forecasts will be made to clarify the role of the annual cycle in interannual variability. The interdecadal sensitivity of ENSO forecast skill to realistic marine stratus clouds will be further examined. The coupled model's response to observed cloud radiative forcing will be explored. For this purpose, high, middle, and low cloud amount and cloud optical depth fields will be specified, globally, from ISCCP data.

Analysis of seasonal coupled model ensemble forecasts will be extended to compare the ensemble distributions to observations for a variety of ocean and atmosphere fields (yy). In particular, the skill of coupled GCMs in predicting the frequency of tropical storm occurrence with seasonal lead times will be evaluated. Additional ensemble members will be

produced to increase statistical confidence and to examine predictions started from other seasons.

Analysis of cloud/convection/radiation feedback will continue with an emphasis on the sensitivity to air-sea exchanges. The surface heat balance processes and winds of the coupled model will be compared to observations from TOGA-COARE and TAO moorings.

Analysis of TIO's from coupled GCM ensembles and an investigation of the sensitivity of the TIO to changes in the convective parameterization will be performed. Studying the TIO from longer integrations that sample more ENSO cycles should help to clarify the relationship between the two tropical phenomena.

The equatorial temporal variability of surface fluxes and other variables from long term coupled and uncoupled GCM integrations will be analyzed. Results from the latter integrations (with specified SSTs) will be compared with NCEP re-analyses and COADS analyses.

The preliminary analysis of decadal oceanic predictability will be completed. The coupled model ensemble experiments have pointed to the relevance of a linear stochastic perspective for understanding the thermohaline variability simulated in the GFDL climate model. Namely, the model's low frequency North Atlantic variability is indicative of a damped linear oscillator (the thermohaline circulation) driven by random forcing (the atmospheric synoptic variability). This framework is being further tested with experiments in which the frequency of coupling between the oceanic and atmospheric portions of the model is altered. Such coupling time experiments are meant to further address questions related to the dependence of the low frequency oceanic response on the high frequency atmospheric variability.

4.4 OCEAN DATA ASSIMILATION

R. Gudgel *M. Harrison*
A. Rosati

ACTIVITIES FY96

An improved quality control procedure has been developed which is general enough that multiple data types and sources may be processed for assimilation into the global ocean model. An ocean reanalysis of the 1984-1994 period has been run with MOM 2 and 50 vertical levels using the NCEP reanalysis wind stress. Comparison with observations show that both the mean and variability of the thermal structure is well captured. However, the currents are not well reproduced.

PLANS FY97

A comparison of the assimilated sea level will be made with Lamont-Doherty Earth Observatory and NCEP analyses. Salinity data will also be assimilated and its impact evaluated. The effect of various data sources and data types will be assessed within the framework of the analyses and coupled model forecasts. Model physics modifications will be evaluated in the context of improving the simulation of the currents. The mean correction field from the assimilation will be used to evaluate model performance.

4.5 OCEAN-ATMOSPHERE INTERACTION

A. Bush
D. Gu
S. Harper
G. Lambert
V. Larichev
S. Masina
S.G.H. Philander

ACTIVITIES FY96

Although the 1980's was a period of rapid progress in the ability to explain, simulate and predict the Southern Oscillation/El Niño phenomenon, the prolonged persistence of warm surface waters over the eastern tropical Pacific during the early 1990's was unanticipated, and is apparently beyond the scope of current theories. Analyses of time-series data from the TOGA-TAO array (bo) suggest that this warming should be viewed not as an extended El Niño, but as part of a decadal fluctuation that is governed by different physical processes. Whereas interannual fluctuations such as El Niño amount to a horizontal redistribution of warm surface waters within the tropics, decadal fluctuations involve exchanges between the tropical and extratropical oceans. Those exchanges can alter the properties of the tropical thermocline, its mean depth and vertical temperature gradient for example, and hence can influence interactions between the ocean and atmosphere. An understanding of the processes that can change the tropical thermocline sheds light on a variety of phenomena, including glacial climates, and also contributes to the development of coupled ocean-atmosphere models intended for predictions of phenomena such as the prolonged warming of the eastern tropical Pacific during the early 1990's.

4.5.1 Decadal Variability

The sharp, shallow tropical thermocline, the salient feature of the thermal structure of the tropical oceans, is maintained by a shallow meridional circulation driven by easterly winds that cause poleward Ekman flow in the surface layers, and equatorward geostrophic flow in the thermocline in response to the eastward pressure force established by the westward winds. Upwelling at the equator and subduction in the extratropics close the circulation. Studies with a realistic oceanic GCM show that one important subduction zone, off the coast of Peru, provides water parcels with a relatively direct window to the equatorial thermocline. Parcels that subduct in another important zone, off the coast of California, follow a circuitous route to the equator. First they travel southwestward to approximately 10°N and then either join an equatorward western boundary current or flow eastward in the North Equatorial Countercurrent while slowly moving equatorward. Presumably these are the routes available

to disturbances that bring unusually cold or warm waters from the surface layers of the extratropics to the equatorial thermocline. Initial results from experiments with the oceanic GCM MOM forced with heat and momentum fluxes appropriate for the period 1970 onwards indicate that, whereas interannual variations in the tropics are locally forced, decadal variations in low latitudes have an extratropical origin. While these studies are underway, we have been exploring the consequences of fluctuations in the exchanges between the tropical and extratropical oceans.

Consider a disturbance in the form of unusually warm surface waters over the northern Pacific Ocean. Those waters converge onto the subduction zone and in due course find their way to the equatorial thermocline. (This could be the origin of the warming of the eastern Pacific equatorial thermocline evident in the TOGA TAO time-series of the early 1990's.) This change in the thermocline affects ocean-atmosphere interactions in such a manner as to result in conditions similar to El Niño: warm surface waters and relaxed easterly winds in the tropics, an equatorward shift of the jet stream and relatively cold surface waters in the extratropics. In other words, the original warm disturbance in the extratropics in due course is followed by a cold disturbance in that region. These arguments imply decadal climate fluctuations that have been explored by means of a simple box-model of the coupled tropical plus extratropical ocean-atmosphere (bn). Fig. 4.4 shows the temperature fluctuations in the surface layers of the tropics (solid lines) and extratropics (dashed lines) in the absence of stochastic noise (upper panel), and when such noise is present (lower panel). These results indicate that the slow oceanic link between the extratropics and tropics, and the rapid atmospheric link in the reverse direction can result in self-sustaining decadal climate fluctuations.

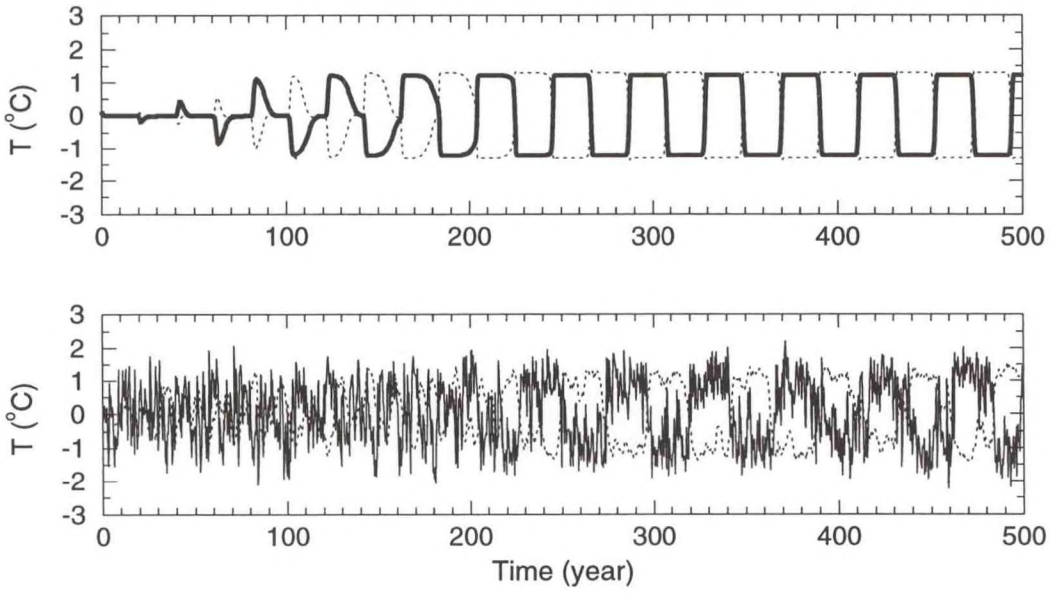

Fig. 4.4 Interdecadal oscillations with a delay time of 20 years for extratropical surface water reaching to the tropical thermocline. Solid line is for extratropical SST and dotted line for tropical SST. The lower panel includes the introduction of a white noise forcing on the extratropical surface ocean. These results suggest that a slow oceanic link between the extratropics and tropics might lead to decadal climate fluctuations.

Consider next a disturbance in the form of unusually cold surface waters over the extratropics. This case is relevant to conditions during the last glacial maximum some 18,000 years ago and can shed light on the controversy concerning temperatures in the tropics during that period. Although paleoclimatologists at first believed that the tropics then were as warm as they are today, recent observations indicate that the tropics were significantly cooler, by as much as 5°C. A simple coupled ocean-atmosphere model, of the type used to predict El Niño, has been used to explore how a cooling of the equatorial thermocline might affect ocean-atmosphere interactions and hence sea surface temperatures in low latitudes. The results indicate that the oceanic exchanges between the tropics and extratropics mentioned above may result in a significant cooling of the tropics during glacial climates.

4.5.2 Simulation of the Tropical Climate with Coupled GCMs

An R30 atmospheric spectral model, coupled to the MOM oceanic GCM and forced with seasonally varying solar radiation reproduces the time-averaged climate of the tropics and its seasonal variations with reasonable realism (as regards the winds, rainfall patterns, oceanic currents) except that sea surface temperatures are too low by approximately 2°C throughout the tropics, and the cold tongue along the equator is too prominent. (Keep in mind that the amplitude of observed interannual variability is approximately 2°C.) During the past year a number of experiments have all failed to remedy this problem. These experiments involved, among other things, changes in the parameterization of stratus clouds, of oceanic mixing, of evaporation from the ocean surface, and changes in the resolution of the oceanic model.

4.5.3 Seasonal Cycle in the Tropical Atlantic

The seasonal cycles in both the equatorial Pacific and Atlantic are characterized by a prominent annual harmonic even though the sun "crosses" the equator twice a year. In the case of the Pacific, the explanation involves the ocean-atmosphere interactions and the asymmetry, relative to the equator, of the time-averaged climate (aj). A recent study for the Atlantic shows that, in that ocean and especially in the Gulf of Guinea, continental geometry is of enormous importance. An atmospheric GCM forced with seasonally varying solar radiation, and with time invariant sea surface temperatures specified to have their annual mean values, nonetheless reproduces surface winds with realistic seasonal variations in the eastern tropical Atlantic. Seasonal variations in the heating of the west African land mass drive the motion. Over the western tropical Atlantic ocean-atmosphere interactions come into play.

4.5.4 Stability of Tropical Currents

Energetic fluctuations, inhomogeneous in space and time, with a period near 30 days and a wavelength on the order of 1000 km are prominent in the surface layers of the equatorial Pacific Ocean. Analyses of simulated fluctuations, in a realistic, high resolution oceanic GCM, show that their origin is the baroclinic instability of currents just north of the equator where the surface mixed layer of the ocean has large north-south, but small vertical temperature gradients. A southward flux of energy initiates barotropic instability of the currents south of the equator where the latitudinal shear of the currents is large.

PLANS FY97

The development of coupled GCMs capable of realistic simulations of the tropical climate and its seasonal, interannual and decadal fluctuations will continue. In parallel, by means of simpler models, the nature of the exchanges between the tropical and extratropical oceans will be explored. Particular attention will be paid to 1) the subduction process, especially the manner in which seasonal and interannual signals are filtered out from disturbances as they subduct so that only decadal signals survive at depth, 2) the paths that water parcels follow as they move equatorward --- do they conserve vorticity and if so, are they capable of crossing the ridge of the thermocline near 10°N? -- and 3) the manner in which changes in the thermocline influence sea surface temperatures. Some of the implications of these exchanges for past climates, those associated with glacial and interglacial conditions, will be explored.

5. OCEANIC CIRCULATION

GOALS

To develop a capability to predict the large-scale behavior of the World Ocean in response to changing atmospheric conditions through detailed, three-dimensional models.

To identify practical applications of oceanic models to human marine activities by the development of a coastal ocean model.

To incorporate biological effects in a coupled carbon-cycle/ocean GCM.

To study the dynamical structure of the ocean through detailed analyses of tracer data.

5.1 WORLD OCEAN STUDIES

5.1.1 Water Masses and Thermohaline Circulation

B. Samuels J.R. Toggweiler

ACTIVITIES FY96

A diagnostic study has been carried out of the sources and sinks of available potential energy in ocean GCMs following the method of Oort et al. (1223). The work done by buoyancy forces and wind forces to drive the large-scale, time-mean circulation has been directly compared for the first time. The current study evaluates energy sources and sinks in two coarse-resolution ocean GCMs. One is a global model (1156, 1157, 1313, 1315) which includes an open circumpolar channel and an Antarctic Circumpolar Current (ACC). The other is a sector model[1] of a single idealized ocean basin which does not include an open circumpolar channel. Both models are forced with similar boundary conditions.

The energy analysis shows that the work done by buoyancy forces is approximately equal to the work done by wind forces in the sector model, but is substantially smaller in the global model, especially in relation to the work done by the winds. The difference is explained by two factors: 1) winds blowing over an open circumpolar channel do much more work on the circulation system than the same winds blowing over a closed basin; and 2) the existence of a circumpolar current changes the site where deep water wells up to the surface. Most of the deep water in the sector model rises to the surface in the tropics where surface buoyancy forces do a lot of work adding heat to the upwelled water. Most of the deep water in the

1. Bryan, F., Parameter sensitivity of primitive equation ocean general circulation models, *J. Phys. Oceanogr., 17,* 970-985, 1987.

global model rises to the surface south of the ACC. Here deep water is lifted to the surface by the winds and buoyancy forces do very little to modify the density of the upwelled water.

The global model maintains a very large stock of available potential energy in its density field which is not present in the sector model. The extra potential energy takes the form of horizontal density differences between the great mass of ocean north of the ACC and the region south of the ACC. The extra potential energy is an essential feature of the global model which allows the momentum added to the ACC by the wind to pass into topographic obstructions on the sea floor. The work done to maintain this energy in the system comes entirely from the wind.

The energetic analysis also helps explain the link between circumpolar winds and deep-water formation in the North Atlantic (1313). The ACC maintains a large north-south pressure difference within the Atlantic basin in which the sea surface north of the ACC is significantly elevated with respect to the sea surface in the North Atlantic. This pressure difference provides an important northward "push" which helps maintain the overturning. The analysis shows that this ACC effect significantly enhances the overturning and northward heat transport in the Atlantic without much extra work being done by buoyancy forces. These results strongly support the idea that a large, wind-driven circumpolar current is an important factor in the ocean's so-called "thermohaline" circulation.

PLANS FY97

The new energy diagnostic will be applied to higher resolution models which resolve the seasonal cycle and have more energetic currents. It will also be applied to help understand fluctuations in the thermohaline circulation observed in other studies (1387).

5.1.2 Stability of North Atlantic Deep Water Formation

M. Winton

ACTIVITIES FY96

The deep Atlantic overturning is one of the main heat transporting circulations of the climate system. Several studies have been undertaken to better understand its stability properties and to help assess its simulation in climate models.

Twentieth century observations of North Atlantic SST's suggest significant variation on an interdecadal time scale. The GFDL coupled climate model also produces similar climatic changes associated with variations in North Atlantic Deep Water (NADW) formation. Recently, some interest has been focused upon the mechanism for the model's variability. Many idealized thermohaline circulation models produce self-sustaining interdecadal oscillations with simple buoyancy flux boundary conditions. To help determine the relevance of these idealized studies to the coupled model behavior, the oscillatory nature of models with flat and bowl shaped basins was compared under the fixed buoyancy flux boundary conditions (bv). It was found that the flat bottomed model was much more prone to oscillation. This difference

arises from the radically different way in which currents adjust to continental coasts when a vertical wall is replaced by a continental slope. The results of this study suggest that the coupled model oscillation mechanism is different than that of the flat-bottom ocean experiments.

One enigma of the paleorecord is the stability of NADW formation in the current warm period, compared to its continuous instability during the last glacial era. This is contrary to expectation since NADW instability is generally thought to be promoted by poleward atmospheric water transport which was likely reduced in cold glacial times. A simple coupled climate model (a two-dimensional ocean with an energy balance atmosphere) was used to examine changes in NADW as a function of mean atmospheric temperature (bg). It was found that warm climates are more favorable to NADW formation, with cold climates typically favoring southern sinking (Fig. 5.1) or continuous oscillation (deep-decoupling or flush cycles). In this model it was found that atmospheric cooling is generally equivalent to increased high latitude freshening (*e.g.*, the progression of circulations seen in Fig. 5.1 could also have been induced by increased atmospheric water transport). The source of the equivalence is a convective instability encountered at low temperatures where the thermal expansion coefficient becomes small (seawater expands less per degree of warming at low temperature). High latitude convection is driven by the *upward* buoyancy flux associated with surface heat loss and suppressed by the *downward* buoyancy flux associated with surface freshening. Because of the nonlinear equation of state, at lower temperatures, the buoyancy flux associated with a given heat flux is reduced and the stratifying effect of surface freshening is favored.

While the results of the simple coupled model are provocative, an important aspect of NADW formation is not properly represented. In the real ocean, the region of NADW formation (the Nordic Seas) is separated from the deep basin which NADW eventually occupies. In the flat-bottom model, the region of deep water formation falls within the model's single basin. The abrupt appearance of deep stratification in the bottom panel of Fig. 5.1 would correspond to a shallowing of Nordic seas outflow in nature. The processes that contribute to the sinking of this outflow to depth in the subpolar North Atlantic are therefore of key importance. Idealized experiments have been undertaken to identify these processes. Preliminary results point to the importance of baroclinic eddies in the sinking of the Nordic seas outflow to depth in the subpolar North Atlantic.

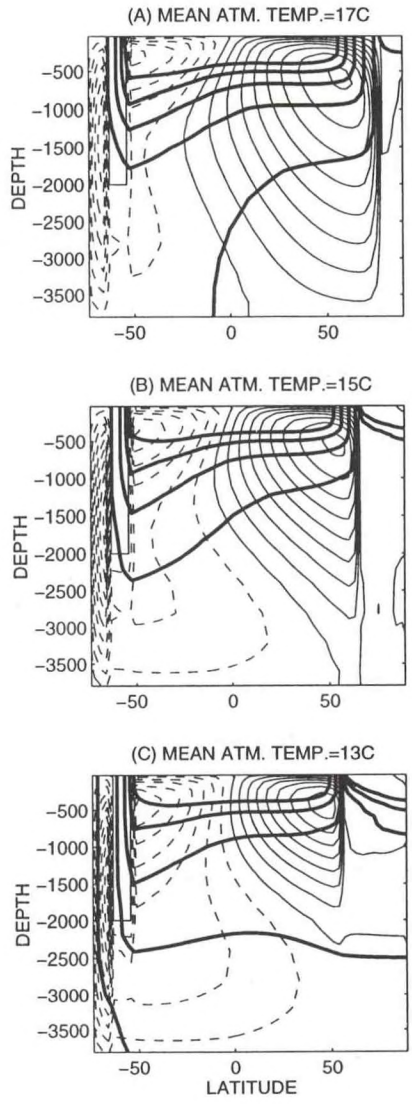

Fig. 5.1 Streamlines of meridional overturning (thin contours) and isopleths of temperature (bold contours) in an Atlantic basin with three different mean atmospheric temperatures. As the climate cools, the Antarctic Bottom Water undercuts the North Atlantic Deep Water further to the north. Nutrient proxies suggest a similar change in circulation between the present day and the Last Glacial Maximum circulation.

PLANS FY97

Work will continue toward understanding the physical processes involved in the sinking of the Nordic seas outflow. The sensitivity of these processes to stratification will be studied. Should the processes turn out to require parameterization in climate models, appropriate parameterizations will also be investigated.

5.1.3 Stability of the Thermohaline Circulation in Coupled Models

S. Griffies *E. Tziperman*
R. Stouffer

ACTIVITIES FY96

The ocean's meridional thermohaline circulation (THC) carries a large amount of heat poleward and significantly affects high latitude climates. The stability of this circulation is of great interest to studies of past and current climate change and variability. A series of model simulations has been carried out using the GFDL coupled climate model in which the initial THC in the model's control run is systematically strengthened and weakened. Analysis of these simulations indicates that active states of the North Atlantic THC that are weaker than the present day THC by 25% or more are spontaneously unstable. When initialized with one of the weak THC states, the coupled model THC does not remain near the initial state given by its control run. The coupled model enters a new and different climatic regime, often with strong THC oscillations. The unstable regimes are also prone to THC collapse. These results may shed light on past climate behavior seen in the paleorecord, as well as on other coupled model results in response to fresh water input into the North Atlantic Ocean and to a four times increased atmospheric CO_2 scenario which predicted THC reductions in excess of 25%.

PLANS FY97

As a side benefit of the THC stability study, a suite of 500 year experiments now exists for which there is an apparent direct correlation between North Atlantic salinity gradient and amplitude of variability in the THC. The mechanisms determining this correlation will be further elaborated in a future study.

5.1.4 Thermohaline Circulation in Isopycnal Coordinates

R. Hallberg *J.R. Toggweiler*

ACTIVITIES FY96

The sinking branch of the thermohaline circulation has long been known to consist of relatively few regions of deep convection. The upwelling branch of the thermohaline circulation is usually thought to consist of a widely distributed upwelling through the thermocline, but measured diapycnal diffusivities are about an order of magnitude less than would be required. Recent studies have suggested that much of the upwelling is actually the result of Ekman pumping in the Southern Ocean (1313).

Isopycnal coordinate ocean models are ideally suited for studying the thermohaline circulation. Numerical diapycnal diffusion can be eliminated entirely; all diapycnal mass fluxes are explicitly parameterized. A global 2° resolution simulation with weak (0.1 $cm^2\ s^{-1}$) interior diapycnal diffusion and real bathymetry, forced with ECMWF annual mean winds and by restoring the surface density to the observed annual mean value of potential density

referenced to 2000 dbar, has been partially spun-up from a resting, homogeneous state. Water mass production rates and current transports are reasonable. Preliminary results confirm the suggestion (1313) that Ekman suction in the Southern Ocean is overwhelmingly important in maintaining the thermocline structure and in closing the thermohaline circulation.

PLANS FY97

Once the global simulation has spun up, it will be possible to diagnose exactly where the diapycnal mass fluxes of the upwelling branch of the thermohaline circulation are. Sensitivity studies will explore the relative importance of the diapycnal diffusivity and the strength of the wind stress in the Southern Ocean in determining the thermocline structure and the strength of the thermohaline circulation.

5.1.5 High-Resolution North Atlantic Studies

W. Hurlin *M. Winton*

ACTIVITIES FY96

An important component of the Atlantic thermohaline circulation is the formation of deep water in the Labrador Sea due to convection in the central basin. Observations indicate that convection in the central basin was greatly diminished during the mid 1960's through the early 1970's during a time when the Labrador basin was capped with a layer of low-salinity water, an event known as the "Great Salinity Anomaly". The fresh water which triggered the collapse of convection does not appear to have come into the basin locally from the atmosphere, but appears to have been advected into the region via the Labrador Current. The Labrador Current picks up low-salinity water from the Arctic and Greenland Seas to the north and then transports low-salinity water around the perimeter of the Labrador basin.

The object of the current study is to see how a salinity anomaly introduced around the perimeter of the Labrador Basin influences convection in the central basin. Does the salinity anomaly in the central basin simply spread outward from an unusually fresh Labrador Current, or is the spreading of the salinity anomaly related to local processes in the Labrador Basin? What role do eddies play? Are resolved eddies critical to a successful simulation of the salinity anomaly and its effect on convection?

A model of the North Atlantic basin has been configured to study convective processes in the Labrador Basin and eddy effects on convective processes. The first step in this study was to configure a model that produces seasonal convective events. Lateral boundaries also have an important effect in basin models. Numerous experiments were conducted to determine the most realistic way to configure the lateral boundaries. Restoring boundaries (or sponge layers) were found to reduce convection by artificially maintaining stable stratification in the interior. The spatial location of convection, and the amount of convection itself (and hence overturning) is very sensitive to small changes in the surface freshwater flux.

PLANS FY97

Ongoing experiments are investigating the role of eddies on convective processes in a model with vigorous seasonally occurring convection. The interaction between baroclinic eddies and convection in the Labrador Basin will be investigated.

5.1.6 Using CFCs as Ocean Tracers

K. Dixon

ACTIVITIES FY96

The ventilation of ocean waters on decadal time scales can play an important role in determining climate change patterns. The simulation of such ventilation processes in the ocean component of the GFDL coupled ocean atmosphere climate model has been examined using anthropogenic chlorofluorocarbons (CFCs) dissolved in seawater as analysis aids. Observed and simulated oceanic CFC distributions have been found to be qualitatively consistent with one another (Fig. 5.2) and with the coupled model's predictions that the ocean may delay greenhouse gas induced warming of surface air temperatures at high southern latitudes (1380).

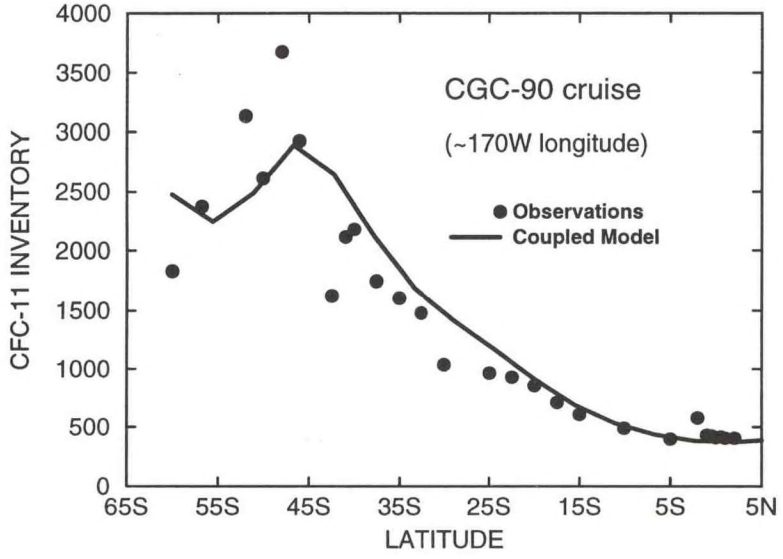

Fig. 5.2 A comparison of observed and modeled vertically integrated CFC-11 column inventories calculated along 170°W showing that the GFDL coupled climate model successfully simulates the CFC penetration up through 1990. The filled circles represent column inventories computed from observations. Results from the ocean component of the GFDL coupled model are shown as the solid line (units = nanomoles m^{-2}).

Additional analyses have been initiated to investigate to what extent the global ocean model's simulated uptake and redistribution of the CFC transient is analogous to transient oceanic warming patterns associated with increasing greenhouse gases. Findings could lend insight as to whether one should expect to find the greatest warming in ocean regions where the CFC signal is strongest. Preliminary results show general agreement for very large scale features, such as an interhemispheric asymmetry. However, at smaller scales marked differences in the CFC and ocean warming patterns are evident. Especially large dissimilarities are found in sea ice regions, where the factors governing the fluxes of CFC and heat across the ocean surface are quite different.

PLANS FY97

Collaborations with researchers at NOAA/PMEL will continue in order to increase the number of high quality oceanic CFC observations available for comparison with ocean model simulations. The sensitivity of modeled CFC uptake to the choice of subgrid scale mixing parameterization will be examined in relatively coarse resolution global ocean models. Analyses comparing the simulated patterns of CFCs and greenhouse warming of ocean waters will be continued.

5.1.7 Nutrient Dynamics in the Equatorial Zone

S. Carson *J.R. Toggweiler*

ACTIVITIES FY96

A simple ecosystem model (1155,1166) has been coupled with a high-resolution model of the equatorial Pacific (758) to study the dynamics of nutrient cycling. The coupled biological/physical model has been used to simulate the input of nitrate into the equatorial upwelling system by the Equatorial Undercurrent and the uptake of nitrate by organisms (1340). This project is part of the JGOFS (Joint Global Ocean Flux Study) Equatorial Pacific Process Study, the field phase of which was completed in 1992.

One of the most important outputs of biogeochemical models is a prediction of the sinking flux of organic matter at the base of the euphotic layer in the upper 50-100 m. The various JGOFS field programs were designed in large part to measure this flux. Constraining the sinking flux has turned out to be very difficult, as different techniques for directly measuring or estimating the flux often fail to agree within a factor of two to four. This means that characterizations of upper ocean biological systems remain fairly incomplete: a system with sinking fluxes at the low end of the observed range has to recycle most of its carbon and nutrients within the euphotic layer in order to maintain its carbon and nutrient stocks, whereas a system with sinking fluxes at the high end of the observed range can afford to lose a relatively large fraction of its organic production to particles which sink deeper into the thermocline before being remineralized. This distinction has implications for the general circulation because the downward sinking flux must be balanced in the time mean by an upward flux of dissolved inorganic carbon and nutrient elements driven by upwelling and vertical mixing. A biological system which efficiently recycles its carbon and nutrients coexists with a physical

system in which diabatic mixing effects are weak. A leaky biogeochemical system can only coexist with a physical system in which lots of mixing occurs.

The coupled biological/physical model has been used to help pin down the absolute magnitude of the sinking flux in the equatorial Pacific. This effort exploits an independent constraint on sinking fluxes, namely the distribution of dissolved oxygen in the thermocline. Parameters of the coupled model are tuned so that the model will reproduce the observed levels of nitrate in surface waters of the equatorial Pacific. Subsurface oxygen concentrations in the depth range between 100 and 400 m are strongly affected by vertical processes but are not used in tuning the coupled model. Oxygen levels at these depths reflect a balance between losses due to organic remineralization and resupply by horizontal advection. If predicted vertical fluxes are excessive, the losses will be greater than the resupply and predicted oxygen concentrations will decline relative to observed levels.

Parallel equatorial simulations were set up with "strongly recycling" and "leaky" ecosystem parameters, respectively. Mixing parameters of the circulation model were adjusted so that each coupled system maintains similar upper ocean nitrate levels. The strongly recycling system run with a background vertical diffusion coefficient of 0.1 cm^2/s is more realistic. Predicted oxygen levels in the leaky simulation (run with a diffusion coefficient of 0.3 cm^2/s) diverge more strongly from observed levels mainly within a few degrees of the equator where the predicted sinking flux overwhelms oxygen resupply via the Equatorial Undercurrent.

PLANS FY97

The sensitivity of the oxygen simulations to other components in the coupled model needs to be checked. These include gas exchange rates, remineralization ratios, and the drag coefficient used to produce a wind stress from the wind data products used to force the model. Similar simulations will be run with an embedded carbon system in order to predict the partial pressure of CO_2 at the surface, an additional diagnostic of the biogeochemical system for which many measurements exist.

5.2 OCEAN PROCESSES

5.2.1 Analysis of High Resolution, Eddy Resolving Ocean Circulation Models

K. Bryan *R.D. Smith**
*J. Dukowicz**

**Los Alamos National Laboratory*

ACTIVITIES FY96

Ocean circulation models used in coupled ocean-atmosphere models for climate sensitivity and climate change studies do not have enough resolution to resolve mesoscale eddies. The stirring effect of eddies is parameterized by simple lateral mixing operating along

flat horizontal surfaces or sometimes along isopycnal surfaces. Various parameterizations have been proposed to represent the mixing of mesoscale eddies in a more realistic way, but these schemes are difficult to justify on the basis of scanty direct observations of mesoscale eddy velocity fields.

High-resolution model calculations offer another means of testing these parameterizations. An analysis of high-resolution results from the Los Alamos version of the GFDL global ocean model indicates that the actual eddy density fluxes of the model have a very complex behavior. In particular, the relationship between local isopycnal thickness gradients and local isopycnal "thickness mixing" seems to be very weak. The relationship between eddy transport of density and the eddy transport of passive tracers also appears to be much more complicated than envisioned in the proposed parameterizations.

PLANS FY97

The ocean model developed at GFDL, and used by many other laboratories around the world, has systematic errors that appear to be connected with its vertical coordinate system. In particular, the model has difficulty in handling deep overflows and deep western boundary currents. This has motivated an effort to generalize the vertical coordinate to include some of the apparent advantages of terrain-following and isopycnal coordinate models. The goal is to develop a flexible code which could be used to carry out multiple experiments to test the sensitivity of results to different vertical coordinate systems. This will be a joint effort with Los Alamos carried out in collaboration with modelers at GFDL.

5.2.2 Interactions Between Topography and Stratified Flow

R. Hallberg

ACTIVITIES FY96

Bottom topography in a basin with planetary vorticity gradients strongly affects the vertical structure of the linear topographic and planetary Rossby waves that spin up the ocean circulation. In particular, there is no barotropic mode in models with large amplitude topography and stratification. It has been shown (cd) that two-layer quasigeostrophic waves that exist with stratification, planetary vorticity gradients, and large amplitude bottom topography are more strongly concentrated in the vertical than Burger number 1 scaling would indicate (for most orientations of the wavevector) except where the bottom slope is nearly meridional. The vertical concentration increases with decreasing frequency. Ray tracing in a channel with large amplitude topography, depicted in Fig. 5.3, suggests that the two layers are linearly coupled in regions with parallel or antiparallel topographic and planetary vorticity gradients, but elsewhere small amplitude motion in the two layers is largely independent. Primitive equation simulations agree with the quasigeostrophic results, and indicate that the localized linear coupling between surface and bottom intensified flow pertains to a continuous stratification (cd).

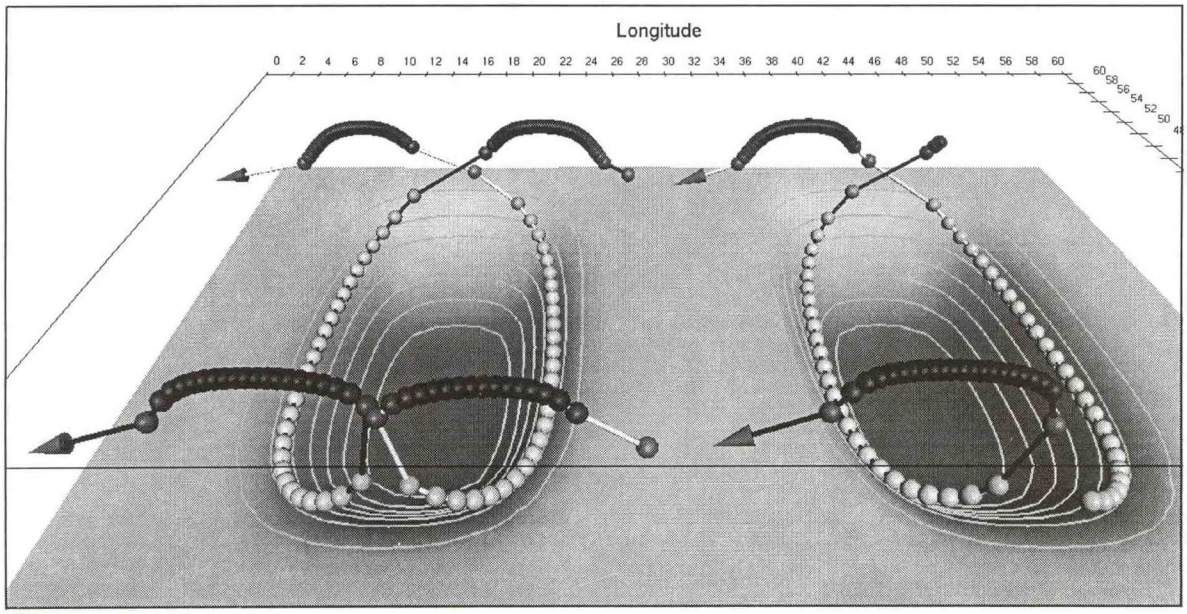

Fig. 5.3 Quasigeostrophic ray paths showing the propagation of information in a two-layer channel with two basins. The balls mark the ray position every day. The shading of the ball and the vertical position indicate the vertical structure of the rays. Surface intensified rays have dark balls and bottom intensified rays have light balls. The ray is in the middle of the upper layer when the magnitude of the flow in the two layers is equal. The connecting lines are either white or black all along a ray. Bottom intensified rays tend to follow the bathymetry, while surface intensified rays propagate westward along the upper layer potential vorticity contours. Rays make a transition between describing surface and bottom intensified flow in the north or south of the basins, where the topographic and planetary vorticity gradients are parallel or anti-parallel. Two rays exchange energy where they make transitions in the opposite sense. Surface and bottom intensified flow are coupled where the rays change their layer of intensification.

In a separate study, the wind-driven stratified flow in an ocean basin with sloping sides is compared with an otherwise identical flow in a flat bottom basin. Eastern boundary topography has only a minor influence on the circulation, but a sloping western boundary dramatically alters the circulation by modifying the interior potential vorticity structure. With a sloping western boundary, the subtropical gyre becomes surface intensified, while the subpolar gyre is expressed more strongly at depth and extends equatorward along the western boundary beneath the subtropical gyre. The extent of outcropping in the subpolar gyre is greatly reduced and the western boundary current separation point is shifted equatorward. Deep regions of homogenous potential vorticity in the flat bottom case are replaced by a tongue of cyclonic potential vorticity extending into the interior from the western boundary current separation point. It is hypothesized that non-quasigeostrophic effects may contribute to stripping cyclonic potential vorticity off of the sloping boundary. Most of the differences between topographic and flat bottom simulations can be directly tied to the changes in the deep potential vorticity structure. This suggests that accurate portrayal of the large-scale ocean circulation may be crucially dependent on the rather small scale flow over the topography along the ocean margins.

PLANS FY97

Continued study will further explore the effect of large amplitude topography on the potential vorticity dynamics of the large-scale ocean circulation. The mechanisms behind the modification of the deep potential vorticity structure with a sloping western boundary will be elucidated.

5.2.3 Ocean Mixed Layer Dynamics

A. Gnanadesikan

ACTIVITIES FY96

The oceanic mixed layer consists of a number of different dynamical regimes, the structure of which has become clear only in recent years. These include a wave-stirred surface layer, a shear layer in which shear and stratification are governed by scaling similar to that found in the atmosphere, a mixed layer interior in which large eddies are responsible for much of the transport, and an entrainment layer at the top of the thermocline. Significant contributions have been made in the past year towards understanding each of these layers. Major achievements include a model intercomparison study which documents the relative mixing strengths in different models and evaluates their importance for photochemical cycling (1371). Another study evaluated the importance of vertically distributed forcing due to wave-current interaction in forcing eddies within the mixed layer interior (1402). An observational study demonstrated that wave-current interaction is an important mechanism for forcing the large eddies (br). A fourth study documents the existence of a wave-stirred layer and a shear layer similar to that found in the atmospheric boundary layer (cz). A model developed in the latter study demonstrates the importance of air injection in limiting the depth of penetration of the wave-injected turbulence.

PLANS FY97

Over the next year, this work will be extended to examine the effects of wave breaking on gas exchange and to evaluate new models within the context of MOM.

5.3 MODEL DEVELOPMENT

5.3.1 MOM 2

R.C. Pacanowski

ACTIVITIES FY96

New features are being added as MOM 2 development continues. These developments are described in the MOM 2 documentation which also has been updated to reflect the current status of the model. All diagnostics have been given an interface to generate NetCDF formatted output which allows easy access to results without intermediate

analysis code. An option for coarse grained parallelism (microtasking) has been added which makes more efficient use of multiple processors than the fine grained (autotasking) approach. This has relevance on platforms such as the CRAY T90 when using tens of processors.

A new isopycnal diffusion formulation which does not increase tracer variance has been developed and is being tested (5.3.2). Options exist for both the small angle approximation and full tensor. A fourth order advection scheme for tracers, the flux-corrected transport (FCT) scheme of Gerdes, Köberle and Willebrand (1991), the pressure gradient averaging technique of Brown and Campana (1978), the "Neptune effect" of Holloway (1992), a general grid rotation, and the open boundaries of Stevens (1990) have also been added. There has also been some restructuring of the memory window to allow for a more robust implementation of fourth order schemes.

PLANS FY97

Future plans include extension of the coarse grained parallelism option to include distributed systems like the CRAY T3E, addition of a third order advection scheme for tracers very similar to the "Quick" scheme of Leonard (1979), and a nonlocal "K-profile parameterization" (KPP) of Large et al. (1994). A new release of MOM 2 is planned in order to make these new options available to the oceanographic community.

5.3.2 Isopycnal Diffusion in MOM 2

A. Gnanadesikan V. Larichev
S. Griffies R.C. Pacanowski

ACTIVITIES FY96

The mixing of ocean tracers occurs predominantly along surfaces of local potential density, also known as isopycnal surfaces. This mixing is thought to be one of the fundamental processes determining water mass properties of the world ocean. A substantial part of this mixing can be parameterized as simple downgradient diffusion. In the mid-1980's, Cox released a version of the GFDL ocean model in which the diffusion tensor was rotated in order to align the directions of tracer diffusion parallel to the local isopycnal directions. The implementation of this scheme improved the model's fidelity quite substantially. Unfortunately, the scheme contains numerical problems which prevent it from being run without an added background diffusion which can act across isopycnals. It turns out that this added background diffusion can counteract certain benefits of the along-isopycnal diffusion.

A reanalysis of the isopycnal diffusion discretization has revealed the essential shortcomings with the original scheme, which include the unphysical tendency to increase tracer variance, the presence of computational modes, and the unphysical effect of diffusing density when it is a nonlinear function of a single active tracer. A new scheme which corrects these problems is currently being implemented in the MOM 2 version of the GFDL ocean model. This scheme will be made available to the user community with the next release of

MOM 2. Combined with a stable advection scheme, such as the flux-corrected transport (FCT) scheme currently in MOM 2, or various other advection schemes being developed for MOM 2, the GFDL ocean model will have the potential to be run in a much more adiabatic mode than previously possible.

PLANS FY97

Extensive tests are planned for the next year in order to fine-tune the scheme, to assess its impact on simulations, and to combine its effects with further higher order parameterizations of isopycnal mixing by oceanic mesoscale eddies.

5.3.3 Isopycnal Coordinate Model Development

R. Hallberg

ACTIVITIES FY96

Isopycnal coordinate ocean models offer several potentially important advantages over traditional level models. Isopycnal models avoid numerical diapycnal diffusion. Arbitrary topography can be accurately represented, since the bottom boundary can be treated as a coordinate surface. Also, with a Lagrangian vertical coordinate, resolution automatically migrates to the locations with the highest stratification and hence vertical shear; flow is represented more accurately with an isopycnal model than a *z*-level model with the same number of layers. However, some aspects, such as the treatment of pressure gradients near the sloping bottom, are numerically more difficult to implement in isopycnal models than they are in *z*-level models. Accurate numerical discretizations of the primitive equations in isopycnal coordinates are being developed.

External gravity waves are often treated separately from the remaining ocean dynamics in the interest of computational efficiency. They may be filtered by using a rigid lid, but this requires solution of a Poisson equation at every time step and may be very inefficient, especially with complicated coastlines, bathymetry, and islands. Alternately, the external gravity waves may be treated implicitly or explicitly with a simplified, two-dimensional subset of the full equations. If care is not taken, the barotropic and baroclinic gravity waves may resonate, and the whole split time stepping scheme may be linearly unstable at some wavelengths. Criteria for a split time stepping scheme to be stable has been developed (ct), and a scheme is suggested which is stable at all wavelengths subject to a CFL criterion based on the internal gravity wave speed.

PLANS FY97

One great difficulty with isopycnal models is treatment of a detraining mixed layer. If a bulk mixed layer is coupled to an isopycnal interior, water being detrained from the mixed layer does not generally match the density of one of the isopycnal layers. The idea will be explored that a variable density buffer layer between the mixed layer and the isopycnal interior may be able to smoothly couple the two. Treatment of the Coriolis terms and the

Montgomery potential gradient (the isopycnal model equivalent of the pressure gradient) in the model under development is different from other, more widely used isopycnal coordinate models. These different parameterizations will be compared using simple cases with analytic solutions or solutions which can found with very high resolution simulations and tested at lower resolutions.

5.4 COASTAL OCEAN MODELING AND PREDICTION

5.4.1 Sigma Coordinate Ocean Model Development

T. Ezer *G. Mellor*

ACTIVITIES FY96

The Princeton Ocean Model (POM) is a sigma coordinate, free surface model which includes a second order turbulence scheme for modeling of coastal processes and boundary layer dynamics. The number of model users has increased dramatically in recent years (to more than 200 by August 1996), and model applications have expanded from mostly small-scale coastal modeling in previous years, to process studies, ocean prediction systems and large-scale climate modeling (for more information, see the POM home page on the web at http://www.aos.princeton.edu/htdocs.pom).

The first POM users group was held at Princeton in June 1996 (1374) and included more than 40 presentations and about 100 participants. During the meeting, a new code, "pom96", was introduced, accompanied by a new POM users guide. The new code includes, among other things, more comprehensive open boundary condition choices, a topographic test case, and a generally cleaner code.

PLANS FY97

Several model improvements and new schemes introduced during the POM meeting, such as new advection schemes and corrections to the turbulence mixing scheme, will be tested further and made available to users. The role of Princeton University in supporting the POM modeling community by providing information, code updating, and code distribution will continue.

5.4.2 Data Assimilation and Model Evaluation Experiments

T. Ezer *G. Mellor*

ACTIVITIES FY96

As part of the U.S. Navy sponsored project, Data Assimilation and Model Evaluation Experiments, DAMEE (1291), a high resolution Model of the North Atlantic Ocean has been set up and tested. Open boundary conditions are derived from a large-scale sigma coordinate

model of the entire Atlantic Ocean. This and other models will be initialized and forced by common datasets, provided to all participants in this project, in order to evaluate and compare different model architectures (*e.g.*, sigma, isopycnal and z-level models) and different assimilation schemes.

PLANS FY97

The data assimilation methodology, previously developed for regional models, will be tested for the North Atlantic Ocean. Model resolution will be further refined, and intercomparisons with other models will be performed using the same data for forcing and assimilation.

5.4.3 The Coastal Ocean Forecast System

P. Chen *G. Mellor*
T. Ezer

ACTIVITIES FY96

The Coastal Ocean Forecast System (COFS) is a project supported by NOAA's Coastal Ocean Program; it is a collaborative project involving scientists from Princeton University, GFDL, the National Center for Environmental Prediction (NOAA/NCEP), and the National Ocean Service (NOAA/NOS). The Princeton Ocean Model is forced by the NCEP mesoscale ETA model in order to provide continuous nowcast and forecast information for the U.S. east coast. The system runs operationally at NCEP every 12 hours, providing 24 hour forecasts (zb). Parallel systems are implemented at Princeton and NOS and are used for evaluation and testing.

Evaluation of the model results shows considerable skill in the prediction of subtidal coastal sea level changes and the seasonal SST changes when compared to tide gauges and offshore buoy data. Several enhancements and improvements have been made to the system during the last year; including the use of a higher resolution (29 km) ETA model, improved vertical resolution in the ocean model, and the addition of tidal forcing. However, the tidal component, developed first for a two-dimensional version of COFS (yn), needs further testing in the three-dimensional system. During the past year, some of the COFS products have been distributed (on an individual customized basis) for uses such as boating, rescue, and as boundary forcing and initialization for regional ecological models and coupled hurricane models. The hope is to eventually provide such forecasts to the general public on a regular basis, as is the case for other NCEP operational products.

PLANS FY97

Data collection and analysis has started to facilitate the development and implementation of a full data assimilation capability, taking advantage of experience gained to date (1249, xf). This component, which is still missing from the current version of the operational system, will be the main focus of the research in following years.

5.4.4 Atlantic Ocean Climate Variability Studies

T. Ezer *G. Mellor*

ACTIVITIES FY96

In collaboration with scientists from NASA/Goddard as part of NOAA's Atlantic Climate Change Program (ACCP), long-term prognostic calculations of Atlantic Ocean variability are now being made (co, cp) with a model of the entire Atlantic Ocean and the Greenland Sea. This effort follows diagnostic calculations which tested POM in a basin-scale configuration of the North Atlantic Ocean for the first time (1250, 1327). The model is driven at the surface by observed SST and wind data from the new COADS analysis and executed for the period 1950 to 1989. Sensitivity studies with different surface boundary conditions have been conducted in order to better understand how the ocean responds to interannual and interdecadal variations at the surface. Fig. 5.4 shows a comparison between the observed sea level at Bermuda and three different model simulations. The large drop in sea level around

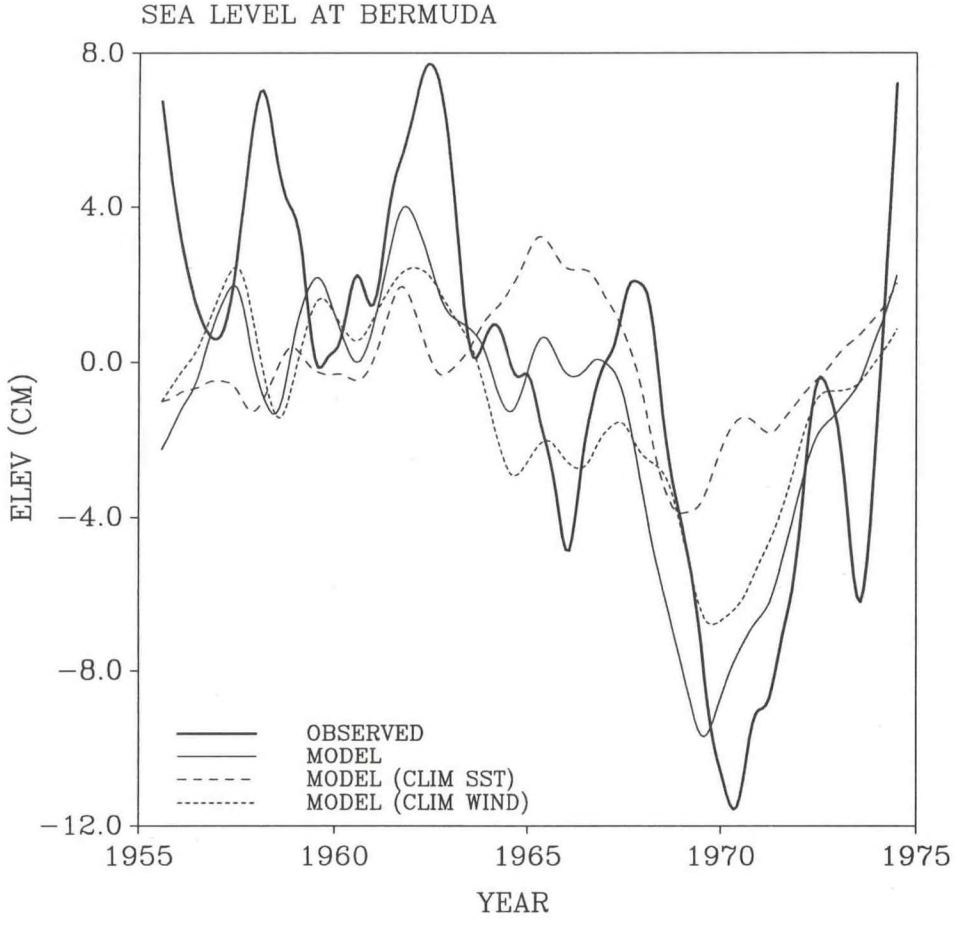

Fig. 5.4 Simulation of long-term sea level changes in Bermuda. Annual cycle and high frequency changes have been filtered. The wide solid line is from tide gauge observed data, the solid, dashed and dotted lines are from three model runs using different surface forcing: observed SST with observed wind; climatological SST with observed wind; and observed SST with climatological wind, respectively. Model forced with observed SST and observed winds produces the most realistic results.

1970 corresponds to the North Atlantic Oscillation and is accompanied by observed changes in the thermohaline circulation and wind patterns. Model sea level calculated using observed SST and observed wind for this period have produced the best comparison with the observations. If either the observed SST or the observed wind is replaced by climatological data, the simulation is less realistic. The shorter time scale variations of five years or so are not simulated very well in any of the cases.

PLANS FY97

Long-term simulations with higher resolution Atlantic and Arctic models will continue in order to study the influence of the high latitude dynamics and water formation on the climatology of the Atlantic.

5.4.5 Formation of Mediterranean Water Eddies (Meddies) and the Exchange Flow Through the Strait of Gibraltor

J.H. Jungclaus G. Mellor

ACTIVITIES FY96

High-resolution simulations of the outflow of warm, saline Mediterranean Outflow Water (MOW) into the North Atlantic have continued (cx). The water mass transition in the outflow layer and routing of the flow by various canyons in the Gulf of Cadiz agree favorably with observations. In order to investigate the instability of an initially bottom-arrested gravity current in more detail, model experiments have been carried out using an idealized continental slope topography. The intruding, relatively dense MOW interacts with the overlaying slope water by inducing vortex compression and stretching. In the slope water, strong cyclones and somewhat weaker anticyclones are formed periodically and travel in the direction of the bottom flow. MOW is injected laterally from the boundary current into the interior over the entire depth range of the plume. The intrusion forms a warm, saline density anomaly in the ambient water and undergoes an adjustment process that results in the formation of isolated anticyclonic eddies, resembling meddies (Fig. 5.5). Additional experiments have been carried out studying the effect of varying bottom slope and topographic anomalies.

To investigate the exchange flow through the Strait of Gibraltar, a new curvilinear model grid has been set up that includes parts of the Western Mediterranean (Alboran Sea) and the Gulf of Cadiz. The model is initialized with seasonal climatologies for the Atlantic and the Mediterranean side. The evolution of the exchange flow after the initial "dam-break" between the Mediterranean and the Atlantic is studied with and without the presence of tidal forcing.

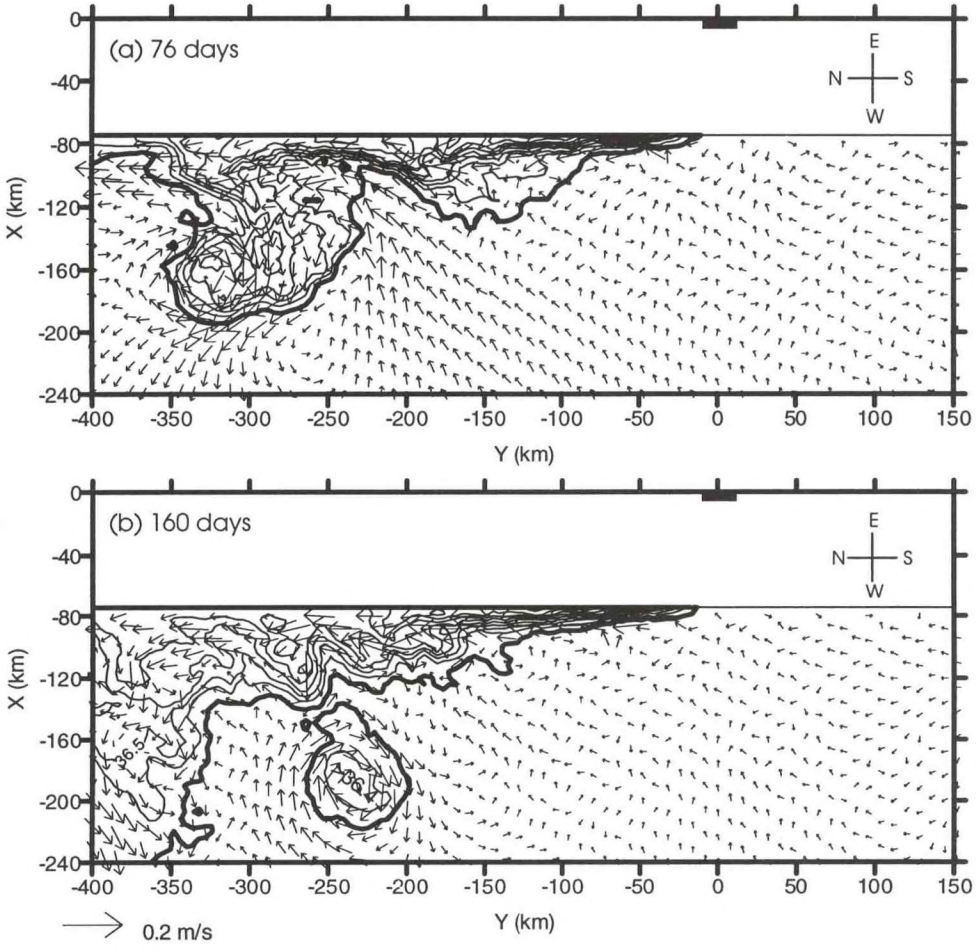

Fig. 5.5 Instability of a dense bottom current intruding into an idealized stratified ambient water body. Mediterranean-like outflow water enters the model domain from the east (top) in a 20-km gap at x = 0, y = 0. Results show salinity (c.i. = 0.1 psu) and velocity vectors at 1200-m depth down the sloping eastern boundary are shown after (a) 76 and (b) 160 days of simulation. The heavy contour line (36.3 psu) marks the boundary of the Mediterranean outflow water that initially flows along the sloping bottom. First, a dipole is formed and shed from the outflow current (a). Second, the anticyclonic eddy increases in size and strength. Third, this eddy separates from the smaller cyclonic eddy and starts to move independently from the boundary current (b).

PLANS FY97

Experiments with the Strait of Gibraltar model will be continued. The evolution and time-dependence of the Alboran Gyres will be studied, as will the pathway and water mass transformation of the outflowing Mediterranean water as it is funneled through the Strait.

5.5 CARBON SYSTEM

5.5.1 Anthropogenic CO_2

D. Baker
S. Fan
*V. Garcon**
E. Gloor
*N. Gruber***
T. Hughes
C. Le Quéré
R. Murnane
J. Olszewski
*S. Pacala****
J. Sarmiento

**C.N.R.S., Toulouse, France*
***University of Berne, Switzerland*
****Dept. of Ecology and Evolutionary Biology, Princeton University*

ACTIVITIES FY96

The Carbon Modeling Consortium (CMC), with support from the NOAA Office of Global Programs, has made significant progress over the past year. The long term goal of the CMC is to develop an integrated carbon system model capable of providing assessments of future oceanic and terrestrial biosphere sinks for anthropogenic carbon. The CMC includes collaborators from AOML, PMEL, and CMDL, as well as from several non-NOAA institutions.

The GFDL SKYHI and GCTM models are crucial components in the CMC efforts. As a first step, transport simulations for a variety of tracers have been compared with observations. Both GCMs predict meridional gradients of ^{85}Kr in good agreement with observations over the Atlantic Ocean. Inversion studies using concentrations and fluxes provided by the GCTM show that CO_2 fluxes from 7 terrestrial and 10 oceanic source regions can be recovered from model concentrations. Terrestrial source regions have fluxes associated with fossil fuel emissions, land use changes, and net primary production.

Several inversion schemes have been tested using results from the GCTM. The first scheme is based on monthly rates of change in concentrations caused by constant emissions. The second scheme is based on the monthly mean concentration deviations from annual trends caused by the various sources. Preliminary results show that: (a) inversions based on deviations from the yearly trend were able to recover fluxes with a 20% accuracy if they are supplemented with a mass conservation constraint; (b) inversions based on the concentration increase rates recovered annual fluxes with an error of 10% and are unaffected by a mass conservation constraint; (c) the accuracy of inversion was improved with an increasing number of observation sites. Different sets of observation stations were used in the test inversions. Preliminary results of network optimization point to the need for additional stations in the Southern Hemisphere, especially in the Indian and Pacific Oceans.

A model of the oceanic carbon cycle has been embedded in the GFDL coupled atmosphere-ocean model (1146) to study the relationship between CO_2 uptake by the ocean and global warming due to the enhanced greenhouse effect (dh). The ocean surface temperature warms 2.4°C and 4.9°C as a result of doubling and quadrupling the atmospheric

CO_2 content at a rate of 1% per year. The reduction in CO_2 uptake by the ocean due to the lower solubility of CO_2 at higher temperatures is found to be of secondary importance compared to the reduction due to the slowing of the ocean's deep overturning circulation. The weakening ($2xCO_2$) or collapse ($4xCO_2$) of the North Atlantic thermohaline circulation, and simultaneous reductions in Antarctic Bottom Water formation, reduce by 38% and 49% the cumulative uptake of CO_2 by the ocean over 350 years relative to a model with a fixed circulation. Such large reductions in ocean uptake would have a major impact on the future growth rate of atmospheric CO_2 and on permissible CO_2 emissions required to stabilize atmospheric CO_2. A potentially large mitigating role may be played by biology; however, this is difficult to quantify with present knowledge.

An atmospheric ^{13}C budget based on atmospheric measurements, documented anthropogenic emissions, and an ocean carbon cycle model with ^{13}C suggests that the size of the labile terrestrial carbon reservoir is currently underestimated. The budget suggests that $2300x10^{15}$ g of terrestrial carbon actively cycle through the atmosphere on 20 year time scales. This is larger than the estimated total terrestrial carbon in the upper meter of soil. A new analysis of GEOSECS and TTO data in the Atlantic allows one to separate anthropogenic carbon from natural carbon in the ocean (df). The analysis suggests that there was $20x10^{15}$ g of anthropogenic carbon in the North Atlantic between 10°N and 80°N during the early 1980's. The highest inventories occur in the subtropical gyres.

The use of bomb-produced radiocarbon (^{14}C) as a tracer of the penetration of anthropogenic CO_2 into the ocean is complicated by two factors: the different atmospheric histories (pulse-like for bomb ^{14}C, exponential increase for CO_2), and the different air-sea equilibration times (~10 years for ^{14}C, ~1 year for CO_2). The atmospheric history can be described by a "mean age", which is the average time since release of all molecules in the combined atmosphere-ocean system, while the definition of a "penetration depth", which is the column inventory divided by the surface concentration, filters differences due to the air-sea equilibration times. The mean age for anthropogenic CO_2 is currently about 30 years, which is also the time since input of bomb ^{14}C. Assuming a unique relationship between the mean age and the penetration depth, the possibility arises of estimating the global average present-day penetration depth of anthropogenic CO_2 from recent extensive surveys of radiocarbon in the world ocean by the World Ocean Circulation Experiment (WOCE) Hydrographic Program. Combined with estimates of the surface CO_2 concentration, this would (in principle) allow a prediction of the global ocean inventory of anthropogenic carbon today.

This concept was explored using results from 3-D simulations of anthropogenic CO_2 and bomb ^{14}C in the GFDL ocean model, coupled to a recent version of the biogeochemical carbon cycle model. The prediction of converging penetration depths for the two tracers in the current decade was confirmed; however, the relationship between the mean age and the global mean penetration depth is less straightforward.

PLANS FY97

Inverse modeling techniques will continue to be a major activity for the CMC. Various techniques will be tested with model data from different GCMs (SKYHI and those of other

laboratories). The inverse modeling techniques will also be applied to atmospheric observations to produce a preliminary estimate of carbon budgets in the 1980s. Study of an optimal monitoring strategy will be intensified. A series of GCTM simulations will be conducted for ^{13}C and O_2. Atmospheric observations of CO_2, CO, CH_4, O_2, and ^{13}C will be acquired and analyzed for inter- and intra-hemispheric gradients and for interannual variability.

Future studies with the coupled atmosphere-ocean model are planned to further examine the consequences of circulation changes for the oceanic CO_2 sink. Simulations with a more realistic historical evolution of atmospheric CO_2 and aerosol forcing since pre-industrial times are already underway, and additional tracers (oxygen, argon, nitrogen) are being added to further examine the roles of changing sea surface temperature and ocean circulation.

A new set of carbon system measurements from the Indian Ocean will be analyzed using the new technique to determine the anthropogenic component of the oceanic carbon. New observations of both ^{14}C and CO_2 in the Pacific will become available very soon and, after processing to separate the bomb/anthropogenic signals from the natural background, may be used to estimate the anthropogenic CO_2 inventory of the North Pacific.

5.5.2 Ocean Carbon Cycle

R. Armstrong
J. Dengg
*V. Garcon**
T. Hughes
*G. Hurtt***
R. Murnane
*S. Pacala***
J. Sarmiento
R. Slater

**C.N.R.S., Toulouse, France*
***Dept. of Ecology and Evolutionary Biology, Princeton University*

ACTIVITIES FY96

The deep ocean exchanges gases with the atmosphere in the North Atlantic and in the Southern Ocean. Both regions are High-Nutrient Low-Chlorophyll (HNLC) regions, where the macro-nutrients phosphate and nitrate are not consumed during the growing season. The existence of HNLC conditions in these areas has a major impact on the ability of the deep ocean to sequester carbon. Understanding what controls the HNLC condition is therefore of fundamental importance for predicting the ocean's role in the global carbon cycle.

Advanced ocean ecosystem models can be used to understand and monitor the HNLC phenomenon. Calibration of a four-compartment ecosystem model using data from the U.S. JGOFS Bermuda Atlantic Time-series Study (BATS) was completed this year (1377). A simultaneous calibration to data from BATS and Ocean Weather Station (OWS) I was also completed. This latter calibration required several improvements, including a parameterization of growth limitation at OWS I by the micronutrient iron.

A carbon-nitrogen ecosystem model has been incorporated into a version of MOM. Pre-industrial air-sea carbon fluxes predicted with the model are generally in good agreement with observed fluxes, but there are local discrepancies. A method for diagnosing the amount and spatial distribution of oceanic "new production" from satellite data has been developed which will be useful for evaluating coupled biological/physical models.

In order to improve coupled biological/physical models with embedded pelagic ecosystems, a study was initiated that concentrates on those aspects of the physics that are of direct relevance to the biological subsystem. As a first testing ground, a $^4/_3$-degree resolution version of the eddy-resolving Kiel Mast Dynamo Model of the North Atlantic was set up. The model attempts to overcome a number of weaknesses found in earlier high-resolution models: 1) an isotropic grid provides higher horizontal resolution at higher latitudes; 2) an open southern boundary reduces the artificial vertical motions encountered at closed boundaries; and 3) a larger model domain combined with modified forcing data provides for a better simulation of the formation and overflow of deep water from the Greenland Basin. To improve the description of the near-surface mixing processes, a Kraus-Turner mixed-layer submodel has been added. To better accommodate the ecological model, the vertical resolution has been increased. First tests with the new model concentrated on the influence of the open boundary and prescribed inflows, and on the effects of different vertical mixing mechanisms.

Simulations of the ocean carbon cycle suggest that, although there is little inter-hemispheric transport of total carbon by the ocean, there is a significant amount of northward transport of isotopic anomaly (120×10^{15} gC ‰ per year) across the equator. The transport must be balanced by a southward atmospheric transport, or by a large net flux of carbon to the atmosphere. For example, a 6×10^{15} gC per year flux of terrestrial carbon with an isotopic composition of -20‰ would be needed to balance this isotopic anomaly flux.

PLANS FY97

The calibrated ecosystem model will be embedded into the ocean GCM, along with estimates of current atmospheric iron deposition rates and a description of iron cycling within and below the mixed layer. The combined model will be tested for its ability to predict the observed distribution of HNLC areas. New parameterizations of the effects of iron on algal growth and of multiple biogeochemically distinct algal taxa will be further developed.

The new North Atlantic model will be coupled to ecosystem codes presently in use. Initial experiments based on the Fasham model (1155) will be compared to earlier experiments with a 2-degree North Atlantic model. Subsequent versions will use a newly developed ecosystem model by Hurtt and Armstrong (1377). Experiments will concentrate on the effects of changes in the physical setup on the ecosystem, with special emphasis on coastal and equatorial upwelling regions and the surface mixed layer.

River fluxes of dissolved and particulate carbon will be introduced to the ocean carbon cycle model so that the alkalinity budget of the ocean can be better constrained.

5.5.3 Measurements

R. Key *C. Sabine*
G. McDonald *J. Sarmiento*
R. Rotter

ACTIVITIES FY96

The Ocean Tracer Lab (OTL) was actively involved in the WOCE survey of the Indian Ocean in FY96. The OTL had responsibility for all of the carbon work on leg I10 which ran from Dampier, Australia to Singapore. Nearly 1,000 discrete water samples were analyzed for both total CO_2 and total alkalinity. The OTL successfully operated an underway pCO_2 system for the entire Indian Ocean expedition which made 200,000 surface water and 50,000 marine air CO_2 measurements. Calibrations and quality control checks of the Indian Ocean data are continuing. An analysis of previous measurements from the Southern Ocean sector of the South Pacific has been completed (di).

PLANS FY97

A survey of the North Atlantic is scheduled to begin in FY97 aboard the R/V Knorr. The OTL has proposed to make underway pCO_2 measurements on the 5 legs planned for 1997. The system may also be run by NOAA scientists on additional legs scheduled for the Knorr in the North Atlantic next year. Synthesized datasets for each of the major ocean basins will be produced using all of the WOCE carbon measurements.

5.6 NITROUS OXIDE

J. Sarmiento *P. Suntharalingham*

ACTIVITIES FY96

The ocean is a significant source of atmospheric nitrous oxide (N_2O), but large uncertainties attend the estimated magnitude of this source, its spatial and temporal distribution, and the processes involved in marine N_2O formation. These issues have been investigated by two separate approaches. The first involves the development of a model of the oceanic N_2O cycle embedded in an ocean GCM. N_2O is treated as a non-conservative tracer subject to biological sources and sinks and gas-exchange at the ocean surface. N_2O source parameterizations are based on relationships between N_2O production and oxygen consumption at depth. A simple linear relationship succeeds in reproducing the large-scale features of the observed N_2O distribution. An oxygen-dependent N_2O source function is also being used to address recent claims that N_2O cycling mechanisms in the low oxygen regions of the global ocean may play a significant role in the oceanic N_2O distribution and sea-air flux.

A second approach uses existing oceanic N_2O observations to construct continuous maps of surface N_2O concentration which can be used to derive estimates of the global oceanic flux. The flux of N_2O to the atmosphere estimated from the mapped N_2O distribution

is 1.9 to 4.0x10^{12} g N per year. This result, and the results of the model simulation, are within the range of the IPCC estimated ocean flux of 1-5x10^{12} g N per year, out of an implied total global source of 13 to 20x10^{12} g N per year.

PLANS FY97

The N_2O modeling analysis will be completed.

5.7 OCEAN CIRCULATION TRACERS

R. Key *J. Sarmiento*
G. McDonald *J.R. Toggweiler*
R. Rotter

ACTIVITIES FY96

For the past five years, the Ocean Tracer Laboratory (OTL) has been the principal U.S. laboratory responsible for collection and interpretation of radiocarbon samples in the WOCE Hydrographic Program. The Ocean Tracer Laboratory participated in the WOCE survey of the Indian Ocean and collected large volume samples for standard beta counting techniques and small volume samples for analysis by accelerator mass spectrometry. Several completed studies describe the analytical and sampling techniques (dj), present the radiocarbon data (dl), and provide basin-scale interpretations of ocean circulation based on the data (dk, dm, dn).

The OTL continues to make major contributions to radiocarbon studies in the WOCE. The radiocarbon program completed sampling during Indian Ocean WOCE legs I1, I2, and I10 and from the WOCE Antarctic section S4 between Capetown and Fremantle.

PLANS FY97

The program will undertake sampling in the North Atlantic and analysis of measurements.

The OTL will begin a new sampling program in the North Atlantic.

6. OBSERVATIONAL STUDIES

GOALS

To determine and evaluate the physical processes by which the earth's climate and the atmospheric and oceanic general circulations are maintained in the mean, and by which they change from year to year and from decade to decade, using all available observations.

To compare results of observational studies with similar diagnostic studies of model atmospheres and model oceans developed at GFDL and thereby develop a feedback to enhance understanding in both areas.

6.1 ATMOSPHERIC DATA AND DATA PROCESSING

M.W. Crane *A.H. Oort*
G. Gahrs *A. Raval*
J.R. Lanzante *B.J. Soden*

ACTIVITIES FY96

6.1.1 Biases in Radiosonde and Satellite Measures of Upper Tropospheric Humidity

A project involving a comparison of daily observations of radiosonde and satellite upper tropospheric humidity (UTH) measurements is nearing completion. While radiosonde instruments are known to have particular difficulty in measuring humidity under very dry conditions, satellite humidity measurements are hindered by the presence of extensive cloud cover, which are typically associated with very moist conditions. The current work addresses the geographical and seasonal aspects of these relative observing biases using a limited global network of "high quality" radiosonde stations (the network of James Angell) and TOVS (Tiros Operational Vertical Sounder) data from a single satellite (NOAA10) during the period 1987-91. This project has sought to develop a general framework for the comparison of redundant measurement systems and is an extension and further development of some of the issues examined previously (1379).

Results to date suggest that a significant (~5-10% in terms of relative humidity expressed as a percentage) satellite "clear sky" bias in UTH can be detected in the tropical regions. The bias pattern appears to "follow" the seasonal north-south migration of the tropical convection zones. The bias was also found to be proportional to the relative humidity. In addition to this "clear-sky" bias which results from systematic elimination of moist cases from the satellite record, the relative bias between the two systems when both systems reported a valid observation was also examined. This latter bias is such that, for most stations, the satellite measure is ~10% higher (in terms of relative humidity expressed as a percentage). The latter bias was also found to be proportional to the relative humidity, which implies that when

comparing maps of satellite and radiosonde UTH, horizontal gradients should be enhanced in the former relative to the latter. This enhancement is greatest where the horizontal gradients are largest. However, it is not possible to determine which measure is closer to "reality".

6.1.2 Enhancement and Distribution of Software and Algorithms

A guidance document (xr) which describes "resistant, robust and nonparametric" statistical techniques has been placed on the World Wide Web. This class of statistical methods and procedures are designed to deal with "messy data", *i.e.*, that which contains outliers or is not drawn from a normal distribution. The manuscript provides alternatives to most of the common techniques routinely employed by meteorologists. Included are illustrative examples using real data as well as the formulas and algorithms. The intention is to encourage the use of these techniques which are not well known or appreciated by meteorologists.

Two libraries of Fortran routines for statistical analysis have been revised for easier use and have been made almost entirely portable (machine independent). These are packages for "statistical eigenvector analysis" and for "resistant, robust and nonparametric statistics". These are intended for use within GFDL and for outside collaborators. Both libraries are already being used by several researchers at GFDL.

6.1.3 Enhancing the Information Content of Radiosonde Temperature Data

A collaborative effort with Dian Gaffen of the Air Resources Laboratory (ARL) and Ted Habermann of the National Geophysical Data Center (NGDC) was begun. The purpose of this effort is to utilize both a unique compilation of "meta-data" describing historical changes in global radiosonde instruments (created at ARL) and advanced statistical methods (created at GFDL and NGDC) to improve the quality of radiosonde temperature data as well as the metadata itself. A library of nonparametric statistical routines discussed in 6.1.2 was transferred from GFDL to ARL for this purpose.

6.1.4 Objective Analysis Scheme for Global Monthly-Mean Fields

A complete write up on the new interpolation routine, called ANAL95, for obtaining global fields from irregularly spaced meteorological data has been completed and has been made available on the World Wide Web (1397). It includes a "Guide for the Use of ANAL95", the Fortran source code, and examples for testing the routine. ANAL95 has been used throughout the history of the Observational Studies Group at GFDL to analyze time-averaged values such as the wind, temperature and humidity fields, as well as their variances and covariances, on a variety of constant-pressure levels. ANAL95 is now available for use by any researcher interested in interpolating data from an irregularly spaced network onto a regular grid.

6.1.5 Graphics for Publication

Considerable efforts have been devoted to the designing of figures for a second edition of the book "Physics of Climate". Advances in computer graphics technology make

it possible and feasible to update the atmospheric statistics for the 2nd Edition from the original 10-year basis (1963-1973) to a 26-year basis (1964-1989).

PLANS FY97

Attempts will be made to utilize both radiosonde and satellite measures of upper tropospheric humidity in order to estimate water vapor trends. It will be necessary to use an approach which minimizes the influence of artificial (non-climatic) changes.

Collaboration will continue with Dian Gaffen of ARL and Ted Habermann of NGDS on a project to utilize "meta-data" and advanced statistical and data analysis techniques in an attempt to improve the quality of upper air temperature measurements and subsequently to estimate temperature trends.

The development of advanced graphical displays of the observed and model-generated climate statistics will continue.

6.2 CLIMATE OF THE ATMOSPHERE

M.W. Crane *A.H. Oort*
J.R. Lanzante *J.P. Peixoto**
N.-C. Lau *P. Peng*
M.J. Nath *F. Vitart*

**University of Lisbon, Portugal*

ACTIVITIES FY96

6.2.1 Westward Propagating Phenomena in Observed and Model Atmospheres

The nature of the westward migrating atmospheric fluctuations in subpolar latitudes has been investigated using observational records in postwar years as well as output from very long integrations with GCMs. By using analysis tools such as cross-spectrum and rotated singular value decomposition, it has been demonstrated that the GCMs are capable of reproducing the observed sites of occurrence, time scale, propagation speed, and spatial pattern of these phenomena. In the model atmosphere, the westward travelling features are discernible in the high latitudes of both hemispheres, and in both summer and winter. These retrograding phenomena are particularly active in regions with weak climatological zonal winds, so that the local advection of planetary vorticity by eddies is comparable to or stronger than the advection of eddy vorticity by the time mean flow. A more complete understanding of the origin of these perturbations, which have typical periods of about 20 days and which can attain substantial amplitudes, should contribute to improved long-range weather prediction. In particular, the skill of monthly and seasonal forecasts would depend critically on the accurate prediction of such slowly varying phenomena. Individual members of an ensemble of GCM runs subjected to the same boundary forcing are known to differ

considerably from each other (6.3.1). A portion of such inter-sample variability may be attributed to the random occurrence of the retrograding fluctuations.

6.2.2 15-Year Global Climatology of Relative Humidity

For the first time, a reliable description of the main characteristics of the relative humidity distribution in the atmosphere has been produced, based on 15 years of data from more than 1,000 radiosonde stations (zp).

The relationships between the global fields of relative humidity, temperature, specific humidity, and vertical motion have been explored further through correlation techniques. In testing whether the correlations are statistically significant, the number of degrees of freedom was determined in each case by carefully studying the structure of the various fields and by the use of scatter plots. Striking differences were found between the tropics and midlatitudes. In the tropics, relative humidity is primarily determined by the specific humidity, whereas in mid latitudes it is mainly a function of the temperature variations. As expected, convective processes dominate in the tropics with strong positive correlations between rising motion and high relative humidity, and vice versa.

A high degree of variability in space and time is found in the observed relative humidity, in contrast with some GCM simulations that show a tendency for a more constant relative humidity (1326,1368).

6.2.3 Long-Term Variability in the Hadley Circulation and its Connection to ENSO

Based on a 26-year set of daily global upper-air wind data for the period January 1964-December 1989, the interannual variability in the strength of the tropical Hadley cells has been investigated. Significant correlations are observed between the Hadley cells and the El Niño-Southern Oscillation phenomenon.

The anomalies in the strength of the Hadley cells are strongly and inversely correlated with the anomalies in the strength of the Walker oscillation. Much effort was spent on establishing the significance of the various computed correlations. As in the case of relative humidity mentioned above, there is the difficulty of estimating the appropriate number of degrees of freedom (Ndf). An unpublished, but very useful, technique to estimate Ndf, developed by the late J. Murray Mitchell in 1963, was adopted and will be published in an Appendix to (yq). According to this measure, most of the computed correlations between the measures of the ENSO, Hadley cell and Walker oscillation phenomena were found to be highly significant. Thus, during El Niño conditions (warm sea surface temperatures in the eastern equatorial Pacific), the Hadley cells tend to strengthen and the Walker oscillation tends to weaken, and vice versa during La Niña conditions (cold sea surface temperatures in the eastern equatorial Pacific).

6.2.4 Hydrology of the North African Desert

In an early study of the global budget of water vapor, Starr and Peixoto (1958) found that over the desert regions the computed evaporation tended to exceed the computed precipitation, forming an apparent source of water vapor for the atmosphere. This tentative conclusion, that deserts would supply water vapor to the atmosphere, was very surprising and remains a much-debated issue.

In the present work, four-times daily NCEP/NCAR Reanalyses for the years 1985 through 1993 have been used to investigate the hydrological cycle over the North African desert. The novelty of this work is that, for the first time, the influence of the diurnal cycle (*i.e.*, land and sea breezes) on the budget of water vapor can be properly investigated[1]. Significant diurnal variations were found in the fluxes of atmospheric water vapor and in the water vapor flux convergence and divergence across North Africa. Nevertheless, the statistics show a small, but apparently significant, excess of evaporation over precipitation over the central North African desert throughout the day. However, more research is needed to clarify the effects of gaps in the upper data, and to estimate the magnitude of possible contributions due to inflow or outflow of condensed water in clouds into the desert regions. The flux of cloud water has been neglected in analyses to date.

6.2.5 Evidence for Human Influence on the Thermal Structure of the Atmosphere

In a joint study with a large group of investigators both inside and outside GFDL (1384), which was based on the temperature statistics analyzed and produced in the Observational Studies Group at GFDL, a search was conducted for human influences on the thermal structure of the atmosphere. It was found that the observed spatial patterns of temperature change in the free atmosphere from 1963 to 1987 were similar to those predicted by state-of-the-art climate models. These models incorporated various combination of changes in carbon dioxide, sulphate aerosol and stratospheric ozone concentrations.

6.2.6 Creation of a Set of 26-year Mean Atmospheric Statistics

A large set of individual monthly statistics has been combined into a 26-year mean dataset of atmospheric statistics for the period January 1964 through December 1989. These data give one of the most representative pictures of the climate of the free atmosphere in existence. The 26-year mean statistics are being used to update the statistics in the book "Physics of Climate" for a future second edition. Surprisingly, most of the 26-year statistics are almost identical to the previously used 10-year mean statistics. This result represents new evidence of the great reproducibility and stability of the present statistics of the atmospheric circulation and climate in the free atmosphere.

---

1. Vitart, F., A.H. Oort, and Kingtse Mo, New results on the hydrology of the North African desert, in *Proceedings of the 20th Climate Diagnostics Workshop*, October 23-27, 1995, Seattle, WA, pp.191-194, 1995.

PLANS FY97

Research on the hydrology over North Africa will continue based on the NCEP/NCAR Reanalyses, with special emphasis on the influence of the diurnal cycle.

The updating and extension of the various Chapters for a future second Edition of the book "Physics of Climate" will continue.

6.3 AIR-SEA INTERACTIONS

S. Klein
N.-C. Lau
M.J. Nath
P. Peng
B.J. Soden

ACTIVITIES FY96

6.3.1 Sensitivity of the Atmospheric Circulation to Sea Surface Temperature Anomalies at Various Locations

A continuing effort has been made to examine the role of air-sea interaction in oceanic and atmospheric variability on interannual time scales. A series of four parallel GCM runs has been completed using prescribed observed month-to-month sea surface temperature (SST) anomalies in only the tropical Indian Ocean during the 1946-93 period. The output from this experiment has been compared in detail with that from an analogous experiment with prescribed SST anomalies in only the tropical Pacific Ocean. It has been demonstrated that the global atmospheric response to tropical Indian SST changes has a polarity which is opposite to that of the response to tropical Pacific anomalies. This finding is primarily attributed to the spatial displacement of the near-equatorial rainbelt when a SST anomaly in the tropical Pacific is replaced by a SST anomaly of the same sign in the Indian Ocean. This perturbation of the rainfall distribution leads to changes in the location of the tropical heating, the phase of the Southern Oscillation in the sea level pressure field, the configuration of the divergent circulation field in the upper troposphere, and the Rossby wave source. The latter field is in turn linked to the phase of the teleconnection pattern in the Northern Hemisphere extratropics.

A detailed diagnosis has been conducted of the ensemble of 13 parallel runs with prescribed global SST anomalies observed during the 1950-95 period. These runs were made using a triangular 40-wavenumber, 18-layer model at the National Centers for Environmental Prediction (NCEP). The results indicate that a substantial fraction of the extratropical model variability might be attributed to internal dynamics involving interactions between the seasonally averaged circulation and the transient eddies. The midlatitude response to changing SST conditions at the lower boundary, which accounts for a relatively smaller fraction of the total variability, is in good agreement with the observational results. The characteristic pattern of model variability on decadal time scales bears some spatial resemblance to the observed counterpart, but has a much weaker amplitude. The principal patterns of intersample variability of the simulated seasonal mean circulation are strongly correlated with the vorticity forcing by transient disturbances with subseasonal time scales.

The correlation between the atmospheric variations appearing in the 13 individual samples and fluctuations in the tropical heat sources and sinks is much weaker. The ability of the NCEP model to replicate the observed midlatitude anomaly in individual El Niño events has been critically assessed. The model skill is notably higher during El Niño events with strong SST anomalies, such as that occurring in the 1982/83 winter. The availability of the multiple samples in this suite of integrations also facilitates an estimation of the number of model runs required to establish stable ensemble means. For strong El Niño episodes, only 2-3 runs are sufficient to reliably determine the mean response. Larger samples (more than six runs) are needed to ascertain the response in weaker events.

The impact of SST anomalies in different geographical sites on extratropical atmospheric variability, and the possible role of the atmospheric circulation in linking oceanic changes at these individual sites, have been reported in a series of recent articles (1256, zy). Several review papers on this general subject area have been prepared, citing results from a coordinated set of GCM experiments performed at GFDL (1366, bx, by).

6.3.2 Atmospheric Bridge Linking Sea Surface Temperature Changes in Various Parts of the Tropical Oceans

In order to understand the lag correlations between the El Niño phenomenon in the Pacific and SST anomalies in the Indian Ocean, tropical North Atlantic and South China Sea (zv), an extensive analysis has been performed using the Comprehensive Ocean-Atmosphere Data Set (COADS). This analysis is focussed on the mechanisms that connect the warming in the Pacific to the warming in the other tropical oceans. In the South China Sea, the tropical North Atlantic, and the northern part of the Indian Ocean, the net heat flux into the ocean increases at the same time as the El Niño events in the Pacific. Due to the thermal inertia of the ocean, this increase in net heat flux forces a warming of the Atlantic, South China Sea and Indian Ocean a few months later. In each ocean, the change in net heat flux is due to a different combination of changes in cloud cover and evaporation. In many ways, this mechanism is similar to the "atmospheric bridge" concept (zy) used to explain the connections of midlatitude SST to the El Niño phenomenon in the tropical Pacific.

An attempt has also been made to identify the changes in large-scale circulation that cause the increase of the net heat flux into the tropical oceans outside the Pacific. For example, in the tropical North Atlantic, the increase in net heat flux arises from a reduction of evaporation that occurs only during the January-April period. The reduction in evaporation results from a reduction in the trade winds over the tropical North Atlantic. One possible cause for the reduction in the trade winds is the anomalous low pressure center over the southeast U.S., which is part of the Pacific-North American (PNA) pattern. Another possible cause is the weakening of the local Hadley cell over the Atlantic sector accompanying the drought conditions in the Nordeste region of Brazil.

PLANS FY97

Multiple runs with SST forcing corresponding to selected El Niño-Southern Oscillation events using a rhomboidal 30-wavenumber (R30) version of the GFDL Climate GCM will be completed. The findings from these integrations will be compared with previous runs based on

the rhomboidal 15-wavenumber version. This comparison will highlight the roles of eddy/mean flow interactions and tropical heating (both of which are better simulated in the R30 version) in determining the pattern and amplitude of the midlatitude response. Some of the sensitivity experiments involving variable SST forcing at selected sites will be repeated using GCMs with improved spatial resolution, model physics, and sampling.

An analysis will be made of the output from a GCM run with historically observed SST anomalies in the tropical Pacific and a 50-meter mixed layer ocean everywhere else. The ability of this experiment to simulate the atmospheric bridges linking the tropical Pacific to the other tropical oceans will be critically examined. In addition, analysis of radiosonde records and GCM runs will be performed in order to determine the processes responsible for the rise in mean tropical tropospheric temperature several months after the El Niño-related warming in the Pacific.

6.4 SATELLITE DATA

M. Crane *M.J. Nath*
N.-C. Lau

ACTIVITIES FY96

6.4.1 Comparison of Satellite and Surface Observations of Synoptic-Scale Cloud Patterns

The organization of various cloud types in relation to midlatitude cyclone waves and tropical convective disturbances has been examined using data from the International Satellite Cloud Climatology Project (ISCCP) and synoptic reports from surface observers at land stations and ships of opportunity. The cloud patterns derived from these two independent data sources were superposed on the concurrent wind and geopotential height fields obtained from the European Centre for Medium-Range Weather Forecasts (ECMWF) analyses. The results based on ISCCP data (1309) were found to be in generally good agreement with the composites using surface observations (Fig. 6.1). Specifically, both the satellite and surface-based data reveal well-defined cloud patterns associated with frontal features in extratropical baroclinic waves and with tropical convective disturbances. By combining the results from the ISCCP dataset (which provides information on cloud-top altitudes) and those from the surface observations (which identify cloud types according to the altitude of the cloud base), it is possible to estimate the vertical extent of the cloud cover in different sectors of the midlatitude cyclones and tropical disturbances. The ISCCP data underestimate the amount of stratus clouds lying beneath clouds with higher tops in the warm sector of the extratropical cyclones.

The consistency among the satellite-based and surface-based cloud types in recurrent meteorological features demonstrates the usefulness of both cloud products for depicting various facets of the atmospheric circulation. For instance, the spatial displacement of the cloud shield from the center of maximum ascent (as inferred from ECMWF analyses and from surface weather reports) in extratropical cyclones is indicative of the strong advective effects of the enhanced jetstream in the upper troposphere.

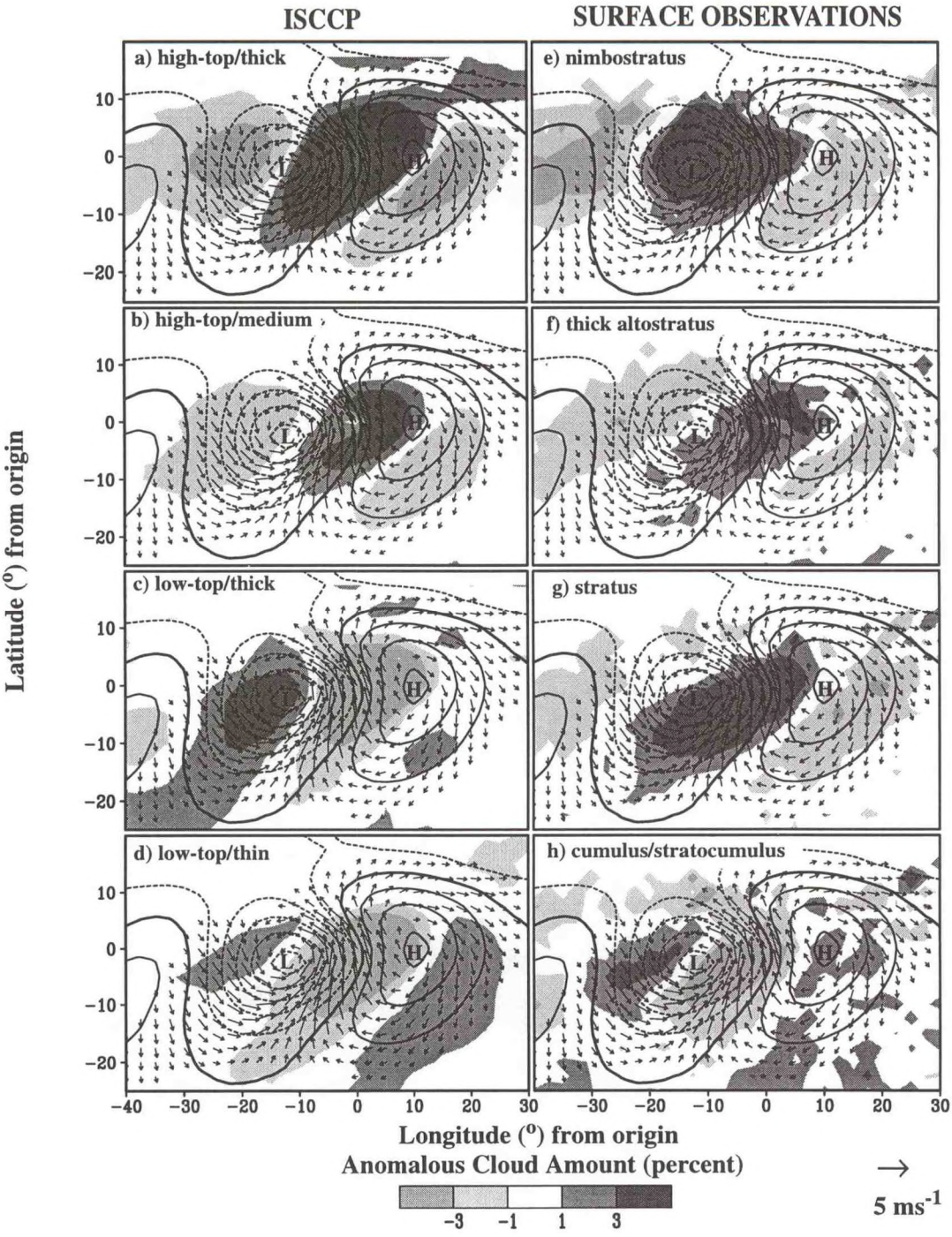

Fig. 6.1 Composite patterns of the anomalous amount of various cloud types for the ISCCP dataset and surface synoptic reports. Superposed on each panel are the corresponding composites of horizontal wind vector (arrows, see scale at bottom right) and geopotential height at 1000 mb (contours), as obtained from ECMWF analyses. All quantities are expressed as devations from the climatological wintertime average. The composite procedure is based on selected cloudy events at 20 reference sites in the North Atlantic during the cool seasons in the 1983-90 period. The ordinate (abscissa) of each panel represents latitudinal (longitudinal) displacements from the common origin, to which the composite charts for individual reference sites are aligned. Note the general agreement among the ISCCP and surface composites for most of the cloud types shown. Also note the underestimation of stratus clouds in the ISCCP composite (compare panels (c) and (g)).

PLANS FY97

Further efforts will be made to discern the interactions between the atmospheric circulation and cloud properties associated with stratus decks in subtropical high pressure regions, and with precipitating systems along subtropical frontal zones. Particular emphasis will be placed on the role of atmospheric dynamics in the temporal evolution of these cloud systems. The mesoscale cloud organization in frequently occurring circulation systems will be studied using ISCCP products with higher spatial resolution (approximately 30 km).

7. HURRICANE DYNAMICS

GOALS

To understand the genesis, development and decay of tropical disturbances by investigating the thermo-hydrodynamical processes using numerical simulation models.

To study small-scale features of hurricane systems, such as the collective role of deep convection, the exchange of physical quantities at the lower boundary and the formation of organized spiral bands.

To investigate the capability of numerical models in predicting hurricane movement and intensity, and to facilitate their conversion to operational use.

7.1 HURRICANE PREDICTION SYSTEM

ACTIVITIES FY96

7.1.1 Performance in The 1995 Hurricane Season

M.A. Bender R.E. Tuleya
Y. Kurhiara

The GFDL Hurricane Prediction System, which became an official operational model for the National Weather Service beginning in the 1995 hurricane season, made 257 forecasts for the Atlantic tropical cyclones, including depressions, and 105 forecasts for the Eastern Pacific basin. The tropical cyclone activity was unusually high in 1995. The system produced substantial improvement in track forecasts, with 35% improvement relative to Cliper (Climate-Persistence method) in the Atlantic at the two and three days forecast time, respectively, and 22% and 17% at the corresponding times in the Eastern Pacific. Position errors of several models (averaged for homogeneous cases) in the two basins are listed in Table 7.1. In the Atlantic, the improvement relative to the next best model at 36, 48 and 72 hour are 14%, 19% and 25%, respectively. In the Eastern Pacific, the GFDL system is the best performer after 24 hours. Apparently, the improvement results from the model's nested fine mesh which can better represent the compact three-dimensional structure of a tropical cyclone at the initial time and throughout the forecasting period. It should be noted that accurate track guidance for two to three days ahead provides much-increased lead time for preparedness activities during the approach of tropical cyclones. In the Atlantic, prediction skill was extremely high in cases of Hurricane Luis and Hurricane Marilyn. On the other hand, track predictions in the Gulf of Mexico, *e.g.*, the forecasts of Hurricane Opal and Roxanne, tended to show westward bias.

The GFDL system was also employed to carry out the experimental prediction of the typhoons in the Western Pacific. This basin is generally warmer than the Atlantic and more

TABLE 7.1 Hurricane track forecast errors in the 1995 hurricane season. Average errors (in km) for homogeneous cases.

Atlantic basin

Model	GFDL	BAMD	BAMM	BAMS	A90E	VBAR	CLIPER
12h(218 cases)	95	97	105	121	90	88	100
24h(209 cases)	165	185	199	235	167	180	215
36h(194 cases)	218	265	284	344	253	269	337
48h(177 cases)	270	333	356	430	343	352	452
72h(146 cases)	395	530	546	630	590	560	666

Eastern Pacific basin

Model	GFDL	BAMD	BAMM	BAMS	PSS	P91E	CLIPER
12h(86 cases)	81	88	95	99	74	74	75
24h(76 cases)	139	158	179	194	151	148	158
36h(67 cases)	190	218	270	292	220	208	234
48h(58 cases)	248	273	355	384	285	256	304
72h(37 cases)	305	321	437	526	425	332	420

intense storms tend to develop. In total, 125 forecasts were made for 16 storms. Compared to both the NOGAPS global model forecasts of the U.S. Navy's Fleet Numerical Meteorology and Oceanography Center and the Joint Typhoon Warning Centers official forecasts, the GFDL system exhibited considerably higher skill, *e.g.*, improvement of 37% and 26% at 48 and 72 hours, respectively, against NOGAPS. Forecast of tracks of Typhoon Faye and Typhoon Ward were especially skillful. In contrast, better forecasts of Typhoon Janis were provided by the NOGAPS model.

7.1.2 Post-season Analysis

M.A. Bender *R.E. Tuleya*
Y. Kurihara *C.-C. Wu**

**National Taiwan University*

The spatial distribution of the position errors for the GFDL model forecasts for the 1995 season was investigated. Interestingly, the smallest error (~100 km for 48h) is found in the open ocean region of the central Atlantic, as shown in Fig. 7.1. Relatively large errors are found in the Gulf of Mexico, along the East Coast of the U.S. and to the north of Guyana. One significant source of errors in the Gulf of Mexico is the westward bias of the GFDL forecast tracks. Other possible sources are related to the initial synoptic scale analysis, the structure of the initially specified vortex, and also to the absence of hurricane-ocean feedback processes in the current system.

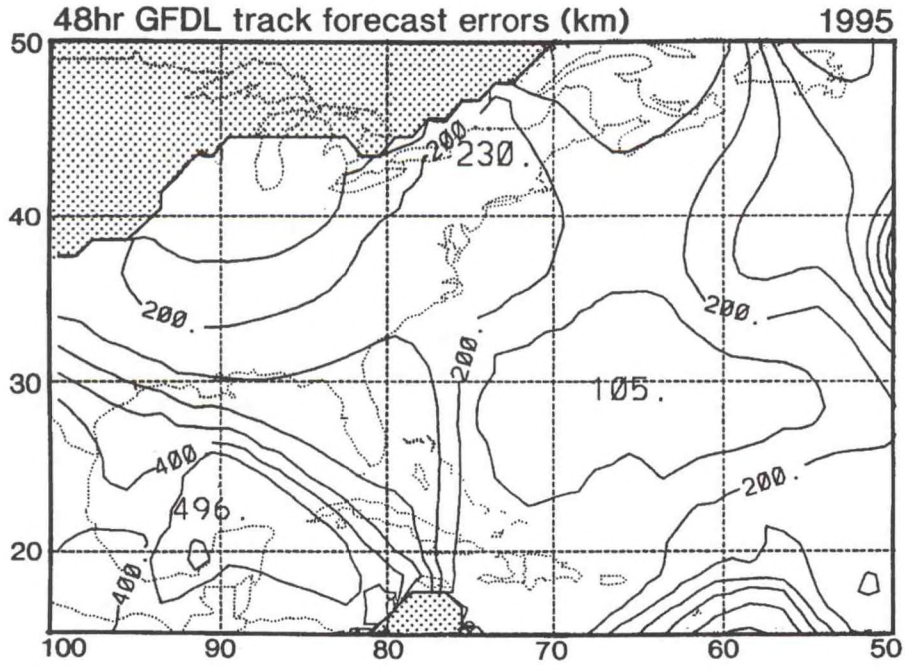

Fig. 7.1 Distribution of the average track forecast errors (in km) by the GFDL model at 48 hour forecast time in the Atlantic basin in the 1995 hurricane season. The contour interval is 50 km. No storms were observed in the shaded regions.

Evaluation of intensity forecasts by the GFDL model indicates a tendency to overpredict intensity of weak systems and underpredict the intensity of strong systems in all basins. This problem seems to be related to the simple initialization scheme of vortex spin-up in which the axially asymmetric structure observed in many storms is removed.

Several major changes were proposed in the global forecast/assimilation system of NCEP. The impact of these proposed modifications, including the use of the satellite water vapor wind data and a change in the vortex bogusing, on the track prediction of the GFDL model was examined. The improved NCEP analysis was found to have a positive impact, reducing the forecast errors by 10% to 20%.

An evaluation of prediction capabilities in the Western Pacific was performed. The forecast errors were extensively analyzed in terms of systematic bias and error scatters.

7.1.3 The 1996 Hurricane Season

M.A. Bender R.E. Tuleya
Y. Kurihara

The GFDL Hurricane Prediction System was modified for the 1996 season by imposing an upper limit of 1000 km on the radius of the specified vortex and also by implementing a

scheme to reduce noise near the lateral boundary caused by strong outflow. In general, the system continues to provide improved storm track guidance. The track forecasts of Hurricane Edouard were particularly skillful. However, forecasts of Hurricane Dolly showed a systematic southward bias. Also, problems were observed in tracking weak storms located in the vicinity of the Mexican coast in the Eastern Pacific.

Collaboration with the U.S. Navy resulted in the successful combination of the GFDL Prediction System with their NOGAPS global forecast/analysis system, providing forecasters with guidance for the typhoon prediction in the Western Pacific starting this season. A system was instituted in which parallel runs are performed using the AVN analysis of NCEP, constituting what may be regarded as a "mini-ensemble" forecast. So far, forecast results from the two different analyses are both quite impressive and the difference between the forecast position errors in terms of distance (from the operational fixes) are not statistically significant.

PLANS FY97

Performance of the GFDL system in the remaining 1996 hurricane season will be carefully monitored and the post-season analysis of the forecast results will be conducted. High resolution forecast experiments will be initiated.

7.2 HURRICANE PREDICTION CAPABILITY

ACTIVITIES FY96

7.2.1 Sensitivity of Forecasts to the Environmental Wind Analysis

M.A. Bender *B. Soden*
Y. Kurihara *R.E. Tuleya*
*S.J. Lord**

**National Center for Environmental Prediction*

A recent study demonstrating the positive impact of Omega dropwindsonde data on the tropical cyclone forecasts with the GFDL model using the NCEP global analysis was completed (bs). The average improvement in the track prediction amounts to ~50 km for one and two day forecasts and ~100 km for three day forecasts. Also, an apparent improvement of 5 knots in the wind intensity forecasts was found at forecast ranges of 2-3 days.

A study was initiated to evaluate the usefulness of the satellite water vapor wind data for the tropical cyclone track forecasts. In a preliminary investigation, the data were combined with the NCEP global analysis to provide the modified environmental flow. Small improvements of the track prediction due to the addition of the water vapor wind data were found in some of the cases examined.

7.2.2 A New Method of Vortex Generation

M.A. Bender R.E. Tuleya
Y. Kurihara

One of the reasons why the improved intensity forecast skill of the GFDL system is not obtained until after a day or two into the forecast period is the presumption of a symmetric structure of the vortex generated in the current GFDL initialization scheme. A new scheme for vortex generation was formulated and numerical tests of the scheme have begun. It is anticipated that a more realistic vortex will be generated, including effects of the existing environmental flow.

7.2.3 Extended Prediction

R.E. Tuleya

Motivated by the substantial improvement of the tropical cyclone track forecast skill with the GFDL model for periods up to three days, the forecasts for 24 cases in the Atlantic in the 1995 season were further extended to five days and their skills were assessed. The mean forecast errors at four and five days are 290 nm and 380 nm, respectively. The case to case variability was large, with track forecast errors as large as 1000 nm in a few difficult cases of Hurricane Felix.

7.2.4 Ensemble Forecast

S.D. Aberson *R.E. Tuleya*
M.A. Bender

**Hurricane Research Division/AOML*

An effort to conduct ensemble forecasts of tropical cyclone tracks was initiated in cooperation with NCEP by combining the GFDL Prediction System with the NCEP operational ensemble forecasts. Preparatory work is underway.

PLANS FY97

The formulation of the new method of vortex generation will continue and the new scheme will be extensively tested. The impact of the satellite water vapor wind will be assessed in the continuing study. Ensemble forecasts may be tested at NCEP.

7.3 BEHAVIOR OF TROPICAL CYCLONES

ACTIVITIES FY96

7.3.1 Landfall of Tropical Cyclones

M.A. Bender *R.E. Tuleya*
Y. Kurihara

Hurricane Opal (1995) exhibited an interesting intensity change during its approach to the land. Investigation is underway of the behavior of the storm in the GFDL model during this period as well as after landfall.

7.3.2 Tropical Cyclone-Ocean Interaction

M.A. Bender *Y. Kurihara*
*I. Ginis**

**University of Rhode Island*

In order to study the effects of tropical cyclones on the structure of the ocean, in particular that of the mixed layer, and its feedback mechanism influencing the storm behavior, a coupled model consisting of the GFDL hurricane model and the Princeton ocean model was constructed. This coupling was facilitated by the specification of both lateral and bottom boundaries of the Princeton ocean model. A 72h coupled simulation experiment was performed for one case of Hurricane Gilbert (1988) for the period from its entering in the Gulf of Mexico to after its landfall over Mexico. A cooling of the sea surface temperature of up to 4 K was generated. As a result, the over-intensification of the hurricane previously observed in simulations run without ocean coupling was considerably reduced, resulting in an improved intensity forecast as shown in Fig. 7.2. The coupled model was also run for two cases of Hurricane Opal and an energy budget analysis is in progress to investigate the impact of any sea surface cooling on the intensity and track forecasts.

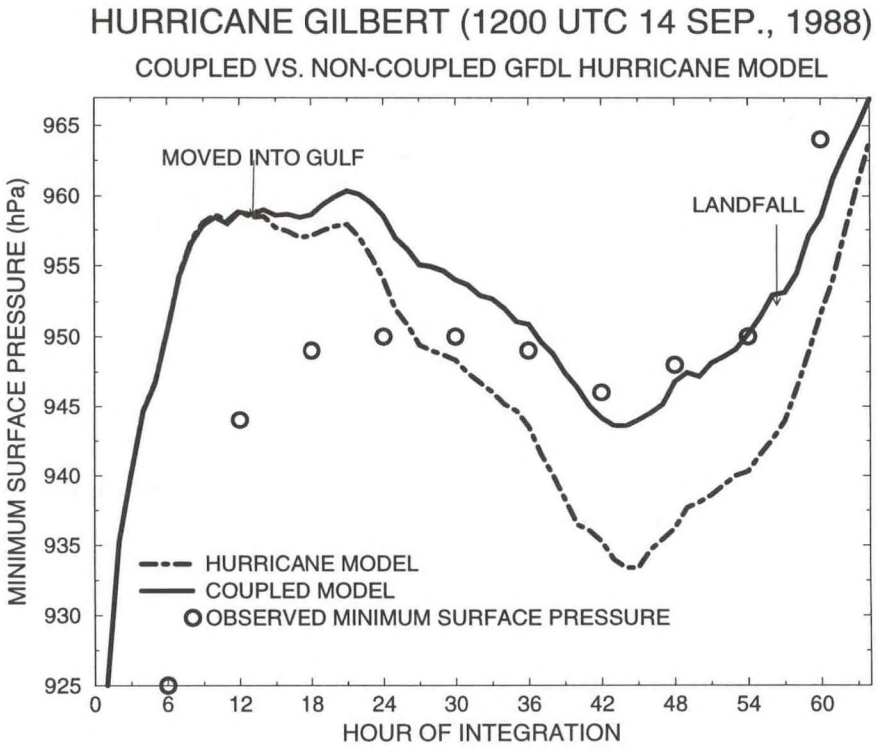

Fig. 7.2 Time series of the minimum sea surface pressure in the hurricane-ocean coupled model vs. the non-coupled model for a case of Hurricane Gilbert starting at 1200UTC 14 September, 1988.

PLANS FY97

Studies of hurricane behavior conducted in FY96 will continue. Expedient deployment of a GFDL coupled tropical cyclone-ocean forecast system may result from an increase in the collaboration with Isaac Ginis at the University of Rhode Island.

7.4 STRUCTURE OF TROPICAL CYCLONES

M.A. Bender Y. Kurihara

ACTIVITIES FY96

7.4.1 Asymmetric Structure

Further analysis of the quasi-steady asymmetric structure of the vortex developed in idealized environmental conditions was performed. In the previous analysis, the strong relationship between the asymmetric pattern and the winds relative to the storm motion was revealed. It was found that the impact of the asymmetric relative winds on the relative vorticity field of the symmetric flow is subtle. Namely, the vorticity tendency due to the advection of the

symmetric vorticity by the relative wind balanced fairly well with the tendency associated with the stretching of the symmetric vorticity caused by the asymmetric divergence.

7.4.2 Transition to an Extratropical System

A study was made of the transition process of Hurricane Luis (1995) to an extratropical system in the vicinity of Nova Scotia, Canada. Analysis results suggest that, at a certain stage in the transition, the effects of strong vertical shear of the environmental winds in suppressing the tropical characteristics of the storm begin to dominate the effects of the circulation in maintaining or restoring the tropical storm characteristics. It seems the cooler sea surface temperature weakened the latter effects as the storm moved northward.

PLANS FY97

The analysis of tropical cyclone structure and structure change will continue using numerical results from the GFDL forecasts.

7.5 MODEL IMPROVEMENT

M.A. Bender *R.E. Tuleya*
Y. Kurihara

ACTIVITIES FY96

The GFDL vortex specification technique used in the 1995 hurricane season was evaluated, particularly with respect to the sensitivity of storm track forecasts to the radius of the inserted specified vortex. As a result, it was decided to limit the vortex radius to 1000 km in the 1996 hurricane season. This change affects the structure of the initial vortex, as well as the initial fields in the vicinity of the storm, in cases of large storms. Together with the revised version of the NCEP global analysis, it is expected that track errors could be reduced by ~20% for 12-36hr forecasts, and to a lesser degree for longer forecast periods.

The weights used in the smoothing of fields near the domain boundary were found to be insufficient to suppress noise in some cases of strong outflow. To deal with this problem, the smoothing weights were made dependent on the wind angle at the lateral boundary. This change was implemented in the GFDL system in 1996.

Upgrading of the model initialization phase requires significant coding changes in the specification of the target wind field as well as in the vortex generation. A large portion of this recoding has been completed.

PLANS FY97

Efforts will continue in developing the new method for vortex specification. The storm tracking algorithm will be reexamined in order to better handle cases involving mountain effects.

8. MESOSCALE DYNAMICS

GOALS

To produce accurate numerical simulations of mesoscale processes in order to understand what role synoptic scale parameters play in their generation and evolution.

To understand the dynamics of mesoscale phenomena and their interaction with larger and smaller scales.

To determine the practical limits of mesoscale predictability by means of sensitivity studies using numerical simulations of mesoscale phenomena.

8.1 THE LIFE CYCLE OF MIDLATITUDE CYCLONES

I. Orlanski *J. Sheldon*
L. Polinsky

ACTIVITIES FY96

8.1.1 Cyclone Evolution Along Storm Tracks

Understanding the nature of cyclone evolution along storm tracks requires looking beyond the life-cycle of individual eddies. The synergy between the cyclone and planetary scale is profound. This interaction is clearly evident in the most active regions of storm tracks. In particular, cyclones behave and interact differently with the environment in the entrance and exit regions of storm tracks. North America, bounded by the exit of the Pacific storm track and the entrance of the Atlantic storm track, is affected by the differences in cyclone evolution in these regions. The different mechanisms producing cyclones are in part responsible for the difference in forecast skill for eastern and western regions of the North American continent.

An ongoing investigation aims to characterize the behavior of cyclones in the observed entrance and exit regions of storm tracks. Preliminary results indicate that a distinct circulation over the eastern Pacific Ocean could be responsible for lowering mid-range (5-10 day) forecast skill. The 500 mb height anomaly correlation for the five day forecasts produced by the ECMWF, UKMO and NCEP has been used as a filter for a regression analysis in various regions of the Northern Hemisphere midlatitudes. The time-lagged regressions of 500 mb heights and meridional wind from the ECMWF dataset have been computed for the five year period 1986-1990. Fig. 8.1 shows the regression of the 500 mb heights corresponding to periods when the averaged anomaly correlations are higher than 0.77 (High Skill) and when they are lower than 0.67 (Low Skill). Wavelet decomposition (8.1.2) was used to separate the planetary and synoptic scales from global scales in the height anomalies. The regression

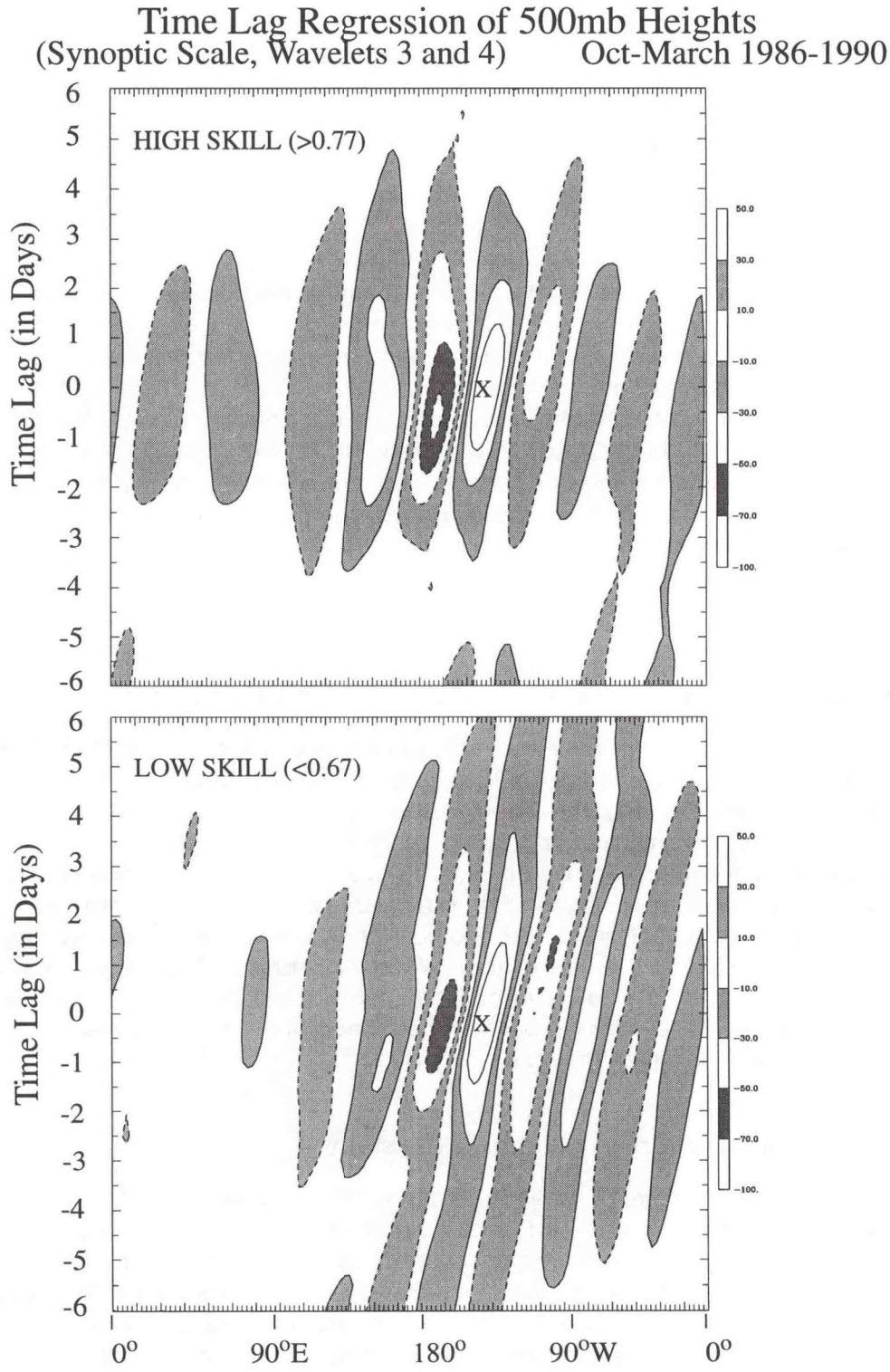

Fig. 8.1 Time-lagged regression (in meters) of 500 mb heights corresponding to high skill (top) and low skill (bottom). "Skill" is defined as the average 500 mb height anomaly correlation based on 5-day forecasts from ECMWF, UKMO, and NCEP. The zonal scale of the 500 mb heights used in this analysis is between 3000 km and 5000 km (Wavelets 3 and 4). In cases of high skill, the eddies have a lifecycle of 5-6 days and progress eastward, while in cases of low skill the eddies become more long-lived and stationary near the eastern Pacific ridge.

variable was located in a 10° meridional band centered at (42.5°N, 140°W), in the eastern Pacific Ocean where the storm track spreads meridionally due to the presence of a standing ridge. A clear difference between the signatures of the high and low skill cases can be seen. Cases with high skill correspond to eddies that seem to have a life cycle of 5 to 6 days with an amplitude maximum that progresses eastward (1177). However, in cases with low skill, the eddies become elongated and more nearly stationary at a position corresponding to the ridge.

Regression analyses of the meridional velocities show similar patterns. All of these results are consistent with the fact that when the eastern Pacific ridge is weak, synoptic disturbances can leak through and enter North America on the west coast of the U.S. However, in periods when the ridge is strong, transient eddies are blocked at these latitudes and their entrance into North America is shifted northward into Canada and Alaska. These results also suggest that the transient disturbances are not only blocked by the ridge, but actually seem to maintain the ridge as they propagate poleward along the storm track. Although the polar deflection of the storm track is stronger in winter than in fall, the energy of the synoptic scale eddies are comparable in both seasons. The seasonal evolution of the synoptic scale disturbances along the storm track is presently under investigation. An understanding of this behavior could have profound implications for improving forecasts for North America.

8.1.2 Wavelet Analysis for Detection of Baroclinic Packets in Storm Tracks

In the analysis of cyclone evolution along storm tracks, it is often difficult to identify wave-packets in the presence of complex flows characterized by different scales. An analysis technique based on wavelet decomposition can be a powerful tool for such detection. The wavelets used in this analysis are orthogonal and act like band-pass filters of Fourier components. Each wavelet represents a band of wavenumbers, and an individual wavelet can represent a entire packet of waves if they are present in the signal. The time evolution of the wavelet amplitude which characterizes the packet can denote precisely the length and speed of the packet along the storm track. Wavelet analysis of idealized storm track simulations is able to distinguish between baroclinic waves characterized by high and low wavenumbers and clearly identifies the propagation speed of individual eddies as well as the baroclinic wave packets in which they are imbedded.

8.1.3 Stages in the Energetics of Baroclinic Systems

A comprehensive picture of "downstream baroclinic evolution" can be developed by analyzing local energetics in idealized and case studies (1345). This viewpoint offers a complementary alternative to the more conventional descriptions of cyclone development. The local energetics approach permits one to define an energy flux vector which accurately describes the magnitude and direction of energy dispersion and clarifies the role of neighboring systems in local development. In this view, the development of a system's energetics is divided in three stages. In *Stage 1*, a pre-existing disturbance well upstream of an incipient trough loses energy via ageostrophic geopotential fluxes directed downstream through the intervening ridge, generating a new energy center there. In *Stage 2*, this new energy center grows vigorously, at first due to the convergence of these fluxes, and later by baroclinic conversion as well. As the center matures, it begins to export energy via

geopotential fluxes to the eastern side of the trough, initiating yet another energy center there. In *Stage 3*, this new energy center continues to grow while that on the western side decays due to dwindling energy fluxes from the older upstream system and its own export of energy downstream. As the eastern energy center matures, it exports energy further downstream, and the sequence begins anew.

Midlatitude and high-latitude case studies were used to test the limits to which this conceptual sequence might apply. One of the cases used was the notorious "Blizzard of '93" (8.2.1). Despite the extraordinary magnitude of this event, it was shown that the evolution of the trough associated with the storm fits the conceptual picture of downstream baroclinic evolution quite well, with geopotential fluxes playing a critical role in its development (1345).

PLANS FY97

An investigation into the seasonal evolution of the storm track and the synoptic scale disturbances within it will employ both data analyses and idealized simulations using a new version of the hydrostatic Zeta model expressed in spherical coordinates (8.4.1). One particular goal will be the accurate modelling of the poleward deflection of the storm track during the transition from autumn to winter. Efforts aimed at correlating the structure of eddy activity with the local environmental characteristics at the entrance and exit of storm tracks will continue. The relationship between the stability and changes in the monthly mean flow and its ability to support different regimes of eddy activity, including packets, will remain a focus of investigation.

8.2 SENSITIVITY STUDIES OF MIDLATITUDE CYCLONES

G. Balasubramanian *I. Orlanski*
S. Garner *J. Sheldon*

ACTIVITIES FY96

8.2.1 The Blizzard of '93

Various case studies seem to indicate that downstream fluxes are an inseparable contributor to the development of all energy centers associated with baroclinic systems (8.1.3). However, it is also possible that baroclinic conversion alone could, in some cases, initiate such a disturbance on its own. In an effort to determine whether an event could be precipitated by purely baroclinic means, local energetics were analyzed in the record-setting Blizzard of '93, which moved up the east coast of the U.S. on 13-14 March 1993. It was found that even in an event as explosive as this, geopotential fluxes played a key role. Fluxes from a decaying system over the Pacific converged over the west coast and initiated the development of an energy center, altering the basic flow and causing the jet stream to push south into Mexico. Subsequently, fluxes from this new energy center became strongly convergent over the Texas gulf coastal region, initiating strong development of an energy center there. This energy center, in turn, tapped into the baroclinicity of a weakly stable area over the Gulf of Mexico. Strong local baroclinic conversion combined with continued convergence of fluxes from the energy center on the west side of the trough (itself maintained

by baroclinic conversion in the sinking cold air) to produce the spectacular strengthening of this record-breaking storm (1345).

8.2.2 Nonlinear Baroclinic Wave Equilibration

The interaction between baroclinic eddies and the zonal-mean or time-mean circulation has implications for the jet stream, storm tracks, stationary wave patterns and blocking events. A previous study (ai) of planetary-scale waves (zonal wavenumber 6) identified a positive feedback between the zonal-mean wind and meridional eddy momentum flux which accounts for starkly different lifecycle patterns in different model geometries and background shear. This work has been extended to explain the preference for cyclonic equilibration at wavenumber 8 and in narrow jets (cb). It has also been possible to identify possible mechanisms that determine whether eddies zonalize or organize into coherent structures at the end of their lifecycles. The combined lifecycle studies have led to the classification shown in Table 8.1

Table 8.1. Classification of nonlinear equilibration on the sphere

Waves	Zonalizing?	Type of Equilibration	Momentum Flux
Long (wavenumbers 5, 6)	Yes	Anticyclonic breaking	Poleward
Short (8, 9, 10,...)	Yes	Cyclonic breaking	Equatorward
Intermediate (7)	Yes	Both types of breaking	Poleward and Equatorward
Long waves with cyclonic barotropic shear	No	Coherent cyclonic vortices	Weak

The distinction between long and short waves is summarized in rows 1 and 2. At all stages of development, the long waves are dominated by poleward momentum flux, while the short waves show mainly equatorward flux. A positive feedback with the time-dependent zonal-mean wind forces the outcome described under "type of equilibration". The direction of flux is related to the meridional scale of the eddy, which was discovered by examining wavenumber 6 in a narrow jet and wavenumber 7 after 2 days of growth. The distinction between zonalizing (rows 1-3) and long-lived (row 4) eddies lies in the amount of warm air that "secludes" during the growth phase. The short waves, though cyclonic, develop relatively little warm temperature anomaly at low levels and thereby become vulnerable to large-scale deformation.

PLANS FY97

The lifecycle studies will be made more realistic by including latent heating and by shifting to a forced-dissipative climate system in which statistical relationships can be established between lifecycle behavior and local environments.

8.3 TOPOGRAPHIC INFLUENCES IN ATMOSPHERIC FLOWS

S. Garner *B. Gross*

ACTIVITIES FY96

8.3.1 Total Wave Drag in a Two-dimensional Model

Assessing the role of mountain torque in the atmosphere starts with an analysis of the total momentum sink at the lower boundary. Using a two-dimensional mesoscale model, the modulation of total mountain drag by surface friction and large-scale baroclinicity has been investigated. Surface friction is introduced with a one-dimensional boundary-layer model that includes height-dependent diffusivity. The large-scale baroclinicity was shown in a previous study to enhance blocking in warm advection.

Adding a frictional boundary layer enhances not only the frictional momentum sink but also the topographic drag in some cases, especially in high-drag solutions. The resolved disturbance in the current set of experiments is nearly hydrostatic, but the friction due to a gravitationally stable boundary layer can be thought of as the nonhydrostatic response to unresolved topography. Previous studies have shown that resolving nonhydrostatic mountain waves can add a significant drag. We conclude that the failure to resolve or parameterize all of the surface roughness may have a larger impact on the total momentum sink than is represented by the friction alone.

Large-scale baroclinicity has a negligible effect on drag at small amplitude. However, steady-state drag is highly sensitive to nonlinearity in the case of large-scale warm advection. In the case of cold advection or no advection, the sensitivity is concentrated at the threshold for wavebreaking, where the steady-state drag rises precipitously. High drag in warm advection is reached more smoothly, with no sharp transition at the onset of wavebreaking.

8.3.2 Frontal Interaction with Orography in a Nonhydrostatic Compressible Model

The nonhydrostatic Zeta model (8.4.2) has been used to simulate the interaction of an idealized three-dimensional cold front with an isolated mountain ridge. A similar experiment with the hydrostatic Zeta model showed that deceleration of cold postfrontal air creates a high pressure anomaly on the windward slope that can accelerate air over the peak in a shallow ageostrophic gravity current (1232). The effects of compressibility, the Boussinesq approximation, and nonhydrostatic motions on this scenario have been evaluated by comparing the two model integrations. Preliminary results indicate that both compressibility and the decrease of density with height weaken surface frontogenesis as the gravity current descends the lee slope, possibly due to the relatively slow development of the baroclinic wave in atmospheres with compressibility (as) or a finite density scale height. Nonhydrostatic effects were difficult to evaluate because nonhydrostatic features, particularly those in the gravity current, cannot be adequately resolved at the horizontal resolution of the simulations (20 km). Even so, the difference between the hydrostatic and nonhydrostatic pressures were less than 10% throughout the nonhydrostatic model run, even during the descent of the front down the lee slope.

PLANS FY97

The assessment of topographic wave drag will be extended using the recently-developed three-dimensional, compressible, grid-point model. Of particular interest is the way in which the mesoscale topographic forcing alters the synoptic-scale disturbances and thereby feeds back on itself. The effects of compressibility, the Boussinesq approximation, and nonhydrostatic motions on the interaction of a front with a mountain will continue to be evaluated.

8.4 MODEL DEVELOPMENT

G. Balasubramanian *I. Orlanski*
B. Gross *L. Polinsky*

ACTIVITIES FY96

8.4.1 Improvements to the Hydrostatic Zeta Model

The primitive equation Zeta model uses the terrain-following coordinate

$$Z = e^{-\varepsilon\left(\frac{z-h(x,y)}{H-h(x,y)}\right)},$$

where $h(x,y)$ represents the topographic height and H is the height of the rigid lid. The original version of the model is dry, inviscid, and adiabatic (except that weak second-order diffusion is included to control noise), and employs the hydrostatic and Boussinesq approximations. A complete description of the model has been provided (1200). A new version of this model is expressed in spherical coordinates to more accurately simulate large-scale and synoptic-scale dynamics (8.2.2). Parameterizations of surface heat fluxes and surface drag have been introduced in order to more realistically examine the effects of baroclinicity and surface friction on cyclone development and its long-term statistics within storm tracks.

8.4.2 Improvements to the Nonhydrostatic Compressible Zeta Model

A three-dimensional, nonhydrostatic, fully compressible version of the hydrostatic Zeta model has been used to investigate mesoscale atmospheric circulations and for evaluating nonhydrostatic and compressibility effects by direct comparison with the hydrostatic Zeta model. The current version of the nonhydrostatic compressible model uses velocity as a dependent variable and expresses advection as second or fourth order finite-differences rather than in flux form. The vertical pressure gradient and vertical divergence of vertical velocity are integrated semi-implicitly in the vertical. Other features of the model have been fully documented (as). A version of the model expressed in spherical coordinates is also available. All versions exploit some features of Fortran-90 and can run on the Cray T90 and SGI workstations available at GFDL. The three-dimensional model has been verified against the hydrostatic Zeta model with idealized simulations of barotropic and baroclinic instability (8.4.4).

8.4.3 Development of a Dynamical Core of Grid-point GCM

The pressure coordinate, hydrostatic PE model in Cartesian coordinate employed in a recent normal mode lifecycle simulation (ai) has undergone substantial improvements. The model is now expressed in sigma coordinates on a horizontal C-grid, and spherical metric terms have been added. The walls have been removed and now its meridional extent is from the south pole to the north pole. This grid-point GCM represents a valuable extension of the set of limited area models currently being used in synoptic and mesoscale studies. The baroclinic lifecycle simulated by this model on the sphere is in excellent agreement with that simulated with a global spectral model. The climate simulated by this grid-point GCM is currently being tested against the results of other dynamical cores. The normal modes for baroclinic basic states in this sigma-coordinate model are being compared with the normal modes for similar basic states in the hydrostatic Boussinesq Zeta model on the sphere.

8.4.4 Model Intercomparisons

The addition of the nonhydrostatic Zeta model to several other two- and three-dimensional hydrostatic and nonhydrostatic models provides a suite of tools with which a variety of atmospheric phenomena can be explored. With these tools, nonhydrostatic and compressibility effects can be assessed in three dimensional flows. Such an assessment was made in order to verify the nonhydrostatic Zeta model by comparing hydrostatic and nonhydrostatic simulations of idealized barotropic and baroclinic instability (as). A linear stability analysis shows that the growth rates for both instabilities decrease with compressibility, as measured by the inverse acoustic phase speed. An examination of the perturbation energy equations indicate that the work done against elasticity during compression represents a source of perturbation internal energy and a sink of perturbation kinetic energy, thereby diminishing the growth rate. Simulations of barotropic and baroclinic instability with the nonhydrostatic compressible Zeta model are nearly identical to those using the hydrostatic Boussinesq Zeta model, but show that relatively slow growth continues well into the nonlinear regime.

In order to simplify model intercomparisons, initialization procedures that allow the output from one model to be input by another continue to be developed. The introduction of spherical coordinates into both the hydrostatic and nonhydrostatic compressible Zeta models have substantially simplified these procedures. However, initializing non-Boussinesq models with output from the Boussinesq hydrostatic Zeta model still requires solving a nonlinear balance system using the potential vorticity based on the Boussinesq solution.

PLANS FY97

Moist processes and boundary layer physics will continue to be incorporated into both the hydrostatic and nonhydrostatic Zeta models. Moderate resolution (1°) idealized storm-track simulations with the new spherical-coordinate models should clarify the most important processes in the development, maintenance, and decay of these storm tracks. High resolution (10-20 km) nonhydrostatic simulations of baroclinic waves will allow the investigation of phenomena such as frontal collapse and equilibration and the role of nonhydrostatic circulations in the development and decay of these systems. Development of the adjoints of

the hydrostatic and nonhydrostatic Zeta models will continue to be investigated, and sensitivity studies will be undertaken to clarify the features most important to the aforementioned development, equilibration, and decay processes.

9. COMPUTATIONAL SERVICES

GOAL

To provide a computational facility to support research conducted at GFDL with emphasis on supercomputing and interactive capabilities for developing, running, and analyzing numerical models and on file serving capabilities for managing large amounts of data.

9.1 COMPUTER SYSTEMS

L. Lewis *R. White*
T. Taylor *W. Yeager*
L. Umscheid

ACTIVITIES FY96

GFDL operated a Cray Y-MP/8 and a Cray C90/16 throughout most of FY96. The Y-MP was operated at reduced cost without a maintenance contract beginning November 1995. After one processor failed during February 1996, the Y-MP continued in operation using seven processors. The Y-MP was retired from service during June 1996 and its data archive was moved to the C90. High capacity helical scan tape drives (STK Redwoods) were installed on the C90 in February 1996 as originally scheduled. There was a phased delivery of high capacity cartridges with a total capacity of 30 terabytes (TB). Operationally, files larger than 100 megabytes are automatically archived on the high capacity media. Some of the large files which were stored on IBM 3490E compatible cartridges before the installation of the Redwoods were moved to the high capacity media in a manner transparent to users.

Replacement of the C90 with a T90 was postponed by Cray Research until August 1996. The T90 successfully completed a one-month acceptance period on September 28. The T90 system includes 20 processors that use IEEE floating point arithmetic, an increase of central memory from 256 megawords (MW) to 512 MW, and an increase of solid state disk from 1 gigaword (GW) to 2 GW. The data archives and 355 gigabytes (GB) of rotating disk storage were moved from the C90 to the T90. The T90 system has approximately 1.5 times the computational power of the C90.

Preparation for the transition to the T90 included four Fortran 90 training classes at GFDL. There was also access for a core set of users to a IEEE T90 at Cray Research headquarters for conversion of codes. Two Cray on-site analysts also provided valuable local assistance for code conversion.

In addition to the T90, GFDL's computer facility includes three Silicon Graphics (SGI) servers, three Sun Microsystems servers, and a variety of text and graphics printers. Distributed

throughout GFDL are 119 desktop workstations including 17 SGI Indigo2 R4400XZs, 34 SGI Indigo R4000XZs, 10 SGI 4D/35s, 35 SGI 4D/25s, 5 Sun SPARCstation-1s, and 18 Sun 3/50s. The workstations are interconnected by eight Ethernet segments and a Network Systems Corporation (NSC) router; the T90 and the servers are interconnected by a Fiber Distributed Data Interface (FDDI) network which connects to the Ethernet network through the NSC router.

Network performance was significantly improved by replacing all old fiber-optic repeaters. All servers that were not connected to the FDDI network were attached via an Ethernet-FDDI switch. An automated network backup system was implemented to backup data stored on individual SGI workstations. The SGI software server was upgraded to a faster model. New networked PostScript printers were acquired that virtually eliminated printing backlogs. Fortran 90 was installed on SGI workstations after an evaluation of several Fortran 90 compilers. New hardware and software maintenance contracts for the SGI workstations were negotiated. Two SGI Indigo2 R4400XZ workstations were ordered.

The number of user processor hours for each month and the cumulative amount of total archive data in billions of bytes for the Y-MP are shown in Table 9.1. Table 9.2 shows the same information as Table 9.1, but for the C90 and T90. The number of C90 user processor hours is approximately double a typical Y-MP/8 month due to having twice the number of processors. Similarly, the number of T90/20 user processor hours in September is approximately 25% greater than a typical C90/16 month due to having 25% more processors.

Table 9.1 Cray Y-MP User Processor Time and Amount of Total Archive Data

Month	Hours	Gigabytes
Oct 95	5,993	11,809
Nov 95	5,450	11,808
Dec 95	5,708	11,880
Jan 96	5,720	11,965
Feb 96	4,939[1]	12,025
Mar 96	5,086[1]	12,041
Apr 96	4,774[1]	12,102
May 96	4,047[1]	12,281
Jun 96	1,382[1,2]	12,213

[1] 7 processors beginning Feb. 20

[2] Use terminated June 21

Table 9.2 Cray C90/T90 User Processor Time and Amount of Total Archive Data

Month	Hours	Gigabytes
Oct 95	11,659	2,017
Nov 95	11,254	2,611
Dec 95	10,029	3,053
Jan 96	10,849	3,309
Feb 96	10,728	4,395[1]
Mar 96	11,281	5,445
Apr 96	10,801	6,393
May 96	11,560	7,286
Jun 96	10,939	8,272
Jul 96	11,632	9,225
Aug 96	8,562[2]	9,991
Sep 96	13,312[3]	11,104

[1] Redwood high capacity tape drives installed

[2] C90 use terminated Aug. 26

[3] T90 accounting begun Sep. 10

PLANS FY97

The T90 is scheduled to be upgraded with more processors in January 1997 to approximately 2.15 times the computational power of the C90. At the same time, an upgrade of the I/O subsystem is also scheduled, with an increase in disk storage of 87 GB to a total of 442 GB, an upgrade in the speed of the central memory, and delivery of a Redwood compression chip which will increase the effective capacity of the data archive. A 40 processor Cray T3E scalable system is scheduled for delivery early in FY97. An additional 30 TB of high capacity media will be delivered in August 1997.

Operating strategies for the T90 will be assessed in light of the increased capabilities of the system and the advent of multitasked jobs. The remaining large files on 3490E cartridges will be moved to high capacity media and, after the installation of the compression chip, all uncompressed data on Redwoods will be compressed. This will be achieved transparently to users.

Network performance will be monitored and possible options for upgrading the workstation network will be investigated. Pending availability of funds, older Sun workstations will continue to be replaced with SGI workstations.

9.2 DATA MANAGEMENT AND VISUALIZATION

J. Sheldon *R. White*
H. Vahlenkamp

ACTIVITIES FY96

The foundation of an integrated data management and visualization infrastructure has been laid over the past year, based on last year's analysis of the immediate and strategic needs of the laboratory. Efforts this year have focused primarily on 1) establishing core capabilities, 2) extensive individualized assistance to users, and 3) preparation of a complete guide to all the available data management and visualization resources.

Central to the laboratory's mission is the ability to store data in a reliable, well-documented, and easily-accessed form. Last year, the Network Common Data Format (NetCDF) developed by Unidata was adopted as the laboratory's "common" data format, based on its wide acceptance in the meteorological and oceanographic community, as well as the wide variety of tools and packages which support the manipulation and visualization of netCDF data. The number of users at GFDL using netCDF has grown significantly since then, fueled largely by a netCDF output option in MOM2, by the choice of netCDF as the default output option for the Climate group's GCM, and by a new data-management facility built by the Experimental Prediction group to store their data in netCDF. The recent release of the NCEP Reanalysis data in netCDF has also led to a significant increase in user interest in netCDF.

The conversion to netCDF was made possible largely because of the set of high-level "shell" routines developed at GFDL which insulate the user from the detailed netCDF library itself. These routines also enforce a set of conventions for how to organize data within the netCDF paradigm, making the files extremely portable. A great deal of effort has been expended in refining and optimizing this interface and adapting it to GFDL's new IEEE T90. An extensive series of tests were conducted to optimize both read and write performance using Cray's Flexible File I/O (FFIO) layer. A number of netCDF utilities have also been collected and/or built to support the management and manipulation of netCDF files.

A subset of graphics packages was identified as constituting an important extension of the laboratory's visualization capabilities. "Ncview" permits a simple, but rapid, survey of a dataset using color-shaded slices and animation, and is useful for quickly finding features of interest or potential trouble spots. "Freud" produces more detailed plots, including map projections and annotation, via a Graphical User Interface (GUI), thereby greatly minimizing the amount of time required for the researcher to produce his or her first plot. "Explorer" takes the laboratory's visualization capabilities into the 3rd spatial dimension, producing sophisticated isosurfaces, cutting planes, trajectories and other objects which give the scientist an entirely new way to explore data, as well as a very effective method of conveying

complex insights to colleagues and the public. An extensive set of "modules" have been written for Explorer and now comprise a very robust set of visualization capabilities. These modules have also been made publicly available via GFDL's web site (http://www.gfdl.gov/~jps/Explorer_intro.html), which includes an extensive set of sample images, movies, and maps. In addition to the laboratory's internal use of Explorer for research purposes, a number of products were generated for other agencies and the media as part of GFDL's outreach program.

Perhaps one of the most important developments of the past year, from the standpoint of helping scientists make best use of the tools available to them, has been the development of an extensive hypertext "Scientific Visualization Guide" (http://www.gfdl.gov/~jps/GFDL_Vis_Guide.html). This guide documents all of the steps and tools necessary for the researcher to generate datasets, explore them, and prepare publication and presentation quality visualizations. It covers netCDF, multidimensional visualization, image manipulation, animation, and a host of other functions. As a result, the researcher has more options available than ever before with better information on how to use them.

Lastly, a review was conducted of the technology and products available for the projection of hi-resolution images and movies from the lab's SGI workstations onto the screen in the Smagorinsky Seminar Room. The laboratory subsequently purchased a new high-resolution projection panel which will permit demonstrations, lectures, classes, and other visually intensive presentations to be given to a larger audience with a picture quality matching that available on a workstation screen.

PLANS FY97

Efforts will focus on 1) performance, modularization, and enhancement of the netCDF "shell" routines, 2) the potential synthesis of the myriad netCDF tools into a smaller number of integrated functions, and 3) broadening the actual user-base of Explorer. As new versions of netCDF, tools, and various visualization packages become available, they will be tested. The Scientific Visualization Guide and other web information sources will be expanded and updated as needed, and parts may be redesigned.

APPENDIX A

GFDL STAFF MEMBERS

and

AFFILIATED PERSONNEL

during

Fiscal Year 1996

PERSONNEL SUMMARY

September 30, 1996

GFDL/NOAA	
Full Time Permanent (FTP)	82
Part Time Permanent (PTP)	3
Intermittent (INT)	1
PRINCETON UNIVERSITY (PU)	
AOS Visiting Scientists	12
Graduate Students	7
Professors	3
Research Scientists	1
Research Staff	6
Support Staff	3
Technical Staff	6
Visiting Senior Research Scientist	1
OTHER INSTITUTIONS	
U.S. Geological Survey (USGS)	2
University Corporation for Atmospheric Research (UCAR)	1
VENDORS	
Cray Research Inc. Computer Support Staff	5
IBM Research Staff	1
TOTAL	**134**

CLIMATE DYNAMICS

Manabe, Syukuro	Senior Scientist at GFDL	FTP
Baker, David F.	Graduate Student	PU
Broccoli, Anthony J.	Meteorologist	FTP
Delworth, Thomas L.	Meteorologist	FTP
Hall, Alexander	Graduate Student	PU
Hayashi, Yoshikazu	Meteorologist	FTP
Golder, Donald G.	Meteorologist	FTP
Held, Isaac M.	Senior Scientist at GFDL	FTP
Chen, Shuo	Graduate Student	PU*
Kushner, Paul	AOS Visiting Scientist	PU
Larichev, Vitaly	AOS Visiting Scientist	PU*
Phillipps, Peter J.	Meteorologist	FTP
Swanson, Kyle	AOS Visiting Scientist	PU*
Treguier, Anne Marie	AOS Visiting Scientist	PU*
Weill-Zrahia, Anne	AOS Visiting Scientist	PU*
Zhang, Yunqing	Graduate Student	PU
Zhang, Zhojun	AOS Visiting Scientist	PU*
Knutson, Thomas R.	Meteorologist	FTP
Milly, P.C.D.	Hydrologist	USGS**
Dunne, Krista	Physical Scientist	USGS**
Schlosser, Adam	AOS Visiting Scientist	PU
Numaguti, Atusi	AOS Visiting Scientist	PU*
Spelman, Michael J.	Meteorologist	FTP
Stouffer, Ronald J.	Meteorologist	FTP
Wetherald, Richard T.	Meteorologist	FTP
Williams, Gareth P.	Meteorologist	FTP

*Affiliation terminated prior to September 30, 1996.
**United States Geological Survey (USGS), on detail to GFDL.

RADIATION AND CLOUDS

Ramaswamy, V.	Physical Scientist	FTP
Donner, Leo J.	Physical Scientist	FTP
Reisin, Tamir	AOS Visiting Scientist	PU*
Seman, Charles J.	Physical Scientist	FTP
Freidenreich, Stuart	Meteorologist	FTP
Haywood, James	AOS Visiting Scientist	PU
Li, Jiangnan	AOS Visiting Scientist	PU*
Orris, Rebecca	Graduate Student	PU*
Schwarzkopf, M. Daniel	Meteorologist	FTP
Soden, Brian J.	Physical Scientist	FTP

MIDDLE ATMOSPHERE DYNAMICS AND CHEMISTRY

Mahlman, Jerry D.	Director	FTP
Goldberg, Charles	Scientific Visitor	UCAR*
Hamilton, Kevin P.	Meteorologist	FTP
Wilson, R. John	Meteorologist	FTP
Hemler, Richard S.	Meteorologist	FTP
Kerr, Christopher L.	Scientific Visitor	IBM**
Levy II, Hiram	Physical Scientist	FTP
Hirsch, Adam	Technical Staff	PU*
Klonecki, Andrzej	Graduate Student	PU
Moxim, Walter J.	Meteorologist	FTP
Perliski, Lori	Physical Scientist	FTP
Taubman, Steven J.	Scientific Visitor	UCAR*

*Affiliation terminated prior to September 30, 1996.
**International Business Machines, on detail to GFDL.

EXPERIMENTAL PREDICTION

Anderson, Jeffrey L.	Meteorologist	FTP
Gordon, C. Tony	Meteorologist	FTP
Griffies, Stephen M.	Physical Scientist	FTP
Harrison, Matthew	Physical Scientist	FTP
Ploshay, Jeffrey J.	Meteorologist	FTP
Rosati, Anthony J.	Physical Scientist	FTP
Gudgel, Richard G.	Meteorologist	FTP
Sirutis, Joseph J.	Meteorologist	FTP
Stern, William F.	Meteorologist	FTP
Smith, Robert G.	Computer Assistant	FTP
Vitart, Frederic	Graduate Student	PU
Wittenberg, Andrew	Graduate Student	PU
Wyman, Bruce L.	Meteorologist	FTP
Yang, Xiu-Qin	AOS Visiting Scientist	PU

OCEANIC CIRCULATION

Toggweiler, J. R.	Oceanographer	FTP
Carson, Steven R.	Physical Scientist	FTP
Dixon, Keith W.	Meteorologist	FTP
Gnanadesikan, Anand	AOS Visiting Scientist	PU
Griffies, Stephen	UCAR Fellow	PU*
Hallberg, Robert	AOS Visiting Scientist	PU
Harrison, Matthew	Research Associate	NOAA**/*
Hurlin, William J.	Meteorologist	FTP
Pacanowski, Ronald C.	Oceanographer	FTP
Samuels, Bonita L.	Oceanographer	FTP
Tziperman, Eli	AOS Visiting Scientist	PU
Winton, Michael	Oceanographer	FTP

*Affiliation terminated prior to September 30, 1996.
**NOAA Corps, on assignment to GFDL.

OBSERVATIONAL STUDIES

Oort, Abraham H.	Meteorologist	FTP
Lanzante, John	Meteorologist	FTP
Lau, Ngar-Cheung	Meteorologist	FTP
Crane, Mark	Meteorologist	FTP
Klein, Steven	AOS Visiting Scientist	PU
Nath, Mary Jo	Meteorologist	FTP
Peng, Peitao	AOS Visiting Scientist	PU*

HURRICANE DYNAMICS

Kurihara, Yoshio	Meteorologist	FTP
Bender, Morris A.	Meteorologist	FTP
Tuleya, Robert E.	Meteorologist	FTP

MESOSCALE DYNAMICS

Orlanski, Isidoro	Meteorologist	FTP
Balasubramanian, G.	AOS Visiting Scientist	PU
Garner, Stephen	Meteorologist	FTP
Gross, Brian	Physical Scientist	FTP
Polinsky, Larry	Meteorologist	FTP

*Affiliation terminated prior to September 30, 1996.

MANAGEMENT FRAMEWORK

Administrative and Technical Structure

Mahlman, Jerry D.	Director	FTP
Ross, Bruce B.	Assistant Director	FTP
Ghosh, Koushik	Applications Analyst	CRI
Haller, Gail T.	Library Technician	PTP
Amend, Beatrice E.	Office Automation Clerk	INT
Lewis, Lawrence J.	Leader, COMPUTER SYSTEMS	FTP
Marshall, Wendy H.	Editorial Assistant	FTP
Pege, Joan M.	Management Analyst	FTP
Raphael, Catherine	Scientific Illustrator	PTP
Sheldon, John	Graphics Specialist/Meteorologist	FTP
Vahlenkamp, Hans	Scientific Visitor	UCAR
Umscheid, Ludwig J.	Major Systems Specialist	FTP*
Urbani, Elaine B.	Transportation Assistant	FTP
Uveges, Frank J.	Supervisory Computer Specialist	FTP
Byrne, James S.	Junior Technician	FTP
Shearn, William F.	Leader, COMPUTER OPERATIONS	FTP
Varanyak, Jeffrey	Scientific Illustrator	FTP
Williams, Betty M.	Secretary	FTP

Scientific Structure

Mahlman, Jerry D.	Director and Leader, MIDDLE ATMOSPHERE DYNAMICS AND CHEMISTRY	FTP
Anderson, Jeffrey L.	Leader, EXERIMENTAL PREDICTION	FTP
Kurihara, Yoshio	Leader, HURRICANE DYNAMICS	FTP
Manabe, Syukuro	Leader, CLIMATE DYNAMICS	FTP
Oort, Abraham H.	Leader, OBSERVATIONAL STUDIES	FTP
Orlanski, Isidoro	Leader, MESOSCALE DYNAMICS	FTP
Ramaswamy, V.	Leader, RADIATION AND CLOUDS	FTP
Toggweiler, J. R.	Leader, OCEANIC CIRCULATION	FTP

*Affiliation terminated prior to September 30, 1996.

COMPUTER SYSTEMS

Lewis, Lawrence J.	Computer Specialist	FTP
Rao, Ramesh	Applications Analyst	CRI
Taylor III, Thomas E.	Computer Specialist	FTP
White, Robert K.	Computer Specialist	FTP
Yeager, William T.	Computer Specialist	FTP

COMPUTER OPERATIONS SUPPORT

Shearn, William F.	Operations Manager	FTP
Hopps, Frank K.	Supervisory Computer Operator	FTP
King, John T.	Lead Computer Operator	FTP
Duggins, Marsha	Peripheral Equipment Operator	FTP
Harrold, Renee M.	Computer Operator	FTP
Yacovelli, Deborah	Peripheral Equipment Operator	FTP
Hand, Joseph S.	Supervisory Computer Operator	FTP
Cordwell, Clara L.	Lead Computer Operator	FTP
Ledden, Jay H.	Computer Operator	FTP
Lim, Jennifer J.	Computer Operator	PTP
Deuringer, James A.	Supervisory Computer Operator	FTP
Blakemore, Geneve	Computer Operator	FTP
Dahl, Tania	Computer Operator	FTP
Krueger, Scott R.	Lead Computer Operator	FTP
Henne, Ronald N.	Computer Assistant	FTP

ATMOSPHERIC AND OCEANIC SCIENCES PROGRAM

Philander, S.G.H.	Professor, Program Director	PU
Bryan, Kirk	Visiting Senior Research Scientist	PU
Bush, Andrew	AOS Visiting Scientist	PU
Callan, Johann V.	Technical Research Secretary	PU
Goddard, Lisa M.	Graduate Student	PU*
Gu, Daifang	Research Staff	PU
Harper, Scott	Graduate Student	PU
Lambert, Gregory	Technical Staff	PU*
Rossi, Laura	Program Manager	PU
Valerio, Anna	Technical Research Secretary	PU
Mellor, George	Professor Emeritus	PU
Chen, Ping	AOS Visiting Scientist	PU
Ezer, Tal	Research Staff	PU
Jungclaus, Johann	AOS Visiting Scientist	PU*
Kim, Namsoug	Technical Staff	PU
Sarmiento, Jorge	Professor	PU
Armstrong, Robert	Research Staff	PU
Dengg, Joachim	AOS Visiting Scientist	PU
Fan, Song-Miao	Research Staff	PU
Garcon, Veronique	Research Scientist	PU*
Hughes, Tertia	Technical Staff	PU
Key, Robert M.	Research Scientist	PU
LeQuere, Corrine	Technical Staff	PU*
McDonald, Gerard	Technical Staff	PU
Murnane, Richard J.	Research Staff	PU
Olszewski, Jason	Research Staff	PU*
Rossmassler, Julie E.	Technical Staff	PU
Rotter, Richard	Technical Staff	PU
Sabine, Christopher L.	Research Staff	PU
Slater, Richard D.	Technical Staff	PU
Webb, Vincent	Graduate Student	PU*

*Affiliation terminated prior to September 30, 1996.

CRAY RESEARCH INCORPORATED

Siebers, Bernard	Analyst in Charge	CRI
Braunstein, Mark	Field Engineer	CRI
Ghosh, Koushik	Applications Analyst	CRI
Rao, Ramesh	Applications Analyst	CRI
Weiss, Ed	Engineer in Charge	CRI

APPENDIX B

GFDL

BIBLIOGRAPHY

1993-1996

GFDL PUBLICATIONS

This is a partial listing of GFDL publications. A copy of the complete bibliography can be obtained by calling (609) 452-6502, or by writing to:

Director
Geophysical Fluid Dynamics Laboratory
Post Office Box 308
Princeton, New Jersey 08542

* (1116) Orlanski, I., and E.K.M. Chang, Ageostrophic Geopotential Fluxes in Downstream and Upstream Development of Baroclinic Waves, *Journal of the Atmospheric Sciences, 50(2),* 212-225, 1993.

* (1117) Anderson, L.A., The Determination of Redfield Ratios for Use in Global Oceanic Nutrient Cycle Models, Ph.D. Dissertation, Atmospheric and Oceanic Sciences Program, Princeton University, 1993.

(1118) Hayashi, Y., and D.G. Golder, Tropical 40-50- and 25-30-Day Oscillations Appearing in Realistic and Idealized GFDL Climate Models and the ECMWF Dataset, *Journal of the Atmospheric Sciences, 50(3),* 464-494, 1993.

(1119) Ploshay, J., W. Stern, and K. Miyakoda, A Summary Report on FGGE Re-analysis at GFDL, *Data Assimilation Systems,* BMRC Research Report No. 27, pp. 29-53, Melbourne, Australia, 1991.

(1120) Hamilton, K., What We Can Learn from General Circulation Models about the Spectrum of Middle Atmospheric Motions, in *Coupling Processes in the Lower and Middle Atmosphere,* edited by E.V. Thrane et al., pp. 161-174, Kluwer Academic Publishers, 1993.

(1121) Manabe, S., and R.J. Stouffer, Reply to Comments on "Two Stable Equilibria of a Coupled Ocean-Atmosphere Model", *Journal of Climate, 6(1),* 178-179, 1993.

* (1122) Schwarzkopf, M.D., and V. Ramaswamy, Radiative Forcing due to Ozone in the 1980s: Dependence on Altitude of Ozone Change, *Geophysical Research Letters, 20(2),* 205-208, 1993.

(1123) Broccoli, A.J., and S. Manabe, The Effects of Orography on Midlatitude Northern Hemisphere Dry Climates, *Journal of Climate, 5(11),* 1181-1201, 1992.

* (1124) Oort, A.H., and H. Liu, Upper-Air Temperature Trends Over the Globe, 1958-1989, *Journal of Climate, 6(2),* 292-307, 1993.

* (1125) Chang, E.K.M., and I. Orlanski, On the Dynamics of a Storm Track, *Journal of the Atmospheric Sciences, 50(7),* 999-1015, 1993.

(1126) Bryan, K., Ocean Circulation Models, in *Strategies for Future Climate Research,* edited by M. Latif, pp. 265-285, Max Planck Institute fur Meteorologie, Hamburg, Germany, 1991.

(1127) Lau, N.-C., Climate Variability Simulated in GCMs, in *Climate System Modeling,* edited by K.E. Trenberth, pp. 617-642, Cambridge University Press, 1992.

(1128) Lanzante, J.R., A Comparison of the Stationary Wave Responses in Several GFDL Increased CO_2 GCM Experiments, *Proceedings of the Sixteenth Annual Climate Diagnostics Workshop,* Lake Arrowhead, CA, pp. 241-246, 1991.

*In collaboration with other organizations

* (1129) Milly, P.C.D., Sensitivity of the Global Water Cycle to the Water-Holding Capacity of Soils, in *Exchange Processes at the Land Surface for a Range of Space and Time Scales*, IAHS Pub. No. 212, Yokohama, Japan, pp. 495-501, 1993.

* (1130) Savoie, D.L., J.M. Prospero, S.J. Oltmans, W.C. Graustein, K.K. Turekian, J.T. Merrill, and H. Levy II, Sources of Nitrate and Ozone in the Marine Boundary Layer of the Tropical North Atlantic, *Journal of Geophysical Research, 97(D11)*, 11,575-11,589, 1992.

(1131) Held, I.M., Large-Scale Dynamics and Global Warming, *Bulletin of the American Meteorological Society, 74(2)*, 228-241, 1993.

* (1132) Imbrie, J., E.A. Boyle, S.C. Clemens, A. Duffy, W.R. Howard, G. Kukla, J. Kutzbach, D.G. Martinson, A. McIntyre, A.C. Mix, B. Molfino, J.J. Morley, L.C. Peterson, N.G. Pisias, W.L. Prell, M.E. Raymo, N.J. Shackleton, and J.R. Toggweiler, On the Structure and Origin of Major Glaciation Cycles, 1. Linear Responses to Milankovitch Forcing, *Paleoceanography, 7(6)*, 701-738, 1992.

(1133) Donner, L.J., A Cumulus Parameterization Including Mass Fluxes, Vertical Momentum Dynamics, and Mesoscale Effects, *Journal of the Atmospheric Sciences, 50(6)*, 889-906, 1993.

(1134) Mahlman, J.D., Modeling Perspectives on Global Monitoring Requirements, *Proceedings of the NOAA Workshop on Assuring the Quality and Continuity of NOAA's Environmental Data*, Silver Spring, MD, December 1991, pp. 19-26, 1993.

* (1135) Murray, J.W., M.W. Leinen, R.A. Feely, J.R. Toggweiler, and R. Wanninkhof, EqPac: A Process Study in the Central Equatorial Pacific, *Oceanography, 5(3)*, 134-142, 1992.

* (1136) Freidenreich, S.M., and V. Ramaswamy, Solar Radiation Absorption by CO_2, Overlap with H_20, and a Parameterization for General Circulation Models, *Journal of Geophysical Research, 98(D4)*, 7255-7264, 1993.

* (1137) Kasibhatla, P.S., H. Levy II, and W.J. Moxim, Global NO_x, HNO_3, PAN, and NO_y Distributions from Fossil Fuel Combustion Emissions: A Model Study, *Journal of Geophysical Research, 98(D4)*, 7165-7180, 1993.

(1138) Held, I.M., and P.J. Phillipps, Sensitivity of the Eddy Momentum Flux to Meridional Resolution in Atmospheric GCMs, *Journal of Climate, 6(3)*, 499-507, 1993.

(1139) Kurihara, Y., M.A. Bender, R.E. Tuleya, and R.J. Ross, Hurricane Forecasting with the GFDL Automated Prediction System, in *Preprints, 20th Conference on Hurricanes and Tropical Meteorology*, 10-14 May 1993, San Antonio, TX, pp. 323-326, American Meteorological Society, Boston, MA, 1993.

(1140) Ross, R.J., and Y. Kurihara, Hurricane-Environment Interaction in Hurricanes Gloria and Gilbert, *Preprints, 20th Conference on Hurricanes and Tropical Meteorology*, 10-14 May 1993, San Antonio, TX, pp. 27-30, American Meteorological Society, Boston, MA, 1993.

* (1141) Hakkinen, S., G.L. Mellor, and L.H. Kantha, Modeling Deep Convection in the Greenland Sea, *Journal of Geophysical Research, 97(C4)*, 5389-5408, 1992.

* (1142) Sarmiento, J.L., Biogeochemical Ocean Models, in *Climate System Modeling*, edited by K. Trenberth, pp. 519-551, Cambridge University Press, Cambridge, MA, 1992.

* (1143) Sarmiento, J.L., and J.C. Orr, The Iron Fertilization Strategy, *Proceedings of the Conference "Oceans, Climate, Man"*, Fondazione, San Paolo, Italy, 1992.

* (1144) Lee, S., and I. Held, Baroclinic Wave Packets in Models and Observations, *Journal of the Atmospheric Sciences, 50(10)*, 1413-1428, 1993.

*In collaboration with other organizations

(1145) Delworth, T., and S. Manabe, Climate Variability and Land Surface Processes, *Advances in Water Resources, 16,* 3-20, 1993.

(1146) Manabe, S., and R.J. Stouffer, Century-Scale Effects of Increased Atmospheric CO_2 on the Ocean-Atmosphere System, *Nature, 364(6434),* 215-218, 1993.

(1147) Kurihara, Y., M.A. Bender, and R.J. Ross, An Initialization Scheme of Hurricane Models by Vortex Specification, *Monthly Weather Review, 121(7),* 2030-2045, 1993.

(1148) Bender, M.A., R.J. Ross, R.E. Tuleya, and Y. Kurihara, Improvements in Tropical Cyclone Track and Intensity Forecasts Using the GFDL Initialization System, *Monthly Weather Review, 121(7),* 2046-2061, 1993.

(1149) Anderson, J.L., The Climatology of Blocking in a Numerical Forecast Model, *Journal of Climate, 6(6),* 1042-1056, 1993.

* (1150) Yuan, L., Statistical Equilibrium Dynamics in a Forced-Dissipative f-plane Shallow-Water Model, Ph.D. Dissertation, Atmospheric and Oceanic Sciences Program, Princeton University, 1993.

* (1151) Levy II, H., W.J. Moxim, and P.S. Kasibhatla, Impact of Global NO_x Sources on the Northern Latitudes, in *The Tropospheric Chemistry of Ozone in the Polar Regions,* edited by H. Niki and K.H. Becker, pp. 77-88, NATO ASI Series I, Vol. 7, Springer-Verlag, Berlin, 1993.

(1152) Kurihara, Y., Hurricanes and Atmospheric Processes, in *Relating Geophysical Structures and Processes: The Jeffreys Volume,* edited by K. Aki and R. Dmowska, pp. 19-26, Geophysical Monograph 76, IUGG, Vol. 16, American Geophysical Union, 1993.

* (1153) Manzini, E., and K. Hamilton, Middle Atmospheric Traveling Waves Forced by Latent and Convective Heating, *Journal of the Atmospheric Sciences, 50(14),* 2180-2200, 1993.

* (1154) Chang, E.K.M., Downstream Development of Baroclinic Waves as Inferred from Regression Analysis, *Journal of the Atmospheric Sciences, 50(13),* 2038-2053, 1993.

* (1155) Sarmiento, J.L., R.D. Slater, M.J.R. Fasham, H.W. Ducklow, J.R. Toggweiler, and G.T. Evans, A Seasonal Three-Dimensional Ecosystem Model of Nitrogen Cycling in the North Atlantic Euphotic Zone, *Global Biogeochemical Cycles, 7(2),* 417-450, 1993.

(1156) Toggweiler, J.R., and B. Samuels, Is the Magnitude of the Deep Outflow from the Atlantic Ocean Actually Governed by Southern Hemisphere Winds?, in *The Global Carbon Cycle,* edited by M. Heimann, pp. 303-331, NATO ASI Series I, Vol. 15, Springer-Verlag, Berlin, 1993.

(1157) Toggweiler, J.R., and B. Samuels, New Radiocarbon Constraints on the Upwelling of Abyssal Water to the Ocean's Surface, in *The Global Carbon Cycle,* edited by M. Heimann, pp. 333-366, NATO ASI Series I, Vol. 15, Springer-Verlag, Berlin, 1993.

* (1158) Matano, R.P., On the Separation of the Brazil Current from the Coast, *Journal of Physical Oceanography, 23(1),* 79-90, 1993.

* (1159) Matano, R.P., and S.G.H. Philander, Heat and Mass Balances of the South Atlantic Ocean Calculated from a Numerical Model, *Journal of Geophysical Research, 98(C1),* 977-984, 1993.

* (1160) Ezer, T., G.L. Mellor, D.-S. Ko, and Z. Sirkes, A Comparison of Gulf Stream Sea Surface Height Fields Derived from Geosat Altimeter Data and Those Derived from Sea Surface Temperature Data, *Journal of Atmospheric and Oceanic Technology, 10(1),* 76-87, 1993.

* (1161) Hakkinen, S., and G.L. Mellor, Modeling the Seasonal Variability of a Coupled Arctic Ice-Ocean System, *Journal of Geophysical Research, 97(C12),* 20,285-20,304, 1992.

*In collaboration with other organizations

* (1162) Nakamura, N., Momentum Flux, Flow Symmetry, and the Nonlinear Barotropic Governor, *Journal of the Atmospheric Sciences, 50(14)*, 2159-2179, 1993.

* (1163) Gerdes, R., A Primitive Equation Ocean Circulation Model Using a General Vertical Coordinate Transformation, 1: Description and Testing of the Model, *Journal of Geophysical Research, 98(C8)*, 14,683-14,701, 1993.

* (1164) Gerdes, R., A Primitive Equation Ocean Circulation Model Using a General Vertical Coordinate Transformation, 2: Application to an Overflow Problem, *Journal of Geophysical Research, 98(C8)*, 14,703-14,726, 1993.

* (1165) Sarmiento, J.L., Ocean Carbon Cycle, *Chemical and Engineering News, 71*, 30-43, 1993.

* (1166) Fasham, M.J.R., J.L. Sarmiento, R.D. Slater, H.W. Ducklow, and R. Williams, Ecosystem Behavior at Bermuda Station "S" and Ocean Weather Station "India", A General Circulation Model and Observational Analysis, *Global Biogeochemical Cycles, 7*, 379-415, 1993.

* (1167) Kasibhatla, P.S., NO_y from Sub-sonic Aircraft Emissions: A Global, Three-Dimensional Model Study, *Geophysical Research Letters, 20(16)*, 1707-1710, 1993.

(1168) Hamilton, K., A General Circulation Model Simulation of El Niño Effects in the Extratropical Northern Hemisphere Stratosphere, *Geophysical Research Letters, 20(17)*, 1803-1806,1993.

* (1169) Ting, M.-F., and N.-C. Lau, A Diagnostic and Modeling Study of the Monthly Mean Wintertime Anomalies Appearing in a 100-Year GCM Experiment, *Journal of the Atmospheric Sciences, 50(17)*, 2845-2867, 1993.

* (1170) Armstrong, R.A., A Comparison of Index-Based and Pixel-Based Neighborhood Simulations of Forest Growth, *Ecology, 74(6)*, 1707-1712, 1993.

* (1171) Ramaswamy, V., and C.-T. Chen, An Investigation of the Global Solar Radiative Forcing Due to Changes in Cloud Liquid Water Path, *Journal of Geophysical Research, 98(D9)*, 16,703-16,712, 1993.

(1172) Hamilton, K., Notes and Correspondence: An Examination of Observed Southern Oscillation Effects in the Northern Hemisphere Stratosphere, *Journal of the Atmospheric Sciences, 50(20)*, 3468-3473, 1993.

* (1173) Siegenthaler, U., and J.L. Sarmiento, Atmospheric Carbon Dioxide and the Ocean, *Nature, 365*, 119-125, 1993.

* (1174) Sarmiento, J.L., Atmospheric CO_2 Stalled, *Nature, 365*, 697-698, 1993.

* (1175) Slater, R.D., J.L. Sarmiento, and M.J.R. Fasham, Some Parametric and Structural Simulations with a Three Dimensional Ecosystem Model of Nitrogen Cycling in the North Atlantic Euphoric Zone, in *Long-Term Monitoring of Global Climate Forcings and Feedbacks*, pp. 1-5, NASA Conference Publication 3234, 1993.

* (1176) Stephenson, D.B., and I.M. Held, GCM Response of Northern Winter Stationary Waves and Storm Tracks to Increasing Amounts of Carbon Dioxide, *Journal of Climate, 6(10)*, 1859-1870, 1993.

(1177) Orlanski, I., and J. Sheldon, A Case of Downstream Baroclinic Development over Western North America, *Monthly Weather Review, 121(11)*, 2929-2950, 1993

(1178) Hamilton, K., Model Simulation of the Stratospheric Penetration of the Southern Oscillation, *Toga Notes, 13*, 7-11, 1993.

* (1179) Xue, H.-J., and G.L. Mellor, Instability of the Gulf Stream Front in the South Atlantic Bight, *Journal of Physical Oceanography, 23(11)*, 2326-2350, 1993

*In collaboration with other organizations

(1180) Milly, P.C.D., An Analytic Solution of the Stochastic Storage Problem Applicable to Soil Water, *Water Resources Research, 29(11)*, 3755-3758, 1993.

* (1181) Imbrie, J., A. Berger, E.A. Boyle, S.C. Clemens, A. Duffy, W.R. Howard, G. Kukla, J. Kutzbach, D.G. Martinson, A. McIntyre, A.C. Mix, B. Molfino, J.J. Morley, L.C. Peterson, N.G. Pisias, W.L. Prell, M.E. Raymo, N.J. Shackleton, and J.R. Toggweiler, On the Structure and Origin of Major Glaciation Cycles, 2. The 100,000-year Cycle, *Paleoceanography, 8(6)*, 699-735, 1993.

(1182) Delworth, T., S. Manabe, and R.J. Stouffer, Interdecadal Variations of the Thermohaline Circulation in a Coupled Ocean-Atmosphere Model, *Journal of Climate, 6(11)*, 1993-2011, 1993.

* (1183) Held, I.M., R.S. Hemler, and V. Ramaswamy, Radiative-Convective Equilibrium with Explicit Two-Dimensional Moist Convection, *Journal of the Atmospheric Sciences, 50(23)*, 3909-3927, 1993.

* (1184) Xie, S.P., A. Kubokawa, and K. Hanawa, Evaporation-Wind Feedback and the Organizing of Tropical Convection on the Planetary Scale, Part II: Nonlinear Evolution, *Journal of the Atmospheric Sciences, 50(23)*, 3884-3893, 1993.

* (1185) Tziperman, E., and K. Bryan, Estimating Global Air-Sea Fluxes from Surface Properties and from Climatological Flux Data using an Oceanic General Circulation Model, *Journal of Geophysical Research, 98(C12)*, 22,629-22,644, 1993.

(1186) Mahlman, J.D., Monitoring Issues from a Modeling Perspective, in *Long-Term Monitoring of Global Climate Forcings and Feedbacks*, pp. 1-5, NASA Conference Publication 3234, 1993.

* (1187) Chen, C.-T., Sensitivity of the Simulated Global Climate to Perturbations in Low Cloud Microphysical Properties, Ph.D. Dissertation, Atmospheric and Oceanic Sciences Program, Princeton University, 1994.

* (1188) Nakamura, H., Notes and Correspondence: Horizontal Divergence Associated with Zonally Isolated Jet Streams, *Journal of the Atmospheric Sciences, 50(14)*, 2310-2313, 1993.

* (1189) Nakamura, H., and J.M. Wallace, Synoptic Behavior of Baroclinic Eddies during the Blocking Onset, *Monthly Weather Review, 121(7)*, 1892-1903, 1993.

(1190) Kurihara, Y., Surface Conditions in Tropical Cyclone Models, in *Modelling Severe Weather*, Papers presented at the Fourth BMRC Modelling Workshop, 26-29 October 1992, BMRC Research Report #39, edited by J.D. Jasper and P.J. Meighen, pp. 69-74, 1993.

(1191) Kurihara, Y., R.E. Tuleya, M.A. Bender, and R.J. Ross, Advanced Modeling of Tropical Cyclones, *Proceedings of ICSU/WMO International Symposium on Tropical Cyclone Disasters*, 12-16 October 1992, pp. 190-201, Beijing, China, 1993.

(1192) Manabe, S., and R.J. Stouffer, Multiple Century Response of a Coupled Ocean-Atmosphere Model to an Increase of Atmospheric Carbon Dioxide, *Journal of Climate, 7(1)*, 5-23, 1994.

* (1193) Mahlman, J.D., J.P. Pinto, and L.J. Umscheid, Transport, Radiative, and Dynamical Effects of the Antarctic Ozone Hole: A GFDL "SKYHI" Model Experiment, *Journal of the Atmospheric Sciences, 51(4)*, 489-508, 1994.

(1194) Manabe, S., R.J. Stouffer, and M.J. Spelman, Response of a Coupled Ocean-Atmosphere Model to Increasing Atmospheric Carbon Dioxide, *Ambio, 23(1)*, 44-49, 1994.

(1195) Held, I.M., Lectures on the General Circulation of the Atmosphere, *Proceedings of the Atmosphere-Ocean Dynamics and Interannual Climate Variability*, Friday Harbor Summer School, University of Washington, 19 July-21 August 1993, 35 pp., 1994.

*In collaboration with other organizations

(1196) Delworth, T.L., Tracer Transport in a Quasi-Geostrophic Ocean Model, *Proceedings of the Atmosphere-Ocean Dynamics and Interannual Climate Variability,* Friday Harbor Summer School, University of Washington, 19 July-21 August 1993, 13 pp., 1994.

* (1197) Hamilton, K., R.J. Wilson, and H. Vahlenkamp, Three-Dimensional Visualization of the Polar Stratospheric Vortex, *Canadian Meteorological and Oceanographic Society Bulletin, 22(4),* 4-6, 1994.

* (1198) Bender, M., I. Ginis, and Y. Kurihara, Numerical Simulations of Tropical Cyclone-Ocean Interaction with a High-Resolution Coupled Model, *Journal of Geophysical Research, 98(D12),* 23,245-23,263, 1993.

(1199) Tuleya, R., Tropical Storm Development and Decay: Sensitivity to Surface Boundary Conditions, *Monthly Weather Review, 122(2),* 291-304, 1994.

(1200) Orlanski, I., and B.D. Gross, Orographic Modification of Cyclone Development, *Journal of the Atmospheric Sciences, 51(4),* 589-611, 1994.

* (1201) Stouffer, R.J., S. Manabe, and K.Ya. Vinnikov, Model Assessment of the Role of Natural Variability in Recent Global Warming, *Nature, 367,* 634-636, 1994.

* (1202) Bryan, K., and F.C. Hansen, A Stochastic Model of North Atlantic Climate Variability on Multidecadal Time-Scales, in *Natural Climate Variability on Decade-to-Century Time Scales,* edited by D.G. Martinson, K. Bryan, M. Ghil, M.M. Hall, T.R. Karl, E.S. Sarachik, S. Sorooshian, and L.D. Talley, National Academy Press, Washington, DC, 1995.

* (1203) Lau, N.-C., and K.-H. Lau, Simulation of the Asian Summer Monsoon in a 40-Year Experiment with a General Circulation Model, in *Proceedings of Second International Conference on East Asia and Western Pacific Meteorology and Climate,* 7-10 September 1992, edited by W.J. Kyle and C.P. Chang, pp. 49-56, World Scientific, Publishing Co., Singapore, 1993.

* (1204) Xie, S.P., On Preferred Zonal Scale of Wave-CISK with Conditional Heating, *Journal of the Meteorological Society of Japan, 72(1),* 19-30, 1994.

* (1205) Pavan, V., Parameter Study of the Statistically Steady-State of a Multi-Layer Quasi-Geostrophic Model, Ph.D. Dissertation, Atmospheric and Oceanic Sciences Program, Princeton University, 1994.

* (1206) Murnane, R.J., J.K. Cochran, and J.L. Sarmiento, Estimates of Particle-and Thorium-Cycling Rates in the Northwest Atlantic Ocean, *Journal of Geophysical Research, 99(C2),* 3373-3392, 1994.

* (1207) Murnane, R., Determination of Thorium and Particulate Matter Cycling Parameters at Station P: A Reanalysis and Comparison of Least Squares Techniques, *Journal of Geophysical Research, 99(C2),* 3393-3405, 1994.

* (1208) Chao, Y., and S.G.H. Philander, On the Structure of the Southern Oscillation, *Journal of Climate, 6(3),* 450-469, 1993.

* (1209) Peixoto, J.P., and A.H. Oort, On the Forced Regime of the General Circulation of the Atmosphere, *Transactions of the Academy of Sciences,* Lisbon, Portugal, Vol. 32, pp. 111-148, 1993.

* (1210) Peixoto, J.P., and A.H. Oort, The Forcing of the Zonal Mean State of the Atmosphere, *Transactions of the Academy of Sciences,* Lisbon, Portugal, Vol. 32, pp. 149-179, 1993.

* (1211) Sun, D.-Z., and R.S. Lindzen, A PV View of the Zonal Mean Distribution of Temperature and Wind in the Extratropical Troposphere, *Journal of the Atmospheric Sciences, 51(5),* 757-772, 1994.

*In collaboration with other organizations

* (1212) Ramaswamy, V., Perturbation of the Climate System due to Stratospheric Ozone Depletion, *Chemistry of the Atmosphere Symposium Proceedings*, Preprints, American Chemical Society, Division of Petroleum Chemistry, 37(4), 1546-1551, 1993.

(1213) Knutson, T.R., and S. Manabe, Impact of Increasing CO_2 on the Walker Circulation and ENSO-like Phenomena in a Coupled Ocean-Atmosphere Model, in *Preprints, 6th Conference on Climate Variations*, 23-28 January 1994, Nashville, TN, pp. 80-81, American Meteorological Society, Boston, MA, 1994.

(1214) Najjar, R.G., and J.R. Toggweiler, Reply to the Comment by Jackson, *Limnology and Oceanography, 38(6)*, 1331-1332, 1993.

* (1215) Liu, Z., Thermocline Forced by Varying Ekman Pumping, Part II: Annual and Decadal Ekman Pumping, *Journal of Physical Oceanography, 23(12)*, 2523-2540, 1993.

* (1216) Anderson, J.L., and H.M. van den Dool, Skill and Return of Skill in Dynamic Extended-Range Forecasts, *Monthly Weather Review, 122(3)*, 507-516, 1994.

* (1217) Liu, Z., Notes and Correspondence: Interannual Positive Feedbacks in a Simple Extratropical Air-Sea Coupling System, *Journal of the Atmospheric Sciences, 50(17)*, 3022-3028, 1993.

(1218) Donner, L.J., Radiative Forcing by Parameterized Ice Clouds in a General Circulation Model, in *Preprints, The 8th Conference on Atmospheric Radiation*, 23-28 January 1994, Nashville, TN, pp. 110-112, American Meteorological Society, Boston, MA, 1994.

(1219) Stouffer, R.J., The Geophysical Fluid Dynamics Laboratory (GFDL) Model Integration, in *An Intercomparison of Selected Features of the Control Climates Simulated by Coupled Ocean-Atmosphere General Circulation Models*, pp. 3-7, WCRP-82, WMO/TD No. 574, 1993.

(1220) Hamilton, K., Interdecadal Climate Variations Over the High-Latitude North Atlantic as Seen in 235 Years of Surface Air Temperature Data, *Canadian Meteorological and Oceanographic Society Bulletin, 22(2)*, 11-14, 1994.

(1221) Lau, N.-C., Environmental Crisis of the Twenty-First Century: Air and Sunshine, Part I: (in Chinese), *"Twenty-First Century" Bimonthly, No. 21*, February 1994, pp. 69-76, published by Institute of Chinese Studies, Chinese University of Hong Kong, 1994.

(1222) Lau, N.-C., Environmental Crisis of the Twenty-First Century: Air and Sunshine, Part II: (in Chinese), *"Twenty-First Century" Bimonthly, No. 22*, April 1994, pp. 69-77, published by Institute of Chinese Studies, Chinese University of Hong Kong, 1994.

* (1223) Oort, A.H., L.A. Anderson, and J.P. Peixoto, Estimates of the Energy Cycle of the Oceans, *Journal of Geophysical Research, 99(C4)*, 7665-7688, 1994.

* (1224) Strahan, S.E., and J.D. Mahlman, Evaluation of the GFDL SKYHI General Circulation Model using Aircraft N_20 Measurements: 1. Polar Winter Stratospheric Meteorology and Tracer Morphology, *Journal of Geophysical Research, 99(D5)*, 10,305-10,318, 1994.

* (1225) Strahan, S.E., and J.D. Mahlman, Evaluation of the GFDL SKYHI General Circulation Model using Aircraft N_20 Measurements: 2. Tracer Variability and Diabatic Meridional Circulation, *Journal of Geophysical Research, 99(D5)*, 10,319-10,332, 1994.

(1226) Hamilton, K., Modelling Middle Atmosphere Interannual Variability, *Proceedings of the Fifth Cospar Colloquium*, Columbia, MD, August 1993, edited by M. Teague, D. Baker and V. Papitashvi, pp. 751-757, Pergammon Press, 1994.

(1227) Milly, P.C.D., and K.A. Dunne, Sensitivity of the Global Water Cycle to the Water-Holding Capacity of Land, *Journal of Climate, 7(4)*, 506-526, 1994.

*In collaboration with other organizations

(1228) Tziperman, E., J.R. Toggweiler, Y. Feliks, and K. Bryan, Instability of the Thermohaline Circulation with Respect to Mixed Boundary Conditions: Is it Really a Problem for Realistic Models?, *Journal of Physical Oceanography, 24(2)*, 217-232, 1994.

* (1229) Matano, R.P., and S.G.H. Philander, On the Decay of the Meanders of Eastward Currents, *Journal of Physical Oceanography, 24(2)*, 298-304, 1994.

* (1230) Raval, A., A.H. Oort, and V. Ramaswamy, Observed Dependence of Outgoing Longwave Radiation on Sea Surface Temperature and Moisture, *Journal of Climate, 7(5)*, 807-821, 1994.

(1231) Phillipps, P.J., and I.M. Held, The Response to Orbital Perturbations in an Atmospheric Model Coupled to a Slab Ocean, *Journal of Climate, 7(5)*, 767-782, 1994.

* (1232) Gross, B.D., Frontal Interaction with Isolated Orography, *Journal of the Atmospheric Sciences, 51(11)*, 1480-1496, 1994.

* (1233) Boer, G., R. Colman, M. Dix, V. Galin, M. Helfand, J. Kiehl, A. Kitoh, W. Lau, X.-Z. Liang, V. Lykossov, B. McAvaney, K. Miyakoda, and S. Planton, Cloud Radiative Effects on Implied Oceanic Energy Transports as Simulated by Atmospheric General Circulation Models, PCMDI Report #15, UCRL-ID-116893, University of California, Lawrence Livermore National Laboratory, Livermore, CA, 1994.

* (1234) Kasahara, A., A.P. Mizzi, and L.J. Donner, Diabatic Initialization for Improvement in the Tropical Analysis of Divergence and Moisture using Satellite Radiometric Imagery Data, *Tellus, 46A(3)*, 242-264, 1994.

* (1235) Anderson, L.A., and J.L. Sarmiento, Redfield Ratios of Remineralization Determined by Nutrient Data Analysis, *Global Biogeochemical Cycles, 8(1)*, 65-80, 1994.

* (1236) Sarmiento, J.L., and M. Bender, Carbon Biogeochemistry and Climate Change, *Photosynthesis Research, 39*, 209-234, 1994.

(1237) Orlanski, I., Energy Dispersion vs. Baroclinic Conversion in the Life Cycle of Atmospheric Eddies, *Proceedings of the Life Cycle of Extratropical Cyclone Conference*, Bergen, Norway, 27 June-2 July 1994, 1994.

* (1238) Ohfuchi, W., The Sensitivity of an Atmospheric General Circulation Model to Large Changes in Carbon Dioxide Level, Ph.D. Dissertation, Atmospheric and Oceanic Sciences Program, Princeton University, 1994.

* (1239) Seman, C.J., A Numerical Study of Nonlinear Nonhydrostatic Conditional Symmetric Instability in a Convectively Unstable Atmosphere, *Journal of the Atmospheric Sciences, 51(11)*, 1352-1371, 1994.

* (1240) Colman, R.A., B.J. McAvaney, and R.T. Wetherald, Sensitivity of the Australian Surface Hydrology and Energy Budgets to a Doubling of CO_2, *Australian Meteorological Magazine, 43*, 105-116, 1994.

* (1241) Molinari, R.L., D. Battisti, K. Bryan, and J. Walsh, The Atlantic Climate Change Program, *Bulletin of the American Meteorological Society, 75(7)*, 1191-1199, 1994.

* (1242) Milly, P.C.D., Climate, Soil Water Storage, and the Average Annual Water Balance, *Water Resources Research, 30(7)*, 2143-2156, 1994.

* (1243) Galloway, J.N., H. Levy II, and P.S. Kasibhatla, Year 2020: Consequences of Population Growth and Development on Deposition of Oxidized Nitrogen, *Ambio, 23(2)*, 120-123, 1994.

* (1244) Oltmans, S.J., and H. Levy II, Surface Ozone Measurements from a Global Network, *Atmospheric Environment, 28(1)*, 9-24, 1994.

*In collaboration with other organizations

* (1245) Chameides, W.L., P.S. Kasibhatla, J. Yienger, and H. Levy II, Growth of Continental-Scale Metro-Agro-Plexes, Regional Ozone Pollution, and World Food Production, *Science, 264*, 74-77, 1994.

(1246) Broccoli, A.J., and S. Manabe, Climate Model Studies of Interactions Between Ice Sheets and the Atmosphere-Ocean System, in *Ice in the Climate System*, edited by W.R. Peltier, Springer-Verlag, Berlin, NATO ASI Series I, Vol. 12, pp. 271-290,1993.

* (1247) Soden, B.J., and L.J. Donner, Evaluation of a GCM Cirrus Parameterization using Satellite Observations, *Journal of Geophysical Research, 99(D7)*, 14,401-14,413, 1994.

* (1248) Ezer, T., On the Interaction Between the Gulf Stream and the New England Seamount Chain, *Journal of Physical Oceanography, 24(1)*, 191-204, 1994.

* (1249) Ezer, T., and G.L. Mellor, Continuous Assimilation of Geosat Altimeter Data into a Three-Dimensional Primitive Equation Gulf Stream Model, *Journal of Physical Oceanography, 24(4)*, 832-847, 1994.

* (1250) Ezer, T., and G.L. Mellor, Diagnostic and Prognostic Calculations of the North Atlantic Circulation and Sea Level Using a Sigma Coordinate Ocean Model, *Journal of Geophysical Research, 99(C7)*, 14,159-14,171, 1994.

* (1251) Mellor, G.L., T. Ezer, and L.-Y. Oey, The Pressure Gradient Conundrum of Sigma Coordinate Ocean Models, *Journal of Atmospheric and Oceanic Technology, 11(4)*, 1126-1134, 1994.

* (1252) Koberle, C., and S.G.H. Philander, On the Processes that Control Seasonal Variations of Sea Surface Temperatures in the Tropical Pacific Ocean, *Tellus, 46A*, 481-496, 1994.

* (1253) Armstrong, R.A., Grazing Limitation and Nutrient Limitation in Marine Ecosystems: Steady State Solutions of an Ecosystem Model with Multiple Food Chains, *Limnology and Oceanography, 39(3)*, 597-608, 1994.

* (1254) Scanlon, B.R., and P.C.D. Milly, Water and Heat Fluxes in Desert Soils, 2. Numerical Simulations, *Water Resources Research, 30(3)*, 721-733, 1994.

* (1255) Navarra, A., W.F. Stern, and K. Miyakoda, Reduction of the Gibbs Oscillation in Spectral Model Simulations, *Journal of Climate, 7(8)*, 1169-1183, 1994.

(1256) Lau, N.-C., and M.J. Nath, A Modeling Study of the Relative Roles of Tropical and Extratropical SST Anomalies in the Variability of the Global Atmosphere-Ocean System, *Journal of Climate, 7(8)*, 1184-1207, 1994.

* (1257) Nakamura, H., Rotational Evolution of Potential Vorticity Associated with a Strong Blocking Flow Configuration over Europe, *Geophysical Research Letters, 21(18)*, 2003-2006, 1994.

(1258) Broccoli, A.J., Learning From Past Climates, *Nature* (News and Views), *371*, 282, 1994.

* (1259) Milly, P.C.D., Climate, Interseasonal Storage of Soil Water, and the Annual Water Balance, *Advances in Water Resources, 17*, 19-24, 1994.

* (1260) Ramaswamy, V., and M.M. Bowen, Effect of Changes in Radiatively Active Species upon the Lower Stratospheric Temperatures, *Journal of Geophysical Research, 99(D9)*, 18,909-18,921, 1994.

* (1261) Xie, S.P., The Maintenance of an Equatorially Asymmetric State in a Hybrid Coupled GCM, *Journal of the Atmospheric Sciences, 51(18)*, 2602-2612, 1994.

(1262) Hamilton, K., Meteorology and Climatology, in *Encyclopedia of Applied Physics, 10*, 215-237, VCH Publishers, Inc., 1994.

*In collaboration with other organizations

* (1263) Soden, B.J., S.A. Ackerman, D.O'C. Starr, S.H. Melfi, and R.A. Ferrare, Comparison of Upper Tropospheric Water Vapor from GOES, Raman Lidar, and Cross-chain Loran Atmospheric Sounding System Measurements, *Journal of Geophysical Research, 99(D10)*, 21,005-21,016, 1994.

* (1264) Xie, S.P., and S.G.H. Philander, A Coupled Ocean-Atmosphere Model of Relevance to the ITCZ in the Eastern Pacific, *Tellus, 46A*, 340-350, 1994.

* (1265) Xie, S.P., Oceanic Response to the Wind Forcing Associated with the Intertropical Convergence Zone in the Northern Hemisphere, *Journal of Geophysical Research, 99(C10)*, 20,393-20,402, 1994.

(1266) Broccoli, A.J., Climate Model Sensitivity, Paleoclimate and Future Climate Change, in *Long-Term Climatic Variations*, edited by J.-C. Duplessy and M.-T. Spyridakis, NATO ASI Series I, Vol. 22, Springer-Verlag, Berlin, pp. 551-567, 1994.

(1267) Toggweiler, J.R., The Ocean's Overturning Circulation, *Physics Today, 47(11)*, 45-50, 1994.

(1268) Knutson, T.R., and S. Manabe, Impact of Increased CO_2 on Simulated ENSO-Like Phenomena, *Geophysical Research Letters, 21(21)*, 2295-2298, 1994.

* (1269) Held, I.M., and M.J. Suarez, A Proposal for the Intercomparison of the Dynamical Cores of Atmospheric General Circulation Models, *Bulletin of the American Meteorological Society, 75(10)*, 1825-1830, 1994.

* (1270) Karoly, D.J., J.A. Cohen, G.A. Meehl, J.F.B. Mitchell, A.H. Oort, R.J. Stouffer, and R.T. Wetherald, An Example of Fingerprint Detection of Greenhouse Climate Change, *Climate Dynamics, 10*, 97-105, 1994.

* (1271) Randall, D.A., R.D. Cess, J.P. Blanchet, S. Chalita, R. Colman, D.A. Dazlich, A.D. DelGenio, E. Keup, A. Lacis, H. Le Treut, X.-Z. Liang, B.J. McAvaney, J.F. Mahfouf, V.P. Meleshko, J.-J. Morcrette, P.M. Norris, G.L. Potter, L. Rikus, E. Roeckner, J.F. Royer, U. Schlese, D.A. Sheinin, A.P. Sokolov, K.E. Taylor, R.T. Wetherald, I. Yagai, and M.-H. Zhang, Analysis of Snow Feedbacks in 14 General Circulation Models, *Journal of Geophysical Research, 99(D10)*, 20,757-20,771, 1994.

(1272) Hayashi, Y., and D.G. Golder, Kelvin and Mixed Rossby-Gravity Waves Appearing in the GFDL "SKYHI" General Circulation Model and the FGGE Dataset: Implications for their Generation Mechanism and Role in the QBO, *Journal of the Meteorological Society of Japan, 72(6)*, 901-935, 1994.

(1273) Toggweiler, J.R., Vanishing in Bermuda, *Nature (News and Views), 372*, 505-506, 1994.

(1274) Hamilton, K., R.J. Wilson, J.D. Mahlman, and L.J. Umscheid, Climatology of the SKYHI Troposphere-Stratosphere-Mesosphere General Circulation Model, *Journal of the Atmospheric Sciences, 52(1)*, 5-43, 1995.

(1275) Hamilton, K., Interannual Variability in the Northern Hemisphere Winter Middle Atmosphere in Control and Perturbed Experiments with the GFDL SKYHI General Circulation Model, *Journal of the Atmospheric Sciences, 52(1)*, 44-66, 1995.

* (1276) Yuan, L., and K. Hamilton, Equilibrium Dynamics in a Forced-Dissipative f-Plane Shallow Water System, *Journal of Fluid Mechanics, 280*, 369-394, 1994.

* (1277) Branstator, G., and I.M. Held, Westward Propagating Normal Modes in the Presence of Stationary Background Waves, *Journal of the Atmospheric Sciences, 52(2)*, 247-262, 1995.

(1278) Garner, S.T., Permanent and Transient Upstream Effects in Nonlinear Stratified Flow over a Ridge, *Journal of the Atmospheric Sciences, 52(2)*, 227-246, 1995.

* (1279) Held, I.M., R.T. Pierrehumbert, S.T. Garner, and K.L. Swanson, Surface Quasi-Geostrophic Dynamics, *Journal of Fluid Mechanics, 282*, 1-20, 1995.

*In collaboration with other organizations

* (1280) Liu, Z., and S.P. Xie, Equatorward Propagation of Coupled Air-Sea Disturbances with Application to the Annual Cycle of the Eastern Tropical Pacific, *Journal of the Atmospheric Sciences, 51(24)*, 3807-3822, 1994.

* (1281) Ross, R.J., and Y. Kurihara, A Numerical Study on Influences of Hurricane Gloria (1985) on the Environment, *Monthly Weather Review, 123(2)*, 332-346, 1995.

* (1282) Xie, S.P., On the Genesis of the Equatorial Annual Cycle, *Journal of Climate, 7(12)*, 2008-2013, 1994.

* (1283) Burpee, R.W., J.L. Franklin, S.J. Lord, and R.E. Tuleya, The Performance of Hurricane Track Guidance Models With and Without Omega Dropwindsondes, *Preprint of 21st AMS Conference on Hurricanes and Tropical Meteorology*, 1995.

* (1284) Wu, C.-C., and K.A. Emanuel, Potential Vorticity Diagnostics of Hurricane Movement. Part I: A Case Study of Hurricane Bob (1991), *Monthly Weather Review, 123(1)*, 69-92, 1995.

* (1285) Wu, C.-C., and K.A. Emanuel, Potential Vorticity Diagnostics of Hurricane Movement. Part II: Tropical Storm Ana (1991) and Hurricane Andrew (1992), *Monthly Weather Review, 123(1)*, 93-109, 1995.

(1286) Manabe, S., R.J. Stouffer, and M.J. Spelman, Interaction Between Polar Climate and Global Warming, *Fourth Conference on Polar Meteorology and Oceanography*, Dallas, TX, 15-20 January 1995, American Meteorological Society, Boston, MA, pp. 1-9, 1995.

(1287) Hamilton, K., Aspects of Mesospheric Simulation in a Comprehensive General Circulation Model, in *The Upper Mesosphere and Lower Thermosphere: A Review of Experiment and Theory*, Geophysical Monograph 87, American Geophysical Union, pp. 255-264, 1995.

* (1288) Sarmiento, J.L., C. LeQuéré, and S.W. Pacala, Limiting Future Atmospheric Carbon Dioxide, *Global Biogeochemical Cycles, 9(1)*, 121-137, 1995.

(1289) Lanzante, J.R., Circulation Response in GFDL Increased CO_2 Experiments and Comparison with Observed Data, *Proceedings of the Seventeenth Annual Climate Diagnostic Workshop*, Norman, OK, October 1992, pp. 248-253, 1993.

* (1290) Pierrehumbert, R.T., I.M. Held, and K.L. Swanson, Spectra of Local and Non-Local Two-Dimensional Turbulence, *Chaos, Solitons, and Fractals, 4(6)*, 1111-1116, 1994.

* (1291) Willems, R.C., S.M. Glenn, M.F. Crowley, P. Malanotte-Rizzoli, R.E. Young, T. Ezer, G.L. Mellor, H.G. Arango, A.R. Robinson, and C.-C.A. Lai, Experiment Evaluates Ocean Models and Data Assimilation in the Gulf Stream, *EOS, Transactions*, American Geophysical Union, *75(34)*, 385,391,394, 1994.

* (1292) Moody, J.L., S.J. Oltmans, H. Levy II, and J.T. Merrill, Transport Climatology of Tropospheric Ozone: Bermuda, 1988-1991, *Journal of Geophysical Research, 100(D4)*, 7179-7194, 1995.

* (1293) Gu, D., and S.G.H. Philander, Secular Changes of Annual and Interannual Variability in the Tropics During the Past Century, *Journal of Climate, 8(4)*, 864-876, 1995.

* (1294) Armstrong, R.A., J.L. Sarmiento, and R.D. Slater, Monitoring Ocean Productivity by Assimilating Satellite Chlorophyll into Ecosystem Models, in *Ecological Time Series*, edited by T.M. Powell and J.H. Steele, pp. 371-390, 1995.

(1295) Kurihara, Y., M.A. Bender, and R.E. Tuleya, Performance Evaluation of the GFDL Hurricane Prediction System in the 1994 Hurricane Season, in *Preprints 21st Conference on Hurricanes and Tropical Meteorology*, Miami, FL, 24-28 April 1995, American Meteorological Society, Boston, MA, pp. 41-43, 1995.

*In collaboration with other organizations

* (1296) Zhang, J., Effects of Latent Heating on Midlatitude Atmospheric General Circulation, Ph.D. Dissertation, Atmospheric and Oceanic Sciences Program, Princeton University, 1995.

(1297) Donner, L.J., Validating Cumulus Parameterizations using Cloud (System)-Resolving Models, in *Preprints 21st Conference on Hurricanes and Tropical Meteorology*, Miami, FL, 24-28 April 1995, American Meteorological Society, Boston, MA, pp. 564-566, 1995.

(1298) Bender, M.A., Numerical Study of the Asymmetric Structure in the Interior of Tropical Cyclones, in *Preprints 21st Conference on Hurricanes and Tropical Meteorology*, Miami, FL, 24-28 April 1995, American Meteorological Society, Boston, MA, pp. 600-602, 1995.

(1299) Hayashi, Y., and D.G. Golder, The Generation Mechanism of Tropical Transient Waves: Control Experiments and a Unified Theory with Moist Convective Adjustment, in *Preprints 10th Conference on Atmospheric and Oceanic Waves and Stability*, Big Sky, MT, 5-9 June 1995, American Meteorological Society, Boston, MA, pp. 7-8, 1995.

(1300) Stern, W.F., and K. Miyakoda, Feasibility of Seasonal Forecasts Inferred from Multiple GCM Simulations, *Journal of Climate, 8(5)*, 1071-1085, 1995.

(1301) Hamilton, K., Comment on "Global QBO in Circulation and Ozone. Part I: Reexamination of Observational Evidence," *Journal of the Atmospheric Sciences, 52(10)*, 1834-1838, 1995.

* (1302) Gleckler, P.J., D.A. Randall, G. Boer, R. Colman, M. Dix, V. Galin, M. Helfand, J. Kiehl, A. Kitoh, W. Lau, X.-Z. Liang, V. Lykossov, B. McAvaney, K. Miyakoda, S. Planton, and W. Stern, Cloud-Radiative Effects on Implied Oceanic Energy Transports as Simulated by Atmospheric General Circulation Models, *Geophysical Research Letters, 22(7)*, 791-794, 1995.

* (1303) Shine, K.P., Y. Fouquart, V. Ramaswamy, S. Solomon, and J. Srinivasan, Radiative Forcing, in *Climate Change 1994: Radiative Forcing of Climate Change*, Cambridge University Press, pp. 167-199, 1995.

* (1304) Shine, K.P., K. Labitzke, V. Ramaswamy, P. Simon, S. Solomon, W.-C. Wang, Radiative Forcing and Temperature Trends, in *Scientific Assessment of Stratospheric Ozone Depletion*, 1994, Global Ozone Research and Monitoring Project Report #37, WMO, pp. 8.1-8.26, 1995.

* (1305) Ginis, I., and G. Sutyrin, Hurricane-Generated Depth-Averaged Currents and Sea Surface Elevation, *Journal of Physical Oceanography, 25(6)*, 1218-1242, 1995.

* (1306) Zavatarelli, M., and G.L. Mellor, A Numerical Study of the Mediterranean Sea Circulation, *Journal of Physical Oceanography, 25(6)*, 1384-1414, 1995.

* (1307) Yienger, J.J., and H. Levy II, Empirical Model of Global Soil-Biogenic NO_x Emissions, *Journal of Geophysical Research, 100(D6)*, 11,447-11,464, 1995.

(1308) Rosati, A., R. Gudgel, and K. Miyakoda, Decadal Analysis Produced from an Ocean Data Assimilation System, *Monthly Weather Review, 123(7)*, 2206-2228, 1995.

(1309) Lau, N.-C., and M.W. Crane, A Satellite View of the Synoptic-Scale Organization of Cloud Properties in Midlatitude and Tropical Circulation Systems, *Monthly Weather Review, 123(7)*, 1984-2006, 1995.

* (1310) Chang, E.K.M., and I. Orlanski, On Energy Flux and Group Velocity of Waves in Baroclinic Flows, *Journal of the Atmospheric Sciences, 51(24)*, 3823-3828, 1994.

*In collaboration with other organizations

* (1311) Goddard, L., The Energetics of Interannual Variability in the Tropical Pacific Ocean, Ph.D. Dissertation, Atmospheric and Oceanic Sciences Program, Princeton University, 1995.

(1312) Mehta, V.M., and T.L. Delworth, Decadal Variability of the Tropical Atlantic Ocean Surface Temperature in Shipboard Measurements and in a Global Ocean-Atmosphere Model, *Journal of Climate, 8(2)*, 172-190, 1995.

(1313) Toggweiler, J.R., and B. Samuels, Effect of Drake Passage on the Global Thermohaline Circulation, *Deep-Sea Research, 42(4)*, 477-500, 1995.

(1314) Toggweiler, J.R., Anthropogenic CO_2 - The Natural Carbon Cycle Reclaims Center Stage, *Reviews of Geophysics, (Supplement)*, 1249-1252, 1995.

(1315) Toggweiler, J.R., and B. Samuels, Effect of Sea Ice on the Salinity of Antarctic Bottom Waters, *Journal of Physical Oceanography, 25(9)*, 1980-1997, 1995.

(1316) Lanzante, J.R., Analysis of Climate Data Using Resistant, Robust and Nonparametric Techniques: Some Examples and Some Applications to the Historical Radiosonde Record, *Proceedings of the Nineteenth Annual Climate Diagnostics Workshop*, College Park, MD, 14-18 November 1994, pp. 37-40, 1995.

(1317) Sarmiento, J.L., The Carbon Cycle and the Role of the Ocean in Climate, in *Ecological and Social Dimensions of Global Change*, edited by D.D. Caron, F.S. Chapin III, J. Donoghue, M. Firestone, J. Harte, L.E. Wells, and R. Stewardson, Institute of International Studies, University of California, Berkeley, CA, pp.-4-41, 1994.

(1318) Shaffer, G., and J.L. Sarmiento, Biogeochemical Cycling in the Global Ocean, I. A New, Analytical Model with Continuous Vertical Resolution and High Latitude Dynamics, *Journal of Geophysical Research, 100(C2)*, 2659-2672, 1995.

(1319) Joos, F., and J.L. Sarmiento, Der Anstieg des Atmospharischen Kohlendioxds, *Physikalische Blatter, 51(5)*, 405-411, 1995.

(1320) Sarmiento, J.L., R. Murnane, and C. LeQuéré, Air-Sea CO_2 Transfer and the Carbon Budget of the North Atlantic, *Philosophical Transactions of the Royal Society of London, B348*, 211-219, 1995.

(1321) Anderson, J.L., A Simulation of Atmospheric Blocking with a Forced Barotropic Model, *Journal of the Atmospheric Sciences, 52(15)*, 2593-2608, 1995.

* (1322) Lawrence, M.G., W.L. Chameides, P.S. Kasibhatla, H. Levy II, and W.J. Moxim, Lightning and Atmospheric Chemistry: The Rate of Atmospheric NO Production, in *Handbook of Atmospheric Electrodynamics*, edited by Hans Volland, CRC Press, pp. 189-202, 1995.

(1323) Lau, N.-C., The Antarctic Ozone Hole Story, in *United Bulletin*, United College, Chinese University of Hong Kong, pp. 49-53, 1992-93.

* (1324) Chen, C.-T., and V. Ramaswamy, Parameterization of the Solar Radiative Characteristics of Low Clouds and Studies with a General Circulation Model, *Journal of Geophysical Research, 100(D6)*, 11,611-11,622, 1995.

* (1325) Liu, Z., and S.G.H. Philander, How Different Wind Stress Patterns Affect the Tropical-Subtropical Circulations of the Upper Ocean, *Journal of Physical Oceanography, 25(4)*, 449-462, 1995.

* (1326) Sun, D.-Z., and A.H. Oort, Humidity-Temperature Relationships in the Tropical Troposphere, *Journal of Climate, 8(8)*, 1974-1987, 1995.

*In collaboration with other organizations

* (1327) Ezer, T., G.L. Mellor, and R.J. Greatbatch, On the Interpentadal Variability of the North Atlantic Ocean: Model Simulated Changes in Transport, Meridional Heat Flux and Coastal Sea Level Between 1955-1959 and 1970-1974, *Journal of Geophysical Research, 100(C6)*, 10,559-10,566, 1995.

* (1328) Chylek, P., and J. Li, Light Scattering by Small Particles in an Intermediate Region, in *Optics Communications, 117*, 389-394, 1995.

(1329) Kurihara, Y., M.A. Bender, R.E. Tuleya, and R.J. Ross, Improvements in the GFDL Hurricane Prediction System, *Monthly Weather Review, 123(9)*, 2791-2801, 1995.

(1330) Knutson, T.R., and S. Manabe, Time-mean Response over the Tropical Pacific to Increased CO_2 in a Coupled Ocean-Atmosphere Model, *Journal of Climate, 8(9)*, 2183-2199, 1995.

(1331) Freidenreich, S.M., and V. Ramaswamy, Stratospheric Temperature Response to Improved Solar CO_2 and H_2O Parameterizations, *Journal of Geophysical Research, 100(D8)*, 16,721-16,725, 1995.

(1332) Hamilton, K., Simulation of Vertically-Propagating Waves in Comprehensive General Circulation Models: Opportunities for Comparison with Observations, *Proceedings of the Workshop on Wind Observations in the Middle Atmosphere*, Centre National d'Etudes Spatiales, Paris, France, 15-18 November 1994, pp. 4.3-4.15, 1994.

(1333) Hamilton, K., Comprehensive Simulation of the Middle Atmospheric Climate: Some Recent Results, *Climate Dynamics, 11*, 223-241, 1995.

* (1334) Ramaswamy, V., R.J. Charlson, J.A. Coakley, J.L. Gras, Harshvardhan, G. Kukla, M.P. McCormick, D. Moller, E. Roeckner, L.L. Stowe, and J. Taylor, What are the Observed and Anticipated Meteorological and Climatic Responses to Aerosol Forcing?, in *Aerosol Forcing of Climate*, edited by R.J. Charlson and J. Heintzenberg, Wiley Interscience, pp. 386-399, 1995.

* (1335) Galloway, J.N., W.H. Schlesinger, H. Levy II, A. Michaels, and J.L. Schnoor, Nitrogen Fixation: Anthropogenic Enhancement-Environmental Response, *Global Biogeochemical Cycles, 9(2)*, 235-252, 1995.

* (1336) Shine, K.P., B.P. Briegleb, A.S. Grossman, D. Hauglustaine, H. Mao, V. Ramaswamy, M.D. Schwarzkopf, R. Van Dorland, and W.-C. Wang, Radiative Forcing Due to Changes in Ozone: A Comparison of Different Codes, in *Atmospheric Ozone as a Climate Gas*, edited by W.-C. Wang and I.S.A. Isaksen, NATO ASI Series I, Vol. 32, Springer-Verlag, pp. 373-396, 1995.

* (1337) Larichev, V.D., and I.M. Held, Eddy Amplitudes and Fluxes in a Homogeneous Model of Fully Developed Baroclinic Instability, *Journal of Physical Oceanography, 25(10)*, 2285-2297, 1995.

* (1338) Soden, B.J., and R. Fu, A Satellite Analysis of Deep Convection, Upper Tropospheric Humidity and the Greenhouse Effect, *Journal of Climate, 8(10)*, 2333-2351, 1995.

* (1339) Griffies, S.M., and E. Tziperman, A Linear Thermohaline Oscillator Driven by Stochastic Atmospheric Forcing, *Journal of Climate, 8(10)*, 2440-2453, 1995.

* (1340) Toggweiler, J.R., and S. Carson, What are Upwelling Systems Contributing to the Ocean's Carbon and Nutrient Budgets? in *Upwelling in the Oceans: Modern Processes and Ancient Records*, edited by C.P. Summerhayes, K.-C. Emeis, M.V. Angel, R.I. Smith and B. Zeitzchel, John Wiley & Sons, Ltd., pp. 337-360, 1995.

* (1341) Hamilton, K., and R.A. Vincent, High-Resolution Radiosonde Data Offer New Prospects for Research, *EOS, Transactions*, American Geophysical Union, 76(49), 497, 506-507, 1995.

*In collaboration with other organizations

(1342) Manabe, S., and R.J. Stouffer, Simulation of Abrupt Climate Change Induced by Freshwater Input to the North Atlantic Ocean, *Nature, 378*, 165-167, 1995.

* (1343) Broccoli, A.J., S. Manabe, J.F.B. Mitchell, and L. Bengtsson, Comments on "Global Climate Change and Tropical Cyclones: Part II", *Bulletin of the American Meteorological Society, 76(11)*, 2243-2245, 1995.

* (1344) Jones, P.W., C.L. Kerr, and R.S. Hemler, Practical Considerations in Development of a Parallel SKYHI General Circulation Model, *Parallel Computing, 21*, 1677-1694, 1995.

(1345) Orlanski, I., and J. Sheldon, Stages in the Energetics of Baroclinic Systems, *Tellus, 47A*, 605-628, 1995.

(1346) Wetherald, R.T., Feedback Processes in the GFDL R30-14 Level General Circulation Model, in *Climate Sensitivity to Radiative Perturbations: Physical Mechanisms and Their Validation*, NATO ASI Series I, Vol. 34, 251-266, 1996.

* (1347) Lee, W.-J., and M. Mak, Dynamics of Storm Tracks: A Linear Instability Perspective, *Journal of the Atmospheric Sciences, 52(6)*, 697-723, 1995.

* (1348) Mak, M., Orthogonal Wavelet Analysis: Interannual Variability in the Sea Surface Temperature, *Bulletin of the American Meteorological Society, 76(11)*, 2179-2186, 1995.

* (1349) Donner, L.J., J. Warren, and J. Ström, Implementing Microphysics at Physically Appropriate Scales in GCMs, *Proceedings of the WCRP Workshop on Cloud Microphysics in GCMs*, Kananaskis, Alberta, Canada 23-25 May 1995, pp. 133-139,1995.

* (1350) Santer, B.D., K.E. Taylor, T.M.L. Wigley, P.D. Jones, D.J. Karoly, J.F.B. Mitchell, A.H. Oort, J.E. Penner, V. Ramaswamy, M.D. Schwarzkopf, R.J. Stouffer, and S. Tett, A Search for Human Influences on the Thermal Structure of the Atmosphere, *PCMDI Report, No. 27*, 26 pp., 1995.

(1351) Wyman, B.L., A Step-Mountain Coordinate General Circulation Model: Description and Validation of Medium Range Forecasts, *Monthly Weather Review, 124(1)*, 102-121, 1996.

(1352) Wetherald, R.T., and S. Manabe, The Mechanisms of Summer Dryness Induced by Greenhouse Warming, *Journal of Climate, 8(12)*, 3096-3108, 1995.

(1353) Hamilton, K., Do Historical "Zero Depth" Hydrographic Data Contain Useful Information on Climate Trends? *Canadian Meteorological and Oceanographic Society Bulletin, 23(6)*, 6-8, 1995.

* (1354) Broccoli, A.J., and E.P. Marciniak, Comparing Simulated Glacial Climate and Paleodata: A Re-examination, *Paleoceanography, 11(1)*, 3-14, 1996.

(1355) Anderson, J.L., Selection of Initial Conditions for Ensemble Forecasts in a Simple Perfect Model Framework, *Journal of the Atmospheric Sciences, 53(1)*, 22-36, 1996.

(1356) Mahlman, J.D., Toward a Scientific Centered Climate Monitoring System, *Climatic Change, 31*, 223-230, 1995.

* (1357) Overland, J.E., P. Turet, and A.H. Oort, Regional Variations of Moist Static Energy Flux into the Arctic, *Journal of Climate, 9(1)*, 54-65, 1996.

* (1358) Oey, L.-Y., Simulation of Mesoscale Variability in the Gulf of Mexico: Sensitivity Studies, Comparison with Observations, and Trapped Wave Propagation, *Journal of Physical Oceanography, 26(2)*, 145-175, 1996.

(1359) Manabe, S., and R.J. Stouffer, Low Frequency Variability of Surface Air Temperature in a 1,000-Year Integration of a Coupled Atmosphere-Ocean-Land Surface Model, *Journal of Climate, 9(2)*, 376-393, 1996.

*In collaboration with other organizations

* (1360) Frey, R.A., S.A. Ackerman, and B.J. Soden, Climate Parameters from Satellite Spectral Measurements, Part I: Collocated AVHRR and HIRS/2 Observations of Spectral Greenhouse Parameter, *Journal of Climate, 9(2)*, 327-344, 1996.

* (1361) Milly, P.C.D., Effects of Thermal Vapor Diffusion on Seasonal Dynamics of Water in the Unsaturated Zone, *Water Resources Research, 32(3)*, 509-518, 1996.

* (1362) Held, I.M., and V.D. Larichev, A Scaling Theory for Horizontally Homogeneous, Baroclinically Unstable Flow on a Beta-Plane, *Journal of the Atmospheric Sciences, 53(7)*, 946-952, 1996.

(1363) Hamilton, K., Tides, in *The Encyclopedia of Climate and Weather*, Oxford University Press, pp. 761-764, 1996.

* (1364) Li, J., and V. Ramaswamy, Four-Stream Spherical Harmonic Approximation for Solar Radiative Transfer, *Journal of the Atmospheric Sciences, 53(8)*, 1174-1186, 1996.

(1365) Anderson, J.L., and W.F. Stern, Evaluating the Predictive Utility of Ensemble Forecasts in a Perfect Model Setting, *Journal of Climate, 9(2)*, 260-269, 1996.

(1366) Lau, N.-C., Variability of the Midlatitude Atmospheric Circulation in Relation to Tropical and Extratropical Sea Surface Temperature Anomalies, in *From Atmospheric Circulation to Global Change*, Monograph in Celebration of the 80th Birthday of Professor T.C. Yeh, edited by The Institute of Atmospheric Physics, Chinese Academy of Sciences, Beijing, China, China Meteorological Press, pp. 549-572, 1996.

* (1367) Soden, B.J., and F.P. Bretherton, Interpretation of TOVS Water Vapor Radiances in Terms of Layer-Average Relative Humidities: Method and Climatology for the Upper, Middle, and Lower Troposphere, *Journal of Geophysical Research, 101(D5)*, 9333-9343, 1996.

* (1368) Sun, D.-Z., and I.M. Held, A Comparison of Modeled and Observed Relationships between Interannual Variations of Water Vapor and Temperature, *Journal of Climate, 9(4)*, 665-675, 1996.

* (1369) Pavan, V., and I.M. Held, The Diffusive Approximation for Eddy Fluxes in Baroclinically Unstable Jets, *Journal of the Atmospheric Sciences, 53(9)*, 1262-1272, 1996.

(1370) Wilson, R.J., and K. Hamilton, Comprehensive Model Simulation of Thermal Tides in the Martian Atmosphere, *Journal of the Atmospheric Sciences, 53(9)*, 1290-1326, 1996.

* (1371) Gnanadesikan, A., Modeling the Diurnal Cycle of Carbon Monoxide: Sensitivity to Physics, Chemistry, Biology, and Optics, *Journal of Geophysical Research, 101(C5)*, 12,177-12,191, 1996.

* (1372) Moxim, W.J., H. Levy II, and P.S. Kasibhatla, Simulated Global Tropospheric PAN: Its Transport and Impact on NO_x, *Journal of Geophysical Research, 101(D7)*, 12,621-12,638, 1996.

* (1373) Mellor, G.L., and T. Ezer, Sea Level Variations Induced by Heating and Cooling: An Evaluation of the Boussinesq Approximation in Ocean Models, *Journal of Geophysical Research, 100(C10)*, 20,565-20,577, 1995.

* (1374) Ezer, T., (Ed.), Proceedings from the Princeton Ocean Model (POM) Users Meeting, Princeton, NJ, 10-12 June 1996, Program in Atmospheric and Oceanic Sciences, Princeton University, 56 pp., 1996.

* (1375) Pinardi, N., A. Rosati, and R.C. Pacanowski, The Sea Surface Pressure Formulation of Rigid Lid Models. Implications for Altimetric Data Assimilation Studies, *Journal of Marine Systems, 6*, 109-119, 1995.

*In collaboration with other organizations

(1376) Hamilton, K., Comprehensive Meteorological Modelling of the Middle and Upper Atmosphere: A Tutorial Review, *Journal of Atmospheric and Terrestrial Physics, 58(14)*, 1591-1628, 1996.

* (1377) Hurtt, G.C., and R.A. Armstrong, A Pelagic Ecosystem Model Calibrated with BATS Data, *Deep-Sea Research, 43*, 653-683, 1996.

* (1378) Vinnikov, K.Ya., A. Robock, R.J. Stouffer, and S. Manabe, Vertical Patterns of Free and Forced Climate Variations, *Geophysical Research Letters, 23(14)*, 1801-1804, 1996.

(1379) Soden, B.J., and J.R. Lanzante, An Assessment of Satellite and Radiosonde Climatologies of Upper Tropospheric Water Vapor, *Journal of Climate, 9(6)*, 1235-1250, 1996.

* (1380) Dixon, K.W., J.L. Bullister, R.H. Gammon, and R.J. Stouffer, Examining a Coupled Climate Model using CFC-11 as an Ocean Tracer, *Geophysical Research Letters, 23(15)*, 1957-1960, 1996.

* (1381) Chen, C.-T., and V. Ramaswamy, Sensitivity of Simulated Global Climate to Perturbations in Low Cloud Microphysical Properties, Part I: Globally Uniform Perturbations, *Journal of Climate, 9(6)*, 1385-1402, 1996.

* (1382) Kushnir, Y., and I.M. Held, Equilibrium Atmospheric Response to North Atlantic SST Anomalies, *Journal of Climate, 9(6)*, 1208-1220, 1996.

* (1383) Masina, S., Tropical Instability Waves in the Pacific Ocean, Ph.D. Dissertation, Atmospheric and Oceanic Sciences Program, Princeton University, 1996.

* (1384) Santer, B., K. Taylor, T.M.L. Wigley, T.C. Johns, P.D. Jones, D.J. Karoly, J.F.B. Mitchell, A.H. Oort, J.E. Penner, V. Ramaswamy, M.D. Schwarzkopf, R.J. Stouffer, and S. Tett, A Search for Human Influences on the Thermal Structure of the Atmosphere, *Nature, 382*, 39-46, 1996.

* (1385) Mellor, G.L., and X.-H. Wang, Pressure Compensation and the Bottom Boundary Layer, *Journal of Physical Oceanography, 26(10)*, 2214-2222, 1996.

* (1386) Mellor, G.L., *Introduction to Physical Oceanography*, AIP Press, 300 pp., 1996.

* (1387) Toggweiler, J.R., E. Tziperman, Y. Feliks, K. Bryan, S.M. Griffies, and B. Samuels, Reply to Comment by S. Rahmstorf, *Journal of Physical Oceanography, 26(6)*, 1106-1110, 1996.

* (1388) Murnane, R.J., J.K. Cochran, K.O. Buesseler, and M.P. Bacon, Least Squares Estimates of Thorium, Particle, and Nutrient Cycling Rate Constants from the JGOFS North Atlantic Bloom Experiment, *Deep-Sea Research, 43(2)*, 239-258, 1996.

* (1389) Lee, S., and J.L. Anderson, A Simulation of Atmospheric Storm Tracks with a Forced Barotropic Model, *Journal of the Atmospheric Sciences, 53(15)*, 2113-2128, 1996.

(1390) Anderson, J.L., A Method for Producing and Evaluating Probabilistic Forecasts from Ensemble Model Integrations, *Journal of Climate, 9(7)*, 1518-1530, 1996.

* (1391) Hsieh, W.W., and K. Bryan, Redistribution of Sea Level Rise Associated with Enhanced Greenhouse Warming: A Simple Model Study, *Climate Dynamics, 12*, 535-544, 1996.

* (1392) Bryan, K., The Steric Component of Sea Level Rise Associated with Enhanced Greenhouse Warming: A Model Study, *Climate Dynamics, 12*, 545-555, 1996.

* (1394) Ramaswamy, V., M.D. Schwarzkopf, and W.J. Randel, Fingerprint of Ozone Depletion in the Spatial and Temporal Pattern of Recent Lower-Stratospheric Cooling, *Nature, 382*, 616-618, 1996.

* (1395) Slusser, J., K. Hammond, A. Kylling, K. Stamnes, L. Perliski, A. Dahlback, D. Anderson, and R. DeMajistre, Comparison of Air Mass Computations, *Journal of Geophysical Research, 101(D5)*, 9315-9321, 1996.

*In collaboration with other organizations

* (1396) Dunne, K.A., and C.J. Willmott, Global Distribution of Plant-Extractable Water Capacity of Soil, *International Journal of Climatology, 16,* 841-859, 1996.

* (1397) Raval, A., A.H. Oort, and J.R. Lanzante, A New Interpolation Routine ("ANAL95") for Obtaining Global Fields from Irregularly Spaced Meteorological Data, GFDL Web Pages from the URL http://www.gfdl.gov/, 1996.

* (1398) Anderson, L., and J.L. Sarmiento, Global Ocean Phosphate and Oxygen Simulations, *Global Biogeochemical Cycles, 9(4),* 621-636, 1995.

* (1399) Joos, F., M. Bruno, R. Fink, U. Siegenthaler, T.F. Stocker, C. LeQuere, and J.L. Sarmiento, An Efficient and Accurate Representation of Complex Oceanic and Biospheric Models of Anthropogenic Carbon Uptake, *Tellus, 48B,* 397-417, 1996.

(1400) Williams, G.P., Jovian Dynamics. Part 1: Vortex Stability, Structure, and Genesis, *Journal of the Atmospheric Sciences, 53(18),* 2685-2734, 1996.

* (1401) Wu, C.-C., and Y. Kurihara, A Numerical Study of the Feedback Mechanisms on Hurricane-Environment Interaction on Hurricane Movement from the Potential Vorticity Perspective, *Journal of the Atmospheric Sciences, 53(15),* 2264-2282, 1996.

* (1402) Gnanadesikan, A., Mixing Driven by Vertically Variable Forcing: An Application to the Case of Langmuir Circulation, *Journal of Fluid Mechanics, 322,* 81-107, 1996.

(1403) Gordon, C.T., A. Rosati, and R. Gudgel, The Impact of Specified ISCCP Low Clouds in Coupled Model Integrations, in *Preprints 11th Conference on Numerical Weather Prediction,* 19-23 August 1996, Norfolk, VA, American Meteorological Society, Boston, MA, pp. 8-10, 1996.

(1404) Ramaswamy, V., Longwave Radiation, in *Encyclopedia of Climate and Weather,* edited by S.H. Schneider, Oxford University Press, pp. 478-481, 1996.

* (1405) Schimel, D., D. Alves, I. Enting, M. Heimann, F. Joos, D. Raynaud, T. Wigley, M. Prather, R. Derwent, D. Ehhalt, P. Fraser, E. Sanhueza, X. Zhou, P. Jonas, R. Charlson, H. Rodhe, S. Sadasivan, K.P. Shine, Y. Fouquart, V. Ramaswamy, S. Solomon, J. Srinivasan, D. Albritton, I. Isaksen, M. Lal, D. Wuebbles, Radiative Forcing of Climate Change, in *Climate Change 1995: The Science of Climate Change,* edited by J.T. Houghton et al., Cambridge University Press, pp. 65-131, 1996.

*In collaboration with other organizations

MANUSCRIPTS SUBMITTED FOR PUBLICATION

(tg) Oort, A.H., Angular Momentum Cycle in Planet Earth, Contribution to *The Encyclopedia of Planetary Sciences*, February 1993.

(wn) Miyakoda, K., A. Rosati, and R. Gudgel, ENSO Forecasting with a Coupled Model, Part I. The System, *Monthly Weather Review*, May 1994.

* (xf) Ezer, T., and G.L. Mellor, Data Assimilation in the Gulf Stream Region: How Useful are Satellite-Derived Surface Data for Nowcasting the Subsurface Fields?, *Journal of Atmospheric and Oceanic Technology*, August 1994.

(xr) Lanzante, J.R., Resistant, Robust and Nonparametric Techniques for the Analysis of Climate Data: Theory and Examples, Including Applications to Historical Radiosonde Station Data, *International Journal of Climatology*, October 1994.

(xt) Rosati, A., K. Miyakoda, and R. Gudgel, The Impact of Ocean Initial Conditions on ENSO Forecasting with a Coupled Model, *Monthly Weather Review*, October 1994.

* (yj) Lindberg, C., and A.J. Broccoli, Representation of Topography in Spectral Climate Models and its Effect on Simulated Precipitation, *Journal of Climate*, January 1995.

(ym) Delworth, T.L., S. Manabe, and R.J. Stouffer, Interannual to Interdecadal Variability in a Coupled Ocean-Atmosphere Model, *Proceedings of International Workshop on Numerical Prediction of Oceanic Conditions*, Tokyo, Japan, 7-11 March 1995.

* (yn) Chen, P., G.L. Mellor, Determination of Tidal Boundary Forcing using Tide Station Data, in *Coastal Ocean Prediction*, edited by C.N.K. Mooers, AGU Press, November 1955.

* (yq) Oort, A.H., and J.J. Yienger, Observed Long-term Variability in the Hadley Circulation and Its Connection to ENSO, *Journal of Climate*, February 1995.

(ys) Delworth, T.L., North Atlantic Interannual Variability in a Coupled Ocean-Atmosphere Model, *Journal of Climate*, March 1995.

(yz) Miyakoda, K., J. Ploshay, and A. Rosati, Preliminary Study on SST Forecast Skill Associated with El Niño Process, using Coupled Model Data Assimilation, *Atmosphere and Ocean Dynamics*, Canada, March 1995.

* (zb) Aikman, F., G.L. Mellor, T. Ezer, D. Sheinin, P. Chen, L. Breaker, K. Bosley, and D.B. Rao, Toward an Operational Nowcast/Forecast System for the U.S. East Coast, in *Modern Approaches to Data Assimilation in Ocean Modeling*, Elsevier Publishers, April 1995.

* (zd) Kasibhatla, P.S., W.L. Chameides, H. Levy II, and A. Klonecki, Large-Scale Impact of Photochemical Pollution on Boundary-Layer Ozone over the North Atlantic Ocean during Summer, *Science*, March 1995.

* (zj) Kasibhatla, P.S., H. Levy II, and A. Klonecki, A Three-dimensional View of the Large-Scale Tropospheric Ozone Distribution over the North Atlantic Ocean during the Summer, *Journal of Geophysical Research-Atmospheres*, May 1995.

* (zn) Ramaswamy, V., and C.-T. Chen, Climate Sensitivity to Greenhouse and Solar Radiative Perturbations, *Nature*, June 1995.

* (zp) Peixoto, J.P., and A.H. Oort, On the Climatology of Relative Humidity in the Atmosphere, *Journal of Climate*, June 1995.

* (zq) Armstrong, R.A., Structurally and Parametrically Congruent Tree-by-Tree and Landscape-Level Simulators of Forest Growth, *Ecology*, June 1995.

* (zr) Levy II, H., W.J. Moxim, and P.S. Kasibhatla, A Global Three-Dimensional Time-dependent Lightning Source of Tropospheric NO_x, *Journal of Geophysical Research*, June 1995.

*In collaboration with other organizations

(zs) Stern, W.F., Tropical Intraseasonal Variability in the GFDL/DERF GCM during AMIP, *Proceedings of AMIP Scientific Conference*, Monterey, CA, June 1995.

* (zu) Beegle, C.J., K.W. Dixon, and R.H. Gammon, The Chlorofluorocarbon Transient in the North Pacific: A Model-Observation Comparison, *Journal of Physical Oceanography*, July 1995.

(zv) Lanzante, J.R., Lag Relationships Involving Tropical Sea Surface Temperatures, *Journal of Climate*, July 1995.

(zy) Lau, N.-C., and M.J. Nath, The Role of the "Atmospheric Bridge" in Linking Tropical Pacific ENSO Events to Extratropical SST Anomalies, *Journal of Climate (Stan Hayes Special Issue)*, July 1995.

* (zz) Goswami, B.N., Internally Generated and Externally Forced Interannual Variations of Indian Summer Monsoon, *Journal of Climate*, August 1995.

* (ab) Chen, C.-T., E. Roeckner, and B.J. Soden, A Comparison of Satellite Observations and Model Simulations of Column Integrated Moisture and Upper Tropospheric Humidity, *Journal of Climate*, August 1995.

* (ad) Figueroa, H.A., and J.L. Sarmiento, Thermocline Ventilation in a North Atlantic General Circulation Model, *Journal of Geophysical Research*, August 1995.

* (ae) Wacongne, S., and R.C. Pacanowski, Seasonal Heat Transport in a Primitive Equation Model of the Tropical Indian Ocean, *Journal of Physical Oceanography*, August 1995.

* (af) Li, X., P. Chang, and R.C. Pacanowski, A Wave-Induced Mixing Mechanism in the Mid-depth Equatorial Ocean, *Journal of Marine Research*, August 1995.

* (ai) Balasubramanian, G., and S.T. Garner, The Role of Momentum Fluxes in Shaping the Lifecycle of a Baroclinic Wave, *Journal of the Atmospheric Sciences*, August 1995.

* (aj) Li, T., S.G.H. Philander, On the Annual Cycle of the Eastern Equatorial Pacific, *Journal of Climate*, August 1995.

* (ak) Philander, S.G.H., D. Gu, D. Halpern, G. Lambert, N.-C. Lau, T. Li, and R.C. Pacanowski, Why the ITCZ is Mostly North of the Equator, *Journal of Climate*, August 1995.

* (ao) Ramaswamy, V., and J. Li, A High-Spectral Resolution Investigation of Solar Radiative Effects in Vertically Inhomogeneous Low Clouds, *Quarterly Journal of the Royal Meteorological Society*, September 1995.

* (aq) Lee, S., and J.L. Anderson, A Simulation of Atmospheric Storm Tracks with a Forced Barotropic Model, *Journal of the Atmospheric Sciences*, September 1995.

(as) Gross, B.D., The Effect of Compressibility on Barotropic and Baroclinic Instability, *Journal of the Atmospheric Sciences*, September 1995.

* (au) Burpee, R.W., J.L. Franklin, S.J. Lord, R.E. Tuleya, and S.D. Aberson, The Impact of Omega Dropwindsondes on Operational Hurricane Track Forecast Models, *Bulletin of the American Meteorological Society*, September 1995.

* (av) Chen, C.-T., and V. Ramaswamy, Sensitivity of Simulated Global Climate to Perturbations in Low Cloud Microphysical Properties, Part II: Spatially Localized Perturbations, *Journal of Climate*, September 1995.

* (aw) Knutson, T.R., S. Manabe, and D. Gu, Simulated ENSO in a Global Coupled Ocean-Atmosphere Model: Multi-Decadal Amplitude Modulation and CO_2 Sensitivity, *Journal of Climate*, October 1995.

* (ay) Li, J., S.M. Freidenreich, and V. Ramaswamy, Solar Spectral Weight at Low Cloud Tops, *Journal of the Atmospheric Sciences*, October 1995.

*In collaboration with other organizations

(az) Hayashi, Y., and D.G. Golder, United Mechanisms for the Generation of Low- and High-Frequency Tropical Waves, Part I: Control Experiments with Moist Convective Adjustment, *Journal of the Atmospheric Sciences*, October 1995.

(ba) Hayashi, Y., and D.G. Golder, United Mechanisms for the Generation of Low- and High-Frequency Tropical Waves, Part II: Linear Instability Theory with a Partitional Scheme of Moist Convective Adjustment, *Journal of the Atmospheric Sciences*, October 1995.

* (bb) Miyakoda, K., J. Sirutis, A. Rosati, T.C. Gordon, R. Gudgel, W.F. Stern, J. Anderson, and A. Navarra, Atmospheric Model Parameterizations for Coupled Air-Sea Forecasts of ENSO, *Dynamics of Atmosphere and Oceans*, November 1995.

(bc) Sirutis, J., K. Miyakoda, and J. Lanzante, Eastward Propagation of Southern Oscillation Signals, *Journal of the Meteorological Society of Japan*, November 1995.

* (bd) Anderson, J.L., and V. Hubeny, A Reexamination of Methods for Evaluating the Predictability of the Atmosphere, *Journal of the Atmospheric Sciences*, November 1995.

* (bg) Winton, M., The Effect of Cold Climates upon North Atlantic Deep Water Formation in a Simple Ocean-Atmosphere Model, *Journal of Climate*, December 1995.

(bi) Williams, G.P., The Vertical Structure of Jupiter's Atmospheric Circulation, *Nature*, December 1995.

(bj) Held, I.M., Planetary Waves and Their Interaction with Smaller Scales, in *American Meteorological Society - University of Bergen*, based on Bergen Symposium on Extratropical Cyclones, January 1996.

* (bk) Numaguti, A., and Y. Hayashi, Gravity-Wave Dynamics of the Hierarchical Structure of Super Cloud Clusters, *Journal of the Atmospheric Sciences*, January 1996.

(bl) Bender, M.A., The Effect of Relative Flow on the Asymmetric Structure in the Interior of Hurricanes, *Journal of the Atmospheric Sciences*, January 1996.

* (bm) Treguier, A.M., I.M. Held, and V.D. Larichev, On the Parameterization of Quasi-Geostrophic Eddies in Primitive Equation Models, *Journal of Physical Oceanography*, January 1996.

* (bn) Gu, D., and S.G.H. Philander, A Theory for Interdecadal Climate Fluctuations, *Nature*, February 1996.

* (bo) Gu, D., S.G.H. Philander, and M.J. McPhaden, The Seasonal Cycle and Its Modulation in the Eastern Tropical Pacific Ocean, *Journal of Physical Oceanography*, February 1996.

* (bp) Hall, A., and S. Manabe, Can Stochastic Theory Explain Sea Surface Temperature and Salinity Variability? *Climate Dynamics*, February 1996.

* (bq) Chen, T.H., A. Henderson-Sellers, P.C.D. Milly, A.J. Pitman, A.C.M. Beljaars, J. Polcher, F. Abramopoulos, A. Boone, S. Chang, F. Chen, Y. Dai, C.E. Desborough, R.E. Dickinson, L. Dumenil, M. Ek, J.R. Garratt, N. Gedney, Y.M. Gusev, J. Kim, R. Koster, E.A. Kowalczyk, K. Laval, J. Lean, D. Lettenmaier, X.Z. Liang, J.F. Mahfouf, H.-T. Mengelkamp, K. Mitchell, O.N. Nasonova, J. Noilhan, A. Robock, C. Rosenzweig, J. Schaake, C.A. Schlosser, J.-P. Schulz, Y. Shao, A.B. Shmakin, D.L. Verseghy, P. Wetzel, E.F. Wood, Y. Xue, Z.-L. Yang, and Q. Zeng, Cabauw Experimental Results from the Project for Intercomparison of Land-surface Parameterization Schemes (PILPS), *Journal of Climate*, March 1996.

* (br) Gnanadesikan, A., A.J. Plueddemann, and R.A. Weller, Observational Evidence that Langmuir Cells are Driven by Wave-Current Interaction: Scaling the Time-Varying Near-Surface Shear, *Journal of Marine Research*, March 1996.

*In collaboration with other organizations

* (bs) Tuleya, R.E., and S.J. Lord, The Impact of Dropwindsonde Data on GFDL Hurricane Model Forecasts using Global Analyses, *Journal of Weather and Forecasting*, March 1996.

* (bt) Vitart, F., J.L. Anderson, W.F. Stern, Simulation of Interannual Variability of Tropical Storm Frequency in an Ensemble of GCM Integrations, *Journal of Climate*, March 1996.

* (bu) Nakamura, H., M. Nakamura, and J.L. Anderson, The Role of High- and Low-Frequency Dynamics in the Blocking Formation, *Monthly Weather Review*, April 1996.

* (bv) Winton, M., The Damping Effect of Bottom Topography on Internal Decadal-Scale Oscillations of the Thermohaline Circulation, *Journal of Physical Oceanography*, April 1996.

* (bw) Klein, S., Synoptic Variability of Low Cloud Properties and Meteorological Parameters in the Subtropical Trade Wind Boundary Layer, *Journal of Climate*, April 1996.

(bx) Lau, N.-C., Interactions Between Global SST Anomalies and the Midlatitude Atmospheric Circulation, *Bulletin of the American Meteorological Society*, April 1996.

* (by) Trenberth, K.E., G.W. Branstator, D. Karoly, A. Kumar, N.-C. Lau, and C. Ropelewski, Global Atmospheric Diagnostics and Modeling for TOGA, *Journal of Geophysical Research (Special TOGA Issue)*, April 1996.

(bz) Delworth, T.L., Interannual to Decadal Variability in the North Pacific of a Coupled Ocean-Atmosphere Model, *Proceedings of the JCESS/CLIVAR Workshop on Decadal Climate Variability*, Columbia, MD, 22-24 April 1996.

(ca) Anderson, J.L., The Impact of Dynamical Constraints on the Selection of Initial Conditions for Ensemble Predictions: Low-order Perfect Model Results, *Monthly Weather Review*, May 1996.

* (cb) Balasubramanian, G., and S.T. Garner, The Equilibration of Short Baroclinic Waves, *Journal of the Atmospheric Sciences*, May 1996.

(cc) Manabe, S., Early Development in the Study of Greenhouse Warming: The Emergence of Climate Models, *Ambio* (Special volume commemorating 100th year anniversary of the publication of "Arrhenius" paper on Greenhouse Warming), May 1996.

* (cd) Hallberg, R., Localized Coupling Between Surface and Bottom Intensified Flow Over Topography, *Journal of Physical Oceanography*, May 1996.

* (ce) Swanson, K.L., P.J. Kushner, and I.M. Held, Dynamics of Barotropic Storm Tracks, *Journal of the Atmospheric Sciences*, June 1996.

* (cf) Bryan, K., The Role of Mesoscale Eddies in the Poleward Transport of Heat by the Oceans, *Physica D.*, June 1996.

* (cg) Bryan, K., and S. Griffies, North Atlantic Climate Variability on Decadal Time-Scales: Is it Predictable? *Izvestia Atmospheric & Oceanic Physics*, June 1996.

(ch) Soden, B., Does the 1987 El Niño Provide Evidence of Negative Water Vapor Feedback? *Journal of Climate*, June 1996.

(ci) Anderson, J.L., Impacts of Dynamically Constrained Initial Conditions on Ensemble Forecasts, Reprints from the 11th Numerical Weather Prediction Conference, June 1996.

(cj) Stern, W.F., and J.L. Anderson, Interannual Variability of Tropical Intraseasonal Oscillations in the GFDL/DERF GCM Inferred From an Ensemble of AMIP Integrations, Reprints from the 11th Numerical Weather Prediction Conference, June 1996.

* (ck) Jones, P.W., K. Hamilton, and R.J. Wilson, A Very High-Resolution General Circulation Model Simulation of the Global Circulation in Austral Winter, *Journal of the Atmospheric Sciences*, June 1996.

*In collaboration with other organizations

(cl) Sirutis, J.J., and A. Rosati, The Impact of Cumulus Convection Parameterization in Coupled Air-Sea Models, Reprints from the 11th Numerical Weather Prediction Conference, June 1996.

* (cm) Griffies, S.M., and K. Bryan, Ensemble Predictability of Simulated North Atlantic Interdecadal Climate Variability, *Nature*, June 1996.

* (co) Ezer, T., and G.L. Mellor, Simulations of the Atlantic Ocean with a Sigma Coordinate Ocean Model, Part I. Model Setting and Climatology, *Journal of Geophysical Research*, March 1996.

* (cp) Ezer, T., and G.L. Mellor, Simulations of the Atlantic Ocean with a Sigma Coordinate Ocean Model, Part II: Interannual and Interdecadal Variabilities Associated with Variations in Observed Surface Temperatures and Winds, *Journal of Geophysical Research*, March 1996.

* (cq) Klein, S.A., Comments on "Moist Convective Velocity and Buoyancy Scales", *Journal of Atmospheric Sciences*, July 1996.

(cr) Hamilton, K., The Role of Parameterized Drag in a Troposphere-Stratosphere-Mesosphere General Circulation Model, in *Gravity Waves Processes and Their Parameterization in Global Climate Models*, Springer-Verlag, July 1996.

* (cs) Milly, P.C.D., The Reduction in Summer Soil Wetness Caused by Increased Atmospheric Carbon Dioxide: Sensitivity to Change in Plant Rooting Depth, *Nature*, August 1996.

* (ct) Hallberg, R., Stable Split Time Stepping Schemes for Large-Scale Ocean Modeling, *Journal of Computational Physics*, August 1996.

(cu) Broccoli, A.J., and S. Manabe, Mountains and Midlatitude Aridity, in *Global Tectonics and Climate Change*, August 1996.

* (cv) Ramaswamy, V., and C-T. Chen, Linear Additivity of Climate Response for Combined Albedo and Greenhouse Perturbations, *Geophysical Research Letters*, August 1996.

* (cw) Milly, P.C.D., Factors Determining the Partitioning of Precipitation into Evaporation and Runoff, in *Global Energy and Water Cycles*, edited by K. Browning and R. Gurney, August 1996.

* (cx) Jungclaus, J.H., and G.L. Mellor, A Three-Dimensional Model Study of the Mediterranean Outflow, *Journal of Marine Systems*, August 1996.

(cy) Kurihara, Y., R.E. Tuleya, and M.A. Bender, The GFDL Hurricane Prediction System and its Performance in the 1995 Hurricane Season, *Monthly Weather Review*, August 1996.

* (cz) Gnanadesikan, A., and E.A. Terray, Evidence for Wave-Stirred and Wall Layers in a Strongly Forced Mixed Layer, *Journal of Physical Oceanography*, August 1996.

(da) Manabe, S., and R.J. Stouffer, Simulation of Younger Dryas-like Phenomenon by a Coupled Ocean-Atmosphere Model, *Paleoceanography*, August 1996.

(db) Delworth, T.L., S. Manabe, and R.J. Stouffer, Multidecadal Climate Variability in the Nordic Seas and Surrounding Regions: A Coupled Model Simulation, *Geophysical Research Letters*, August 1996.

* (dd) Swanson, K.L., Downstream Development and the Dynamics of Nonlinear Baroclinic Wave Packets, *Journal of the Atmospheric Sciences*, August 1996.

* (de) Levy II, H., P.S. Kasibhatla, W.J. Moxim, A.A. Klonecki, A.I. Hirsch, S.J. Oltmans, and W.L. Chameides, The Human Impact on Global Tropospheric Ozone, *Geophysical Research Letters*, August 1996.

*In collaboration with other organizations

* (df) Gruber, N., J.L. Sarmiento, and T.F. Stocker, An Improved Method for Detecting Anthropogenic CO_2 in the Oceans, *Global Biogeochemical Cycles*, September 1996.

* (dg) Haywood, J.M., V. Ramaswamy, and L.J. Donner, The Effects of Sub-Grid Scale Variations in Relative Humidity and Cloud Upon the Direct Radiative Forcing of Sulfate Aerosol, *Geophysical Research Letters*, September, 1996.

* (dh) Sarmiento, J.L., and C. Le Quéré, Oceanic CO_2 Uptake in a Model of Century-Scale Global Warming, *Science*, September 1996.

* (di) Sabine, C.L., and R.M. Key, Controls on fCO_2 in the South Pacific, *Marine Chemistry*, September 1996.

* (dj) Key, R.M., WOCE Pacific Ocean Radiocarbon Program, *Radiocarbon*, September 1996.

* (dk) Key, R.M., and P.D. Quay, WOCE AMS Radiocarbon I: Pacific Ocean Results: P6, P16, and P17, *Radiocarbon*, September 1996.

* (dl) Stuiver, M., G. Ostlund, R.M. Key, and P.J. Reimer, Large Volume WOCE Radiocarbon Sampling in the Pacific Ocean, *Radiocarbon*, September 1996.

* (dm) Peng, T.-H., R.M. Key, and H.G. Ostlund, Temporal Variations of Bomb Radiocarbon Inventory in the Pacific Ocean, *Marine Chemistry*, September 1996.

* (dn) Broecker, W.S., S. Peacock, S. Walker, R. Weiss, C. Heinze, U. Mikolajewicz, E. Fahrbach, M. Schroeder, R. Key, T.-H. Peng, T. Takahashi, and S. Rubin, How Much Deep Water is formed in the Southern Ocean? Ewing Symposium Monograph, September 1996.

(do) Schwarzkopf, M.D., and V. Ramaswamy, Stratospheric Climatic Effects due to CH_4, N_2O, CFCs, and the H_2O Infrared Continuum: A GCM Experiment, *International Radiation Symposium*, Fairbanks, Alaska, August 1996.

(dp) Donner, L.J., C.J. Seman, and J.P Sheldon, Cloud-Radiative Interactions in High-Resolution Cloud-Resolving Models, *International Radiation Symposium*, Fairbanks, Alaska, August 1996.

(dq) Donner, L.J., C.J. Seman, R.S. Hemler, and J.P. Sheldon, Radiative Transfer in a Three-Dimensional Cloud-System-Resolving Model, *International Radiation Symposium*, Fairbanks, Alaska, August 1996.

*In collaboration with other organizations

BIBLIOGRAPHY
1993-1996
CROSS REFERENCE BY AUTHOR

*In collaboration with other organizations

*In collaboration with other organizations

DELWORTH, T.L.	(1145),(1182),(1196),(1312),(ym),(ys),(bz),(db),
DeMAJISTRE, R.	(1395),
DERWENT, R.	(1405),
DESBOROUGH, C.E.	(bq),
DICKINSON, R.E.	(bq),
DIX, M.	(1233),(1302),
DIXON, K.W.	(1380),(zu),
DONNER, L.J.	(1133),(1218),(1234),(1247),(1297),(1349),(dg),(dp),(dq),
DUCKLOW, H.W.	(1155),(1166),
DUFFY, A.	(1132),(1181),
DUMENIL, L.	(bq),
DUNNE, K.A.	(1227),(1396),
EHHALT, D.	(1405),
EK, M.	(bq),
EMANUEL, K.A.	(1284),(1285),
ENTING, I.	(1405),
EVANS, G.T.	(1155),
EZER, T.	(1160),(1248),(1249),(1250),(1251),(1291),(1327),(1373),(1374),(xf),(zb),(co),(cp),
FAHRBACH, E.	(dn),
FASHAM, M.J.R.	(1155),(1166),(1175),
FEELY, R.A.	(1135),
FELIKS, Y.	(1228),(1387),
FERRARE, R.A.	(1263),
FIGUEROA, H.A.	(ad),
FINK, R.	(1399),
FOUQUART, Y.	(1303),(1405),
FRANKLIN, J.L.	(1283),(au),
FRASER, P.	(1405),
FREIDENREICH, S.M.	(1136),(1331),(ay),
FREY, R.A.	(1360),
FU, R.	(1338),
GALIN, V.	(1233),(1302),
GALLOWAY, J.N.	(1243),(1335),

*In collaboration with other organizations

*In collaboration with other organizations

*In collaboration with other organizations

*In collaboration with other organizations

*In collaboration with other organizations

*In collaboration with other organizations

OORT, A.H.	(1124),(1209),(1210),(1223),(1230),(1270), (1326),(1350),(1357),(1384),(1397),(tg), (yq),(zp),
ORLANSKI, I.	(1116),(1125),(1177),(1200),(1237),(1310), (1345),
ORR, J.C.	(1143),
OSTLUND, G.	(dl),(dm),
OVERLAND, J.E.	(1357),
PACALA, S.W.	(1288),
PACANOWSKI, R.C.	(1375),(ae),(af),(ak),
PAVAN, V.	(1205),(1369),
PEACOCK, S.	(dn),
PEIXOTO, J.P.	(1209),(1210),(1223),(zp),
PENG, T.-H.	(dm),(dn),
PENNER, J.E.	(1350),(1384),
PERLISKI, L.	(1395),
PETERSON, L.C.	(1132),(1181),
PHILANDER,S.G.H.	(1159),(1208),(1229),(1252),(1264),(1293), (1325),(aj),(ak),(bn),(bo),
PHILLIPPS, P.J.	(1138),(1231),
PIERREHUMBERT, R.T.	(1279),(1290),
PINARDI, N.	(1375),
PINTO, J.P.	(1193),
PISIAS, N.G.	(1132),(1181),
PITMAN, A.J.	(bq),
PLANTON, S.	(1233),(1302),
PLOSHAY, J.	(1119),(yz),
PLUEDDEMANN, A.J.	(br),
POLCHER, J.	(bq),
POTTER, G.L.	(1271),
PRATHER, M.	(1405),
PRELL, W.L.	(1132),(1181),
PROSPERO, J.M.	(1130),
QUAY, P.D.	(dk),

*In collaboration with other organizations

RAMASWAMY, V.	(1122),(1136),(1171),(1183),(1212),(1230), (1260),(1303),(1304),(1324),(1331),(1334), (1336),(1350)(1364),(1381),(1384),(1394),(1404), (1405),(zn),(ao),(av),(ay),(cv),(dg),(do),
RANDALL, D.A.	(1271),(1302),
RANDEL, W.J.	(1394),
RAO, D.B.	(zb),
RAVAL, A.	(1230),(1397),
RAYMO, M.E.	(1132),(1181),
RAYNAUD, D.	(1405),
REIMER, P.J.	(dl),
RIKUS, L.	(1271),
ROBINSON, A.R.	(1291),
ROBOCK, A.	(1378),(bq),
RODHE, H.	(1405),
ROECKNER, E.	(1271),(1334),(ab),
ROPELEWSKI, C.	(by),
ROSATI, A.	(1308),(1375),(1403),(wn),(xt),(yz),(bb),(cl),
ROSENZWEIG, C.	(bq),
ROSS, R.J.	(1139),(1140),(1147),(1148),(1191),(1281), (1329),
ROYER, J.F.	(1271),
RUBIN, S.	(dn),
SABINE, C.L.	(di),
SADASIVAN, S.	(1405),
SAMUELS, B.	(1156),(1157),(1313),(1315),(1387),
SANHUEZA, E.	(1405),
SANTER, B.D.	(1350),(1384),
SARMIENTO, J.L.	(1142),(1143)(1155),(1165),(1166),(1173),(1174), (1175),(1206),(1235),(1236),(1288),(1294), (1317),(1318),(1319),(1320),(1398),(1399),(ad), (df),(dh),
SAVOIE, D.L.	(1130),
SCANLON, B.R.	(1254),
SCHAAKE, J.	(bq),
SCHIMEL, D.	(1405),
SCHLESE, U.	(1271),

*In collaboration with other organizations

*In collaboration with other organizations

*In collaboration with other organizations

*In collaboration with other organizations

APPENDIX C

Seminars Given at GFDL

During Fiscal Year 1996

3 October 1995	Dynamics of Super Cloud Clusters Simulated in a Simple Two-Dimensional Model, by Dr. Atusi Numaguti, Atmospheric and Oceanic Sciences Program, Princeton University, Princeton, NJ and Dr. Yoshikazu Hayashi, Geophysical Fluid Dynamics Laboratory, Princeton, NJ
3 October 1995	Analytical Theory and Numerical Experiments for Forcing of Flow at Isolated Topographic Feature, by Dr. Martin Schmidt, Warnemuende, Germany
5 October 1995	The Mesoscale Variability of Nutrients and Plankton as Seen in a Coupled Model of the Southwestern Baltic, by Dr. Thomas Neumann, Institute of Ostseeforschung Rostock, Germany
12 October 1995	Ensemble Forecasting at NCEP (formerly NMC) and the Breeding Method, by Dr. Zoltan Toth, National Center for Environmental Prediction, Washington, DC
17 October 1995	Parameterizing Mesoscale Ocean Eddies, by Dr. Kirk Bryan, Atmospheric and Oceanic Sciences, Princeton University, Princeton, NJ
18 October 1995	Interannual Variability in an Ensemble of AMIP Climate Simulations Conducted with the Canadian Climate Centre GCM2, by Dr. Francis Zwiers, Canadian Centre for Climate Modeling and Analysis, University of Victoria, Victoria, BC Canada
19 October 1995	Hydrostatic Adjustment, by Prof. Peter Bannon, Department of Meteorology, Pennsylvania State University, University Park, PA
24 October 1995	The Temperature of the Glacial Ocean: New Solutions, by Daniel Schrag, Geological and Geophysical Sciences, Princeton University, Princeton, NJ
26 October 1995	Paleotropical SST's at Barbados: Rates of Change and Implications, by Dr. Thomas Guilderson, Lamont-Doherty Earth Observatory, Palisades, NY
31 October 1995	Seasonal and Interannual Variability in the Eastern Tropical Pacific Ocean, by Dr. Daifang Gu and Dr. S.G.H. Philander, Atmospheric and Oceanic Sciences, Princeton University, Princeton, NJ
13 November 1995	Warm Pool, Cold Tongue and the Walker Circulation: A Coupled View, by Dr. Zheng-yu Liu, University of Wisconsin, Madison, WI
14 November 1995	Ocean Convection and Its Parameterization, by Dr. John Marshall, Department of Earth, Atmosphere and Planetary Sciences, Massachusetts Institute of Technology, Cambridge, MA
17 November 1995	The Emergence of Jets and Vortices in Freely Evolving Shallow-Water Turbulent Flows, by Dr. Lorenzo M. Polvani, Department of Applied Physics, Columbia University, New York, NY
21 November 1995	The Mediterranean: A Place to Test Models, by Prof. George Mellor, Atmospheric and Oceanic Sciences, Princeton University, Princeton, NJ

28 November 1995	Atlantic Ocean Simulations with a Sigma-Coordinate Ocean Model, by Dr. Tal Ezer, Atmospheric and Oceanic Sciences, Princeton University, Princeton, NJ
30 November 1995	The Thermohaline Circulation and Coupled Models, by Dr. Andrew Weaver, School of Earth and Ocean Sciences, University of Victoria, Victoria, BC, Canada
5 December 1995	Simulated ENSO in a Global Coupled Ocean-Atmosphere Model: Multi-decadal Amplitude Modulation and CO_2 Sensitivity, by Mr. Thomas Knutson, Geophysical Fluid Dynamics Laboratory, Princeton, NJ
7 December 1995	Long-Term Changes in Two Difficult-to-Assess Greenhouse Gases: Stratospheric Water Vapor and Tropospheric Ozone, by Dr. Samuel Oltmans, Climate Monitoring and Diagnostics Laboratory, Environmental Research Laboratory/NOAA, Boulder, CO
13 December 1995	Climate Sensitivity and Variability: Studies Using an Ocean-Atmosphere Model of Intermediate Degree of Complexity, by Dr. R. Saravanan, National Center for Atmospheric Research, Boulder, CO
18 December 1995	The Diagnostic and Prognostic Experiments of the World Ocean Circulation and Water Masses, by Dr. Shinzou Fujio, Ocean Research Institute, University of Tokyo, Tokyo, Japan
19 December 1995	ZETANG: A New Nonhydrostatic, Compressible Model in Terrain-Following Coordinates, by Dr. Brian Gross, Geophysical Fluid Dynamics Laboratory, Princeton, NJ
5 January 1996	The Use of Tracers to Determine Chemical Change in the Atmosphere: Examples from the Antarctic Spring and the Aftermath of Pinatubo, by Dr. Loretta Mickley, University of Chicago, Chicago, IL
11 January 1996	A Contour-Advective Semi-Lagrangian Numerical Algorithm for Simulating Fine-Scale Conservative Dynamical Fields, by Dr. David Dritschel, Cambridge University, Cambridge, England
11 January 1996	Catastrophic Rainfall from an Upslope Thunderstorm in the Central Appalachians: The Rapidan Storm of June 27, 1995, by Dr. James A. Smith, Department of Civil Engineering, Princeton University, Princeton, NJ
16 January 1996	Annual and Semi-annual Variations of the Indonesian Throughflow, by Dr. Toshio Yamagata, University of Tokyo, Tokyo, Japan
17 January 1996	Seasonal Transport Variations of the Kuroshio, by Dr. Toshio Yamagata, University of Tokyo, Tokyo, Japan
18 January 1996	Interdecadal Variability in a Hierarchy of Coupled Ocean/Atmosphere/Sea-Ice Models, by Dr. Fei Chen, Center for Ocean-Land-Atmosphere Studies, Calverton, MD

30 January 1996	Marine Boundary Layer Clouds - Recent Research and Implications for Parameterization, by Dr. Steven Klein, Atmospheric and Oceanic Sciences Program, Princeton University, Princeton, NJ
2 February 1996	Interaction of Dust and Rain in the Eastern Mediterranean, by Prof. Zev Levin, Tel Aviv University, Tel Aviv, Israel
2 February 1996	Inferring Meridional Mass and Heat Transports in the Indian Ocean by Combining a General Circulation Model with Climatological Data, by Dr. Jochem Marotzke, Massachusetts Institute of Technology, Cambridge, MA
5 February 1996	Global and Regional Variability in a Coupled AOGCM, by Dr. Simon Tett, Hadley Centre, London, United Kingdom
6 February 1996	The Radiative Forcing of Tropospheric Sulfate and Soot Aerosol, by Dr. James Haywood, Atmospheric and Oceanic Sciences Program, Princeton University, Princeton, NJ
7 February 1996	Modification of the Thermodynamic Structure of the Lower Troposphere by the Evaporation of Precipitation: A GEWI Cloud System Study, by Dr. Jack Katzfey, CSIRO, Aspendale, Australia
8 February 1996	The Influence of Land Surface Processes on Precipitation Variability, by Dr. Randy Koster, NASA Goddard Space Flight Center, Greenbelt, MD
13 February 1996	A Delayed Oscillator of Interdecadal Climate Fluctuations, by Dr. Daifang Gu and Dr. George Philander, Atmospheric and Oceanic Sciences Program, Princeton University, Princeton, NJ
15 February 1996	Middle Atmosphere Processes as Seen in UARS, by Dr. Marvin A. Geller, State University of New York, Stony Brook, NY
20 February 1996	An Investigation into the Cloud Absorption Anomaly Problem, by Dr. Jiangnan Li, Atmospheric and Oceanic Sciences Program, Princeton University, Princeton, NJ
21 February 1996	Towards Understanding Gulf Stream Meanders, by Prof. Randolph Watts, University of Rhode Island, Providence, RI
22 February 1996	Applications of Cloud Ensemble Simulation to Cloud Parameterizations, by Dr. Kuan-Man Xu, Colorado State University, Fort Collins, CO
23 February 1996	Moist Convective Velocity and Buoyancy Scales: Theory, Observations, and Implications for Tropical Dynamics, by Dr. Kerry Emanuel, Massachusetts Institute of Technology, Cambridge, MA
27 February 1996	Impact of Dynamical Constraints on Ensemble Prediction, by Dr. Jeffrey Anderson, Geophysical Fluid Dynamics Laboratory, Princeton, NJ
28 February 1996	Some Theoretical Hints about the Ocean's Overturning, by Remi Tailleux, Laboratorie de Modelisation, du Climat et de l'Environment, Saclay, France

5 March 1996	A Preliminary Study on Effective Linear Operators from the 100,000-day GFDL R15L9 GCM Perpetual January Integration, by Dr. Zuojun Zhang, Atmospheric and Oceanic Sciences Program, Princeton University, Princeton, NJ
7 March 1996	Composition and Chemistry of Polar Stratospheric Clouds: Impact on Ozone, by Dr. Margaret Tolbert, University of Colorado, Boulder, CO
14 March 1996	Radiating Instability of Non-zonal Ocean Currents, by Mr. Igor Kamenkovich, Massachusetts Institute of Technology, Cambridge, MA
15 March 1996	Rotating Convection Driven by Differential Bottom Heating and its Application, by Dr. Young-Gyu Park, Woods Hole Oceanographic Institute, Woods Hole, MA
18 March 1996	Are There Natural Bounds on the Earth's Temperature?, by Dr. Hsien-Wang Ou, Lamont-Doherty Earth Observatory, Palisades, NY
18 March 1996	Moisture Sinks/Sources Over the Mediterranean and Arabia-Iraqi Desert, by Prof. Pinhas Alpert, Data Assimilation Office, NASA/Goddard Space Flight Center, Greenbelt, MD
19 March 1995	Sources and Sinks of Mechanical Energy in the Ocean, by Dr. J.R. Toggweiler and Ms. Bonnie Samuels, Geophysical Fluid Dynamics Laboratory, Princeton, NJ
20 March 1996	Water Cycles in Major River Basins of Globe Estimated by Atmospheric Water Balance and GCM, by Dr. Taikan Oki, NASA/Goddard Space Flight Center, Greenbelt, MD
21 March 1996	Mechanisms of Mesoscale Organization of Deep Tropical Convection, by Mr. Venkatramani Balaji, York University, Ontario, Canada
22 March 1996	Tropical Cyclone Intensity Forecasting, by Dr. Mark DeMaria, Tropical Prediction Center, National Hurricane Center, Miami, FL
25 March 1996	Simulation of Interannual Variability of Tropical Storm Frequency in an Ensemble of GCM Integrations, by Frederic Vitart, Atmospheric and Oceanic Sciences Program, Princeton University, Princeton, NJ
26 March 1996	Wind-Driven Circulation in Ocean Basins with Isopycnals Intersecting the Sloping Bottom, by Dr. Robert Hallberg, Atmospheric and Oceanic Sciences Program, Princeton University, Princeton, NJ
28 March 1996	Variational Data Assimilation Using Models with Variable Nonlinearity, by Dr. Tomislava Vukicevic, National Center for Atmospheric Research (UCAR), Boulder, CO
28 March 1996	Continental Ice Sheet Mass Balances as Derived from GCM Climate Simulations, by David Baker, Atmospheric and Oceanic Sciences Program, Princeton University, Princeton, NJ

29 March 1996	Dynamics of the Antarctic Circumpolar Current: Results from a Q-G Two-Layer Model, by Shuo Chen, Atmospheric and Oceanic Sciences Program, Princeton University, Princeton, NJ
29 March 1996	Broadcast Meteorology: Experiences in Radio and Television, by Alan Kasper, WBUD-AM, WKXW-FM, Ewing, NJ
1 April 1996	Interdecadal Modulation of the ENSO Signal: Regions of Subtropical Subduction, by Scott Harper, Atmospheric and Oceanic Sciences Program, Princeton University, Princeton, NJ
4 April 1996	The Seasonal Cycle of Transport in the Lower Stratosphere, by Dr. Karen H. Rosenlof, NOAA Aeronomy Laboratory, Boulder, CO
9 April 1996	Some Issues on the Extratropical Response to El Niño in NCEP GCM, by Dr. Peitao Peng, Atmospheric and Oceanic Sciences Program, Princeton University, Princeton, NJ
11 April 1996	Coupling Chemistry and Climate in the NCAR Climate Model, by Dr. Philip Rasch, National Center for Atmospheric Research, Climate and Global Dynamics Division, Boulder, CO
16 April 1996	The ACC and the Ocean's Thermal Structure, by Dr. J.R. Toggweiler, Ms. B. Samuels, and Mr. M. Harrison, Geophysical Fluid Dynamics Laboratory, Princeton, NJ
18 April 1996	Small-Scale Processes in the Ocean and Their Parameterization, by Dr. Christopher Garrett, University of Victoria, Victoria, BC Canada
19 April 1996	Forcing Mid-Latitude Humidity by Tropical Deep Convection, by Dr. Rong Fu, University of Arizona, Tucson, AZ
23 April 1996	Simulation of Tropical Temperatures During the Last Ice Age, by Mr. Anthony Broccoli, Geophysical Fluid Dynamics Laboratory, Princeton, NJ
25 April 1996	A Mechanism for Decadal Climate Variability, by Dr. Mojib Latif, Max Planck Institute for Meteorology, Hamburg, Germany
30 April 1996	Satellite Remote Sensing of Energy Transfer Processes in the Arctic, by Ms. Jennifer Francis, Rutgers University, New Brunswick, NJ
2 May 1996	Available Potential Energy in the Ocean, by Dr. Rui Xin Huang, Woods Hole Oceanographic Institute, Woods Hole, MA
7 May 1996	Parameterizing Baroclinic Eddies in Large-Scale Ocean Models, by Dr. Isaac Held, Geophysical Fluid Dynamics Laboratory, Princeton, NJ
14 May 1996	Estimating Wind from Time-Lapsed Satellite Imagery: Method and Applications, by Dr. Brian Soden, Geophysical Fluid Dynamics Laboratory, Princeton, NJ

21 May 1996	A Proposal to "Strengthen the U.S. National Climate Modeling Effort," by Dr. Jerry Mahlman, Geophysical Fluid Dynamics Laboratory, Princeton, NJ
21 May 1996	Testing the Gent-McWilliams Parameterization in a Global Eddy-Resolving Model, by Dr. Richard D. Smith, Theoretical Division, Los Alamos National Laboratory, Los Alamos, NM
22 May 1996	Ensemble Forecasting of Hurricane Tracks, by Sim Aberson, HRD Atlantic Oceanographic and Meteorological Laboratory, Miami, FL
28 May 1996	Isopycnal Ocean Model at Greenbelt, by Dr. Paul Schopf, Goddard Space Flight Center, Greenbelt, MD
30 May 1996	The Application of Canonical Correlation Analysis to Seasonal Climate Forecasting, by Anthony Barnston, Climate Prediction Center, National Center for Environmental Prediction, Washington, DC
31 May 1996	Seasonal Variability in UARS and CLAES N_2O, by Dr. Noboru Nakamura, University of Chicago, Chicago, IL
4 June 1996	The Development of the Adjoint for a Model with Moist Physics, by Kevin Raeder, National Center for Atmospheric Research, Boulder, CO
6 June 1996	Strong Asymmetry in Rotating Flows, by Dr. Vladimir Vladimirov, The Hong Kong University of Science and Technology, Hong Kong
17 June 1996	ENSO-like Decade-to-Century Scale Variability, by Prof. John M. Wallace, Joint Institute for the Study of the Atmosphere and Ocean, University of Washington, Seattle, WA
21 June 1996	Deep Water Renewal in Lake Baikal, by Prof. D. Imboden, Swiss Federal Institute of Technology, Zurich, Switzerland
2 July 1996	Problems in Mesoscale Data Assimilation, by Dr. Qin Xu, University of Oklahoma, Norman, OK
3 July 1996	Decadal Variability in the Tropical Atlantic, by Dr. Ping Chang, Texas A & M University, College Station, TX
8 July 1996	Can Poleward Oceanic Heat Flux Explain the Warm Cretaceous Climate?, by Dr. Laurence Mysak, Centre for Climate and Global Change Research, Montreal, Canada
10 July 1996	Gas-To-Particle Conversion of Tropospheric Sulfur, by Dr. Constantin Andronache, Georgia Institute of Technology, Atlanta, GA
22 July 1996	Glacial Cooling: Is Water Vapor the Villain?, by Prof. Wallace S. Broecker, Lamont-Doherty Earth Observatory, Palisades, NY
23 July 1996	Tropical Intraseasonal Oscillations in the GFDL/DERF GCM, by Mr. William Stern, Geophysical Fluid Dynamics Laboratory, Princeton, NJ

23 July 1996	On the Entrainment Instability of the Stratocumulus, by Prof. Hung-Chi Kuo, National Taiwan University, Taipei, Taiwan
30 July 1996	The Impacts of Cumulus Convection Parameterizations and Specified Marine Stratus Clouds on Coupled Model Integrations, by Mr. J. Sirutis and Dr. Tony Gordon, Geophysical Fluid Dynamics Laboratory, Princeton, NJ
1 August 1996	A Prognostic Closure for Cumulus Parameterization, by Dr. Dzong-Ming Pan, Department of Atmospheric Science, Colorado State University, Fort Collins, CO
5 August 1996	Forcings and Chaos in Interannual to Decadal Climate Change, by Dr. James Hansen, Goddard Institute for Space Studies, New York, NY
6 August 1996	On the Proximity of Present-Day Climate to an Instability Threshold, by Dr. Eli Tziperman, Dr. Steve Griffies, and Mr. Ronald Stouffer, Geophysical Fluid Dynamics Laboratory, Princeton, NJ
9 August 1996	Absorption and Solar Radiative Forcing in Cloudy Atmospheres, by Dr. Harshvardhan, Department of Earth and Atmospheric Sciences, Purdue University, West Lafayette, IN
13 August 1996	The Impact of Specified Marine Stratus Clouds on Coupled Model Integrations, by Dr. Tony Gordon, Geophysical Fluid Dynamics Laboratory, Princeton, NJ
19 August 1996	Dynamics of Wintertime Stratospheric Transport in the SKYHI Model, by Dr. Janusz Eluszkiewicz, Massachusetts Institute of Technology, Cambridge, MA
22 August 1996	Forced and Free CO_2 Variations as the Basis for a Unified Dynamical Model of Pleistocene and Pre-pleistocene Climatic Change, by Prof. Barry Saltzman, Department of Geology and Geophysics, Yale University, Newhaven, CT
29 August 1996	Optimal Perturbations and the Onset of Weather Regimes, by Mr. Jeroen Oortwijn, Royal Netherlands Meteorological Institute, De Bilt, The Netherlands
29 August 1996	Empirical Normal Model Analysis of Gravity Waves in the SKYHI Model, by Martin Charron, McGill University, Montreal, Canada
3 September 1996	Anticyclonic and Cyclonic Baroclinic Waves: Part II: Short Waves, by Drs. G. Balasubramanian and Stephen Garner, Geophysical Fluid Dynamics Laboratory, Princeton, NJ
10 September 1996	Human Impact on Tropospheric Ozone, by Dr. Hiram Levy II, Geophysical Fluid Dynamics Laboratory, Princeton, NJ
24 September 1996	Tropical-Extratropical Climate Fluctuations, by Prof. George Philander et al., Princeton University, Princeton, NJ
30 September 1996	The Potential of Isopycnal Models in Ocean Modeling, by Dr. Dingming Hu, Department of Atmospheric Sciences, University of Washington, Seattle, WA

APPENDIX D

Talks, Seminars, and Papers Presented Outside GFDL

During Fiscal Year 1996

3 October 1995	Mr. Anthony J. Broccoli "Simulation of Tropical Temperatures at the Last Glacial Maximum", Paleoclimate Model Intercomparison Project Workshop, Colognes La Rouge, France
4 October 1995	Dr. Jerry D. Mahlman "A High-Resolution SKYHI Experiment on the CM5", DOE CHAMMP Annual Science Team Meeting, Rockville, MD
4 October 1995	Dr. Isaac M. Held "Geostrophic Turbulence and Baroclinic Instability", Courant Institute, New York University, New York, NY
13 October 1995	Dr. Abraham H. Oort "Long-term Variability in Hadley Circulation and Convection with ENSO", University of Utrecht, Utrecht, The Netherlands
13 October 1995	Dr. Syukuro Manabe "The Role of Oceans and Continental Surfaces in Climate Variability and Its Implication for the Detection of Global Warming", NASA/Goddard Scientific Colloquia, Greenbelt, MD
17 October 1995	Mr. Keith W. Dixon "CFC's as Greenhouse Heat Analogues in Coupled Climate Models", Maurice Ewing Symposium on Applications of Trace Substance Measurements to Oceanographic Problems, Oracle, AZ
17 October 1995	Dr. Jerry D. Mahlman "The State of Climate Science: Predictions and Uncertainties", Meeting of the "Roundtable" on North American Energy Policy, Montreal, Canada
17 October 1995	Dr. John R. Toggweiler "Why is the Deep Water Around Antarctica so Old?", Maurice Ewing Symposium on Applications of Trace Substance Measurements to Oceanographic Problems, Oracle, AZ
18 October 1995	Dr. V. Ramaswamy "Stratospheric Temperature Trends Project", Stratospheric Processes and their Role in Climate (SPARC) Meeting, Geneva, Switzerland
18 October 1995	Dr. Jeffrey L. Anderson "Verification of Seasonal Forecasts from Ensemble GCM Integrations", University of Utah, Salt Lake City, UT
23 October 1995	Dr. Abraham H. Oort "New Results on the Hydrology of the North African Desert Based on the NMC Re-Analyses", Climate Diagnostics Workshop, Seattle, WA
24 October 1995	Dr. Leo J. Donner "Cumulus Parameterizations and Cloud Microphysics in General Circulation Models: Observational Requirements for Development and Validation", Cloud Modeling and Measurement Workshop, Boulder, CO

24 October 1995	Dr. Bruce Ross "Status/Accomplishments of the Advanced Computing Panel", NOAA HPCC/ NII Council Meeting, Silver Spring, MD
30 October 1995	Dr. V. Ramaswamy "IPCC Overview of Aerosol Forcing", Aerosol Interdisciplinary Program Meeting, Columbia, MD
2 November 1995	Dr. John R. Toggweiler "Anthropogenic CO_2: The Natural Carbon Cycle Reclaims Center Stage", Frontiers of Science Meeting sponsored by The National Academy of Science, Irvine, CA
2 November 1995	Dr. Jerry D. Mahlman "Report of the Mission to Planet Earth Science Advisory Committee", NASA Advisory Council Meeting, NASA/Ames Research Center, Mountain View, CA
8 November 1995	Dr. Syukuro Manabe "The Role of Thermohaline Circulation in Abrupt Climate Change", Wadati Conference on Global Change and Polar Climate, Tsukuba, Japan
14 November 1995	Dr. Isidoro Orlanski "Stages in the Energetics of Baroclinic Systems", CIMA, Buenos Aires, Argentina
15 November 1995	Dr. Syukuro Manabe "The Role of Thermohaline Circulation in Abrupt Climate Change", Hokkaido University, Sapporo, Japan
16 November 1995	Dr. Jerry D. Mahlman "Uncertainties in Climate Change Modeling", House of Representatives Committee on Science Hearing on Climate Models and Projections of Potential Impacts of Global Climate Change, Washington, DC
16 November 1995	Dr. Isaac M. Held "New Perspectives on Storm Track Dynamics", University of Maryland, College Park, MD
29 November 1995	Dr. Kevin P. Hamilton "Theory of the Quasibiennial Oscillation", Courant Institute, New York University, New York, NY
4 December 1995	Mr. Ronald J. Stouffer "Role of the Oceans in Variability on Long Time Scales", Workshop on Dynamics and Statistics of Secular Climate Variations, Trieste, Italy
4 December 1995	Dr. Jerry Mahlman "Global Warming in the Public Eye", PEI Faculty Research Conference on Environmental Science and Engineering, Princeton University, Princeton, NJ
6 December 1995	Dr. V. Ramaswamy "Aerosols and Climate", IGAC Meeting, Fairfax, VA

7 December 1995	Dr. Leo J. Donner "Cumulus Convection and Cirrus Clouds in General Circulation Models and the Atmosphere", Pennsylvania State University, State College, PA
10 December 1995	Mr. Thomas R. Knutson "Simulated ENSO in a Global Coupled Ocean-Atmosphere Model: Multi-Decadal Amplitude Modulation and CO_2 Sensitivity", American Geophysical Union Fall Meeting, San Francisco, CA
11 December 1995	Mr. Anthony J. Broccoli "Simulation of Tropical Temperatures at the Last Glacial Maximum", American Geophysical Union Fall Meeting, San Francisco, CA
11 December 1995	Dr. Jerry D. Mahlman "Hurricane Prediction: From Tomorrow to 2100", U.S. House of Representatives, Washington, DC
12 December 1995	Dr. Syukuro Manabe "The Interaction Between Thermohaline Circulation and Climate as Simulated by a Coupled Ocean-Atmosphere Model", American Geophysical Union Fall Meeting, San Francisco, CA
12 December 1995	Dr. Brian J. Soden "How Well Can We Monitor Upper Tropospheric Water Vapor?: An Assessment of Satellite and Radiosonde Climatologies", American Geophysical Union Fall Meeting, San Francisco, CA
12 December 1995	Mr. Anthony J. Rosati 1. "A Combined XBT and Altimetry Global Ocean Assimilation System", and 2. "A Coupled B-grid Atmosphere and Ocean Model", American Geophysical Union Fall Meeting, San Francisco, CA
18 December 1995	Dr. V. Ramaswamy "A GCM Simulation of the Effects due to Lower Stratospheric Ozone Loss", Stratospheric Temperature Trends Assessment Meeting, Berlin, Germany
17 January 1996	Dr. V. Ramaswamy "SAGE III-Related Research Performed in 1995", SAGE III Science Team Meeting, Hampton, VA
23 January 1996	Dr. Syukuro Manabe "Role of Thermohaline Circulation in Climate", Geophysical Institute, University of Tokyo, Tokyo, Japan
29 January 1996	Dr. V. Ramaswamy "Climate Forcing", American Meteorological Society Annual Meeting - Global Climate Session, Atlanta, GA

12 February 1996	Dr. John R. Toggweiler 1. "Why is the Deep Water Around Antarctica so Old?", 2. "Dissolved Organic Matter in Marine Systems: Changing Paradigms from a Modeling Perspective", American Geophysical Union Ocean Sciences Meeting, San Diego, CA
23 February 1996	Dr. Jerry Mahlman "Anticipating Global Climate Changes", The Habitability of the Earth Sessions, Princeton University, Princeton, NJ
23 February 1996	Dr. Syukuro Manabe "Natural and Anthropogenic Change of Climate Simulated by a Coupled Ocean-Atmosphere Model", Center for Climate and Global Change, McGill University, Montreal, Canada
26 February 1996	Dr. Leo J. Donner 1. "GCM Cirrus Experiments", 2. "Convection, Anvil Development and Radiation in a Three-Dimensional Cloud System Model", C4 Science Team Meeting, National Center for Atmospheric Research, Boulder, CO
27 February 1996	Mr. Anthony Rosati 1. "Initialization of Coupled Forecast Models", and 2. "Overview of GFDL Seasonal/Interannual Project", WMO-CLIVAR-NEG Meeting, Montego Bay, Jamaica
27 February 1996	Dr. Jerry D. Mahlman "Toward Improving Climate Understanding from NPOESS: The Need for Better Climate Monitoring", NPOESS Climate Requirements Workshop, University of Maryland, College Park, MD
5 March 1996	Mr. R. John Wilson "Selected Aspects of the SKYHI GCM Climatology", GCM-Reality Intercomparison Workshop sponsored by the World Climate Research Program, Victoria, British Columbia, Canada
6 March 1996	Dr. Isaac M. Held "The Dynamics of Global Warming", Physics Colloquium, University of Minnesota, Minneapolis, MN
6 March 1996	Dr. Lori Perliski "Issues in 3-Dimensional Photochemical Modeling", Atmosphere/Ocean Colloquium, Courant Institute, New York University, New York, NY
11 March 1996	Dr. Lori Perliski "The Case of the Missing Ozone: The Tools Scientists Used to Crack It", Fressman Initiative Project - Atmospheric Ozone, Penn State Great Valley Campus, Malvern, PA
22 March 1996	Dr. Syukuro Manabe "Simulation of Younger Dryas-Like Events by a Coupled Ocean-Atmosphere Model", Lamont-Doherty Geological Observatory, Palisades, NY

25 March 1996	Mr. Morris A. Bender "Evaluation of the GFDL Hurricane Prediction System in the Western Pacific", 50th Interdepartmental Hurricane Conference, Miami, FL
26 March 1996	Mr. Robert E. Tuleya "Assessment of Current Skill and Possible Plans for the GFDL Hurricane Prediction System", Interagency Conference on Hurricanes, Miami, FL
28 March 1996	Dr. John R. Toggweiler "Stability of the Interglacial Climate and Ocean Circulation", University of Maine, Orono, ME
1 April 1996	Dr. Kevin P. Hamilton "Drag Effects on the Simulated Climate of the GFDL SKYHI General Circulation Model", NATO Advanced Research Workshop on Gravity Wave Processes and Their Parameterization in Global Climate Models, Santa Fe, NM
2 April 1996	Dr. Brian J. Soden 1. "Satellite Remote Sensing of Upper Troposphere Water Vapor: Applications for Climate Studies", 2. "Improving Hurricane Forecasts Through the Assimilation of Satellite-Derived Winds", Institute for the Study of Planet Earth, University of Arizona, Tucson, AZ
5 April 1996	Dr. Jeffrey L. Anderson "Impacts of Dynamically Constrained Initial Conditions on Ensemble Forecasts", Environmental Modeling Center at NMC/NCEP, Suitland, MD
9 April 1996	Dr. Yoshio Kurihara "Numerical Prediction of Tropical Cyclones", National Center for Atmospheric Research, Boulder, CO
9 April 1996	Dr. Syukuro Manabe "Simulation of Greenhouse Effect: Historical Perspective", Symposium - "Svant Arrhenius and Greenhouse Effect: A Century", Stockholm, Sweden
16 April 1996	Dr. Leo J. Donner "Using ISCCP Data to Evaluate a GCM Parameterization for Ice Clouds", International Workshop on Research Uses of ISCCP Datasets, New York, NY
17 April 1996	Dr. Ngar-Cheung Lau "A Satellite View of Synoptic-Scale Organization of Cloud Properties in Midlatitude and Tropical Circulation Systems", International Workshop on Research Uses of ISCCP Datasets, New York, NY
18 April 1996	Dr. Charles T. Gordon "The Impact of Specified ISCCP Low Clouds in Coupled Model Integrations", International Workshop on Research Uses of ISCCP Datasets, New York, NY
22 April 1996	Dr. Thomas L. Delworth "North Pacific Decadal Variability in the GFDL Coupled Models", JCESS/ CLIVAR Workshop on Decadal Climate Variability, Columbia, MD

22 April 1996	Dr. Michael Winton "Internal Decadal Variability in Ocean GCMs", JCESS/CLIVAR Workshop on Decadal Climate Variability, Columbia, MD
22 April 1996	Dr. Jerry D. Mahlman "Prospects for a Future Northern Hemisphere Ozone Hole", State University of New York at Stony Brook, Stony Brook, NY
22 April 1996	Dr. Syukuro Manabe "Simulation of Natural Climate Variability and Its Implication for the Detection of Global Warming", Cornell University, Ithaca, NY
23 April 1996	Mr. Ronald J. Stouffer "The Role of the Oceans in Natural Variability as Found in a 1000-year Integration of a Coupled Ocean-Atmosphere Model", JCESS/CLIVAR Workshop on Decadal Climate Variability, Columbia, MD
24 April 1996	Dr. Jerry D. Mahlman "Final Report of the Mission to Planet Earth's ESSAAC Committee", NASA Advisory Council Meeting, Washington, DC
25 April 1996	Dr. Y. Kurihara "Numerical Prediction of Hurricanes", Princeton Plasma Physics Laboratory, Princeton University, Princeton, NJ
25 April 1996	Dr. Bruce B. Ross "Mesoscale Modeling at GFDL", NOAA Modeling Meeting, Research Triangle Park, NC
25 April 1996	Dr. Charles Seman "Development of Deep Convection Along an Idealized Baroclinic Dryline", National Center for Environmental Prediction, Washington, DC
26 April 1996	Dr. Jerry D. Mahlman "Anthropogenic Greenhouse Warming: What Do We Really Know?", Global Climate Change Conference, Overland Park, KS
1 May 1996	Dr. Brian Gross "Mesoscale Modeling at GFDL", NOAA Modeling Meeting, Research Triangle Park, NC
7 May 1996	Dr. Jeffrey L. Anderson "The Impacts of Climatological Constraints on the Calculation of Predictability in Dynamical Systems", European Geophysical Society General Assembly, The Hague, Netherlands
7 May 1996	Dr. V. Ramaswamy "Validation Issues Regarding SAGE III Data Retrievals", SAGE III Science Team Meeting, NASA, Langley, VA

10 May 1996	Dr. Jeffrey L. Anderson "The Impact of Dynamical Constraints on the Selection of Initial Conditions for Ensemble Predictions", Royal Dutch Meteorological Institute, De Bilt, The Netherlands
13 May 1996	Dr. Jerry D. Mahlman "NPOESS: Challenges and Opportunities for Climate Research", NASA EOS Investigators' Working Group Meeting, Greenbelt, MD
13 May 1996	Dr. Jeffrey L. Anderson "Coupled Model and Ensemble Prediction Research at GFDL", United Kingdom Meteorological Office, Bracknell, England
14 May 1996	Dr. Ngar-Cheung Lau "The Role of the Atmospheric Bridge in Linking Tropical Pacific ENSO Events to Extratropical SST Anomalies", Goddard Laboratory for Atmospheres/NASA, Greenbelt, MD
14 May 1996	Dr. Jeffrey L. Anderson "The Impact of Dynamical Constraints on the Selection of Initial Conditions for Ensemble Predictions", European Centre for Medium Range Weather Forecasting, Reading, England
15 May 1996	Dr. John R. Toggweiler "Sources and Sinks of Mechanical Energy in the Ocean", Massachusetts Institute of Technology, Department of Earth, Atmospheric and Planetary Science, Cambridge, MA
20 May 1996	Dr. Yoshio Kurihara "Problems in the Tropical Cyclone Prediction", Japan Meteorological Agency, Tokyo, Japan
24 May 1996	Dr. Yoshio Kurihara "Interaction Between Typhoons and the Environment: From a Viewpoint of Typhoon Track Prediction", University of Tokyo, Tokyo, Japan
4 June 1996	Mr. Ronald J. Stouffer "The Role of the Oceans in Natural Variability as Found in a 1000-year Integration of a Coupled Ocean-Atmosphere Model", Lawrence Livermore Laboratory, Livermore, CA
10 June 1996	Dr. Jerry D. Mahlman "Greenhouse Warming: What Do We Really Know?", Goddard Space Flight Center Conference on Global Change and the Americas, Greenbelt, MD
11 June 1996	Dr. Isaac M. Held "Additional Tests for the Dynamical Cores of GCM's", Workshop on Test Cases for Dynamical Cores of GCMs, Breckenridge, CO
11 June 1996	Dr. John R. Toggweiler "GFDL Ocean Circulation Model", Carbon Modeling Center Meeting, Boulder, CO

13 June 1996	Mr. Thomas R. Knutson "Impact of Increased CO_2 on Tropical Storms as Simulated in a GFDL R30-Resolution GCM", Climate Variability and Tropical Cyclone Predictions sponsored by the Risk Prediction Initiative, Tuckers Island, Bermuda
17 June 1996	Dr. Leo J. Donner "Radiative Forcing and Feedbacks by Ice Clouds", Second International Conference on Global Energy and Water Cycle, Washington, DC
10 July 1996	Dr. Jerry D. Mahlman "Anthropogenic Greenhouse Warming: What Do We Really Know?", House of Representatives Meeting on the Science of Climate Change, Washington, DC
17 July 1996	Dr. Leo J. Donner "Elements of Cumulus Parameterization for Microphysics, Radiation and Initialization in Large-Scale Models", NASA/Goddard Space Flight Center, Greenbelt, MD
18 July 1996	Mr. R. John Wilson "Dust Transport in the Martian Atmosphere as Simulated by a GCM", COSPAR Meeting, Birmingham, England
22 July 1996	Mr. R. John Wilson 1. "A Synthesis and Comparison of the Zonal Mean Fields Obtained by Various Modeling Groups", 2. "The Use of Thermal Tide Observations for Constraining Martian GCMs", Martian GCM Intercomparison Workshop, Oxford, England
23 July 1996	Dr. V. Ramaswamy "Cloud-Radiation Issues in General Circulation Modeling", WCRP/GEWEX Radiation Panel Meeting, Dublin, Ireland
23 July 1996	Dr. Jerry D. Mahlman "The Need for International Assessments on Key Sustainable Development Issues, Workshop of the National Research Council Board on Sustainable Development on "The Transition to Sustainability", Bar Harbor, ME
24 July 1996	Dr. Abraham H. Oort "The Energy Cycle of the Earth", GAIA Education Outreach Institute, University of New Hampshire, Temple, NH
30 July 1996	Dr. Syukuro Manabe "Modeling Climate Change", NASA/NOAA Summer School for Earth Science, Process of Global Change, Pasadena, CA
5 August 1996	Dr. Ngar-Cheung Lau "Variability of the Midlatitude Atmospheric Circulation in Relation to Tropical and Extratropical Sea Surface Temperature Anomalies", International Symposium on Climate and Environmental Change, Beijing, China
6 August 1996	Dr. Jeffrey L. Anderson "Predictability of the Coupled Atmosphere-Ocean System", ONR/NRL Workshop on Issues in Atmospheric and Oceanic Predictability, Monterey, CA

13 August 1996	Mr. Ronald Pacanowski "MOM2 Parameterizations and Parallelization", National Center for Atmospheric Research, Boulder, CO
16 August 1996	Dr. Jerry D. Mahlman "NPOESS and Long-Term Climate Products: Opportunities and Challenges for NOAA", NOAA Headquarters Seminar Series, Washington, DC
17 August 1996	Dr. Jeffrey L. Anderson "Design of Modular Physical Parameterizations for Use in a Suite of Coupled Models", American Meteorological Society's Eleventh Conference on Numerical Weather Prediction, Norfolk, VA
19 August 1996	Mr. William Stern "Interannual Variability of Tropical Intraseasonal Oscillations in the GFDL/DERF GCM Inferred from an Ensemble of AMIP Integrations", American Meteorological Society's Eleventh Conference on Numerical Weather Prediction, Norfolk, VA
19 August 1996	Dr. Charles T. Gordon "The Impact of Specified ISCCP Low Clouds in Coupled Model Integrations", American Meteorological Society's Eleventh Conference on Numerical Weather Prediction, Norfolk, VA
19 August 1996	Mr. Matthew Harrison "Initialization of Coupled Model Forecasts using a Global Oceanic Data Assimilation System", American Meteorological Society's Eleventh Conference on Numerical Weather Prediction, Norfolk, VA
19 August 1996	Dr. Jeffrey L. Anderson "Impacts of Dynamically Constrained Initial Conditions on Ensemble Forecasts", American Meteorological Society's Eleventh Conference on Numerical Weather Prediction, Norfolk, VA
19 August 1996	Mr. Joseph Sirutis "The Impact of Cumulus Convection Parameterization in Coupled Air-Sea Models", American Meteorological Society's Eleventh Conference on Numerical Weather Prediction, Norfolk, VA
20 August 1996	Mr. Robert E. Tuleya 1. "Prediction of Hurricane Landfall using the GFDL Model", 2. "Results of the Operational GFDL Hurricane Model at NCEP", American Meteorological Society Eleventh Conference on Numerical Weather Prediction, Norfolk, VA
21 August 1996	Dr. Leo J. Donner "Radiative Transfer in a Three-Dimensional Cloud-System-Resolving Model", International Radiation Symposium, Fairbanks, Alaska
21 August 1996	Dr. V. Ramaswamy 1. "Absorption of Solar Radiation by Water Vapor and Clouds", 2. "Feedbacks and Climate Sensibility to Anthropogenic Solar and Longwave Radiative Forcings", International Radiation Symposium, Fairbanks, Alaska

23 August 1996	Mr. M.D. Schwarzkopf "Effects of Changes in H_20 Continuum in a General Circulation Model", International Radiation Symposium, Fairbanks, Alaska
4 September 1996	Dr. Stephen Griffies "Thermohaline Circulation Predictability on Interdecadal Time Scales", CLIVAR Workshop on Atmospheric-Ocean Interactions and their Influence on Decadal-Scale Climate Variability, Vancouver, Canada
5 September 1996	Mr. Anthony J. Broccoli "The Cold Ocean-Warm Land (COWL) Pattern in Long Integrations of the GFDL Coupled Atmosphere-Ocean Model", CLIVAR Workshop on Atmospheric-Ocean Interactions and their Influence on Decadal-Scale Climate Variability, Vancouver, Canada
6 September 1996	Dr. V. Ramaswamy "Climate Response to Aerosol Radiative Forcing", CHINA-MAP Tropospheric Aerosols Meeting, Boulder, CO
10 September 1996	Dr. Stephen T. Garner "The Role of Momentum Fluxes in Shaping the Life-Cycles of Baroclinic Waves", Joint AMS/RMS Conference on Mesoscale Meteorology, Reading, England
13 September 1996	Mr. Ronald J. Stouffer "A Intercomparison of Three Long (1000 year) Coupled Model Integrations", University of Victoria, Victoria, British Columbia, Canada
16 September 1996	Dr. Jerry D. Mahlman "Greenhouse Warming: A Challenge for Future Generations", 12th Annual Mobile Sources/Clear Air Conference, Crested Butte, CO
20 September 1996	Dr. Kevin P. Hamilton "An Imposed Quasibiennial Oscillation in a GCM: Tropical and Extratropical Effects", Institute for Terrestrial and Planetary Sciences of the State University of New York, Stony Brook, NY
20 September 1996	Dr. Syukuro Manabe "Study of Abrupt Climate Change by Coupled Ocean-Atmosphere-Land Model", Department of Geosciences, Princeton University, Princeton, NJ

APPENDIX E

ACRONYMS

ACRONYMS

AASE	Arctic Airborne Stratospheric Experiment
ABLE	Atmospheric Boundary Layer Experiment
AEROCE	Air Ocean Chemistry Experiment
AGCM	Atmospheric General Circulation Model
AMEX	Australian Monsoon Experiment
AMIP	Atmospheric Model Intercomparison Project
AOML	Atlantic Oceanographic and Meteorological Laboratory/NOAA
AOU	Apparent Oxygen Utilization
ARL	Atmospheric Research Laboratory/NOAA
A94/P95	GFDL Activities FY94, Plans FY95
CCN	Cloud Condensation Nuclei
CEM	Cumulus Ensemble Model
CFC	Chlorofluorocarbon
CHAMMP	Computer Hardware, Advanced Mathematics and Model Physics project
CIRA	COSPAR International Reference Atmosphere
CLIPER	A simple model combining CLImatology and PERsistence used in hurricane prediction.
CMC	Carbon Modeling Consortium
CMDL	Climate Monitoring and Diagnostics Laboratory/NOAA
COADS	Comprehensive Ocean-Atmosphere Data Set
COARE	Coupled Ocean-Atmosphere Response Experiment
COSPAR	Congress for Space Research
CRAY	Cray Research, Inc.
CSIRO	Commonwealth Scientific & Industrial Research Organization
DAMEE	Data Assimilation and Model Evaluation Experiments
DJF	December, January, February (winter)
DU	Dobson units

E	A physical parametrization package in use at GFDL. E physics includes a high-order closure scheme for subgrid turbulence.
ECMWF	European Centre for Medium-Range Weather Forecasts
E"n"	Horizontal model resolution corresponding to "n" points between a pole and the equator on the E-grid.
ENSO	El Niño - Southern Oscillation
EOF	Empirical Orthogonal Function
EPOCS	Equatorial Pacific Ocean Climate Studies
ERBE	Earth Radiation Budget Experiment
FDDI	Fiber Distributed Data Interface
FDH	Fixed Dynamic Heating model
FIRE	First ISCCP Regional Experiment
FY"yy"	Fiscal Year "yy" where "yy" are the last two digits of the year.
GARP	Global Atmospheric Research Program
GATE	GARP Atlantic Tropical Experiment
GCM	General Circulation Model
GCTM	Global Chemical Transport Model
GEOSAT	Geodetic Satellite
GFD	Geophysical Fluid Dynamics
GFDL	Geophysical Fluid Dynamics Laboratory/NOAA
GMT	Greenwich Mean Time
GOES	Geostationary Operational Environmental Satellite
GTE	Global Tropospheric Experiment
HIBU	Federal Hydrological Institute and Belgrade University
HPCC	High Performance Computing and Communications
HRD	Hurricane Research Division/AOML
ICRCCM	InterComparison of Radiation Codes in Climate Models
IGBP/PAGES	International Geosphere-Biosphere Project/Past Global Changes
I/O	Input/Output

IPCC	Intergovernmental Panel on Climate Change
ISCCP	International Satellite Cloud Climatology Project
IT	Information Technology
ITCZ	Intertropical Convergence Zone
JGOFS	Joint Global Ocean Flux Study
JJA	June, July, August (summer)
JPL	Jet Propulsion Laboratory
LAHM	Limited Area HIBU Model
LAN	Limited Area Nonhydrostatic
LBL	Line By Line
LIMS	Limb Infrared Monitor of the Stratosphere
L"n"	Vertical model resolution of "n" levels.
LWP	Liquid Water Path
MLS	Microwave Limb Sounder
MMM	Multiply-nested Movable Mesh
MOM	Modular Ocean Model
MOM2	Modular Ocean Model, Version 2
MOODS	Master Oceanographic Observations Data Set
MPP	Massively Parallel Processor
NABE	North Atlantic Bloom Experiment
NADW	North Atlantic Deep Water
NARE	North Atlantic Regional Experiment
NASA	National Aeronautics and Space Administration
NCAR	National Center for Atmospheric Research
NCDC	National Climate Data Center/NOAA
NH	Northern Hemisphere
NMC	National Meteorological Center/NOAA
NOAA	National Oceanic and Atmospheric Administration

NODC	National Oceanographic Data Center/NOAA
ODA	Ocean Data Assimilation
OLR	Outgoing Longwave Radiation
OTL	Ocean Tracers Laboratory/Princeton University
PCMDI	Program for Climate Model Diagnosis and Intercomparison
PFC	Perfluorocarbon
PILPS	Project for Intercomparison of Land-Surface Parameterization Schemes
PMEL	Pacific Marine Environmental Laboratory
PMIP	Paleoclimate Model Intercomparison Project
PNA	Pacific-North American
POM	Princeton Ocean Model
PSCs	Polar Stratospheric Clouds
QBO	Quasi-Biennial Oscillation
QG	Quasi-Geostrophic
RAS	Relaxed Arakawa-Schubert
RFP	Request for Proposal
R"n"	Horizontal resolution of spectral model with rhomboidal truncation at wavenumber "n".
SAGE	Stratospheric Aerosol and Gases Experiment
SAMS	Stratospheric Aerosol Measurement System
SAVE	South Atlantic Ventilation Experiment
SBUV	Solar Backscatter Ultraviolet (satellite)
SGI	Silicon Graphics, Inc.
SH	Southern Hemisphere
SiB	Simple Biosphere
SKYHI	The GFDL Troposphere-Stratosphere-Mesosphere GCM
SME	Solar Mesosphere Explorer
SOI	Southern Oscillation Index
SPCZ	South Pacific Convergence Zone

SPECTRE	Spectral Radiation Experiment
SST	Sea Surface Temperature
SUN	Sun Microsystems, Inc.
THC	Thermohaline Circulation
TIO	Tropical Intraseasonal Oscillations
T"n"	Horizontal resolution of spectral model with triangular truncation at wavenumber "n".
TOGA	Tropical Ocean and Global Atmosphere project
TOGA/TAO	Tropical Ocean Global Atmosphere/Tropical Atmosphere Ocean
TOMS	Total Ozone Mapping Spectrometer
TOPEX	Topographic Experiment
TOVS	Tiros Operational Vertical Sounder
TTO	Transient Tracers in the Oceans
UARS	Upper Atmosphere Research Satellite
WGNE	Working Group on Numerical Experimentation
WMO	World Meteorological Organization
WOCE/HP	World Ocean Circulation Experiment/Hydrographic Program
XBT	Expendable Bathythermograph
ZODIAC	Gridpoint Climate Model

☆ U.S. GOVERNMENT PRINTING OFFICE: 1997 - 527-505